RV SONNE 252
Cruise Report / Fahrtbericht

Yokohama: 05.11.2016

Nouméa: 18.12.2016

SO252: RITTER ISLAND
Tsunami potential of volcanic flank collapses

Christian Berndt
GEOMAR Helmholtz Centre for Ocean Research Kiel
2017

With contributions by: Sina Muff, Ingo Klaucke, Sebastian Watt, Christoph Böttner, Bettina Schramm, Ann-Marie Völsch, Swaantje Bennecke, Judith Elger, Wu-Cheng Chi, Johannes van Haren, Aaron Micallef, Theresa Roth

Table of content

1. Cruise summary / Zusammenfassung

1.1 German / Deutsch

Flankenzusammenbrüche von Vulkaninseln generieren hochenergetische Erdrutsche, die katastrophale Tsunamis auslösen können. Computersimulationen zeigen, dass sehr große vulkanische Erdrutsche, auch ozeanweite Tsunamis auslösen können (Løvholt et al., 2008; Waythomas et al., 2009). Die Magnitude solcher Tsunamis ist jedoch umstritten, da sie von vielen Faktoren abhängt, insbesondere von den submarinen Transport- und Ablagerungsprozessen (Harbitz et al. 2013). Für eine vollständige Analyse des Gefahrenpotentials, das von Flankenkollapsen ausgeht, ist es daher wichtig, diese Faktoren im Detail zu untersuchen. Aktuelle Studien deuten auf ein weitaus komplexeres Zusammenspiel von Prozessen am Meeresboden hin, als bisher angenommen. Mit einem Kollapsvolumen von etwa 5 km³ ist der Zusammenbruch der Westflanke von Ritter Island in der Bismarck See von 1888 der größte historisch belegte Flankenkollaps. Das Arbeitsgebiet bietet ideale Bedingungen zur Rekonstruktion der submarinen Transport- und Ablagerungsprozesse, da (I) der Zusammenbruch in jüngster geologischer Vergangenheit stattgefunden hat und somit die Ablagerungen im marinen Bereich sehr deutlich erkennbar sind, (II) historische Aufzeichnungen vorhanden sind, die Auskunft über wichtige Parameter wie das kollabierte subareale Volumen geben und (III) die Höhen und Ankunftszeiten des ausgelösten Tsunamis auf mehreren Nachbarinseln gemessen und dokumentiert wurden. Wir schlagen vor, Bathymetrie, hochauflösende 2D und 3D seismische Daten sowie Meeresbodenproben der submarinen Rutschungsablagerungen um Ritter Island zu sammeln, die Aufschluss über die Bewegung und Ablagerungsprozesse des Materials geben, das durch den Flankenkollaps mobilisiert wurde. Das genaue Verständnis der in Verbindung mit dem Zusammenbruch von 1888 stehenden Rutschungsprozesse in Kombination mit guten Randbedingungen, wie sie durch Augenzeugenberichte des Tsunamis gegeben ist, bietet die einzigartige Möglichkeit, die Geschwindigkeit der Rutschung zu bestimmen, welche dann für Gefährdungsanalysen an anderen Ozeaninseln genutzt werden kann.

1.2 English / Englisch

Large volcanic debris flows associated with volcanic island flank collapses may cause devastating tsunamis as they enter the ocean. Computer simulations show that the largest of these volcanic debris flows on oceanic islands such as Hawaii or the Canaries can cause ocean-wide tsunamis (Løvholt et al., 2008; Waythomas et al., 2009). However, the magnitude of these tsunamis is subject to on-going debate as it depends particularly on landslide transport and emplacement processes (Harbitz et al. 2013). A robust understanding of these factors is thus essential in order to assess the hazard of volcanic flank collapses. Recent studies have shown that emplacement processes are far more complex than assumed previously. With a collapsed volume of about 5 km^3 the 1888 Ritter Island flank collapse is the largest in historic times and represents an ideal natural laboratory for several reasons: (I) The collapse is comparatively young and the marine deposits are clearly visible, (II) the pre-collapse shape of the island is historically documented and (III) eyewitness reports documenting tsunami arrival times, run-up heights and inundation levels on neighboring islands are available. We propose to collect bathymetric, high resolution 2D and 3D seismic data as well as seafloor samples from the submarine deposits off Ritter Island to learn about the mobility and emplacement dynamics of the 1888 flank collapse landslide. A comparison to similar studies from other volcanic islands will provide an improved understanding of emplacement processes of volcanic island landslides and their overall

tsunamigenic potential. In addition, a detailed knowledge of the 1888 landslide processes in combination with tsunami constraints from eyewitness reports provides a unique possibility to determine the landslide velocity, which can then be used in subsequent hazard analyses for ocean islands.

2. Participants / Teilnehmer

2.1 Principal investigators / Leitende Wissenschaftler

Prof. Dr. Christian Berndt, GEOMAR

Dr. Morelia Urlaub, GEOMAR

Dr. Sascha Brune, GFZ-Potsdam

2.2 Scientific party / wissenschaftliche Fahrtteilnehmer

Prof. Dr. Christian Berndt	Chief scientist	GEOMAR
Dr. Ingo Klaucke	Leader Hydroacoustics	GEOMAR
Christoph Böttner	Hydroacoustics	GEOMAR
Dr. Judith Elger	Data management	GEOMAR
Dr. Swantje Bennecke	Marine biology	GEOMAR
Dr. Sudipta Sarkar	Geophysics, Watch leader	GEOMAR
Prof. Wu-Cheng Chi	Heat flow, OBS	SINICA
Dr. Aaron Micallef	Seismic	UOM
Sina Muff	Leader P-Cable	GEOMAR
Dr. Sebastian Watt	Volcanology, sedimentology	UBirmingham
Melanie Ray	Volcanology, sedimentology	UCL
Dr. Johannes van Haren	Physical Oceanography	NIOZ
Bettina Schramm	Leader OBS	GEOMAR
Ann-Marie Völsch	OBS, Admin	GEOMAR
Michel Kühn	OBS, Watch keeper	GEOMAR
Nils Peter Finger	OBS, Watch keeper	GEOMAR
Gero Wetzel	Electronical engineer	GEOMAR
Eduard Fabrizius	Electronical engineer	GEOMAR
Torge Matthiessen	Mechanical engineer	GEOMAR
Jan Rindfleisch	Mechanical engineer	GEOMAR
Theresa Roth	Watch leader	GEOMAR
Kristina Popp	Watch leader	GEOMAR
Joel Edwards	Watch keeper	UC Santa Cruz
Kuan-Ting Lin	Watch keeper, Heat flow	GEOMAR
Olga Sanchez	Watch keeper	IEO
Thore Kausch	Watch keeper,	GEOMAR
Inken Schulze	Watch keeper	GEOMAR
Thomas Mommsen	Watch keeper	GEOMAR
Hendrik Rapp	Watch keeper	GEOMAR
Anja Bräunig	Watch keeper	GEOMAR

2.3 Crew / Mannschaft

Oliver Meyer	Master
Jens Göbel	Chiefmate
Lars Hoffsommer	2. Mate
Ulrich Büchele	2. Mate
Anke Walther	Ship's doctor
Dieter Hermesmeyer	Chief
Steffen Genschow	2. Engineer
Tim Stegmann	2. Engineer
Jörg Leppin	Chief Electrician
Matthias Großmann	System operator
Miriam Plöger	System operator
Hendrik Schmidt	Electrician
Henning De Buhr	Electrician
Torsten Bolik	Deck's fitter
Björn Bredlo	Motormann
Jürgen Kraft	Boatswain
Torsten Bierstedt	2. Boatswain
Frank Heibeck	A.B.
Georg Hoffmann	A.B.
Jannik Doliwa	A.B.
Rene Papke	A.B.
Sascha Fischer	A.B.
Stefan Koch	A.B.
Torsten Kruszona	A.B.
Willi Rieger	A.B.
André Garnitz	Cook
Patrick Kosanke	Cook's mate
Alexander Vogt	Steward
Bernardo Carlonio	Steward
Maik Steep	Steward
Sven Kröger	Steward

3. Narrative of the cruise / Ablauf der Forschungsfahrt

Saturday, 5 November

We left Yokohama, Japan at 08:30 local time in the morning setting sail towards the Mariana Trench. With fine weather and a light easterly breeze, we continued through the approaches of Yokohama for several hours before bearing more southward along the volcanic islands of the Izu-Bonin Arc.

Sunday, 6 November

Because of approaching typhoon Meari (class 4) we altered to a more westerly course in order to avoid beating into the centre of the storm. For the next few days we had strong NE winds up to Bft 8 and a pleasant swell following us from port side abating slowly on until Wednesday 10.

Thursday, 10 November

We reached the Challenger Deep in the evening of the November 10 and started to deploy the CTD after first ascertaining that the identified position is indeed the deepest part of the trench by using the EM122 multi-beam system. To protect the depth sensor of the CTD we did a dual cast first down to 8000 m and then terminating the depth sensor and sending the CTD back down all the way to the bottom which was reached at 10905 m water depth based on EM122 depth soundings calibrated with the CTD sound velocity profile afterwards.

Friday, 11 November

In the morning, while the CTD was still coming back to the surface we started the drone to acquire a movie of Sonne to obtain a practice data set. We used this data set to get information on how much video material is needed for the calculation of a three dimensional model of Ritter Island later on. At noon local time, the CTD was back on board and we steamed 8 nm south where we began to deploy the mooring. Deployment took place the whole afternoon in very hot weather. The final anchor weight was dropped at 09:39 UTC at 11° 20,093' N 142° 11,335' E. Afterwards we steamed to the main survey area off Ritter Island.

Tuesday, 15 November

We arrived north of Ritter Island in the morning and running a CTD at 07:30 in 1650 m water depth in order to calibrate the multi-beam and Parasound systems. This was finished 08:30. Staying at the same station, we ran a releaser test for the fourteen OBS releaser, which lasted until 11:30. Three instruments malfunctioned (two not responding, one not releasing), so that we decided to use only eleven OBS for the main survey. At noon, we began with the deployment of the 2D seismic system. The system was up and running at 15:00 when we began to acquire the first line along Ritter Island.

Friday, 18 November

2D seismic shooting continued until the evening of 18 November in largely calm weather conducive to seismic acquisition producing some beautiful data. We managed to cover the entire slide deposit without any problems covering 680 line km in total. The 2D system was retrieved at 18:00 local time and we mounted the gravity corer. We continued gravity coring until 05:30 in the morning when the crane had a technical failure. Most cores only retrieved some volcanic sand in the core catcher confirming the seismic interpretation that Ritter Island mostly consisted of sedimentary strata such as scoria deposits what we had already suspected based on its seismic character.

Saturday, 19 November

At 09:00 we arrived at a location 300 m east of Ritter Island. For the next hour we conducted two drone flights of which the first produced nice footage of the western side of the island which will be used for the 3D reconstruction. At 10:00 we started to deploy the OBS east of Ritter Island (4 OBS) and during the afternoon a further seven inside the slide deposit west of Ritter Island. At 15:00 we sailed to the distal end of the deposit to continue coring. During the night we attempted gravity coring at five sites, but they were largely unsuccessful with minor sediment recovery in the core catchers showing clayey and silty sediments.

Sunday, 20 November

At 08:00 we deployed the P-Cable system east of Ritter Island. The system was fully functioning by 11:00 and we started to acquire 3D seismic data across the landslide. Shooting continued until Saturday 26 of November without major interruptions.

Thursday, 24 November

During the night the airgun line came off twice, but the system was back up and running within one hour each time.

Friday 25 November

Also during the night from Thursday to Friday, the airgun line came off twice and the gun had to be repaired, but the system was up again within a short time. On Friday morning at 08:00 a fishing net got stuck to the P-Cable system but it came off by itself. To check that there was no damage we conducted a drone flight and could find no problems although the seven port side streamers did not transmit data during the time when the fishing net was entangled. In the afternoon (between 04:05 and 04:12) we observed an area of discoloured surface waters at 5°31'7''S 148°04'4'' E that possibly were related of volcanic activity (Fig. 1). Through the binocular it looked as if water was upwelling and turbulent. The phenomenon continued for about 15 minutes. We tried to find evidence for this in the water column imaging data of the EM710 multi-beam echosounder, but there were no indications for rising gas bubbles.

Figure 1: Photograph of the discoloured surface waters in approximately 0.5 nm distance possibly indicating ongoing volcanic activity. (Photograph: Johannes van Haren).

Saturday, 26 November

We started to retrieve the P-Cable system at 09:20. After the system was back on deck by 10:30, we steamed to the first OBS site and began with the recovery of the OBS. During the afternoon the wind picked up to Bft 8 with 2 m waves. Except for OBS2 all OBS surfaced until 18:00 and we conducted heat flow measurements during the night along a transect that runs between Sakar and New Britain islands and up the flank of Ritter Island. Unfortunately, we were not able to penetrate the seafloor at any of the ten attempted sites indicating a very hard seabed and explaining why gravity coring was not successful either.

Sunday, 27 November

At 08:00 we began to locate the OBS by ranging it from four different directions around the deployment point. It was possible to determine its location to within +/- 50 m. At 11:00 we deployed HyBis and ran a search pattern around the determined location. We found the OBS which had its swim line wrapped around the anchor and recovered it using the grab. The operation was finished by 14:00. During the afternoon we collected multi-beam data as close

as possible around Ritter Island. Afterwards we conducted two drone flights that were finished by 17:00 and provided a complete video coverage of the western flank of Ritter Island. In the evening we redeployed the P-Cable system and started collecting 3D seismic data by 20:00.

Tuesday 29 November

We continued shooting seismic data for the next two days. Tuesday afternoon we finished the first run through the cube and continued with infill lines.

Wednesday, 30 November

In the early morning hours a thunderstorm developed. With Bft 9 the wind was quite strong and the vessel had to speed up in order to steer. This caused damage to the data cable and we had to recover the system when the wind had abated to Bft 5 between 03:00 and 05:30. We continued with multibeam and parasound lines north of Ritter Island while the system was repaired. Starting at 08:30 we deployed the video system OFOS and conducted three dives. The first addressed the nature of the cone structures west of Ritter. The second one the head scarp and the new crater, and the third one the trim line of the Ritter Slide on the slope of Umboi Island. Video surveying continued until 21:00. At 23:00 we started to collect more heat flow data along two transect in the proximal area of the slide.

Thursday, 1 December

In the morning we redeployed the P-Cable system in torching heat. The system was up and running at 10:00. Unfortunately, the drone flight to check that everything was deployed properly ended with the loss of the drone, when it touched the A-frame during the landing.

Friday, 2 December

Around noon a big tree that was floating just below the surface got caught in the P-Cable system and we had to spend the entire afternoon trying to get rid of it. By 16:00 the system was up and running again.

Monday, 5 December

We collected more seismic data without any further interruptions until Monday 5, December. At 15:30 we started to retrieve the P-Cable system which was completed at 16:30. Then we rigged the seismic system into two two-section streamers that were connected with a 9.4 m cable. We mounted a weight to the front of the lower streamer and a buoy to the upper streamer and collected data for about one hour until 18:00. The objective was to obtain a data set that can be used for testing multiple and ghost suppression techniques. Afterwards, we ran multi-beam and Parasound profiles during the night to map out the distal part of the landslide deposit in order to quantify better its volume.

Tuesday, 6 December

We finished with the Parasound lines at 9:00 and conducted three HyBis dives throughout the day. First, we took two samples from the newly developing cone, then we dove into the deepest part of the landslide scarp, and finally we have tried to take a sample in the main debris flow plain south of Sakar Island, but the fibre optic winch system failed and we had to recover HyBis before a sample could have been taken. During the night we collected more Parasound and multi-beam data.

Wednesday, 7 December

Because of a winch problem, we could not use HyBis and lost about four hours looking for an insulation problem in the high voltage supply. From 13:00 to 19:00 we ran a long OFOS transect across the block west of the slide scar which appears to be a remnant of the original volcanic edifice although it is not entirely clear if it has been moved during the Ritter Island collapse. During the night we collected more Parasound and multi-beam bathymetry data in the distal part of the slide.

Thursday, 8 December

At 09:00 we deployed HyBis again after the winch had been fixed. We conducted two dives with the OFOS frame mounted underneath HyBis. The first transect ran from the hummocky facies into an erosional channel in the southern part of the failure area north of Umboi. We found evidence for high currents such as ripples and numerous corals on the exposed areas around 500 m water depth but hardly any evidence for strong currents within the channel where they should be expected, which probably means that the channels have been incised during the Ritter Island collapse but were inactive since. The second dive started at the top of the highest cone structure and continued into the main channel with very similar observations as the first dive. At the end of the second dive a voltage meter in the high voltage power supply failed, which had to be fixed during the evening. During the night we sailed out into the very distal area of the landslide collecting more multibeam and Parasound data.

Friday, 9 December

During the day we conducted four HyBis dives from the very distal area progressively closer to Ritter Island. We found a wide range of different seafloor. The most distal part was covered by a fine sand debris flow deposit. The second site only showed hemi-pelagic sediments with big mud clasts. The third site showed typical fine sand and mud debris flow deposits. The fourth site was the most proximal one outside the barrier between Umboi and Sakar islands. The seafloor was flat and we recovered interlayered sands and muds without indications that they were related to the Ritter Island collapse.

Saturday, 10 December

During the day we conducted four HyBis dives in the proximal area between Umboi, Sakar, and Ritter Island. The first dive sampled the flat area close to Umboi where we had thought we had discovered incised channels during the third OFOS transect on November 30. It turned out that the seafloor topography is much more complex in this area with numerous round or oblong depressions and that we must have mistaken them for a channel during the first visit. We took a sample which consisted of poorly sorted debris with a thin hemipelagic mud on top. The second dive was carried out on the flank of a hummock and revealed various volcanoclastic sediments. The third dive visited the flank of the eastern cone structure. We managed to get a sample from the 30-40° steep side of the cone which consists of fresh looking volcanic rocks with numerous rocks that contain xenoliths. The fourth dive went to the flat area south of Sakar area where we tried to sample the dark patches at the break of slope. The seafloor must be very hard because HyBis hardly penetrated, scraping off only the uppermost hemi-pelagic sediments and some fine sand. This was the area where we also bent the gravity corer barrel during an unsuccessful coring attempt. During the night we continued with filling gaps in the EM710 multi-beam coverage mainly between Sakar and Umboi island.

Sunday, 11 December

Starting at 8:30 in the morning we conducted two long HyFos (HyBis with the OFOS video sledge) video transects. The first one started at the southern end of the foot of the new crater all the way up to the crater rim and down into the crater. Inside the crater the visibility was very poor and the very steep seafloor is covered by very fine, brown material that is in the water column draping the volcanic rocks. The dive continued to the southern tip of Ritter Island where a steep at least 30 m-high cliff exists. It consists of dense igneous rocks presumably dike intrusions. The second dive covered a long stretch at the 380 m contour line of Ritter Island's east side to a topographic depression in the slope further south. The slope was covered by small and large blocks, but with more drape than on Ritter Island's western side. The second dive was completed by 16:40. During the night we collected more Parasound and EM710 data.

4. Aims of the Cruise / Zielsetzung der Forschungsfahrt

The overarching aim of this project is to improve our understanding of the general processes and interrelationships that control the submarine continuation and emplacement of landslides caused by volcanic flank collapses. Moreover, the combination of precise knowledge of slide processes (as interpreted from geophysical and geological data collected during the proposed research cruise) and eyewitness reports of the tsunami that was caused by the slide provide the unique opportunity to determine the landslide velocity for the first time.

Objective 1: How was volcanic material from the 1888 flank collapse distributed around Ritter Island?

Extent and facies characteristics of the deposit: Already in 2004 good swath bathymetry and side scan sonar coverage of the 1888 landslide deposit off Ritter Island was achieved and published by US American colleagues at the University of California Santa Cruz (Fig. 5 in Silver et al. 2009). In addition to the interpretation of the spatial extent and identification of different facies of the deposit these data will be re-analyzed with respect to:

- The location, distribution and size of transported blocks
- Topography-driven changes in the direction of emplacement
- Erosional features at the flanks of Umboi and Sakar Islands
- Number and extent of depositional lobes

The results will provide information on the dynamics and mobility of the submarine landslide and are essential parameters for the tsunami modelling in WP 2.

Origin of landslide deposit: The collapse of Ritter Island was not necessarily limited to the subaerial part of the volcano, but could as well have affected its submarine flanks. At the same time, the seafloor may fail as a response to sudden loading by volcanic debris, mobilizing large amounts of marine sediments. To estimate the magnitude of a tsunami it is crucial to know the total landslide volume, the origin of the slid material and the percentages of the distinct landslide masses with different sources (Figs. 1, 2). The combination of already existing bathymetry and side scan sonar data with new 3D and 2D seismic data, gravity cores and HyBIS sampling will help to constrain the following key questions:

- What is the total volume of material involved in the landslide?
- Was the landslide emplaced in a single or in multiple stages?
- How did the landslide disintegrate?
- What mechanisms could have caused seafloor failure?

The 3D seismic investigations will be concentrated on the uppermost part of the flank collapse deposit. This area is crucial for several reasons. First, it is likely that disintegration of the slope material has occurred in this area and we will use the 3D seismic data to document the extent to which material has been broken up in blocks and to which extent it may have moved intact. In the 3D seismic data we will map intact blocks of flank material and evidence for mega-scale slickensides and glide planes. Second, it is important to constrain to which extent the submarine part of the volcano flank has been mobilized. We will use the 3D seismic data together with multibeam bathymetry data to look for evidence for the pre-landslide morphology of the island. While the multibeam bathymetry of areas surrounding the slope failure will be used to determine the general trend of the slope, the 3D seismic data will be used to determine the depth of infill within the landslide scarp. Third and finally, we will use the 3D seismic data to distinguish between volcanic deposits and pre-existing slope sediments that have been mobilized during the slide. The IODP drilling results from Leg 340 suggest that most of the distal part of volcanic island flank collapse deposits consists of mobilized sediments, which would be of little significance for tsunami generation. Therefore, we propose to collect 2D data in the distal part to constrain the overall volume of slumped material and 3D seismic data in the proximal zone, where we need as precise as possible landslide volumes.

The porosity of landslide deposits can be significantly lower than the porosity of the unfailed material due to shear deformation (Dugan 2012). However, during the transport process volcaniclastic as well as hemipelagic sediments experience decompression and swelling (Leroueil et al. 2001), indicating that most of the porosity loss is a consequence of consolidation. Given the young age of the 1888 landslide deposit and the lack of overburden, it is likely that the material has not consolidated significantly yet, and that its porosity is similar to the porosity at its origin. We therefore assume that the volume of the deposit as estimated from 2D and 3D seismic data is directly representative for the volume of the actively moving landslide.

Was the landslide emplaced in one or in multiple stages? Evidence for multistage emplacement are i.a. several depositional lobes that can be identified in side scan sonar data or the presence of mud intervals between subunits of coarser material. Gravity cores and 3D seismic data will determine internal reflectors within the landslide. In addition, the deposits of long-run-out turbidity currents as recovered in distal gravity cores can also be used to determine whether the landslide was emplaced in one or multiple stages (Hunt et al., 2011). Turbidites that comprise multiple fining-up sequences of sand capped by mud indicate emplacement in multiple stages, as mud settles and consolidates slowly. Thicknesses of these mud drapes represent time intervals between the deposition of subsequent units (Hunt et al. 2011). These time intervals are important in defining the interactions of tsunami waves as well as for differentiating the 1888 deposit from potential younger deposits.

Characteristics of older landslides: A thorough understanding of the relationship between landslides and the eruption history of Ritter Island as well as the surrounding volcanoes is important for the assessment of the overall hazard of this region. Knowledge of the number of past landslides will provide recurrence rates. The 1888 flank collapse and landslide is not related to an eruption of Ritter volcano. Does this case represent an exception, or is this a common pattern? We will use the newly collected data to establish a geological landslide record, and juxtapose it to the eruption history of Ritter volcano and its direct neighbors.

Similarities and differences to other volcanic island landslides: Comparing the results of several case studies may lead to new insights into the general behavior of volcanic island landslides. We suggest to compare the results from the proposed project to flank collapses off Montserrat, as a comparable 3D seismic data set is available. By assessing the similarities and differences with respect to seafloor failure, volume, geometry, slope gradients, sediment type, single- vs multistage failure, etc., we aim to single out and identify the factors that control the behavior of volcanic island landslides, and hence their tsunamigenic potential.

Objective 2: Landslide velocity

Numerical modelling of the 1888 tsunami source will integrate the constraints on landslide evolution that were derived in WP 1. By reconstructing slide dynamics, a kinematic landslide model will be developed that is based on the original shape of Ritter Island, the final distribution of landslide material as well as any existing additional constraints on slide evolution. The time-dependent, three-dimensional slide distribution will be used as boundary condition for the numerical tsunami propagation model. Tsunami simulation will be conducted using the established nonlinear shallow-water model TUNAMI-N2 (Imamura et al. 1997) that has been previously modified to account for landslide-tsunami generation (Brune et al. 2009, 2010). In addition to the kinematic model of landslide motion, the tsunami propagation model requires high-resolution bathymetry data that will be collected during the survey and embedded in a regional data set with 30 arc seconds resolution (GEBCO). The aim is to compute tsunamis of multiple plausible slide scenarios and to compare the results to documented run-up heights.

The applicability of non-linear shallow water equations has certain limits that have to be respected during tsunami modelling. Namely the tsunami wavelength has to be much larger than the local water depth. If we find that the Ritter Island Landslide was dominated by small wave lengths, we will have to apply alternative tsunami modelling tools that are not submitted to the shallow water approximation. The most promising alternatives rely on the so-called Boussinesq approximation, whereas the code COULWAVE will be best suited for this project, since it has been already applied in recent investigations of two proposal applicants (Berndt et al. 2009, Brune et al. 2009).

5. Setting of the working area / Beschreibung des Arbeitsgebiets

Ritter Island is an uninhabited, crescent-shaped volcanic island (Fig. 2) located about 100 km northeast of New Guinea. The active Ritter stratovolcano situated between the islands of Umboi and Sakar in the Bismarck Sea belongs to the Bismarck Volcanic Arc (Fig. 3). The island's modern shape is a result of its collapse in 1888. Ritter Island is 1900 m long, approximately 200 m wide and the highest elevation of 140 m forms the center of the island (Fig. 2). The open, crater-shaped side faces west, while the eastern side represents the steep flank of the original volcano (~44°, Johnson 1987). The active volcanic cone in the center of the concave western side is covered by 150 m of seawater. Landslide scars are visible on its flanks. The last known eruption in May 2007 triggered a local tsunami that caused limited damage on neighboring Umboi Island. A subsequent tsunami recorded ten days after the eruption with wave heights of 4-10 m around Ritter Island was probably triggered by a landslide on the island's southern flank. Historical paintings reveal that before 1888 Ritter Island was almost perfectly round with a diameter of about 1170 m. The 780 m high cone was extraordinarily steep with gradients of up to 50°.

Figure 2: Aerial photography of Ritter Island with R/V Sonne in the foreground.

Geological background: Ritter Island is part of the 1000 km long Bismarck Volcanic Arc, which is the result of northward subduction of the small Solomon Plate underneath the Bismarck Plate. The rate of subduction decreases from East to West and ranges between 9-12 cm/a (Baldwin et al. 2012). The prevailing sedimentation patterns, sediment transport processes, and the origin of the marine sediments are hardly known. As Ritter Island is surrounded by steep volcanic islands, it is likely that erosion in the form of landslides on volcanic flanks as well as pyroclastic flows dominate the terrestrial sediment input. Hemipelagic sedimentation rates are unknown.

The 1888 landslide: The Ritter Island flank collapse on 13 March 1888 is the largest historic flank collapse of a volcanic island, involving subaerial material with a volume of about 5 km³. This is about twice the volume of the Mt St Helens collapse in 1980 (Voight 1981). The collapse of Ritter Island was not accompanied by eruptive activity. Although Ritter Island collapsed towards the West, the associated landslide was redirected in northwestern direction between the islands Umboi and Sakar and travelled as far as 70 km. Due to its young age the landslide deposit is not eroded or covered by sediment, and is clearly visible in side scan sonar data (Silver et al. 2009). Within a radius of about 15 km around Ritter Island Silver et al. (2009) mapped densely packed, up to 2 km long blocks. Between 15 km and 35 km smaller blocks are embedded in a matrix. No larger blocks are observed further away. Seafloor photography and dredge samples from this distal debris flow show intraclasts of layered sediments. Silver et al. (2009) observe flow reflection on both sides of the natural channel between Umboi and Sakar several hundreds of meters above the seafloor. These observations along with the elongated shape of the deposit suggest that seafloor failure was involved (Watt et al. 2012).

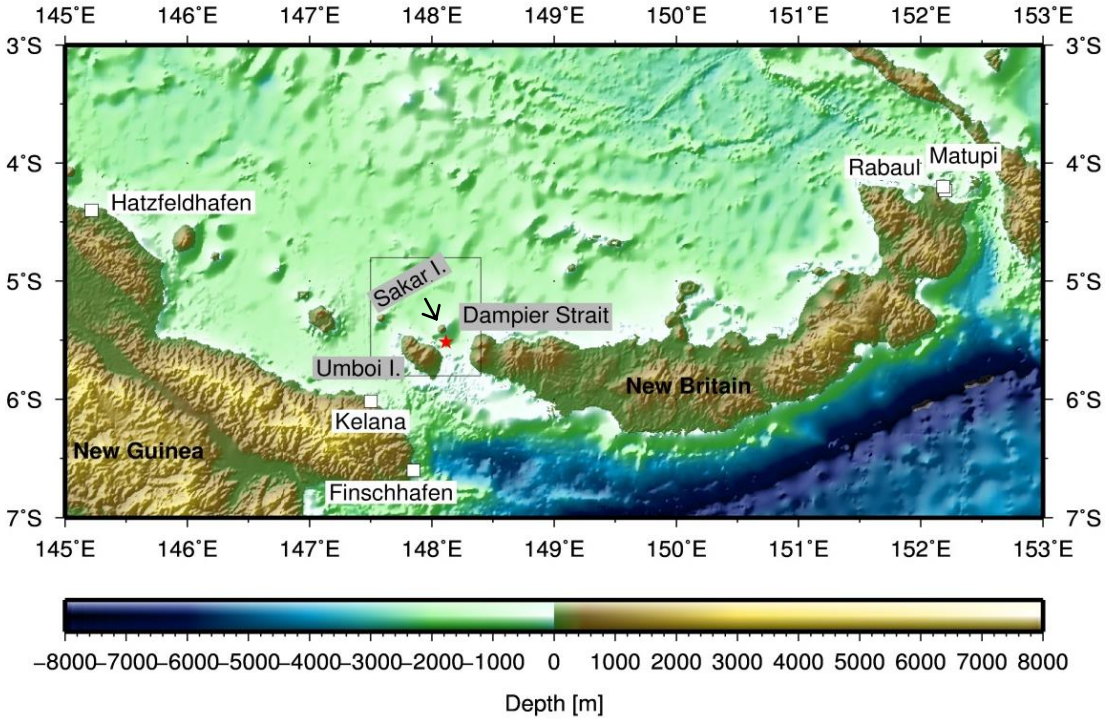

Figure 3: Bathymetric map of the study area (GEBCO). Ritter Island (red star) is located between the islands of Umboi und Sakar. Eyewitness sites of the 1888 tsunami have a white background. Areas with contemporary damage reports are marked with a grey background.

The 1888 tsunami: The tsunami triggered by the 1888 flank collapse caused several hundred fatalities and significant damage on neighboring islands within distances of up to 600 km from Ritter Island (Cooke 1981). In this period German colonists settled in the area between New Guinea and New Britain. Critically, the colonists owned pocket watches so that they documented not only run-up heights but also arrival times of the tsunami at four sites (Table 1). Furthermore, the colonists wrote damage reports with valuable information on the nature of the tsunami.

Table 1: Overview of available boundary conditions from historical eyewitness reports and damage observations (from Cooke 1981). See Fig. 4 for individual locations. 1: Wave arrival time, 2: Duration of anomalous waves, 3: wave period, 4: wave amplitude, 5: run

Location	Type of report	1	2	3	4	5	6
Finschhafen	Eyewitness	x	x	x	x		
Kelana	Eyewitness	x	x	x		x	
Hatzfeldhafen	Eyewitness	x	x	x	x		
Umboi Island	Damage						x
Sakar Island	Damage						x
Neubritannien	Damage						x
Dampier Straße	Eyewitness	x					
Matupi (Rabaul)	Eyewitness	x	x			x	x

Previous studies and existing data: Johnson (1987) conducted the first scientific investigations on and around Ritter Island. During a two-day expedition he acquired single-beam echosounder data down to 1,000 m. The limitation to water depths shallower than 1000 m was due to technical reasons. Hence, he did not image the entire landslide extent on the seafloor. Nevertheless, Johnson (1987) was able to show that a large-scale landslide destroyed Ritter Island, as opposed to an explosive volcanic event.

It was not until 2004 that another scientific cruise led by US scientists collected swath bathymetry and side scan sonar data as well as dredge samples from the seafloor around Ritter Island (Silver et al. 2005, Silver et al. 2009). Thanks to these efforts the submarine extent and major facies changes of the 1888 collapse deposit are relatively well known. All data are available to this project through cooperation with Professor Eli Silver (University of California Santa Cruz, USA). In 2007 the Australian RV Southern Surveyor mapped the area surrounding Ritter Island as part of a larger research program in the Bismarck Strait. The raw data are available from the "CSIRO Marine and Atmospheric Research Laboratories Information Network".

Up to now no seismic investigations were carried out in the study area. The primary reason for this lack of seismic data is the scientific background of the groups that have been active in the area. The complexity of submarine landslides caused by volcanic flank collapses has only recently been recognized and requires 3D seismic data for correct interpretation of landslide processes. Seismic data is essential both for quantifying the amount of material that has moved and for deciphering the break-up processes during the early phase of flank collapse, i.e. to what extent did the material disintegrate before it started to slump? This parameter is crucial for calculating the tsunami potential.

Previous tsunami modelling: Available information regarding arrival times, wave heights and wave train characteristics from eyewitness reports and damage observations are unique for a tsunami triggered by a flank collapse as large as the 1888 Ritter Island one. Ward and Day (2003) used these information as boundary conditions for their modelling of the tsunami. The bathymetry and extent of the debris flow were constrained by data from Johnson (1987). Based on a comparison of historical paintings of the intact Ritter Island and its modern topography Ward and Day (2003) calculated a subaerial collapse volume of 4.6 km^3. The authors simulated the landslide as a single block. The slide velocity was unknown and adjusted with the boundary conditions to give a best fit, which was achieved with 40 m/s. This is comparatively slow given the steep flank gradients and a total height drop of 800 m. The model predicts wave heights of >26 m for the islands of Sakar and Umboi, as well as 20 m for New Britain, whereas eyewitnesses at the individual sites observed 12-15 m. These discrepancies are significant when compared to modern near-field tsunami simulation, where residuals between model and observation are in the order of centimeters (e.g. Yamazaki et al. 2012). It seems likely that one or several assumptions are wrong, and the potential for gaining new insights is high.

Ritter Island as a natural laboratory: Ritter Island is a unique and ideal natural laboratory to study the emplacement dynamics and tsunamigenic potential of a volcanic island landslide for several reasons. It is the biggest historically documented flank collapse, the subaerial collapse volume of which can be reliably reconstructed based on pre-collapse paintings of the island. The resulting tsunami was observed at numerous surrounding islands and thoroughly documented. These information serve as boundary conditions, with which the number of assumptions and thereby the ambiguity of the tsunami models can be greatly reduced. Moreover, eyewitnesses stated that the collapse was not preceded, accompanied or followed by eruptive activity, as opposed for example to the collapse of Krakatau volcano in 1883. Hence, the tsunami simulations do not need to consider an eruption. Due to their young age the submarine landslide deposits are not covered by new sediments so that the individual facies can be imaged by swath bathymetry and sampled with a gravity corer. The shallow water depth (<1500 m) facilitates sampling and allows acquisition of high resolution geophysical data.

6. Work details and first results / Beschreibung der Arbeiten im Detail einschließlich erster Ergebnisse

6.1 Seismic data

6.1.1 2D reflection seismic imaging

Method and experiment setup

The 2D seismic survey aims to map the spatial extent of the volcanic debris derived from the Ritter Island volcanic cone. During the expedition two GI-Guns (105 cubic inch Generator and 105 cubic inch Injector) were used as seismic source. The advantage of using two GI guns of the same volume placed closely together is to produce twice the amplitude. Seismic data were recorded with GeoEel digital streamer segments. Fig. 4 shows the seismic 2D lines acquired during the cruise SO252.

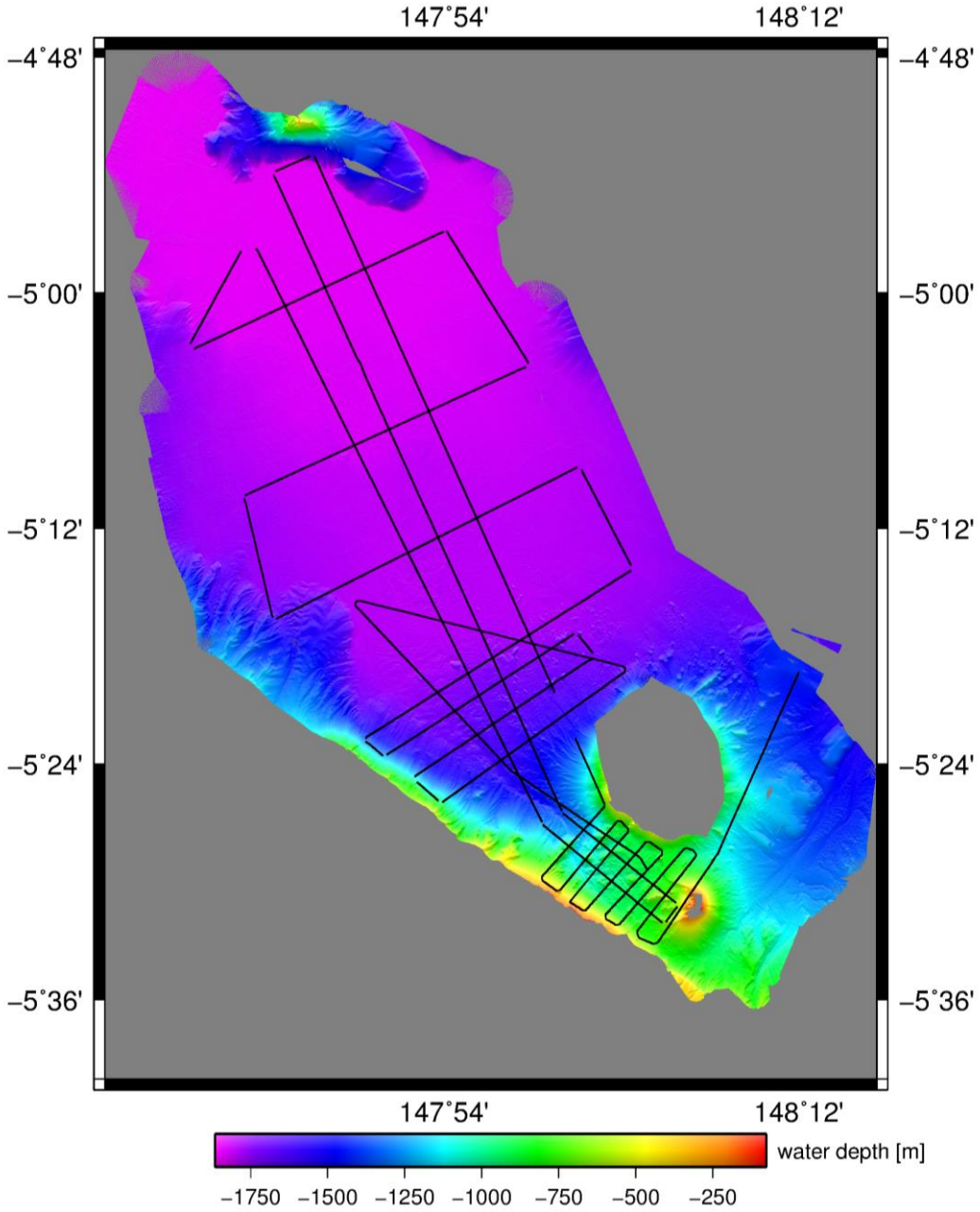

Figure 4: 2D seismic survey lines acquired during the cruise SO252.

Seismic source

During the seismic experiment two GI-Guns were used in harmonic mode as seismic source. Both guns were connected with a stringer hanging on two chains about 70 cm beneath the guns. Two elongated buoys stabilized the guns in a horizontal position at a water depth of ~2 m (Fig. 5). Each GI gun comprised of 105 in^3 generator and 105 in^3 injector chambers. A gun hydrophone provided both the time break and the shape of the near-field signal for permanent monitoring and quality control of the source signal. Due to display problems in the gun controller, the release of the injector pulse was triggered with a delay of 30 ms during the 2D seismic data acquisition with respect to the generator pulse. This delay value was adopted for an approximate source depth of 2 m and a gun pressure of 3000 psi (210 bar). We estimated a delay of -59 ms from the acquired seismic data. The shooting interval was adjusted to 5 seconds, resulting in a shot point distance of 11.25 m with a ship's speed of approximately 4.5 knots in water.

Figure 5: Two standard GI-Guns (105/105 in3) were operated in harmonic mode as seismic source during the cruise SO252. (Photographer: Melanie Ray)

Streamer system

We used different configurations in digital streamer length (Geometrics GeoEel streamer segments) for recording the seismic signal. Deck geometries, streamer configuration and seismic gun setting for the 2D survey are illustrated in Fig. 6. The surveys P1000 and P2000 both have a streamer length of 250.50 m. The seismic streamer consists of a tow cable, one 25 m long vibro-stretch section behind the tow cable and 20 active sections (each 12.5 m long) attached behind the stretch zone. The tow cable had a length of 60 m behind the vessel's stern. Each active section contained 8 hydrophones with a group spacing of 1.56 m. Each active streamer section had an analog-to-digital (AD) converter module. The AD digitizer is a small Linux computer. Communication between the AD digitizer modules and the recording system in the lab was transmitted via TCP/IP protocol. A

repeater was located between the deck cable and the tow cable (Lead-In). The streamer power supply unit managed the power supply and communication between the recording system and the AD digitizer modules. Three birds controlled and monitored the desired streamer depth of 2 m. One was attached to the stretch zone and on two others on the 8th and 13th streamer segments. A small buoy was attached to the tail swivel of the 2D streamer (Fig. 7).

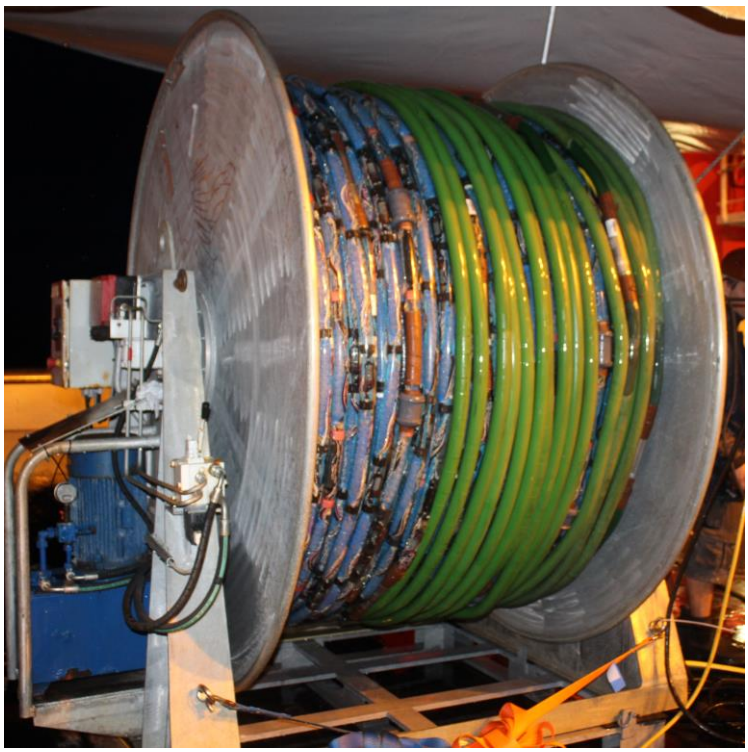

Figure 6: GeoEel streamer segments of 12.5 m length were connected to build up the 2D streamer system. (Photographer: Melanie Ray)

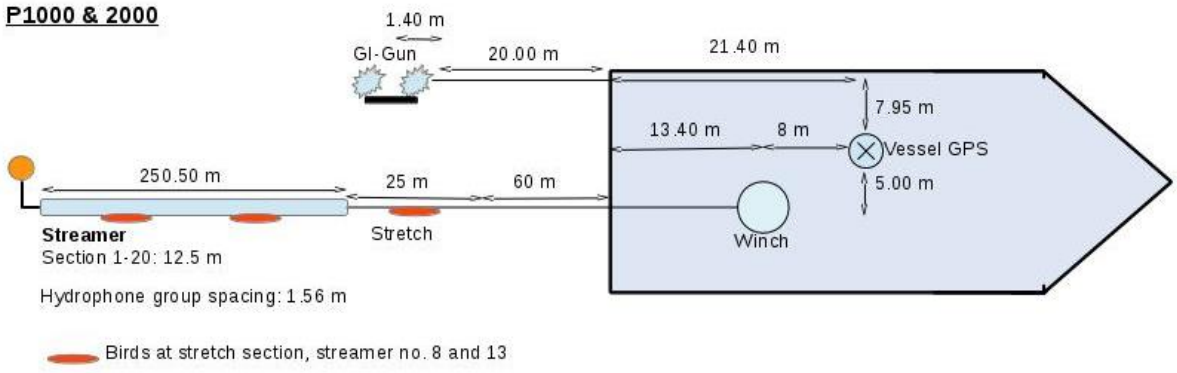

Figure 7: Deck geometries, streamer configuration and gun setting during Cruise SO252.

Bird Controller

Three Oyo Geospace Bird Remote Units (RUs) were deployed on the streamer. The schematic locations of the birds are shown in Fig. 7. The RUs have adjustable wings. A bird controller in the seismic lab controlled the RUs. Controller and RUs communicate via communication coils nested within the streamer. A twisted pair wire within the deck cable connects controller and coils. Designated streamer depth was 2 m in accordance

with good weather conditions and low swell noise. The RUs thus forced the streamer to the chosen depth by adjusting the wing angles accordingly. The birds were deployed at the beginning of a survey but no scanning of the birds was carried out during the survey because bird scans caused false triggers. However, the birds worked very reliably and kept the streamer at the designated depth. This was checked in the frequency spectra of the raw shots for relative position of notches.

Data acquisition systems

Data were recorded with acquisition software provided by Geometrics. The analogue signal was digitized with 2 kHz. The seismic data were recorded as multiplexed SEG-D. Recording length was 4 seconds. One file with all channels within the streamer configuration was generated per shot. The corresponding logged shot file reports shot number and time information contained in the RMC string. The acquisition PC allowed online quality control by displaying shot gathers, a noise window, and the frequency spectrum of each shot. The cycle time of the shots were displayed as well. The vessel's GPS was simultaneously logged in the RMC string along with logged time and position information.

Processing

On-board processing included streamer geometry configuration, delay calculations and source and receiver depth control. From the seismic data a delay of -59 ms was evaluated. A receiver ghost effect in the seismic data could not be detected (Fig. 8). The source-receiver locations were then binned with a common-midpoint bin spacing of 1.5625 m. Different filter tests were performed (Fig. 10) and the frequency spectra (Fig. 9) were analyzed. Seismic traces were balanced and filtered using a bandpass filter with corner frequencies at 10, 45, 250, 400 Hz. Subsequently, a normal move out correction (with a constant velocity of 1495 m/s derived from CTD measurements) and stacking were applied. The stack was migrated with a 2D Stolt algorithm (1500 m/s constant velocity model).

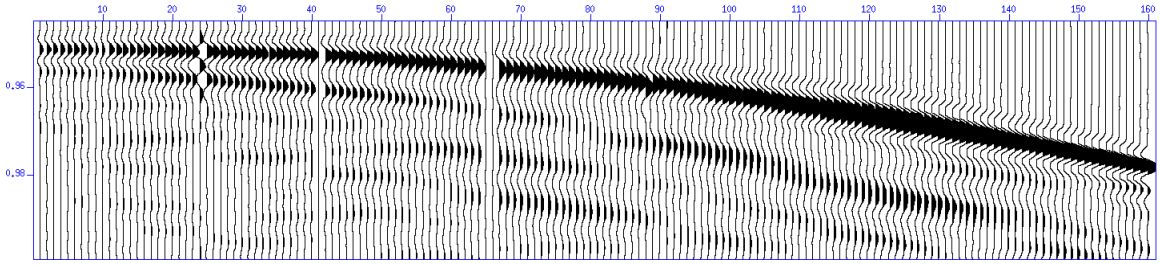

Figure 8: Plotting of the seafloor signal for one shot and 160 channels.

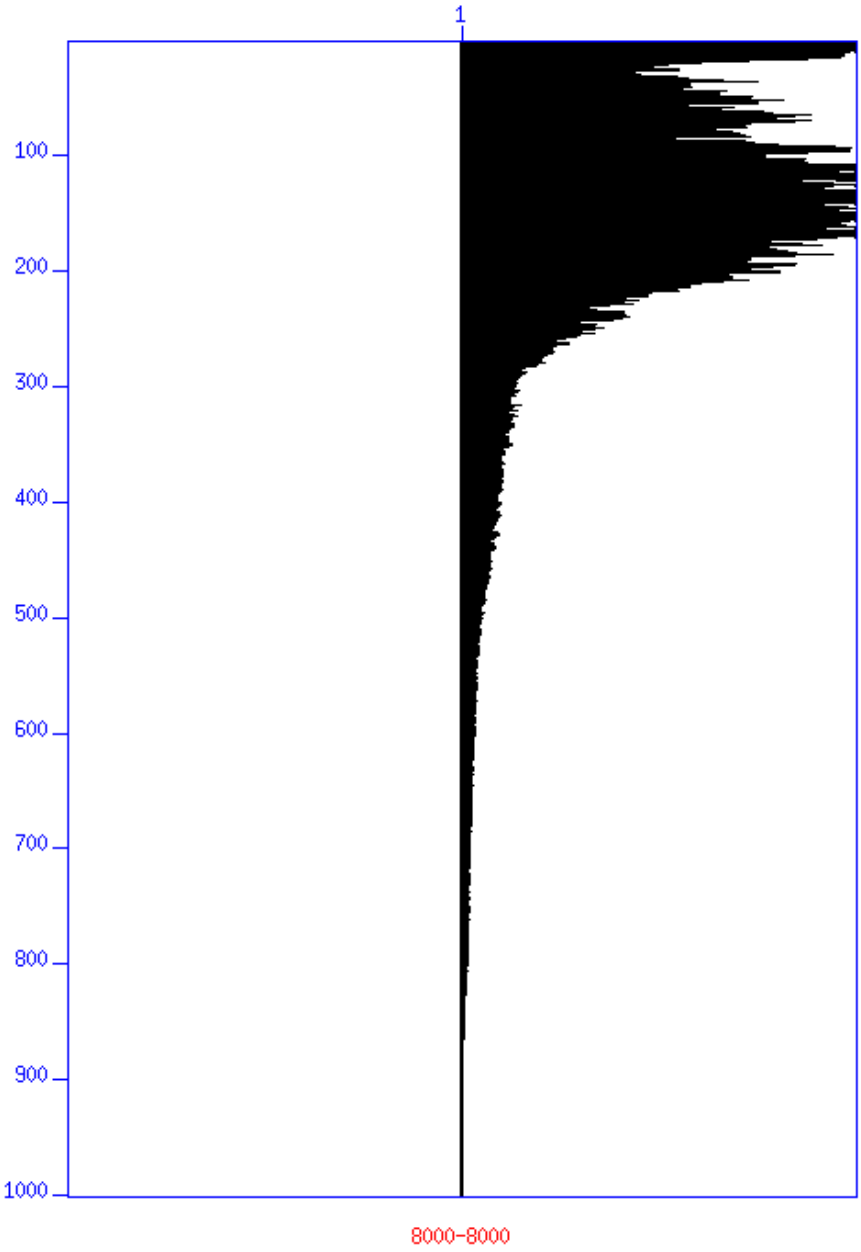

Figure 9: Frequency spectra.

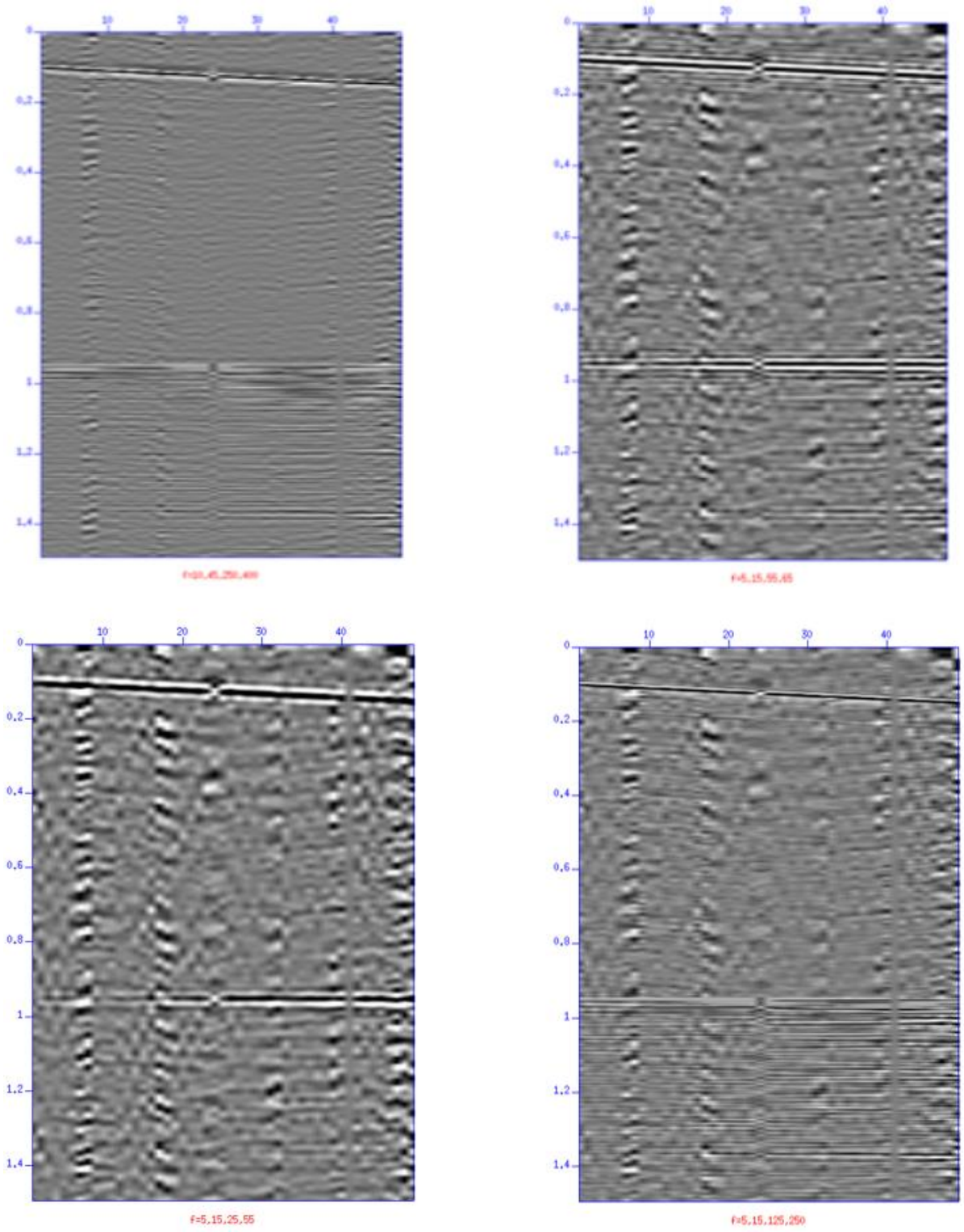

Figure 10: Bandpass frequency

Preliminary results

Preliminary analysis of 2D seismic lines show the overall shape of the debris flow deposit west of Ritter Island. It reaches from Ritter Island to the barrier between Umboi and Sakar islands and is up to 200 ms TWT thick.

Several conical features are observed northwest of the Ritter Island. Central near-vertical conduits inside the cones with low seismic amplitude may represent volcanic

feeder systems. The cones have a clear base, which is marked by downlap of internal reflections. Chaotic facies underlie the cones and in some regions they partially cover the base of the cones. This indicates several phases of the formation of the cones. We interpret the conical features as parasitic volcanic cones which are now inactive.

Several thick buried chaotic units are also observed in the deep basin farther away from Ritter Island. One of the buried chaotic units reveals presence of a frontal ramp, distal thinning and basal thrust faults. We infer this unit as a buried submarine slide. The extent of the buried slide can be traced in the deep part basin as an up to 35 ms-thick unit just below the seafloor.

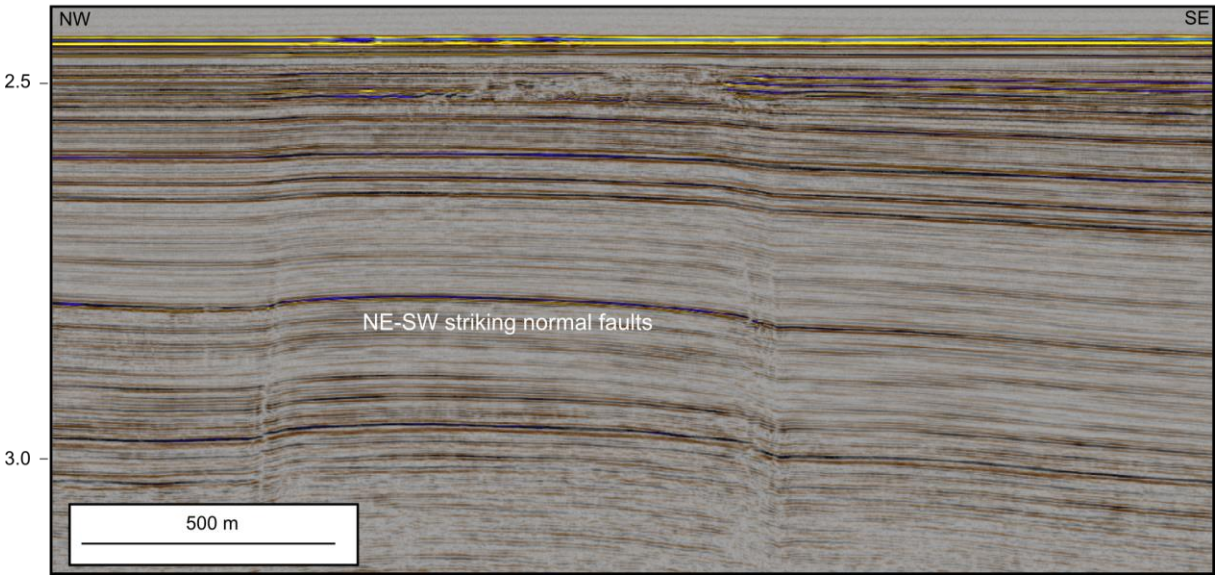

Figure 11: Example of 2D seismic data collected in the distal deposition area showing tectonic faults.

6.1.2 3D seismic acquisition and processing

High-resolution 3D seismic data was acquired with the P-Cable system at the region north west of Ritter Island, covering the main deposit of the Ritter Island flank collapse. To image the region of interest, a NW-SE-striking survey area of 13 km by 4.4 km (Fig. 12) was planned with sail lines spaced 70 m apart.

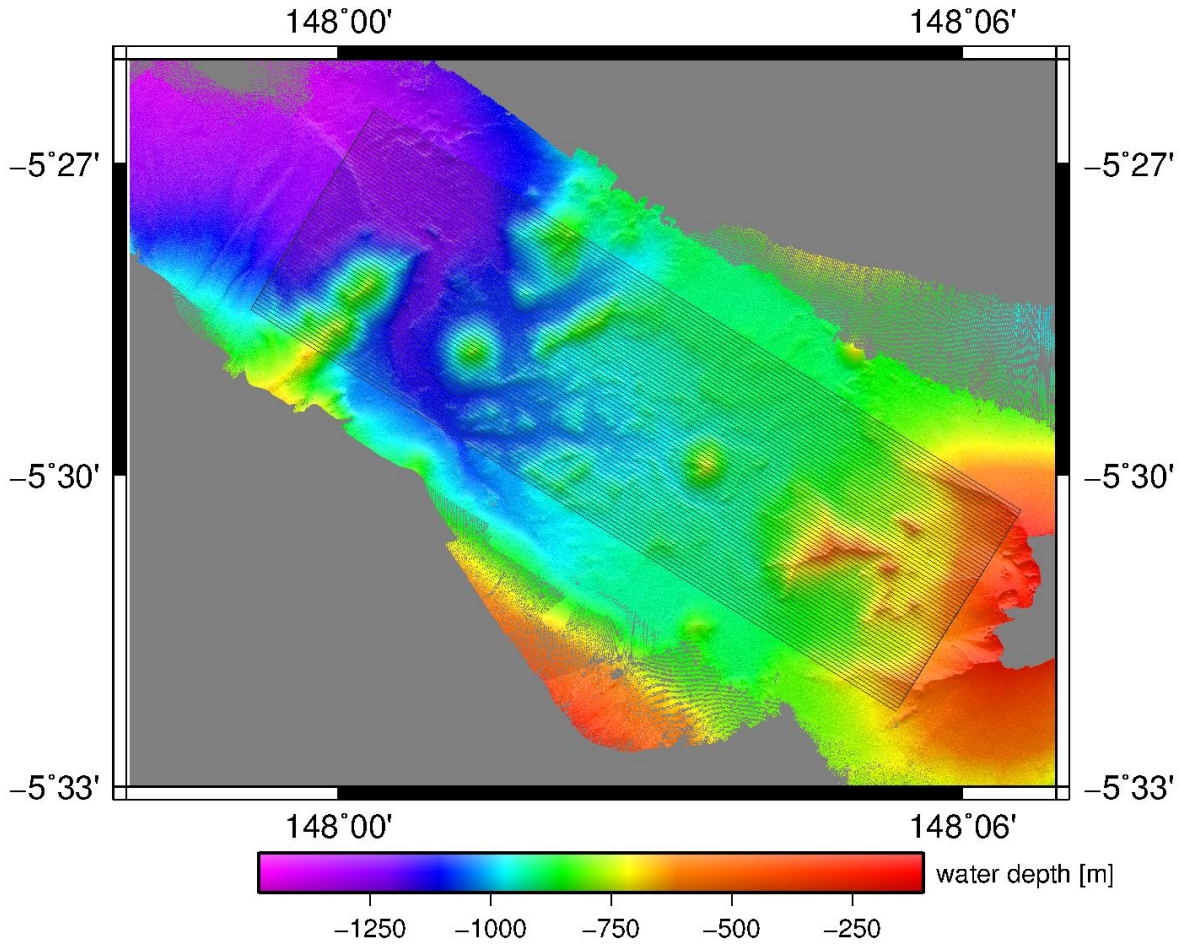

Figure 12: 3D survey cube coverage (grey box) with Ritter Island to the east.

Data Acquisition

We deployed a relatively long cross cable (170.2 m) with 16 streamers attached (Fig. 13). The outer three streamers on each side of the cross cable were spaced approx. 14 m apart and the inner ten were spaced approx. 9 m apart. Two spherical floats were attached to each junction box, except those at the outermost streamers (streamers 1 and 14). Additionally, single floats were tied to the cross cable between the following streamers: 4-5, 6-7, 8-9, 10-11, 12-13. These provided additional buoyancy in the centre of the cross cable where most sag was expected. The system consisted of oil filled streamers and solid state streamers at sections 1, 2, 8, 9, 15, and 16. The paravanes were towed with 100 m of trawl wire rolled off the winch in order to improve the spread of the system. GPS receivers were attached to each paravane and to a known position on the ship for reference. The GPS data show a spread of the system of approx. 150m.

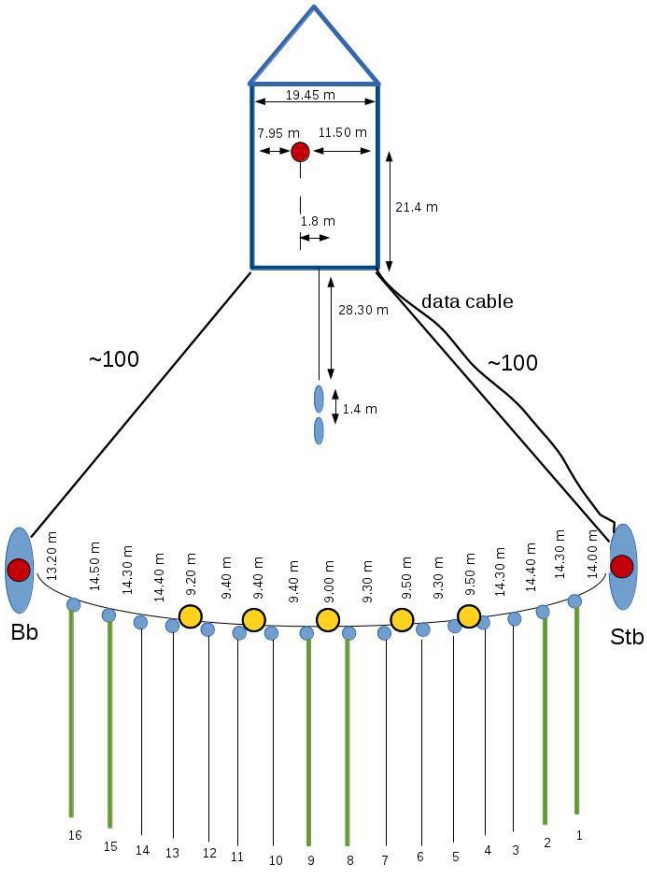

Figure 13: P-cable configuration.

As a seismic source the same GI-Gun configuration was used as during the 2D seismic experiment. The airgun was fired every 5 seconds and we recorded data for 4 seconds at a sampling rate of 0.5 ms. The average ship speed was 3.5 knots through the water; speed over ground varied due to currents, but not to a great extent.

Processing

On-board processing included predictive positioning of the streamers from the paravane locations under the assumption that the cross cable conforms to a catenary curve as it is towed through the water. Direct arrivals from the outermost streamers (streamers 1 and 16) were used to position the gun for every shot of the survey. Receiver locations were then adjusted from the predicted positions such that the direct arrivals at each streamer agreed with the source-receiver offsets. The source-receiver locations were then binned on a grid with 6.25 m by 6.25 m cells resolving in a good fold coverage (Fig. 14). Seismic traces were then balanced and filtered, before an NMO correction (with a constant velocity of 1495 m/s derived from CTD measurements) and the data were stacked. The stacked data were then migrated in two passes (first cross-line then in-line) with a 2D Stolt algorithm (1500 m/s constant velocity model).

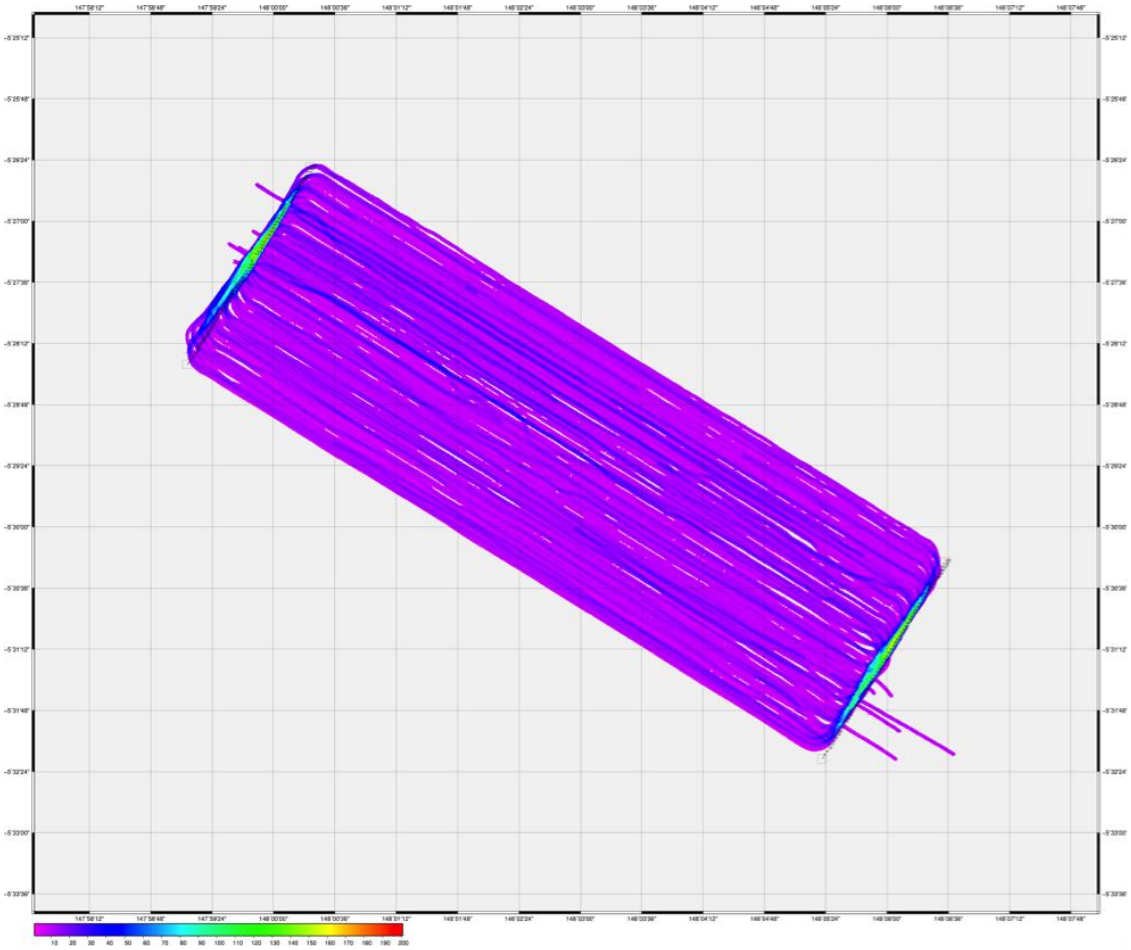

Figure 14: Fold map of the P-Cable survey showing even coverage except for the turns where the ship passed the same location at every sail line.

Preliminary Results

The P-Cable 3D seismic data image the main part of the proximal deposit of the Ritter Island flank collapse. It is this area that must have contributed most to the tsunami. The data show a wide variety of subsurface structures. The undisturbed flank of Ritter Island is well stratified and it can be assumed that the major part of the failed mass was composed similar to the subaerial outcrop of Ritter Island today. West of the main head scarp there is a large block of similar composition which may still be in situ. Further out into the channel between Umboi and Sakar islands is a hummocky terrain with chaotic seismic character which we interpret as the main slide deposit. It is onlapping onto several large cones of transparent seismic charater (Fig. 15). We interpret these cones to be parasitic volcanic cones that predate the Ritter Island flank collapse, although it cannot be ruled out that some may have been active since.

Erosional truncations in the 3D data demonstrate the erosive nature of the channel system that incises into the chaotic seismic facies in the hummocky area in the western part of the cube. A mostly continuous reflector marks the base of the Ritter Island deposit. It is underlain by another unit that onlaps onto the volcanic edifices of Sakar and Umboi islands.

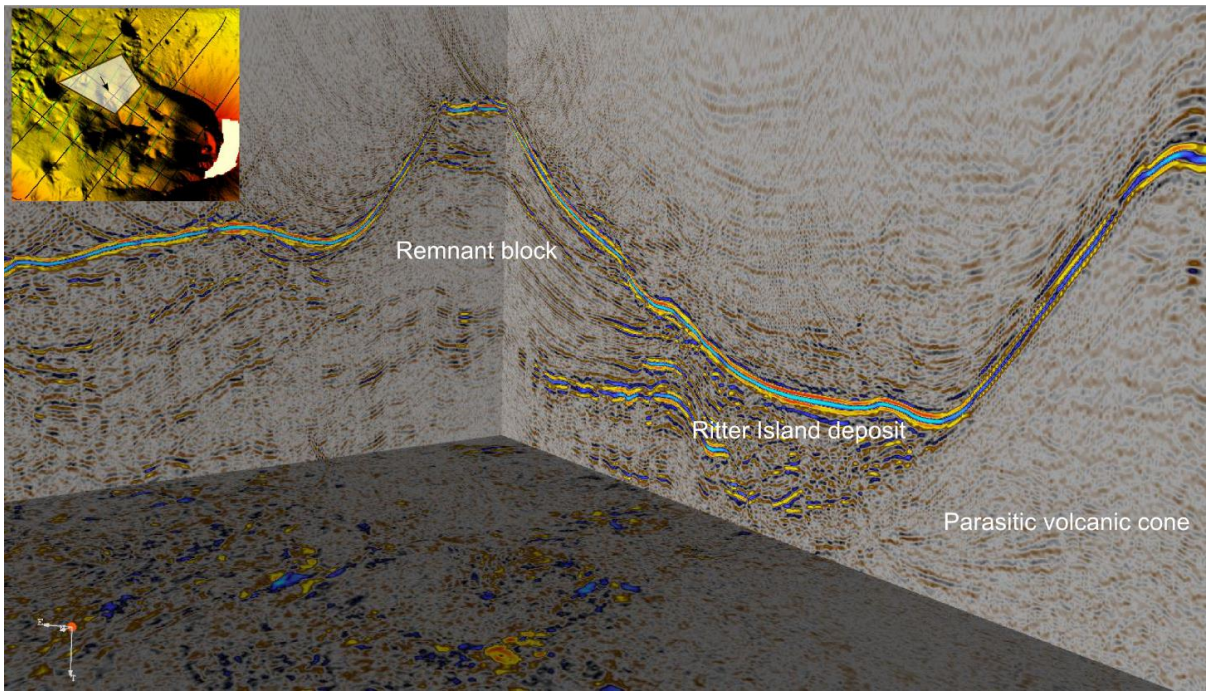

Figure 15: 3D view of the migrated P-Cable data showing the difference in seismic character between the remnant block in the middle of the landslide scarp and one of the parasitic cone structures. The inset shows the location with the arrow pointing in the viewing direction.

6.2 Ocean bottom seismology

The OBS consists of four floats connected to a frame, which carries a three-component seismometer, a hydrophone and a data recorder cased in a high-pressure tube (Fig. 16). The sensors are connected to the recording unit, which continuously records the signals of the sensors. The systems itself floats at the sea surface, so in order to deploy it at the ocean bottom a weight is mounted to the frame with a releaser. The releaser has an acoustic communication unit, which can be addressed from the ship in order to disconnect the weight after the experiment. The OBS will then ascend to the surface and can be recovered. A flashlight, a radio transmitter and a flag are attached to the frame in order to facilitate sighting the OBS. While the OBS continuously records seismic signals an additional data logger on board records the shot times.

Figure 16: OBS deployment (Photograph: Theresa Roth)

The data recorders have to be programmed before the deployment of the system. The sample rate of the OBS recorders was set to 500 Hz, while the time logger recorded at a sample rate of 1000 Hz. The gain of the input channels was set to 15 for the three geophone components and 7 for the hydrophone. The recorder was equipped with one 2 GB and three 1 GB flash cards. The exact recording parameter for the deployments can be found in Appendix C (OBS protocols). The recording units were synchronized with a GPS signal before as well as after the recording period in order to correct the drift of the logger's internal clock.

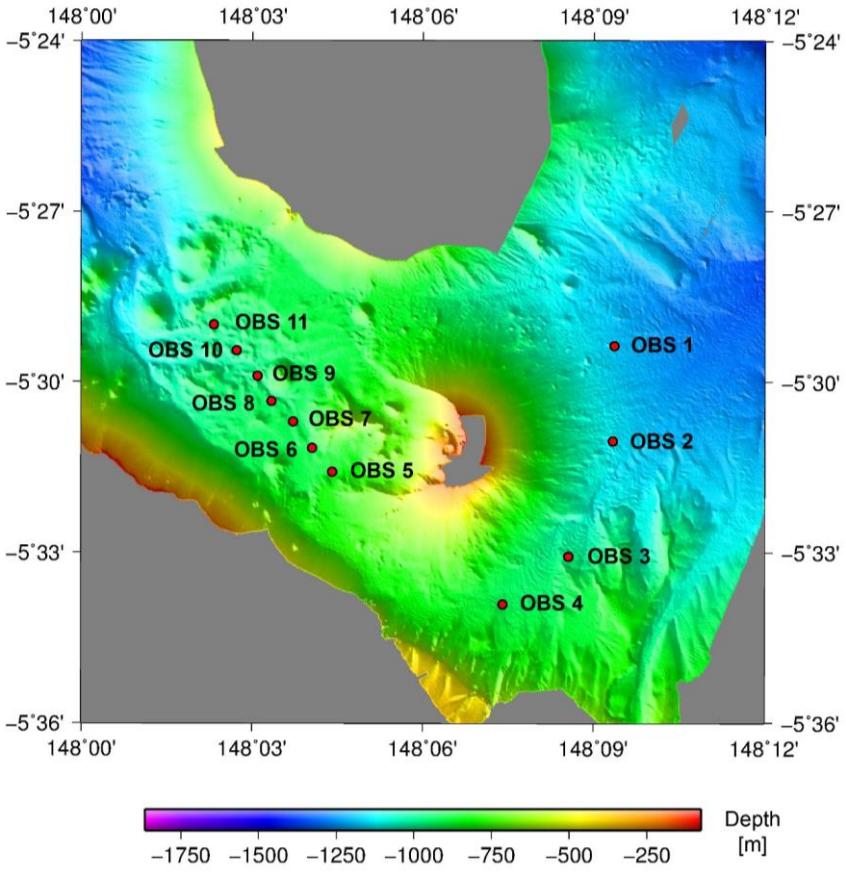

Figure 17: Detailed map of the OBS positions.

In total eleven OBS were deployed around Ritter Island on November the 16th 2016 (Fig. 17). The OBS experiment focused on the 3D reflection seismic cube and included seven OBS. The seven OBS extended on a central profile through the cube on the western flank on top of the collapse material (Fig. 17). The OBS experiment was designed to complement the 3D reflection seismic experiment and to create a velocity model for the processing of the 3D reflection seismic data. Four additional OBS were placed around the eastern flank of Ritter Island (Fig. 17) to get information about the magma chamber below and to notice potential activities of the surrounding volcanoes.

OBS 11, which was deployed at the northwestern end of our central profile, is one of the new KUM designed OBS called Nammu (Fig. 18). This is an OBS, which is very easy to handle and has a more compact design than our standard ones. This is the first time our working group deployed one of these new OBS and everything worked out fine. The whole processing of the data from Nammu will be carried out after the cruise.

Figure 18: Deployment of the new OBS Nammu from KUM (Photograph: Theresa Roth).

Ten of the eleven OBS were recovered on November the 26th and all instruments have recorded data. No instrument showed an error message during synchronization. The OBS recorded between 2,0 and 2,7 GB and no flash card showed any problems. All data have been copied and converted to SEG-Y / PASSCAL files on board. A first quick quality control showed promising data, but a detailed processing will be carried out after the cruise in Kiel (Fig. 19).

OBS 2 did reply to our acoustic release, but did not come up. The ranging showed, that the distance did not change and was slightly less the same than the water depth. The time release was programmed for the next morning, November 27th, but the distance was still the same. Therefore, we located the OBS by ranging it from four different directions around the deployment point. It was possible to determine its location to within +/- 50 m. Then HyBis was deployed and ran a search pattern around the determined location. The OBS was found and its swim line had wrapped around the anchor weight. We recovered it by using the HyBis grab and retrieved the recorded data.

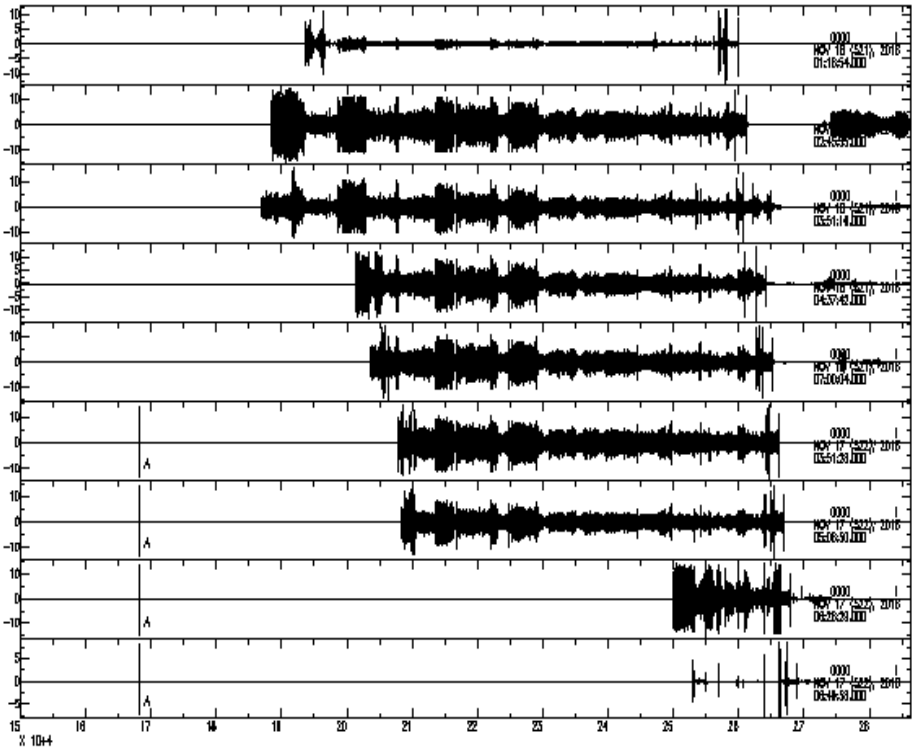

Figure 19: Examples of vertical waveforms from the active source during the GI gun shooting.

6.3 Multi-beam bathymetry

6.3.1 Equipment

RV Sonne is equipped with two Kongsberg Maritime multibeam echosounders: The EM122 system operates at 12 kHz and covers water depths from 20 metres below the transducers up to full ocean depth, while the EM710 system uses 70-100 kHz signals for water depths ranging from 3 m below transducers to roughly 1800 m (2000 m is the maximum range of the system). Two different transmit pulses can be selected: a CW (Continuous Wave) or FM (Frequency Modulated) chirp. In case of the EM710, the latter is part of the full performance version that is installed on RV Sonne. The sounding mode can be either equidistant or equiangle, depending on operation preferences and requirements. Both systems can be operated in single-ping or dual-ping mode, where one beam is slightly tilted forward and the second ping slightly tilted towards the aft of the vessel. The whole beam can also be inclined towards the front of the back and the pitch of the vessel can be compensated dynamically. The EM122 system produces 432 beams covering a swath angle of up to 150° while the EM710 system produces 400 beams for a maximum swath angle of 140°. The swath angle, however, can be reduced, if required.

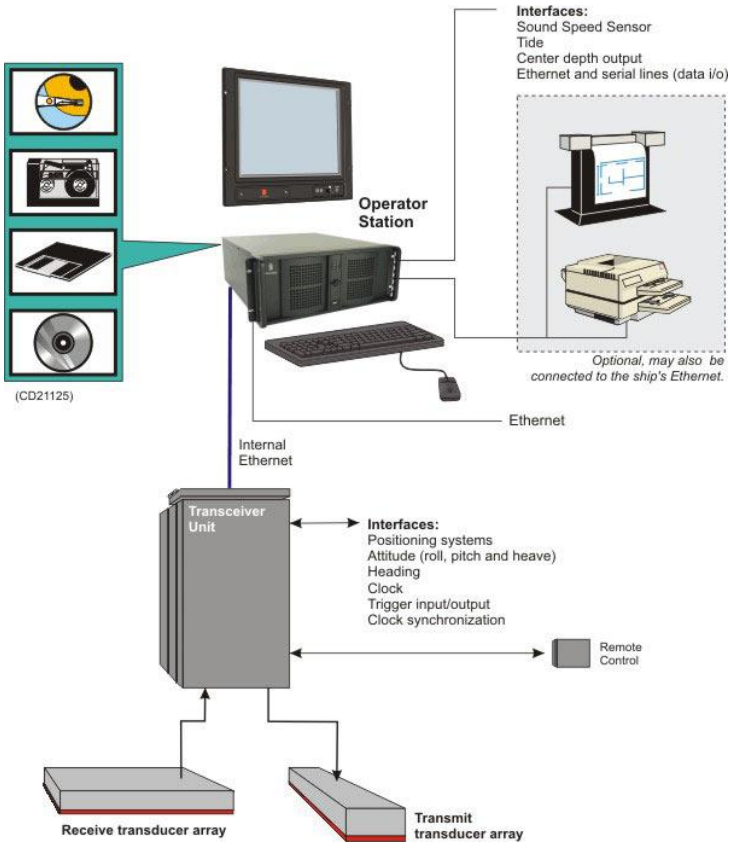

Figure 20: Configuration drawing of the EM122 system units and interfaces.

The transducers of both multibeam echosounder systems of RV Sonne are mounted in a so-called Mills cross array, where the transmit array is mounted along the length of the ship and the receive array is mounted across the ship. The transmit array of the EM122 is about 16m long and can produce a beam with a maximum width of 150° across the ship and 0.5° along the ship. The receive array is about 8m long and can be focused to a beam width of 30° along the ship and 1° across the ship. As a result the beams for producing the soundings

have a size of 0.5° along and 1° across the ship. RV Sonne is the first vessel being equipped with a EM122 system having such a transducer array. Systems on most other vessels are of a 1° x 1° design. The EM710 system installed on RV Sonne is also of a 0.5° x 1° design but transducers are much smaller (2 m across and 1 m along the ship).

The echo signals detected from the seafloor go through a transceiver unit (Kongsberg Seapath) into the data acquisition computer or operator station (Fig. 20). In turn, the software that handles the whole data acquisition procedure is called Seafloor Information System (SIS). In order to correctly determine the point on the seafloor, where the acoustic echo is coming from, information abouth the ship's position, movement and heading, as well as the sound velocity profile in the water column are required. Positioning is implemented onboard RV Sonne with conventional GPS/GLONASS plus differential GPS (DGPS) by using either DGPS satellites or DGPS land stations resulting in quasi-permanent DGPS positioning of the vessel. These signals also go through the transceiver unit (Seapath) to the operator station. However, during this cruise we were located outside DGPS satellite coverage and most of the DGPS land stations were too far away from the ship (2,000km or more). Ship's motion and heading are compensated within the Seapath and SIS by using a Kongsberg MRU 5+ motion sensor. Beamforming also requires sound speed data at the transducer head, which is available from a Valeport MODUS SVS sound velocity probe. This signals goes directly into the SIS operator station. Finally, a sound velocity profile for the entire water column can be obtained from either a sound velocity probe or from a CTD (conductivity, temperature and density) probe. The temperature (T), salinity (S) and pressure (p) data acquired by any CTD (conventional or mounted on the AUV) can be converted into sound speed by using a sound speed function C(S,T,p). During cruise SO252 the function by Delgrosso (1974) has been used.

In addition to bathymteric information both the EM122 and the EM710 system register the amplitude of each beam reflection as well as a sidescan signal for each beam (so-called snippets). Both systems also allow recording the entire water column. The amplitude signals correspond to the intensity of the echo received at each beam. It is registered as the logarithm of the ratio between the intensity of the received signal and the intensity of the output signal, which results in negative decibel values. For each ping EM122 records 432 backscatter intensity values while the EM710 records 400 backscatter values. The water column data correspond to the intensity of the echoes recorded from the instant the output signal is produced. All echoes coming from the water column, the seabed and even below the seabed are recorded for each beam. When the water column data of one ping is divided into a starboard and a port subsets, one can produce two traces, one for each subset. Each trace is build up as a time series in which for each time the highest amplitude is selected from all beams. Then the starboard and the port traces are joint together. In the case of EM122 the side scan sonar data acquired in each ping consists of 1024 pixels.

6.3.2 Acquisition parameters

During cruise SO252 the following settings of the Simrad EM122 system were used. The pulse was FM, ping mode was set to equidistant, dual ping mode was set to dynamic, and depth mode was set to automatic. The beam angle was reduced to 120° during most of the survey, except for survey lines close to the volcanic island, where the maximum coverage was desired. Survey speed varied between 5 and 8 knots. Data were acquired continuously, except for OBS deployment and recovery, coring and video transects and during the acquisition of P-cable 3 D seismic data, during which the EM710 system was used.

Acquisition parameters for the EM710 system were the same as those for the EM122. During transit EM122 data were collected despite higher ship's speed of up to 13 knots. Water column data were recorded throughout the survey. Two CTD casts (Fig. 21) were used for water sound velocity profiles: one at the Challenger Deep in the Marianas Trench, and a second CTD in the distal area of the Ritter Island deposits. A total of almost 4000 km² of the Bismark Sea between the Islands of Umboi, Sakar and New Britain was mapped in great detail (Fig. 22) during the cruise.

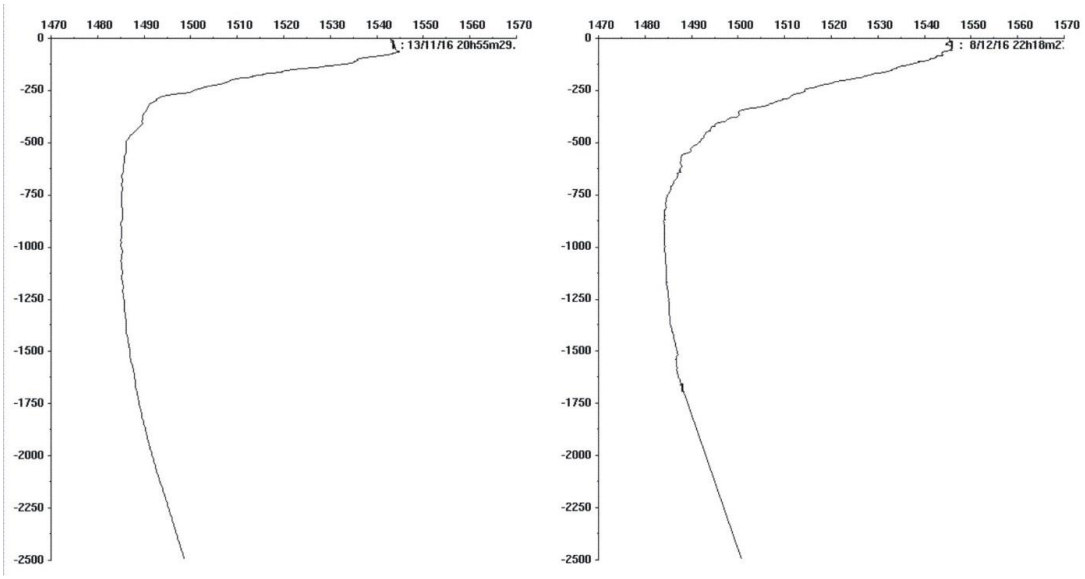

Figure 21: Sound velocity profiles of CTD1 in the Marianas Trench and CTD2 in the Bismark Sea.

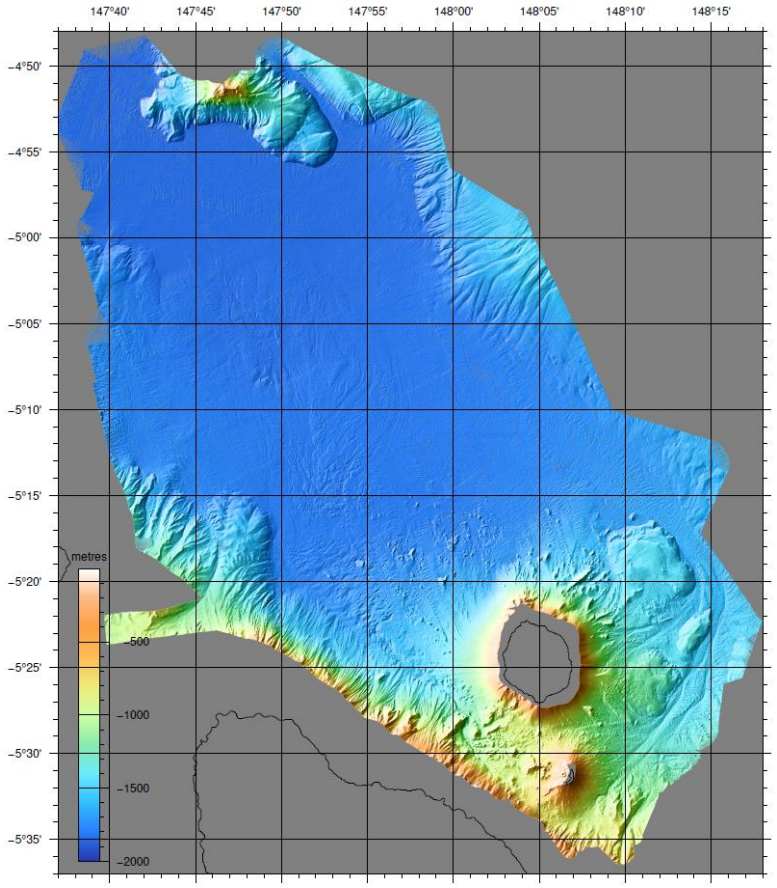

Figure 22: Shaded relief map of the part of the Bismark Sea showing the extent of area mapped during SO252.

Both the Simrad EM122 and EM710 systems were running stable throughout the cruise. Problems with the specular reflection at nadir (a common problem on many previous cruises) were encountered during this cruise, which already points to rather „hard“ deposits in the survey area. Data obtained with the EM122 system show typical spread and increased standard deviation of the soundings with increasing distance from the nadir. Unfortunately, this effect appears twice and affects both the depth soundings based on phase and depth soundings based on amplitude (Fig. 23). This effect is particularly visible in the flat lying areas. EM710 data do not show this effect, although we did not really map flat-lying areas with the EM710 system.

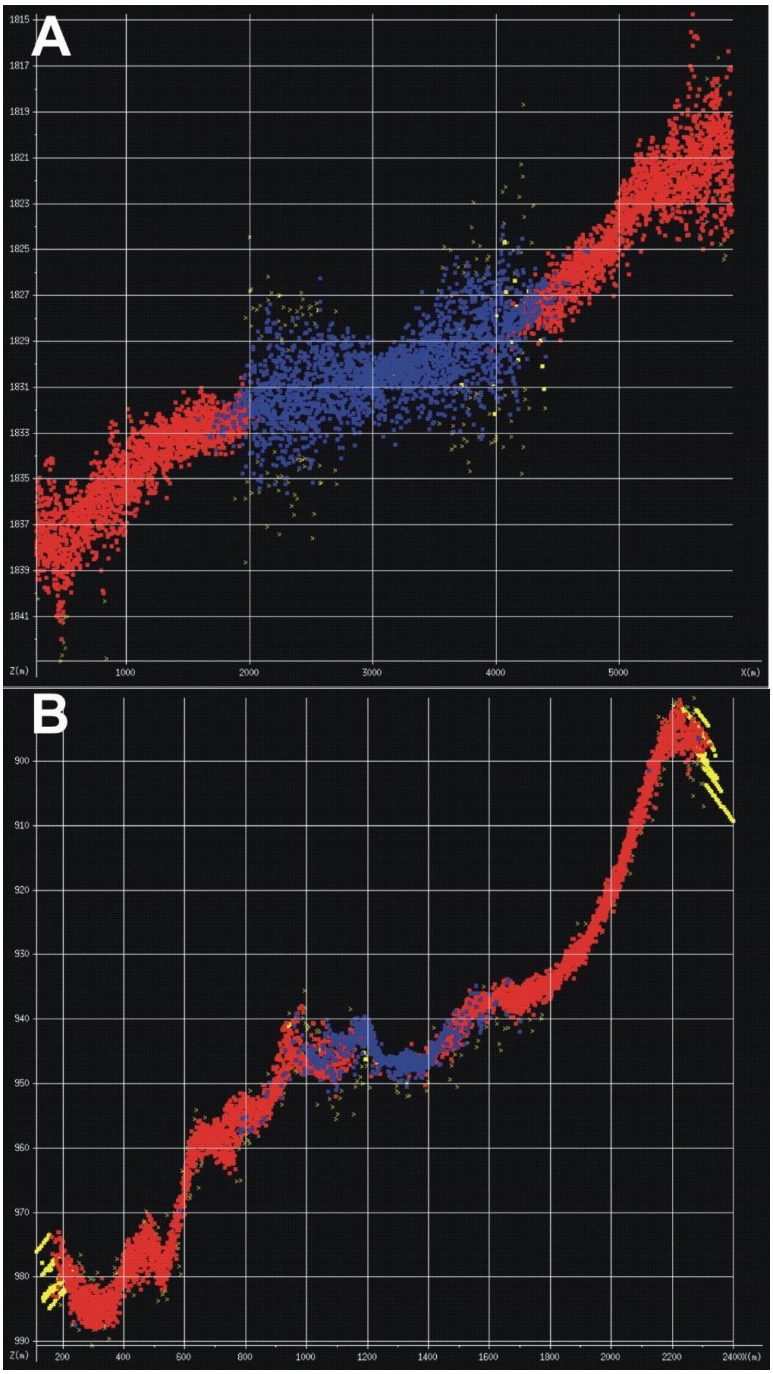

Figure 23: Screenshot of Caraibes editing tool showing increased vertical spreading of the soundings away from the nadir. Blue: soundings determined on phase, Red: soundings determined on amplitude and Yellow: soundings flagged as unvalid. Note the difference in scatter between the EM122 (A) and EM710 (B) systems.

6.6.3 Data processing

Data processing has been carried out onboard using different software packages (CARIS HIPS and SIPS, MB Systems, Fledermaus and mainly Caraibes). Within Caraibes version 3.9 a triangulation filter with 3 iterations was applied to the EM122 data in order to eliminate outliers, and the sounding data were then cleaned manually for further elimination of erroneous soundings. The same filter was not always applicable for the EM710 data that had a very high soundings density. For those data, an initial near-neighbor grid with 10 m grid mesh size and 3 grid cell interpolation was calculated and the soundings filtered against this grid with all sounding in excess of 5 metres from the grid cell average depth being eliminated. The data were subsequently gridded with Caraibes using a near-neighbour algorithm that takes into account two neighbouring cells, eliminates cells with less than two soundings per cell, and interpolates for 3 rows/columns. The soundings were also exported as xyz-data and gridded with GMT using a similar algorithm but no interpolation. The entire survey area was gridded with a 25 metres grid cell size while the area of the P-cable 3D seismic survey (the EM710 data) were gridded with a 5 metres grid celle size. Gradient maps were also calculated based on the bathymetric grids.

6.3.4 Backscatter

The backscatter (amplitude) signal is stored and preprocessed automatically by the Kongsberg software Seafloor Information System (SIS), including altitude processing, time varying gain (TVG) and angle varying gain (AVG). Backscatter data were processed onboard using Caraibes and FMGeocoder. Within Caraibes the backscatter values are compensated for seafloor gradients and unvalid soundings but not for varying beam intensity across the swath, which requires knowledge of the beam emission pattern. The backscatter have been simultaneously processed using FMGeocoder, where radiometric corrections, filtering, anagle-varying gain and anti-aliasing filters are applied to the backscatter data before outputting a georeferenced mosaic.

6.3.5 Water coulmn

Both the EM122 and the EM710 multibeam echosounder produce a second type of raw data files with extension *.wcd, which stores water column data. These files were imported into CARIS Hips&Sips version 9.0.14. The raw multibeam echosounder data (.all format) and associated water column data (.wcd) were placed into a single folder and imported into CARIS HIPS (note: license for Fledermaus mid-water tool was not available). Each line was subsequently opened in Swath Editor and displayed as a curtain image (along track, viewed from starboard side) and a time-series video (across track, viewed from stern). The data were also filtered by intensity. No evidence of backscatter anomalies, which could be indicative of fluid seepage from the seafloor, was observed in the water column data.

6.3.6 Preliminary interpretation

6.3.6.1 Challenger Deep

Although multibeam bathymetry data have been recorded and edited during the entire transit in international waters only those data collected in the vicinity of the Challenger Deep in the Mariana Trench have been looked at in detail (Fig. 24). Here seafloor depths of up to 10,925 metres have been determined based on a 100 x 100 metres grid, which is considerably less than water depths published in a recent paper (Gardner et al., 2014) but in line with older, japanese findings (Nakashimi and Hashimoto, 2011). The Marianas Trench is

rather narrow (less than 100 km wide between the 5000 m contour line on either side of the trench) and bounded by steep flanks. The incoming, oceanic plate also shows a set of bend faults with remarkably high faults scarps of up to 500 meters (Fig. 25).

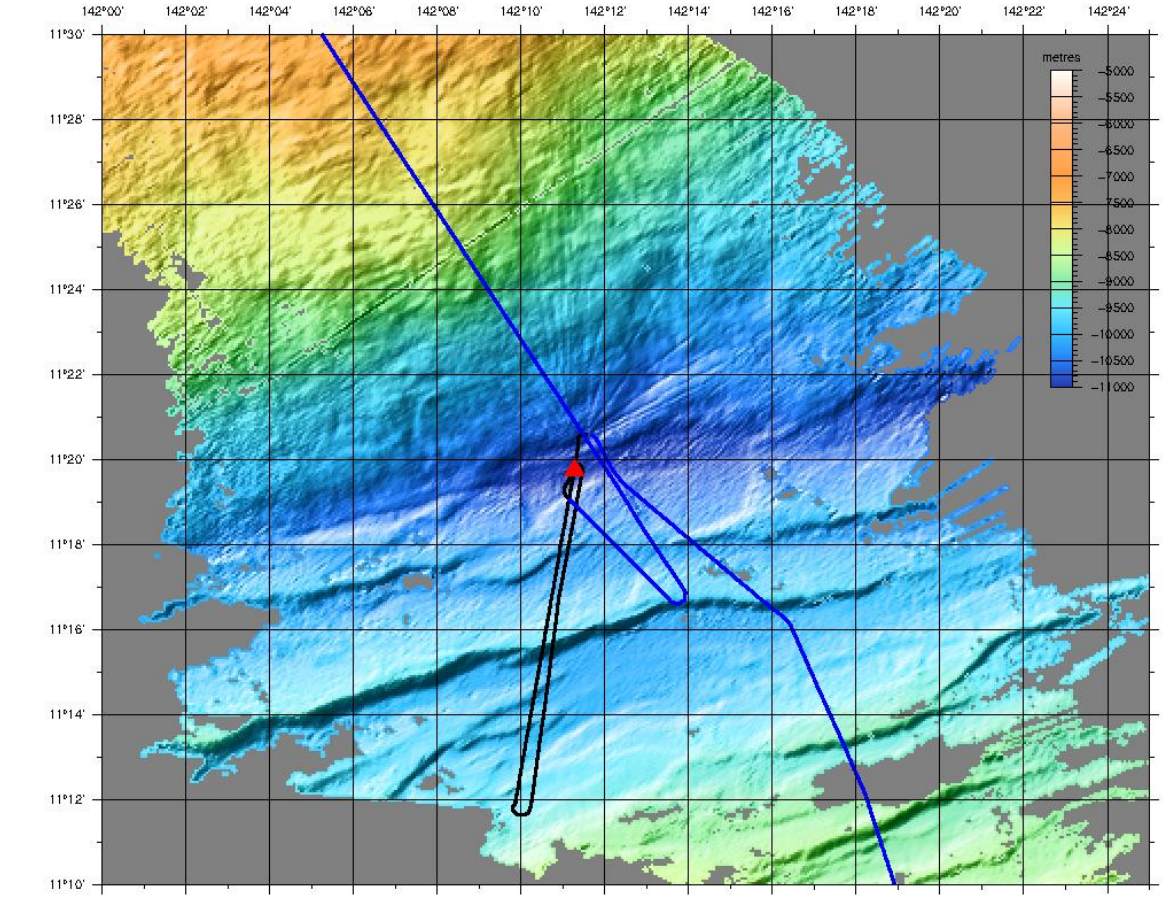

Figure 24: Shaded relief bathymetry of the Marianas Trench. Red star: CTD location. Blue line: High-speed survey ship's track. Black: Low-speed bathymetry survey during mooring lay-out.

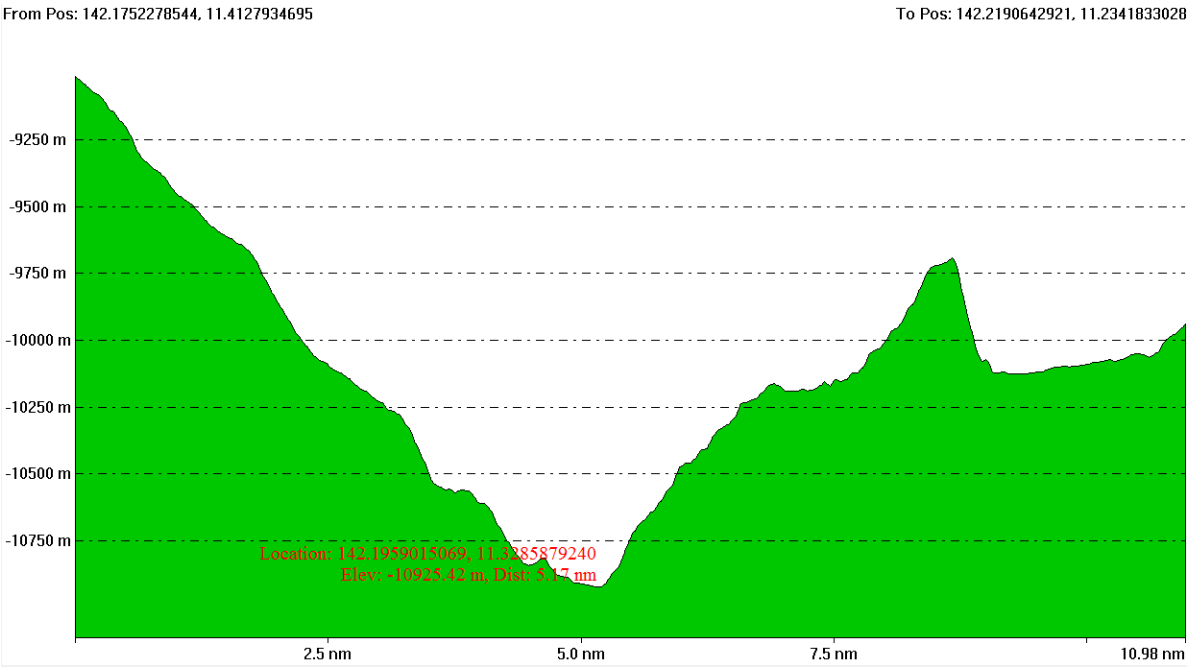

Figure 25: Cross-section of the Marianas Trench at Challenger Deep.

6.3.6.2 Southern Bismark Sea

The working area in the southern Bismark Sea shows an up to 1850 meters deep basin that is bounded in the Southeast by the island of New Britain, in the Southwest by the island of Umboi, in the North by an unnamed seamount and in the Northeast by various seafloor elevations (Fig. 22). In the southwestern corner of this basin two additional volcanic islands are present: Sakar Island and Ritter Island. The flanks of all the volcanic islands (or at least the undisturbed flank, as in case of Ritter Island) show intense gullying that is generally strictly perpendicular to the slope (Fig. 26), except for the northwestern flank of Sakar Island. There, the gullies are diverted northwards at the lower reaches of the island flank.

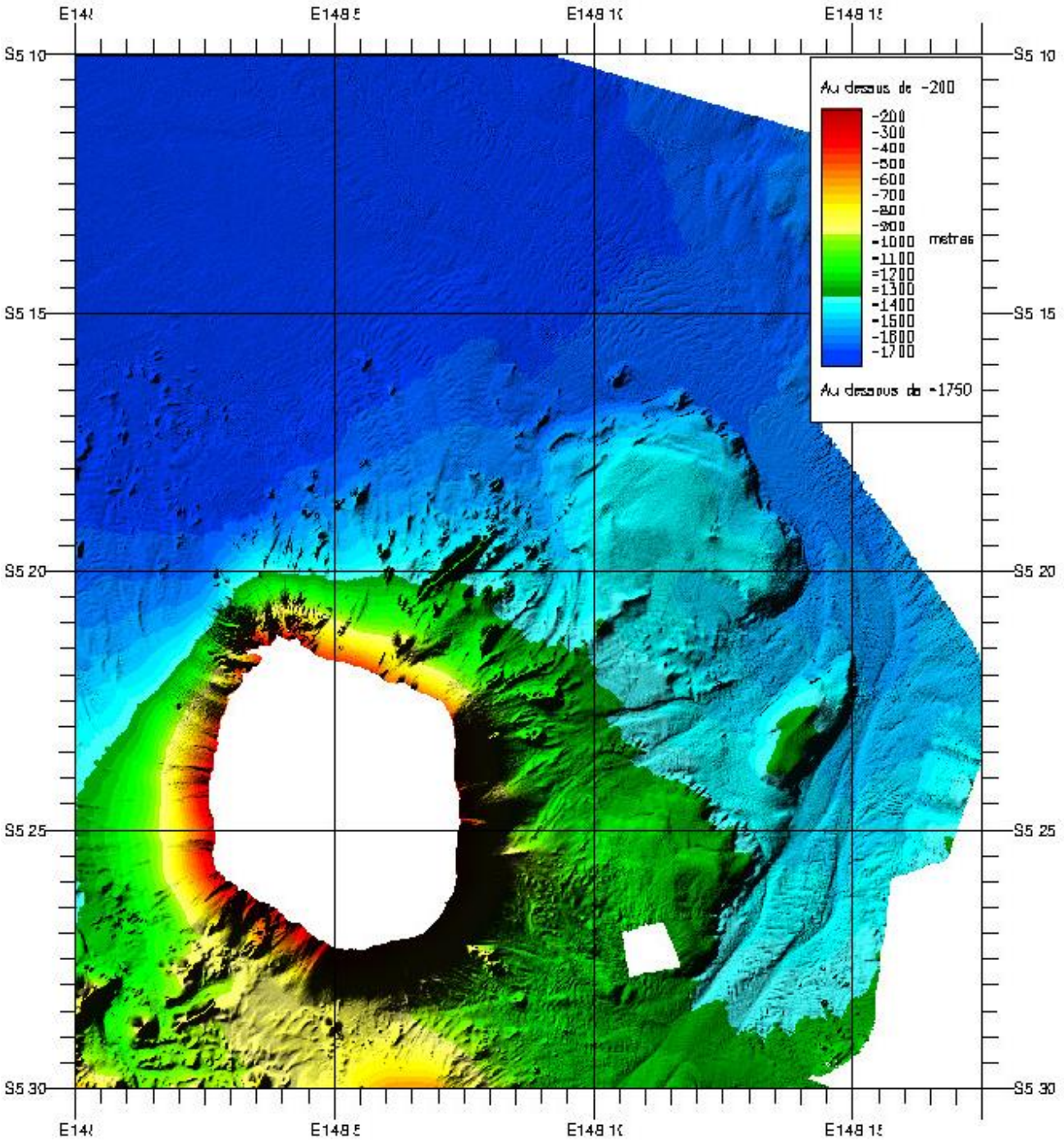

Figure 26: Shaded-relief map of the seafloor between the islands of Sakar, New Britain and Ritter showing intense gullying of the submarine island flanks.

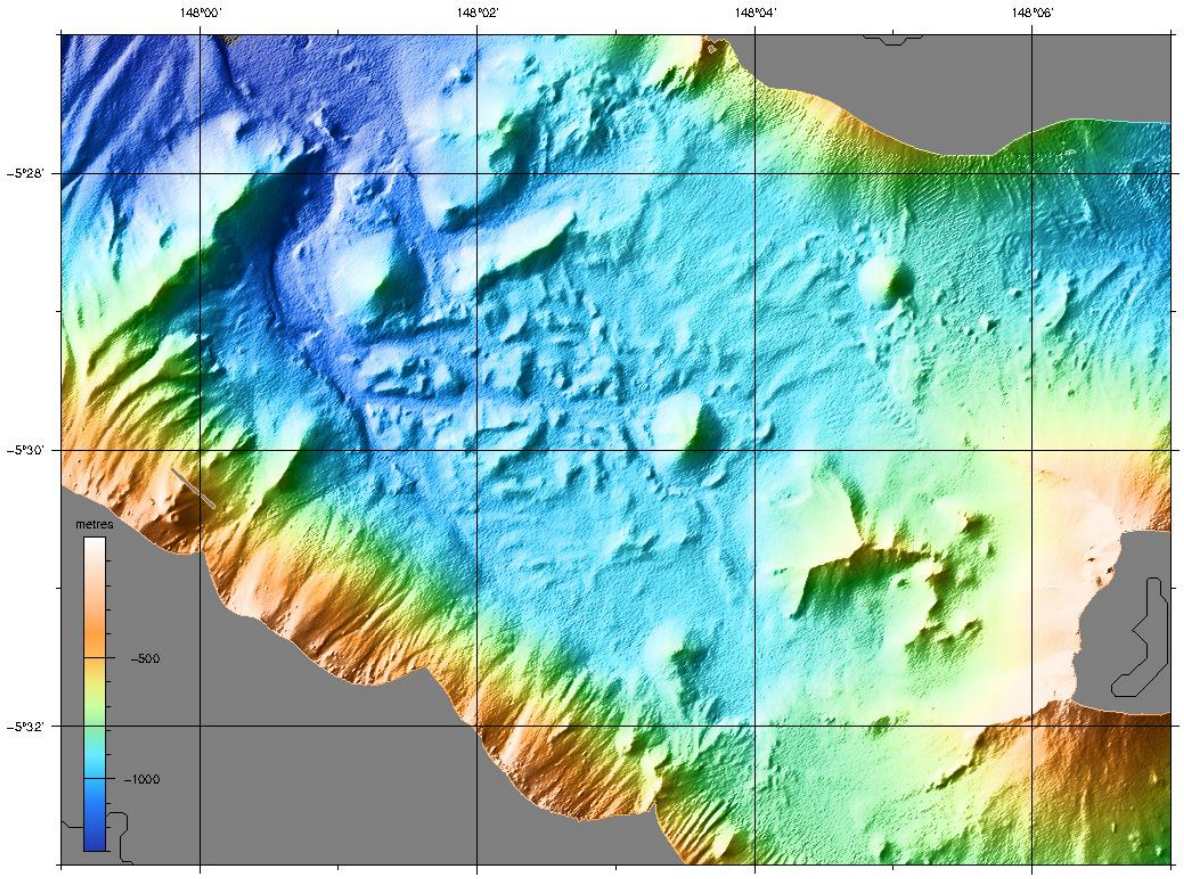

Figure 27: Shaded relief map of the seafloor between the islands of Ritter, Sakar and Umboi.

The main target area of cruise SO252 is located between the islands of Ritter, Sakar and Umboi (Fig. 27). This area has been mapped in great detail due to multiple overlaps of adjacent tracks of EM710 bathymetry. A number of observations can be made. Strikingly regular cone-shaped features of up to 250 meters relief height and steep flanks (Fig. 28) are present in this area that has been directly affected by the failure of Ritter Island in 1888. The bathymetry shows that deposits are abutting against these cones from the Southeast. The cones are characterized by low backscatter intensity on EM122 snippets data (Fig. 29). These deposits are also strongly remodeled by currents that have carved a small irregular channel and left a hummocky-like terrain. Whether these currents were part of the later stages of the Ritter Island event or subsequent flows needs further investigations. The submarine remains of Ritter Island also show some surprising features. A large, 4-crested ridge at the western edge of the Ritter failure scar appears to be a remnant of the original volcanic edifice, suggesting a two-stage failure of the island: towards the northwest and towards the southwest. The inner portion of the failure scar also shows the presence of a smooth cone with a crater on top of it. The cone has two sharp cliffs on its western ride and an irregular, small crest to the North. The cone is located where most probably the center of the original Ritter Island has been situated, and it is more likely a remnant than a new growth. The western end of the proximal reaches are characterized by the presence of a large ridge extending from Umboi and that diverted flows within the small channel to the North. The ridge has not been overspilled by currents and deposits from the Ritter Island event, as erosional gullies on the flank of Umboi north of the ridge is totally unaffected.

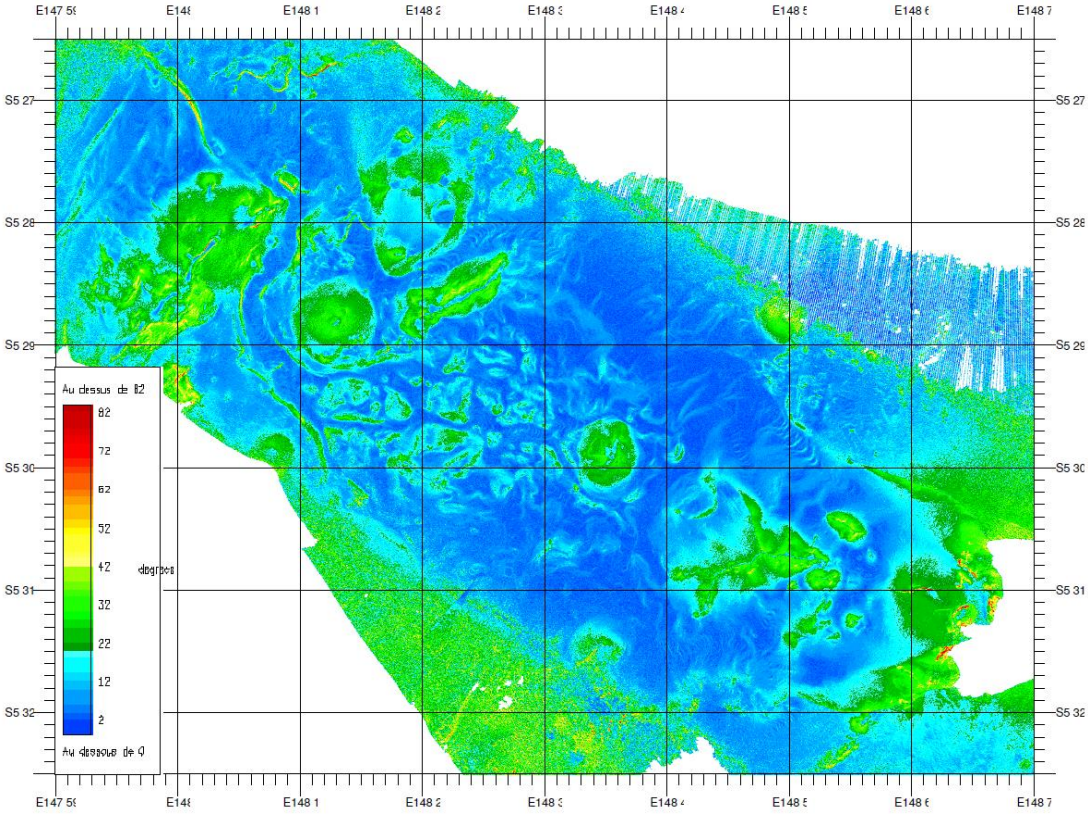

Figure 28: Slope gradient map of the proximal area affected by the Ritter Island event of 1888.

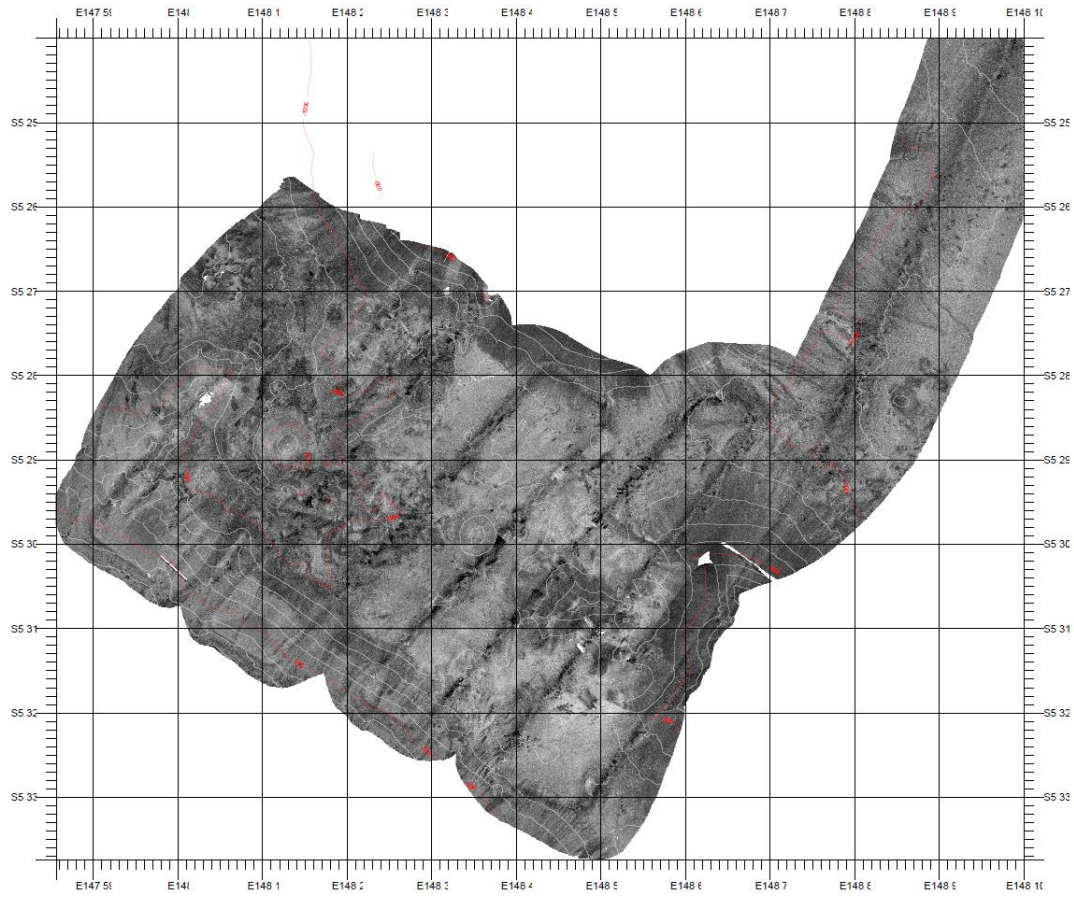

Figure 29: Backscatter intensity map of the proximal area affected by the Ritter Island event of 1888. High backscatter is dark.

The northern, distal part of the basin is relatively flat-lying but shows some striking small-scale relief that most likely represent flow patterns. Whether from one event, a series of genetically closely-related events or several (or many) different event still remains to be elucidated. The pattern is best shown by slope azimuth maps (Fig. 30) and backscatter intensity maps, where an intriguing pattern of high backscatter patches and low backscatter channels is observed (Fig. 31). The southern part shows a widening, channelized flow that seem to overlap and interfinger with flows emanating from the island of Sakar. Towards the North this zone is followed by a braided flow pattern that nevertheless shows a prominent direction towards the North-Northeast. Finally the most distal reaches are smooth in the Northeast and show a renewed anastomozing channel in the Northwest. The end of the basin in the Northwest, where it become rather narrow, has not been mapped. In the North the basin abuts against the steep southern flanks of a large submarine seamount (Fig. 32). This seamount has also been affected by large volcanic flank collapses and it‘s immediate surroundings are heavily faulted.

Despite previous reports of gas of particle emissions from the submerged cone of Ritter Island (Day et al., 2015), the analysis of both EM122 and EM710 water column data (Fig. 33) did not reveal any sign of scattering anomalies in the water column.

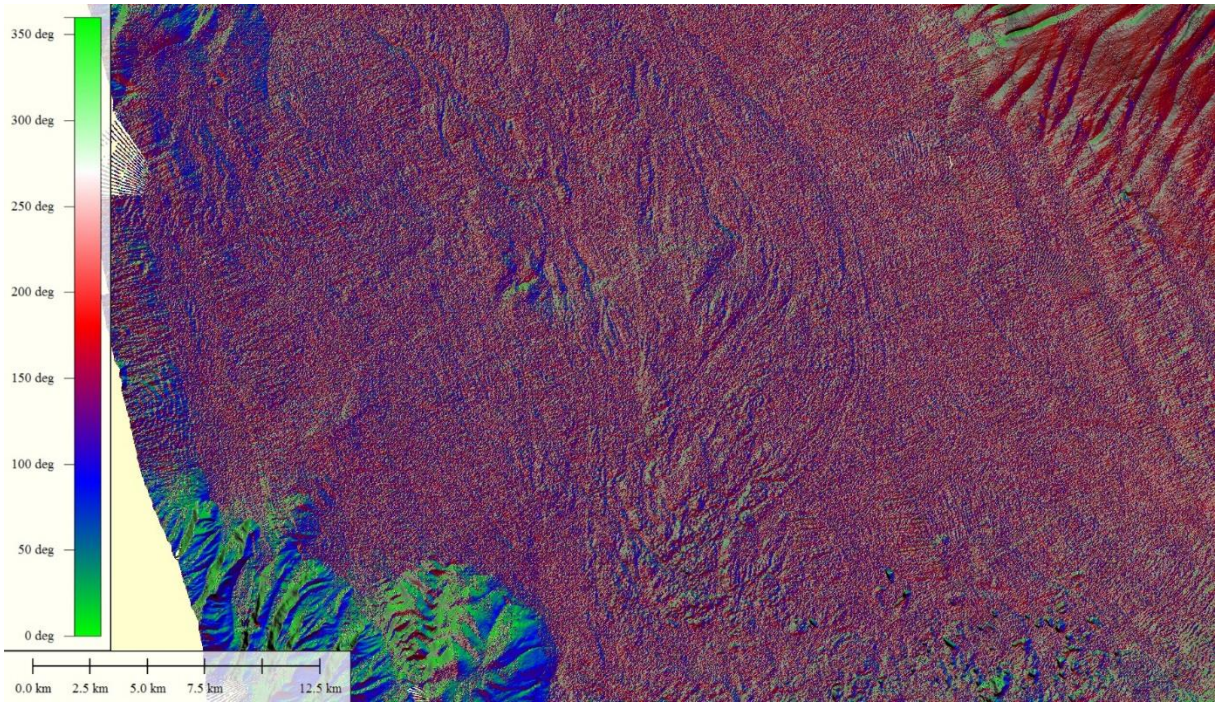

Figure 30: Screenshot of slope azimuth map of the distal reaches of the basin affected by the Ritter Island event.

Figure 31: Backscatter intensity map of the distal area affected by the Ritter Island event of 1888. High backscatter is light.

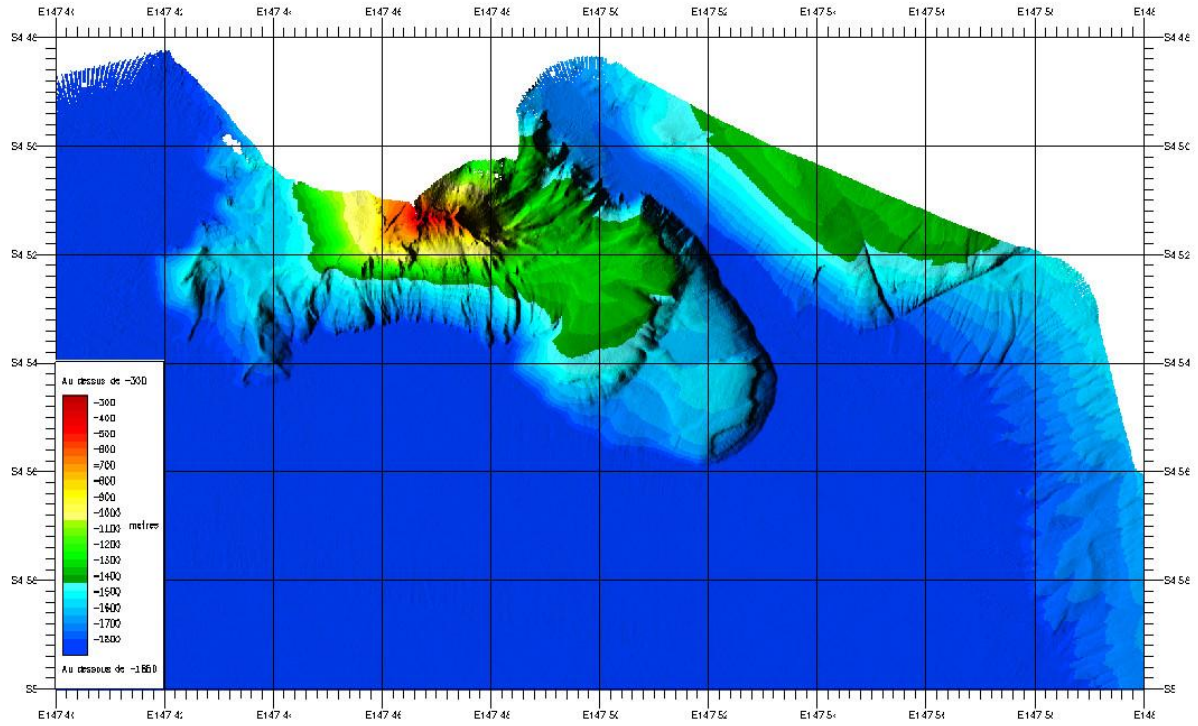

Figure 32: Shaded relief bathymetry of the northern end of the survey area showing a large seamount.

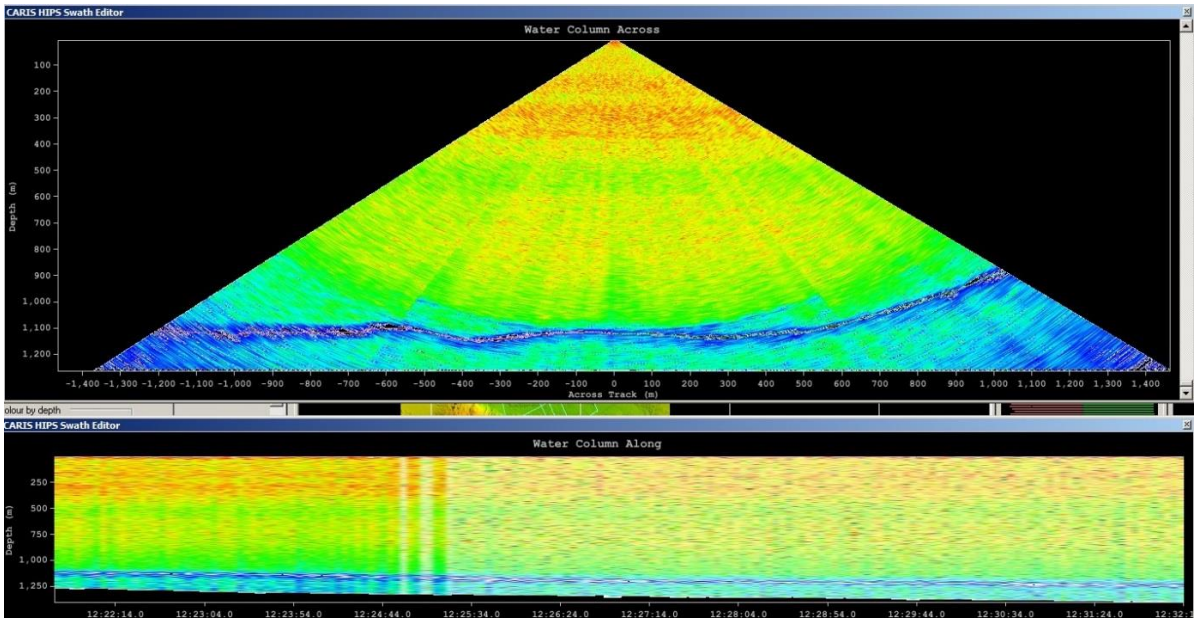

Figure 33: Screenshot from CARIS software showing water column data.

6.4 Parasound

6.4.1 Method

The hull-mounted parametric sub-bottom profiler PARASOUND P70 (Atlas Hydrographic) was operated on a 24-hour schedule for flare imaging and to provide high-resolution (less than 15 cm for sediment layers) information on the uppermost 50-100 m of sediment. The system has a depth range of 10 m to > 11000 m (full ocean depth) and a maximum penetration of 200 m. This high sediment penetration is acquired through the high pulse transmission power of 70 kW.

The RV Sonne is equipped with a PARASOUND P70 system since its commission in 2014. PARASOUND P70 is a narrow beam sediment echo sounder, providing primary frequencies of 18 (PHF) and adjustable 18.5 – 28 kHz, thus generating parametric secondary frequencies in the range of 0.5 – 6 kHz (SLF) and 36.5 – 48 kHz (SHF) respectively. The secondary frequencies are obtained through nonlinear acoustic interaction of the primary waves at high signal amplitudes. This interaction occurs in the emission cone of the high-frequency primary signals, which is limited to a beam width of 4.5° x 5° for the PARASOUND P70. The system consists of four identical transducer modules, each about 0.3 m x 1.0 m. The P70 version includes 384 acoustic elements combined to form 128 stave channels. The resulting footprint size is approx. 4% of water depth and vertical and lateral resolution is significantly improved compared to conventional 3.5 kHz echo sounder systems. The system provides features like recording of the 18 kHz primary signal and both secondary frequencies, continuous recording of the whole water column, beam steering, different types of source signals (continuous wave, chirp, barker coded) and signal shaping. Digitization takes place at 98 kHz to provide sufficient sampling rate for the high secondary frequency. A down-mixing algorithm in the frequency domain is used to reduce the amount of data and allow data distribution over ethernet.

For the standard operation a parametric frequency of 4 kHz and a sinusoidal source wavelet of 3 periods were chosen to provide a good balance between signal penetration and vertical resolution. The 18 kHz signal was also recorded permanently. We used the unique opportunity at the Challenger Deep (10925 m) to test the full ocean range. First results showed that the system provides reasonable data, although it might not be useful for any interpretation due to almost no penetration. However, we can confirm the full ocean depth of the system. At the survey area the system was mainly used for analysis of sedimentary processes, such as the identification of mass transport deposits. Due to low water depth (>2000 m) within the survey area and a rugged morphology of the seafloor close to Ritter Island it was operated in a single pulse mode.

Technical problems occurred rarely and could partly be solved during the cruise. A bug in the PARASTORE software caused loss of data during test runs at the beginning of a hydroacoustic survey around Ritter Island. The bug was reported to ATLAS Hydrographic support in order to find a solution and enhance the PARASTORE software in the future. The system was rebooted a few times due to program crashes (approx. once a week). However, these data gaps rarely exceeded a few minutes and the overall data quality is very good.

All raw data were stored in the ASD data format (Atlas Hydrographic), which contains the data of the full water column of each ping as well as the full set of system parameters. Additionally a 200 m-long reception window centered on the seafloor was recorded in the compressed PS3 data format after resampling the signal back at 12.1 kHz. This format is in wide usage in the PARASOUND user community and the limited reception window provides a detailed view of subbottom structures.

All data were converted to SEG-Y format during the cruise using the software package ps32sgy (Hanno Keil, Uni Bremen). The software allows generation of one SEG-Y file for longer time periods, frequency filtering (low cut 2 kHz, high cut 6 kHz, 2 iterations), subtraction of mean and envelope calculation. If seismic data were collected simultaneously, one SEG-Y file was created for the length of each seismic profile. In all other cases 4h-long pieces were generated (e.g. during transit, long seismic lines). All data were loaded to the seismic interpretation software IHS Kingdom. This approach allowed us to obtain a first

impression of sea floor morphology variations, sediment coverage, sedimentation patterns along the ship's track and imaging of mass transport deposits. In addition the data was converted from time to depth domain with an average velocity of 1495 m/s to select locations for the sediment coring, TV-GRAB, OFOS and HyBis dives.

6.4.2 Initial results

The multibeam bathymetry shows clear boundaries for proximal, medial and distal part of the Ritter Island debris flow. The proximal part is confined by a ridge and characterized by a rugged morphology with cones. The PARASOUND P70 shows good correlation of seafloor depth when compared to the multibeam bathymetry. However, due to high impedance contrast of the volcanic material and steep seafloor morphology, the system does not penetrate deeper than a few meters. Therefore, the data in the proximal area are not very useful (Fig. 34).

In medial to distal parts, entering the Bismarck Sea, the PARASOUND P70 shows very good penetration into the seafloor. The maximum penetration depth during the cruise (~ 60 m) was achieved on the northwestern end of the study area (Fig. 35).

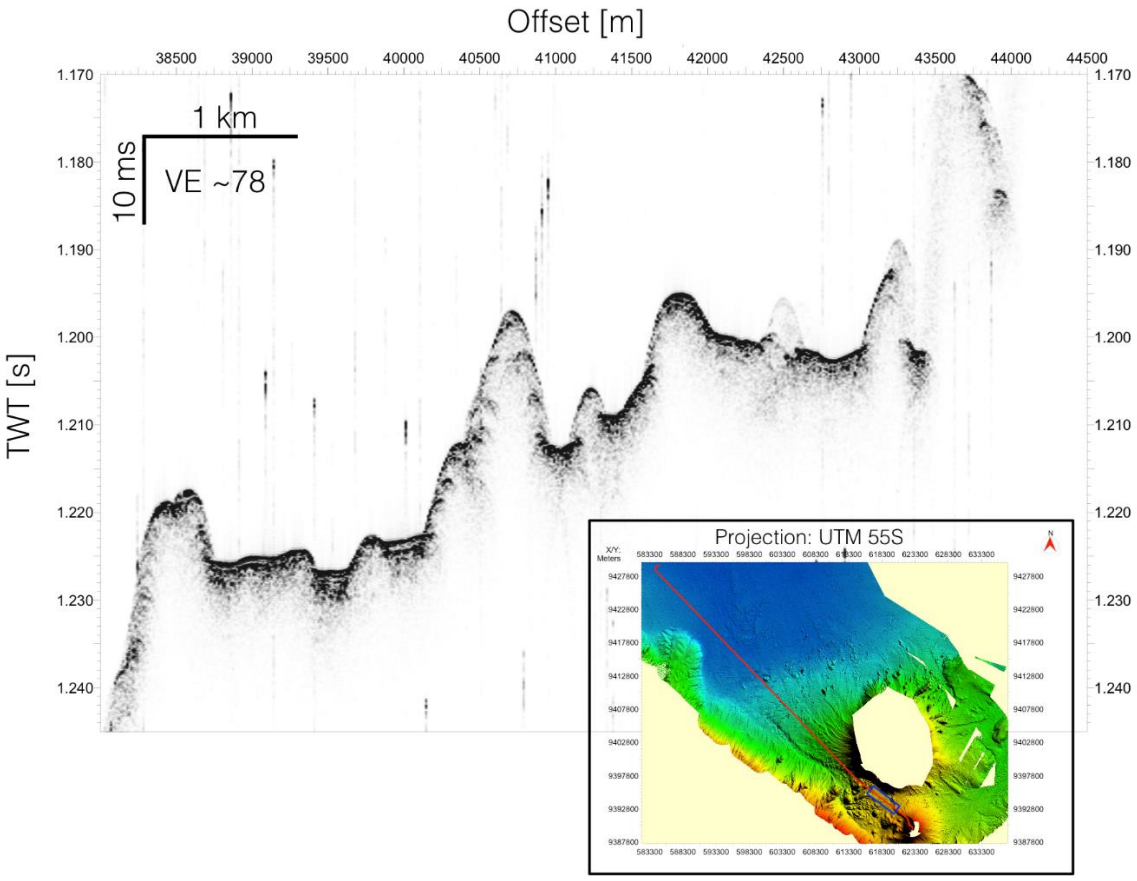

Figure 34: Parasound P70 profile of the secondary low frequency (SLF) of about 4 kHz in the proximal part of Ritter Island in between Sakar Island and Umboi. X-axis is offset in m and y-axis is two-way-traveltime in s. The profile shows low penetration into the seafloor and scattering of energy on mounds and cones.

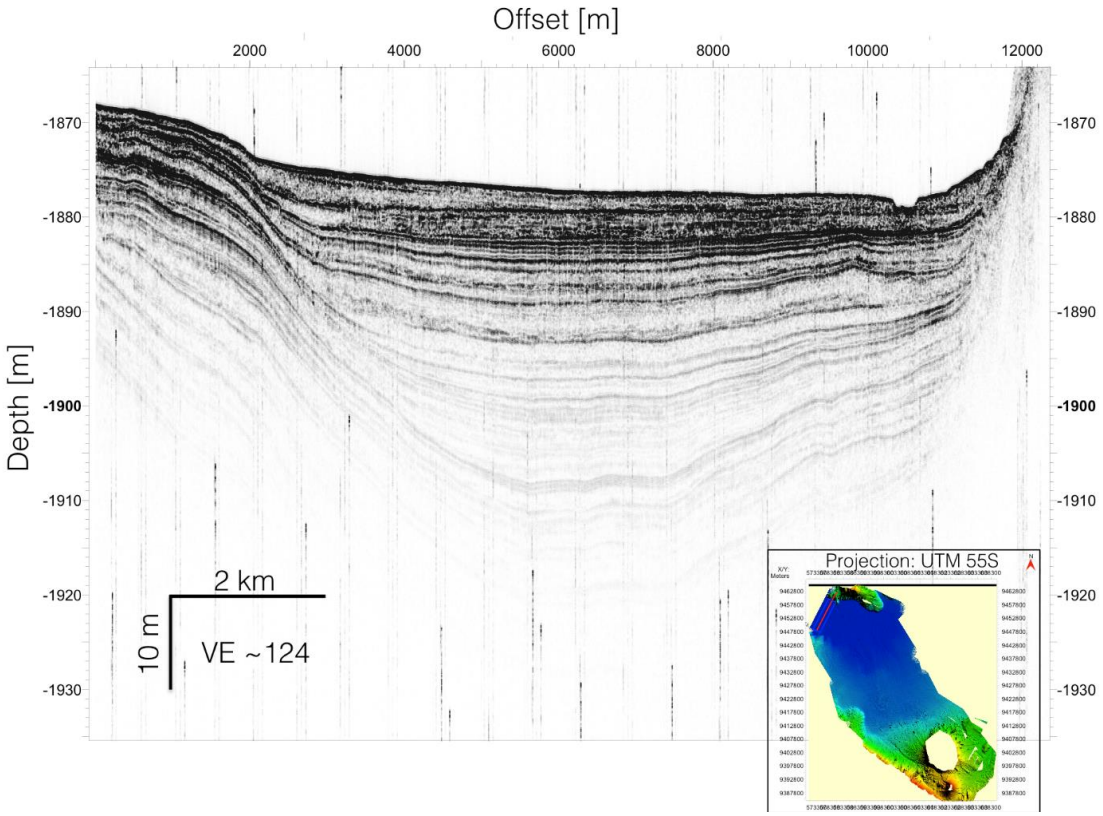

Figure 35: Parasound P70 profile of the secondary low frequency (SLF) of about 4 kHz in the proximal part of Ritter Island inside the Bismarck Sea basin. The x-axis shows offset in m, the y-axis is converted TWT [s] into depth [m] with an average velocity of 1495 m/s derived from the CTD cast. The profile shows high penetration into the seafloor with up to 60 m traceable amplitudes.

We were able to identify and trace the Ritter Island debris flow over a large area covering the basin. Furthermore, we could identify other geological features such as mass transport deposits (turbidites, debris), the overall background sedimentation, sedimentary waves and other forms of contourites as well as channel-levee systems. The data set offers a large potential to analyze the behavior and development of the Ritter Island debris flow in its distal regions. The acquired data enable us to constrain mass transport deposition over a large distance and might give insights into the behavior of the Ritter Island collapse and the subsequent mass transport and deposition at the seafloor.

6.5 HyBis operations

6.5.1 Methods and experimental setup

HyBis is a remotely operated underwater robot manufactured by Hydrolek Ltd., U.K. We ran it on the GEOMAR Hatlapa fibre optic winch supplying 2kV to the instrument. HyBis has three cameras and lights that allow online monitoring of the operation. There is one pan and tilt camera and one fixed camera that are looking forward, and one camera that points downward. These cameras automatically switch from black and white to colour when there is sufficient light.

The instrument has two thrusters that allow some maneuverability and two hydraulic pumps that can be used to manipulate various scientific modules underneath the instrument. During SO252 we used the grab module which allows to sample the top 30 cm of sea floor or pick up objects from the water column, and GEOMAR's OFOS video sledge for high Quality sea floor photography.

6.5.2 Dives

Table 2: Information about HyBIS dives.

		Dive1_HYBIS	Hybis_WP1	Hybis_WP1_2	Hybis_WP2	Hybis_WP3	Dive6_Hybis
start UTC (at bottom)	date	27.11.2016	05.12.2016	06.12.2016	06.12.2016	06.12.2016	09.12.2016
	time	01:48:24	23:37:50	01:12:21	02:31:40	04:20:17	00:36:04
	lat (USBL) [S]	-5°31.0649'	-5°30.9918'	-5°31.0406'	-5°30.7026'	-5°28.9917'	-4°56.5111'
	lon (USBL) [N]	148°09.3502'	148°06.3572'	148°06.3650'	148°06.4410'	148°03.3771'	147°46.4885'
	depth (USBL) [m]	1065.62	277.00	197.55	300.49	863.69	1774.48
end UTC (off bottom)	date	27.11.2016	06.12.2016	06.12.2016	06.12.2016	06.12.2016	09.12.2016
	time	03:37:51	00:20:15	01:25:38	02:44:48	04:48:31	00:51:47
	lat (USBL) [S]	-5°31.0531'	-5°31.0387'	-5°31.0522'	-5°30.7039'	-5°28.9981'	-4°56.5024'
	lon (USBL) [N]	148°09.3202'	148°06.3894'	148°06.3631'	148°06.4373'	148°03.3679'	147°46.4802'
	depth (USBL) [m]	841.53	111.45	193.96	291.63	820.43	1769.5

		Dive7_Hybis	Hybis_Dive8	Hybis_Dive9	Hybis_Dive10	Hybis_Dive11	Hybis_Dive12	Hybis_Dive13
start UTC (at bottom)	date	09.12.2016	09.12.2016	09.12.2016	09.12.2016	10.12.2016	10.12.2016	10.12.2016
	time	03:55:23	07:10:10	09:54:49	22:30:21	01:13:20	03:09:47	04:55:50
	lat [S]	-5°04.7217'	-5°13.1258'	-5°21.5981'	-5°30.9482'	-5°29.5704'	-5°29.9051'	-5°29.0739'
	lon [N]	147°50.1848'	147°52.4227'	147°54.0604'	148°02.3716'	148°02.2213'	148°03.4813'	148°03.2903'
	depth [m]	1769.49	n.a.	1718.00	930.00	927.5	699.89	925.00
end UTC (off bottom)	date	09.12.2016	09.12.2016	09.12.2016	09.12.2016	10.12.2016	10.12.2016	10.12.2016
	time	03:56:07	07:17:02	09:58:27	23:37:22	01:41:53	03:25:37	05:18:50
	lat [S]	-5°04.7215'	-5°13.1258'	-5:21.5982	-5°30.9501'	-5°29.5619'	-5°29.9046'	-5°29.1422'
	lon [N]	147°50.1843'	147°52.4227'	147:54.0610	148°02.3723'	148°02.2110'	148°03.4836'	148°03.3184'
	depth [m]	1764.22	n.a.	1650.33	871.13	748.78	703.92	865.70

6.6 OFOS and HyFOS operations

6.6.1 Methods and experimental setup

OFOS (Ocean Floor Observation System) is a video sledge composed of a downward-looking video camera (standard definition) and a downward-oriented digital still camera (Nikon D7100) with a resolution of 24 megapixels. Two light sources are mounted to the sledge: One light for the video camera that is constantly running during operations and a flash that is connected to the still camera. The maximum amount of photos (~1000) that could be taken during one operation was restricted by the battery of the flash providing light for the still camera. To provide scale to the imagery, three parallel laser pointers are fixed to the video sledge in a triangular arrangement spaced approximately 50 cm apart from each other. The red laser beams can be seen on the videos and photos. OFOS was run on the ship's winch. Overall, 6 OFOS operations were performed during this cruise. Posidonia was attached directly on OFOS for the positioning.

During 4 additional dives, HyBis and OFOS were merged. The HyBis grab was replaced by the video sledge. The forward-facing cameras of HyBis provided an overview over the seafloor while the still camera and laser beams of OFOS allowed for high-resolution imagery. The flash for the still camera was connected to the HyBis' power supply and was not run on a battery. The HyBis and OFOS combination was named HyFOS. Posidonia was attached 30 m above HyFOS for the positioning, for the first dive 50 m.

During OFOS operations, the still camera was programmed to take photos in regular intervals of 9 – 11 seconds depending on the dive time. During HyFOS operations, photos were taken every 5 seconds. A 1.5 m long string with a weight at the end kept the camera in about 1.5-1.7 m above the seafloor.

Ship speed during video tows varied between 1 to 0.1 knots.

6.6.2 OFOS dives

Table 3: Information about OFOS dives.

		Dive1	Dive2	Dive3	Dive4	Dive5	Dive6
start UTC (at bottom)	date	21.11.2016	21.11.2016	29.11.2016	30.11.2016	30.11.2016	07.12.2016
	time	15:46:47	19:59:38	23:53:20	03:00:08	08:33:58	4:21:56
	lat (USBL) [S]	-5°28.6579'	-5°29.9615'	-5°29.9117'	-5°30.4789'	-5°30.9209'	-5°30.8603'
	lon (USBL) [N]	148°03.6560'	148°03.4942'	148°03.5480'	148°06.5874'	148°02.4117'	148°05.3903'
	depth (USBL) [m]	894.50	604.90	740.00	199.39	941.00	655.00
end UTC (off bottom)	date	21.11.2016	21.11.2016	30.11.2016	30.11.2016	30.11.2016	07.12.2016
	time	18:15:49	20:47:16	1:14:48	6:49:39	10:30:31	8:08:51
	lat (USBL) [S]	-5°29.4227'	-5°29.9015'	-5°29.9521'	-5°31.1643'	-5°31.1955'	-5°31.2580'
	lon (USBL) [N]	148°02.9927'	148°03.3956'	148°03.5376'	148°06.2404'	148°01.9908'	148°04.3667'
	depth (USBL) [m]	462.50	820.80	758.00	337.00	799.39	820.49

OFOS Dive 1

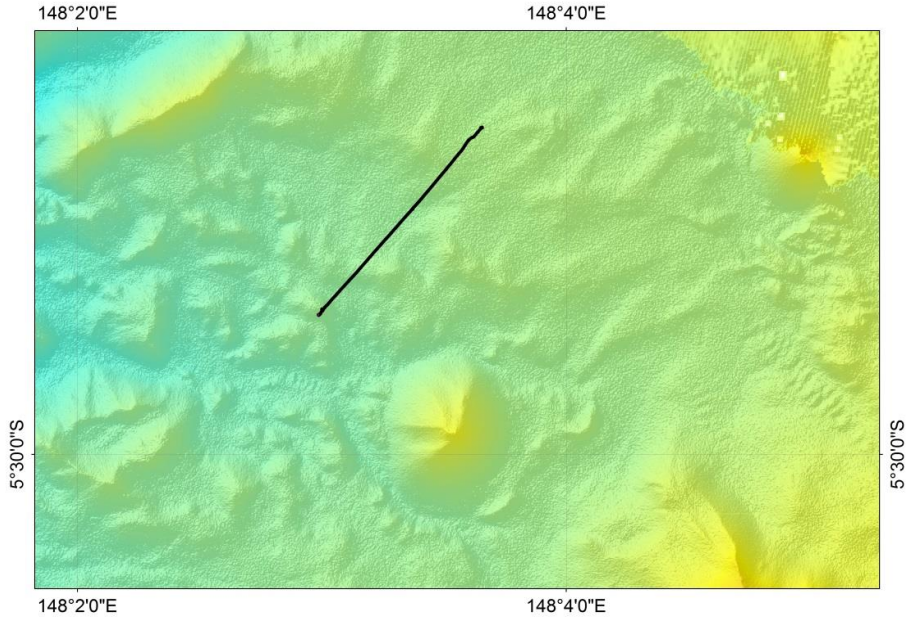

Figure 36: OFOS dive 1.

The first dive transect ran from the northern part of the area between Sakar and Umboi Island, starting in a flat-surfaced region in the north, and travelling SW towards more irregular mounded topography (Fig. 36). The purpose of the dive was to investigate the nature of the seafloor in the flat-surfaced region, and how this changed in the area of irregular topography. The sea floor was very smooth surfaced throughout the dive, with a covering of yellow-brown

hemipelagic mud. No stony material (e.g. cobbles or blocks protruding at the surface) was observed in any part of the dive. Rounded patches of black sand, forming regular ripple structures in places, were observed in the middle part of the dive, generally in areas with slightly higher slope gradient than the entirely mud-covered region. The megafauna was composed of shrimps, sea cucumbers and some bottom-dwelling fish.

OFOS Dive 2

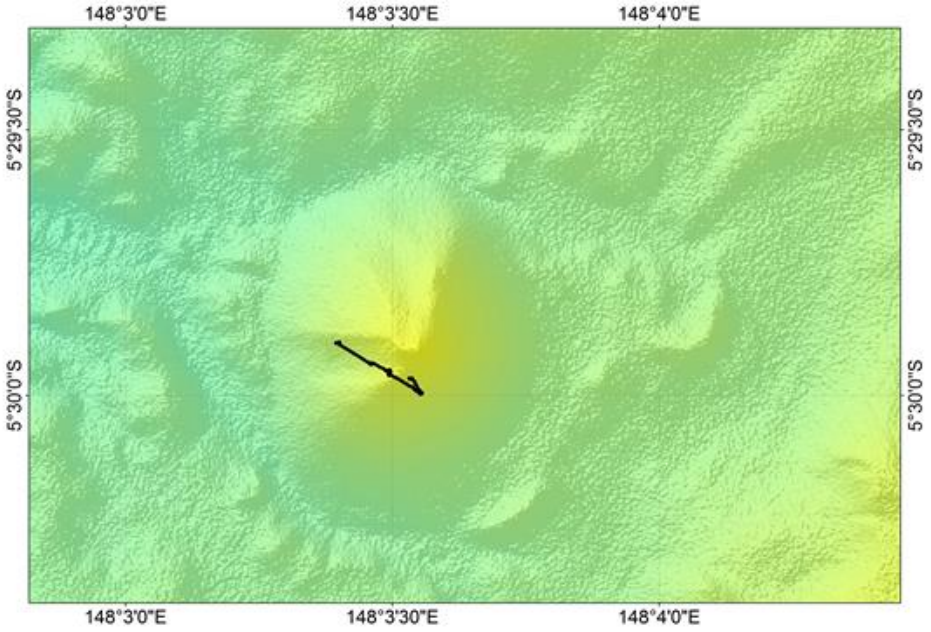

Figure 37: OFOS dive 2.

The second dive transect went from the top of one of the cones west of Ritter Island down its western flank and aimed to better understand the origin of the cone structure (Fig. 37). The top part of the cone is covered by hemipelagic mud and has a very smooth surface, with sandier patches occurring throughout the dive. The ratio of black coarser grains in the sand varied during the dive. More gravelly patches were observed in the middle part of the dive, some with a partial mud drape, and some without a mud cover, exposing sub-angular, irregular, dark grey volcanoclastic gravels, with clast sizes up to a few cm. These are interpreted as partially reworked exposures of scoria derived from the steep sides of a shallow slope failure on the W flank of the cone. The observations support the interpretation that the conical landforms west of Ritter are basaltic scoria cones. The fauna varied along the dive transect. A couple of coral species (e.g. Anthomastus sp.) attached to hard substrate such as cobbles was documented and crinoids were abundant in those areas. Whip corals were very abundant in some areas. Shrimps and bottom-dwelling fish were present.

OFOS Dive 3

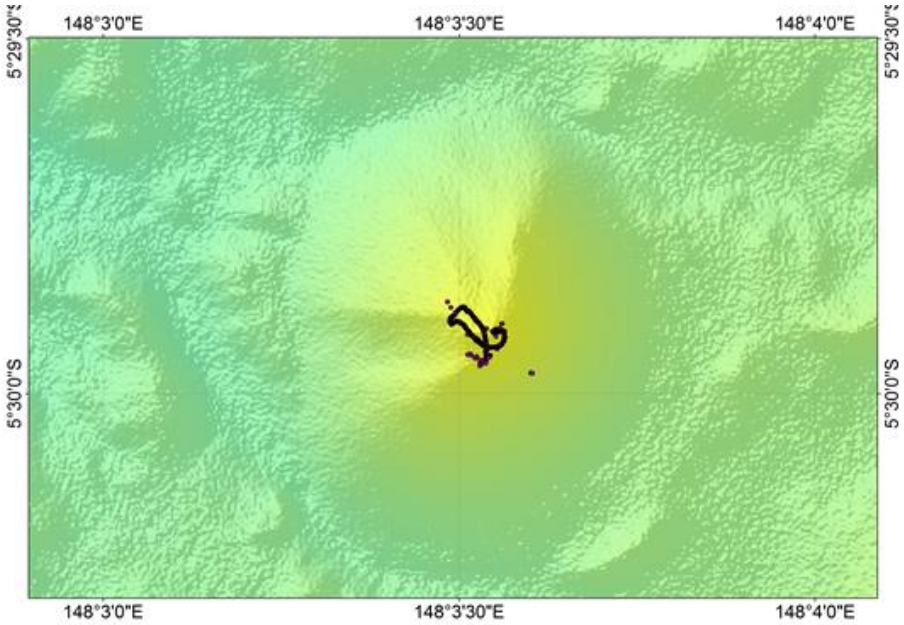

Figure 38: OFOS dive 3.

In order to explore the actual top of cone structure that we missed in dive 2, dive 3 concentrated on the top of the cone to find evidence for its origin, e.g. a crater structure (Fig. 38). The pictures and videos showed predominantly muddy sand with varying ratio of black coarser grains, but overall an extremely smooth surfaced top to the cone, with a gentle flat summit and no evidence for any crater or for any large blocks. Gravelly patches occur around the headwall of a slope failure scarp on the W flank. Scoriaceous clasts up to ~10 cm across were observed. Attached to some of larger clasts corals and crinoids were documented. Multiple shrimp species were found along the transect.

OFOS Dive 4

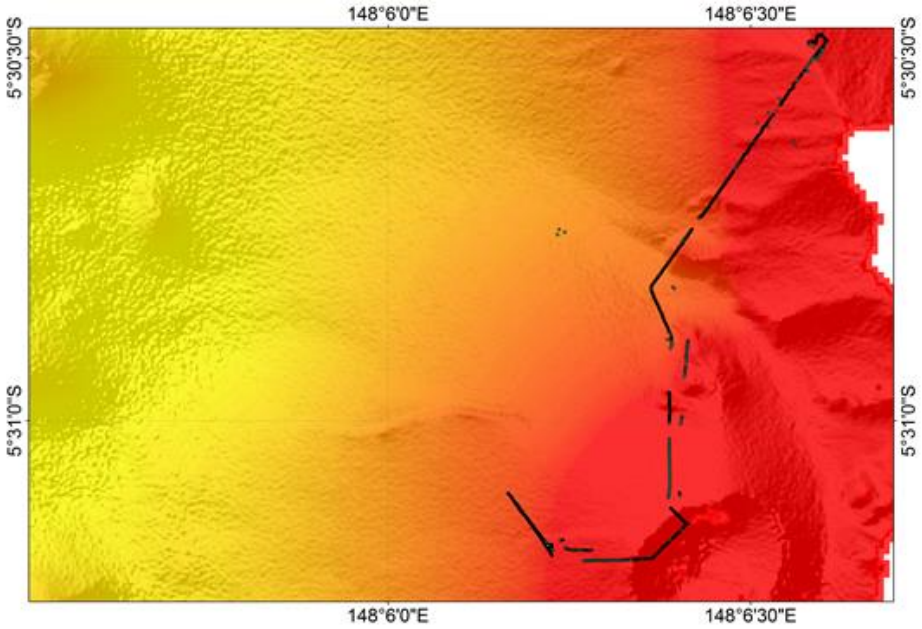

Figure 39: OFOS dive 4.

This transect started at the outer edge of the unfailed slope of Ritter Island in the north and went south down the upper slope of the head scarp from the 1888 failure and the new crater (Fig. 39). The outer flank of Ritter Island is characterized by mixed volcaniclastic gravels and cobbles variably draped by hemipelagic mud. The upper slope of the landslide scar is characterized by facies of bedded gravels of angular grey and generally scoriaceous volcanic clasts, usually well sorted and spanning a range of grain sizes. Some of these areas are draped by hemipelagic mud, while others are very fresh, suggesting recent reworking of the loose slope material. Larger, more angular and dense lava blocks become more frequent in the lower part of the scar, and massive lava bodies and dykes occur here. At the base of the slope there are nearly vertical outcrops of well indurated and poorly sorted layered conglomerates, cut by large (m scale) vertical dykes. The final part of the dive ascended the slope of the post-1888 volcanic cone. This generally has a smooth surface of scoriaceous gravels, showing evidence for downslope transport where the gravel overlies dense lava blocks and hemipelagic mud. An area of rougher topography on the cone is formed by accumulated dense, angular lava boulders and by more massive, intact lava bodies, with steep, jointed faces, protruding ten metres or more from the cone surface. The dive into the new crater had to be aborted because the visibility was poor, with very turbid water occurring at the level of the crater and for around 30 m above this.

Plenty of coral species including whip corals, gorgonians and cup corals were found on the hard substrate at the beginning of the dive at around 200 m depth. Multiple colourful fishes were present.

OFOS Dive 5

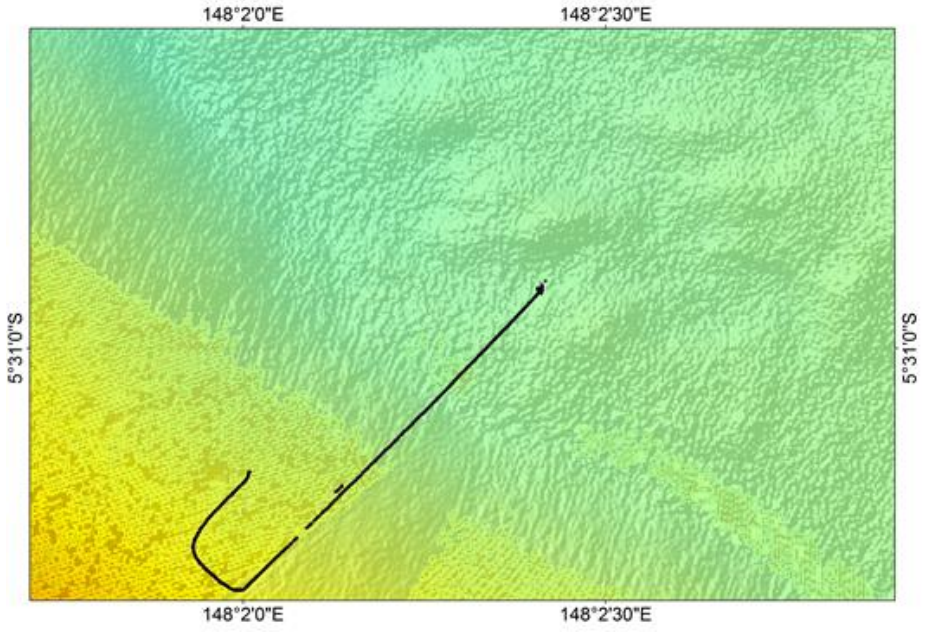

Figure 40: OFOS dive 5.

The transect aimed to investigate the surface deposits on the southern side of the channel between Umboi and Sakar, and a high backscatter strip that occurs at the base of the flank of Umboi, potentially indicating where the slope was scoured by the run-up of the Ritter landslide mass (Fig. 40). The first part of the dive crossed smooth seafloor covered in hemipelagic mud, with several sharp scarps that expose well bedded competent beds of grey sand and mud (a later HyBIS dive shows that these are the sides of circular depressions).

There are very few larger clasts (i.e. gravel or cobbles) visible at the surface. As the high backscatter region is crossed there is no obvious change in the nature of the seafloor; the smooth surfaced, mud-draped facies continues. The only change is that angular boulders of carbonate (with pitting that suggests reef-derived material) occur occasionally, as well as smaller blocks of angular dark volcanic rock. The boulders are present both in the high-backscatter strip and in the lower backscatter region higher up the flank. The only change between these areas is an irregular scarp, several metres in height, that is generally mud-draped by exposes further carbonate boulders. Corals (e.g. bamboo corals) and crinoids were often present on the boulders. In muddy areas, the megafauna was mainly composed of shrimps and bottom-dwelling fish.

OFOS Dive 6

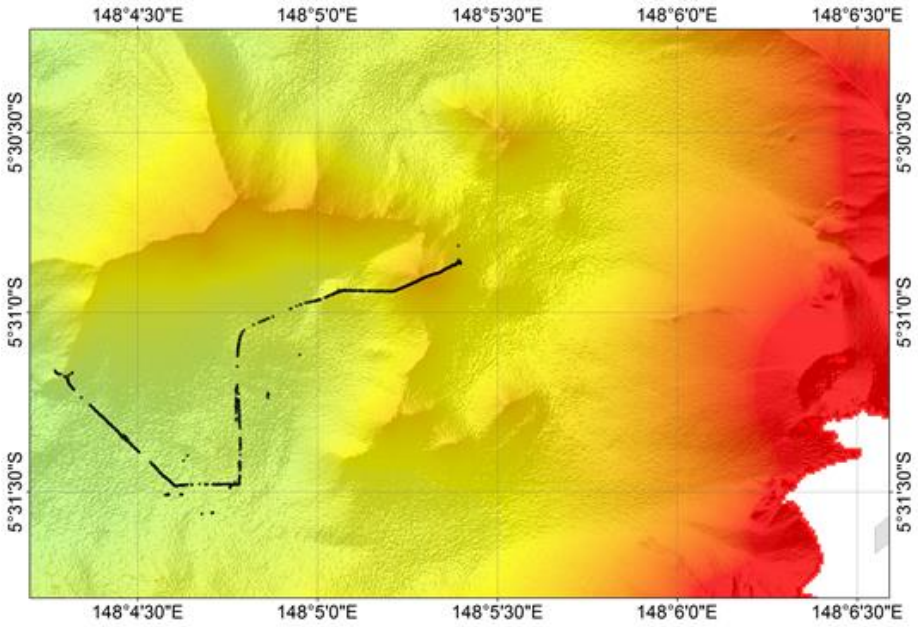

Figure 41: OFOS dive 6.

Dive 6 went across the irregular ridge west of the slide scar and the seafloor beyond (Fig. 41). This material is interpreted as being either remnant of the original volcanic edifice or landslide blocks that remained within the scar region. In the north eastern part of the transect there are various sizes of angular dense lava boulders that form steep slopes in places and are covered with different amounts of sediment. The central part of the dive is characterized by flat, smooth-surfaced mud-draped topography, with occasional angular grey lava cobbles and boulders protruding at the surface, and sandy rippled patches. The dive crossed a channel structure observable in the bathymetry, but no clear change was observed in the dive. Diverse coral species were found attached to rocks and boulders, e.g. black corals, bamboo corals and gorgonians. Some rocks had a dense organic cover that was composed of hydroids and colonial anemones among others. A large red siphonophore got entangled in the rope of the OFOS weight and is visible in some of the pictures.

6.6.3 HyFOS dives

Table 4: Information about HyFOS dives.

		HYFOS1	HYFOS2	HYFOS3	HYFOS4
start UTC (at bottom)	date	08.12.2016	08.12.2016	10.12.2016	11.12.2016
	time	00:55:44	04:12:11	23:29:01	02:44:14
	lat (USBL) [S]	-5°29.3689'	-5°28.8158'	-5°31.3613'	-5°31.4656'
	lon (USBL) [N]	148°02.3140'	148°01.3436'	148°06.3123'	148°07.33172'
	depth (USBL) [m]	964.00	816.33	290.00	344.86
end UTC (off bottom)	date	08.12.2016	08.12.2016	11.12.2016	11.12.2016
	time	02:15:23	05:24:26	01:10:50	06:23:43
	lat (USBL) [S]	-5°29.7106'	-5°29.0677'	-5°31.5015'	-5°32.1808'
	lon (USBL) [N]	148°02.1756'	148°01.0009'	148°06.3930'	148°06.1310'
	depth (USBL) [m]	951.97	948.74	139.00	368.61

HyFOS Dive 1

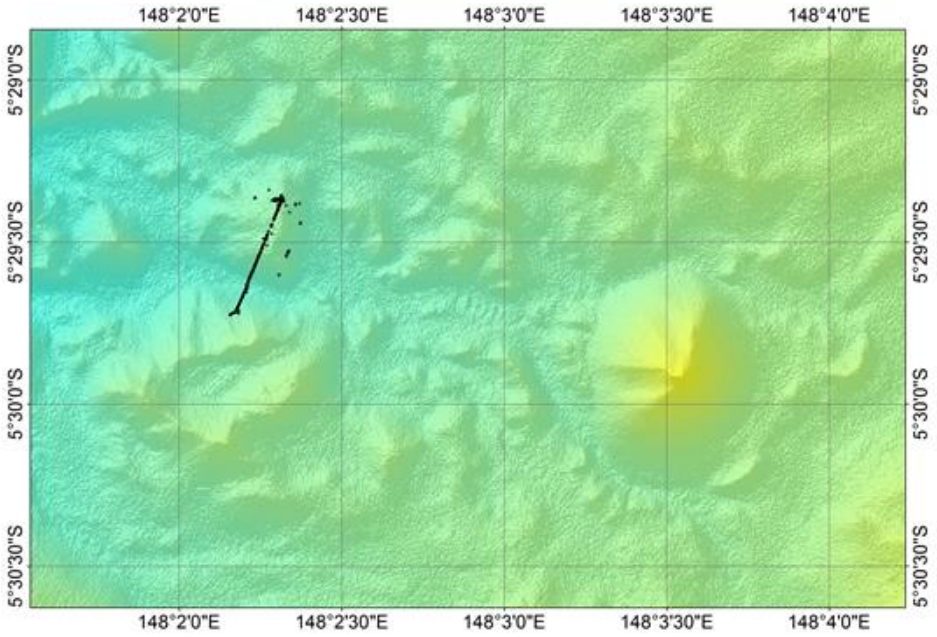

Figure 42: HyFOS dive 1.

The first HyFOS transect ran from the hummocky facies into an erosional channel in the southern part of the failure area north of Umboi Island (Fig. 42). The top of the hummock was extremely smooth surfaced, and covered in yellow-brown hemipelagic mud. Extensive rippled patches occur in places, particularly on the steeper flank of the hummock. On this flank there are also patchy exposures of angular gravel and cobbles of dense, grey volcanic rock. We observed a couple of corals on the exposed areas around 500 m water depth but hardly any evidence for strong currents within the channel where they would be expected if these channels were currently active. This suggests that the channel structures were formed during the Ritter Island landslide within the proximal part of the landslide deposit.

HyFOS Dive 2

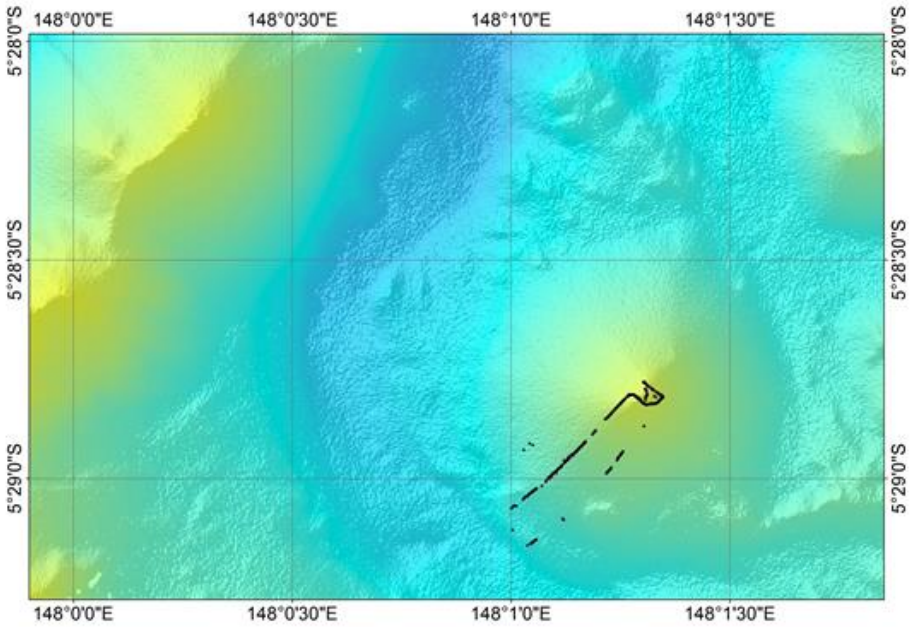

Figure 43: HyFOS dive 2.

The second HyFOS dive started at the top of the highest cone structure and continued into the main channel with very similar observations as the first dive (Fig. 43). The cone was very smooth surfaced and mud-draped, with no summit crater and no exposures of volcanic rock. At the base of the cone the seafloor was smooth and mud-draped, with occasional larger clasts – no scarps were observed. At the end of the second dive a voltage meter in the high voltage power supply failed and the dive was aborted.

Various corals were documented on hard substrates including gorgonians, bamboo corals and numerous black corals. Crinoids and stalked crinoids were present during the dive.

HyFOS Dive 3

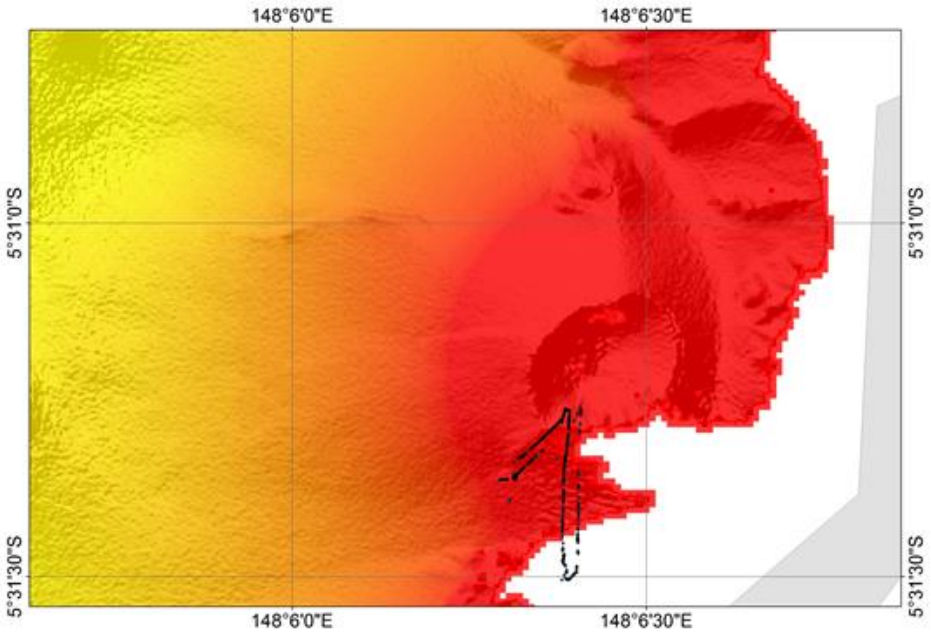

Figure 44: HyFOS dive 3.

This HyFOS dive started at the southern end of the foot of the new crater (Fig. 44). It ran all the way up to the crater rim and down into the crater. Massive lava outcrops were again seen protruding from the flanks of the submarine cone. Inside the crater the visibility was very poor and the very steep seafloor is covered by very fine, yellow material that is in the water column draping the volcanic rocks. The dive continued to the southern tip of Ritter Island where a steep at least 30 m-high cliff exists. It consists of dense igneous rocks (dike intrusions or massive lava bodies). Only little megafauna (e.g. fish and anemones) was observed.

HyFOS Dive 4

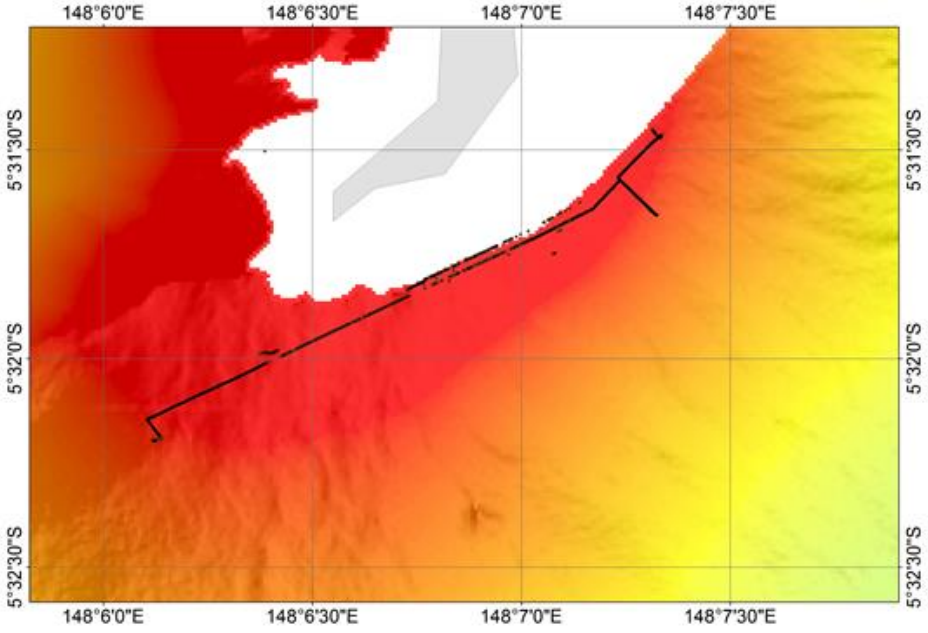

Figure 45: HyFOS dive 4.

The last HyFOS dive covered a long stretch at the 380 m contour line of Ritter Island's east side to a topographic depression in the slope further south (Fig. 45). The slope was covered by small and large blocks, but with more drape than on Ritter Island's western side. The final part of the dive (to the SW) crossed a gentle slope failure scarp, with patches of dense lava boulders occurring inside the scar.

A diverse megafauna was observed including multiple species of sea urchins, corals, large white stalked crinoids, different flat fish and sponges.

Summary biology (video transects)

Overall, around 230 animal species were documented from still images of the 10 video dives (see Appendix C). These were dominated by cnidarians: More than 50 coral species were found. Arthropods (around 30 species) and echinoderms (nearly 50 species of sea stars, brittle stars, sea urchins and sea cucumbers) were abundant and various fish species (> 40) were documented.

Summary biology (grab samples)

A couple of worm tubes/casts and worms were found in samples of soft sediment. Some of these worm tubes were composed of foraminifera. Highest biological diversity was brought up in grab sample "H10", which was taken on a slope and mainly composed of gravel. Hermit crabs, a sea cucumber and multiple worms were present. Strikingly, in sample "H9" a small triggerfish (4 cm) was collected.

6.7 Grab sampling

Samples of seafloor material were collected using the grab module mounted on the base of HyBis, and with the TV Grab.

The grab module on HyBis allows up to 30 cm of seafloor sediment to be collected within the grab buckets. The TV Grab has larger buckets with a wider opening, driven by a battery driven hydraulic system and the 2 tonne weight of the grab. It is able to collect either large rocky samples or to cut approximately 40 cm into the seafloor (the level of seafloor disturbance is greater in the TV grab, given its wider opening angle).

HyBis was used to successfully collect material from 11 sites. A single TV grab sample was also collected (Fig. 46). Sites were selected based on interpretations of Parasound and bathymetry data, on earlier OFOS video transects, and on failed gravity coring sites.

Table 5: Site locations are listed in the table below (H: HyBIS sample; T: TV Grab sample).

Site	Date UTC	Sample Name	Time UTC	Latitude	Longitude	Water depth (m)	Sampled material
H1	06/12/2016	SO252-H-1	00:18	-5.51733	148.1066	250	Lava block (pre-1888?)
H2	06/12/2016	SO252-H-2	01:30	-5.51748	148.1065	244	Post 1888 block and scoria
H3	06/12/2016	SO252-H-3	02:47	-5.51177	148.1074	360	Pre-1888 blocks, N Scar
H4	09/12/2016	SO252-H-4	00:50	-4.9417	147.7748	1840	Distal volcanic sand (?turbidite)
H5	09/12/2016	SO252-H-5	04:00	-5.07865	147.8365	1830	Mud with intraclasts (debris flow deposit)
H6	09/12/2016	SO252-H-6	07:14	-5.21842	147.8736	1790	?Post 1888 stratigraphy (sands and muds)
H7	09/12/2016	SO252-H-7	09:58	-5.36008	147.9011	1720	?Post 1888 stratigraphy (sands and muds)
H8	09/12/2016	SO252-H-8	23:35	-5.51578	148.0397	931	Volcanic sand (?post 1888)
H9	10/12/2016	SO252-H-9	01:35	-5.49265	148.0371	998	Volcanic gravels (1888 landslide material?)
H10	10/12/2016	SO252-H-10	03:25	-5.49835	148.0582	747	Scoria (scoria cone W of Ritter)
H11	10/12/2016	SO252-H-11	05:18	-5.48567	148.0556	927	?Post 1888 volcanic sand
T1	11/12/2016	SO252-T-1	23:27	-5.48453	148.0551	931	?Post 1888 stratigraphy (volcanic sands and muds)

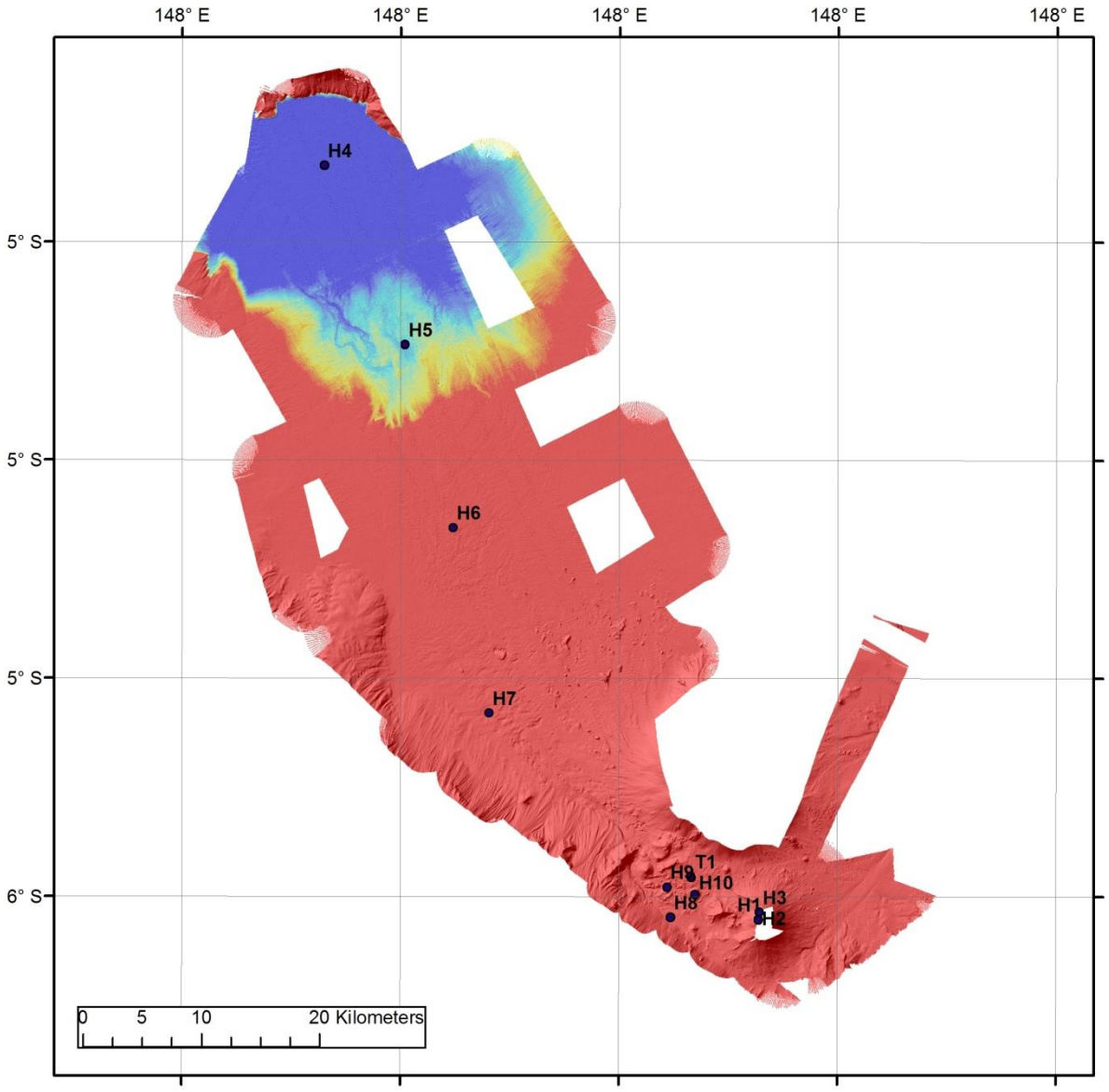

Figure 46: Site Map: HyBIS and TV grab samples (note that T1 and H11 are the same site).

Site and sample descriptions

H1

This site was located high on the N flank of the post-1888 Ritter Island submarine cone. The location is ~50 m upslope from rough topography visible on the bathymetry (protruding from the smooth cone surface), but the seafloor here is littered by large blocks of dense lava, some rounded, and some angular with planar surfaces. This, and later dive observations, suggest that there are frequent rocky exposures, not clear on the bathymetry, at the surface of the young cone. These are interpreted as older rocky topography, possibly mobilised by the landslide, and now partially buried by the young cone (see also 2D seismic profiles).

The H1 sample is a single relatively dense lava block (25 cm across), angular, with roughly planar surfaces. It is moderately encrusted with marine organisms (annelid worm casts, anemones and a biological film) and the outer surface is a rusty grey brown (chips show this is surficial, and the fresh rock is a dark grey). This surface appearance is in contrast with a large block in sample H2, and the block is interpreted as material locally

derived from pre-1888 rocky topography, partially buried by scoria deposits from the post-1888 cone.

The block is very highly crystalline, with a slightly open granular texture. Olivines and pyroxenes are dominant, with some feldspar. A notable feature is angular mid to dark green xenoliths, up to 2.5 cm across.

H2

This sample was collected in the same area as H1 (about 10 m away), with the aim of getting a representative sample of post-1888 pyroclastic deposits from the Ritter Island submarine cone.

The sample comprises a single large block and a bulk sample of coarse gravel and coarse sand (Fig. 47). The large block is rounded, slightly vesicular, mid grey lava, rich in black euhedral pyroxene phenocrysts, in a finely crystalline groundmass. The surface is extremely fresh, with no alteration rim or colonisation (this may reflect that the block was partly buried by gravels, and so not exposed at the actual seafloor). The rounding is in contrast to H1, and could be a result of milling within the vent prior to ejection, implying that the block was deposited as a ballistic clasts ejected from the post-1888 vent. The fresh surface also supports a recent expulsion, rather than a rock that has been exposed at the seafloor since 1888. The lithology is also very different to H1 (olivine is not obviously present as a phenocryst phase, for example, and xenoliths are absent).

The surrounding gravel is a mix of granular to densely scoriaceous lapilli with some denser, more angular fragments (Fig. 48). Dark grey clasts are dominant, but pale grey vesicular pyroclasts make up a significant proportion. Both types are plagioclase and pyroxene-phyric – it is unclear if the colour contrast is simply related to vesicularity, or if there is a compositional difference between the types. The gravel clasts are mostly >1 cm in diameter. A coarse sand fraction occurs alongside this, with similar clast types, but intervening grain sizes are less frequent.

Figure 47: Sample H2, showing the buckets of the HyBIS grab module, and the bulk sample of volcaniclastic gravels with one large, dense rounded block.

Figure 48: A cleaned sample of the volcaniclastic gravel in sample H2 (post 1888 Ritter cone), showing predominant brown scoria (3) and a predominant secondary fraction of pale grey pyroclasts (1).

H3

This site was located near the base of the exposed north scar of the landslide, in a deeply incised region observed in OFOS dive 4. The exposure is in-situ stratigraphy of poorly-sorted volcaniclastic deposits, forming a cliff with vertical rills. The exposure suggests that this unit is well indurated. It is cut by thick (metre scale) vertical dykes. The aim was to collect material that contributed to the landslide and was representative of pre-1888 volcanic rocks from Ritter. The sample couldn't collect the in-situ rock directly, and so a site was chosen at the base of the cliff, on the assumption that it would be dominated by material fallen from this cliff, and possibly also from the dykes.

The sample contains a large number of 10-cm angular blocks. Most are dense, and fall into three types: a dark grey, crystal rich and sometimes vesicular rock rich in very coarse olivines (and/or olivine glomerocrysts) and plagioclase feldspar and pyroxene; a similar dark rock, with a finer groundmass (less/finer plagioclase); and a paler grey pyroxene porphyry (around 30% of the blocks), with a very fine grained groundmass and rich in coarse, euhedral black pyroxene (some with greenish cores, perhaps reflecting overgrowth of olivine).

The sand collected with the blocks contains fine gravel to medium sand (there is no finer material). The sand is rich in olivine fragments, implying (if the sand is from the volcaniclastic sequence) that the olivine rich blocks are likely derived from the bedded volcaniclastic unit, if the same magma fragmented to form the sand. In that case, the pyroxene porphyry may reflect the nature of the local dyke (or one of the submarine lava units observed in OFOS dive 4, which have a similar appearance.

H4

The site was located at the far end of the mapped Ritter Island deposit. The surface deposit is an acoustically transparent unit, interpreted from the Parasound data to be the Ritter Island turbidite, and with discontinuous internal reflections.

The seafloor in the area is flat yellow-brown hemipelagic mud, with no ripples but extensive surface bioturbation. The grab sample penetrated through the mud and into an

underlying sand. This is disturbed by sampling, and the only clear stratigraphy is an overlying mud (5-10 cm thick), grey green at the surface with rusty brown streaks, and very fluid, becoming a more competent grey-brown clay at the base. This overlies a >5 cm dark-grey medium volcaniclastic sand, which in addition to the dominant dark clasts contains red and grey terrigenous clasts and abundant forams (especially at the top of the sand). The sand contains some convoluted muddy intervals, up to 10 mm thick, but not forming a continuous horizon.

H5

The seafloor is similar in appearance to H4: flat and featureless, covered in yellow brown mud with no visible sedimentary structures, but abundant wormcasts. The site was selected as being on the lobe of the distal part of the Ritter Island debris flow deposit (as mapped by Day et al., 2015). The Parasound data supports this interpretation, showing a lobate deposit with a clear front, ponding beyond a subtle topographic step. Upslope seafloor sediment failure (based on steps in the underlying seafloor stratigraphy) is interpreted as contributing to this unit. The sample recovered 4 cm of top hemipelagic mud. The mud is fluid, brown, and rich in wormcasts and forams (i.e. similar to the hemipelagite at the last site). Beneath this is >25 cm of grey fluid mud, structureless and very loose. The only variability within this is the presence of slightly more cohesive fragments, rounded, and dominantly clays, although a few are silty or contain fine sand. These clasts are estimated to comprise around 10% of the mud unit. There is no evidence that they are distributed within any particular part of the sample. There is no change to more cohesive mud at the base of the grab sample. A notable feature is the lack of bioclasts. These are common in the top hemipelagite, but apparently absent in the deeper fluid grey mud (Fig. 49).

Figure 49: A cohesive clay intraclast (grey clay with brown mottling) within fluid grey mud in sample H5.

H6

This site was selected as being in the region where underlying seafloor sediment failure is clearest in the Parasound profiles (i.e. steps at the underlying stratified surface), beneath an acoustically transparent deposit with variable lateral thickness. The site chosen is on a relatively thicker part of this deposit, in an effort to sample this material. The seafloor at this

site is very similar to H4 and H5, being flat and featureless, with a cover of yellow-brown mud and evidence of bioturbation, with some sandy material also visible at the surface. The sample recovered comprised 12 cm of interbedded mud and sand intervals. This is interpreted as being post-1888 sedimentary drape, rather than penetrating into the deposit itself. This drape would not be within the resolution of the Parasound data. There are several potential post-1888 sources for the volcaniclastic sands, including eruption-generated turbidites from Ritter (post-1888 submarine cone) and deposits derived from the nearby flank gully systems on Umboi and Sakar.

The top of the sample recovered 3 cm of hemipelagic brown fluid mud, rich in forams and very similar to the hemipelagite at the previous two sites. Beneath this is a 1 cm grey volcaniclastic fine sand, then a 1 cm brown cohesive mud, a 3 cm dark grey medium volcaniclastic sand, and then 4 cm of grey-brown silty mud. The lower sand has some internal structure, of deformed and rounded mud pellets, 1-2 cm across.

H7

This site was selected to test if the Ritter 1888 deposit was present upslope of H6, in an area of slightly steeper topography (but still very low gradients), marked by several blocks protruding at the surface from an older ?Sakar-derived debris avalanche deposit (see 2D seismic profiles). The area has patchy high backscatter and disrupted sediment wave features, in contrast with equivalent deposits slightly north, where the sediment waves are undisturbed and there is more consistent low backscatter. The Ritter deposit appears to have passed across this area, and is interpreted as potentially causing erosion on the irregular seafloor, leading to high backscatter patches. It is uncertain if the Ritter deposit was depositional in this area (the Parasound doesn't penetrate beneath the irregular seafloor; and the 2D seismic profiles don't provide the vertical resolution to clearly identify a near-surface deposit). The site selected was in a lower backscatter patch. The sample recovered 12 cm of interbedded mud and sand, and as at site H6, this is interpreted as representing the post-1888 sediment drape. The stratigraphy is more complex than at H6, and the two are not easily correlated. The top mud is 1 cm of brown, fluid hemipelagite, thinner than at previous sites. This is underlain by a 1 cm dark grey medium volcaniclastic sand, with an oxidised rusty brown colour in the lowest 2 mm. Beneath this are two thin muds and sands, and then a 2 cm green brown mud with faint horizontal streaks. This is underlain by three further sands and muds, the lowest greenish mud being 1.5 cm and with faint grey streaks. There is then a 4 mm fine mid-grey sand, 7 mm mud, a very faint fine sand band, 4 mm of greenish mud, and then a 4 mm fine to very fine mid-grey sand a the base. The sandy beds are lenticular, and their thickness is slightly variable between the short push cores that were used to sample this deposit within the grab. The beds may have been affected by ripple reworking at the surface, and the measured thicknesses may not be primary.

H8

This site is in the proximal region of the mapped Ritter debris avalanche deposit, on the southern side in an area of relatively flat seafloor, north of the flank of Umboi. It was studied on OFOS dive 5, and is north of the high-backscatter strip at the base of the flank of Umboi. The seafloor in the area is extensively covered in yellow hemipelagic mud, slightly rippled in patches. The sampling area is marked by rounded depressions, some forming enclosed circular structures, and some forming gentle crescent shaped scarps, giving a shallow dune like morphology to the surface. These depressions range in diameter from ~2-15 m. The

scarps at the edge of these are generally gentle, sometimes exposing one or two steps of sandy beds. The origin of the depressions unclear; they may be related to settling and dewatering of the Ritter deposit in this area.

The sample was taken at the base of a scarp, in an attempt to penetrate into material beneath the bedded sequence in the scarp. The sample recovered 12 cm of stratigraphy. The top part of this was 5 cm of fluid brown grey hemipelagic mud, more cohesive at the base. This relatively thick hemipelagite contrasts with sites H6 and H7, and suggests that this site may not have been subjected to the same processes depositing sands at those sites. The mud overlies a 7 cm dark volcaniclastic sand, dominated by dark clasts but with frequent red and white fragments. In the upper few cm of this there are deformed mud intraclasts of cohesive clay.

H9

This site is on the flank of one of the mounds within the central part of the Ritter proximal debris avalanche deposit. The aim of this site was to identify the nature of the material that forms the topography (channels between steep sided hummocks). The seafloor is mud covered and rippled in places, but generally smooth. On the flank of the hummock there are patches where isolated cobbles and patches of smaller, angular cobbles are visible at the surface, partially draped in hemipelagic mud. The sample retrieved is fairly small, due to the difficulty of sampling on the steep slope.

The recovered sample is a fine volcaniclastic gravel/coarse sand, with some coarse larger clasts – angular fragments up to 5 cm across (a few larger cobbles, tens of cm across, were observed on the dive). The blocks are mixed within the gravel and also at the surface, with the cohesive overlying mud. The coarse sand contains crystal and paler crystalline volcanic fragments, and a few bioclasts such as gastropod shells. The blocks are all mafic and crystalline (olivine, pyroxene); several are coarsely vesicular. The overlying mud has not been well sampled – much was likely to have been washed out on sampling.

H10

A site on the conical structure W of Ritter Island. The selected site was on a steep sided shallow-seated flank scar, exposing an active scree slope with streaks of gravels and mud reworked from upslope. The cone has been interpreted as a pre-1888 scoria cone (based on slope degradation, bathymetry and 2D seismic profiles).

The grab collected a large sample of volcaniclastic gravels. The majority is a fine gravel (5 mm clasts), with some coarser cm-scale material. Distributed throughout this are larger blocks, up to 6 cm across. There is no primary stratigraphic information, since everything was sampled from an active scree slope. A few cohesive clay clasts are mixed with gravel, up to 5 cm across, and likely represent the accumulated hemipelagic mud over the cone. The clasts are scoriaceous and variably vesicular, with outer crusted textures around denser interiors (on larger clasts). A striking feature is the abundance of xenoliths (Fig. 50), generally rimmed by basaltic glass, and forming a core to several clasts, especially the larger ones. An initial examination suggests three types of xenoliths: a felsic pale-greenish grey, coarsely crystalline rock with an open, granular texture (monomineralic); finer grained, crystalline greenish brown clasts (a mix of olive green and mid-green crystals, with fine white veins); a finer grained felsic rock, which may be a fine grained equivalent of type 1.

Figure 50: Examples of xenoliths in H10 D, several with a coating of scoriaceous basalt.

H11

A site towards the northern side of the proximal Ritter debris avalanche deposit, in an area of flat seafloor, marked on slightly steeper slopes by ripples, exposing grey sandy patches underneath. The aim was to sample the material that forms this apparently thick, flat-surfaced deposit across the north side of the proximal region affected by the Ritter landslide.

The seafloor through much of the area is monotonous yellow mud. The selected site is in a darker rippled region. HyBIS fails to penetrate deeply into the underlying material, suggesting a relatively hard substrate. The sample preserves around 4 cm of stratigraphy in total: 5 mm of fluid mud (some likely washed out on ascent) overlies 3.5 cm of medium volcaniclastic sand, dominated by dark clasts, but with more frequent white fragments (?needs checking) than the sands at previous sites. There is no evidence of stony material at all within the grab sample; it is unclear why the grab failed to penetrate deeper.

T1

A single site using the TV grab. This site is exactly the same as H11. The aim was to penetrate deeper into this material to ascertain the nature of the underlying flat surface deposit. The grab recovered a full load of sediment (the gates in each grab bucket were overflowing with mid-grey volcaniclastic medium sand) (Fig. 51). This material dominated the outer parts of each grab bucket, and contained mud clasts which may be original or may be created during grab sampling (i.e. relict clasts of either the top hemipelagic clay or underlying clay units; the top hemipelagite is absent from the sample, and so there has clearly been disturbance/loss of the uppermost stratigraphy). A core taken of the outer parts of the bucket entirely comprised this grey volcaniclastic sand, slightly finer in the upper part. The primary thickness of this unit cannot be estimated. It is interpreted as being the same as the volcaniclastic sand in H11, and thus forming the top of the stratigraphy at this site. There were rare coarser clasts dispersed throughout the grab sample as a whole, mixed with this sand, mostly up to 1 cm across, with a single 3 cm clast. These were all low density clasts,

either open-textured brown scoria or white to pale grey pumice (pyroxene and plagioclase phyric).

Within the central part of the grab sample was a domed core of intact stratigraphy, comprising interbedded clays and volcaniclastic sands. The clay beds show strong deformation, with the margins vertically bedded and displaying thrust fractures, all likely reflecting the compression of the stratigraphy during coring. The outer part of the stratigraphy is in contact with the volcaniclastic sand that dominates the grab buckets; the central core is thus interpreted as older stratigraphy. From the top, this older stratigraphy preserves: the dominant volcaniclastic sand (i.e. that in the outer grab buckets; an underlying clay (~2 cm), grading down into a silt and then coarse volcaniclastic sand, with pale coarse interbeds on a mm-scale (the whole sandy unit ~4 cm), then 3 cm of grey clay with a brown oxidised top, and a 3cm dark volcaniclastic sand with a normally graded silty top, underlain by 5mm clay and sand intebeds and a thicker (3.5 cm) dark volcaniclastic sand. Beneath this the material is dominated by dark sand, with discontinuous silty or clay rich intervals, but no well developed clean clays (unlike the sequence above). This lowest sandy unit may thus have been deposited over a short period. The whole sequence is interpreted as a series of volcaniclastic turbidites (rather than fall deposits, given internal structure, normal grading and mixed bioclasts; and the nearby source of multiple recent submarine eruptions), derived from Ritter (although alternative sources are also possible), and thus potentially providing a record of the post-1888 eruptive activity.

Figure 51: Interbedded volcaniclastic sands and clays in the central part of sample T1 (youngest unit to the right of the picture).

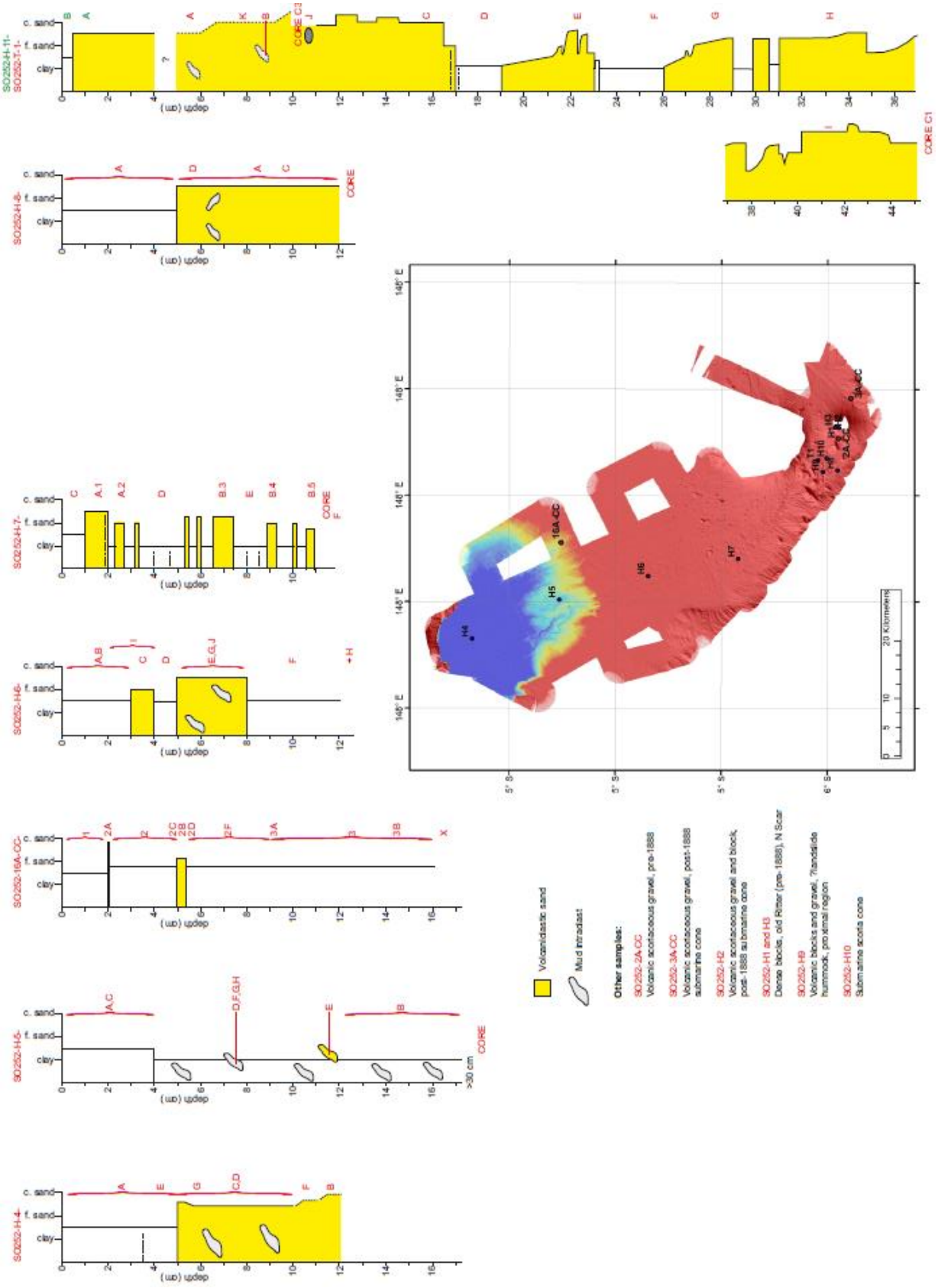

Figure 52: Summary stratigraphy for all recovered sediment sequences and sample list for successful SO252 sampling sites.

6.8 Gravity coring

Initial interpretations of the Ritter Island landslide deposit suggest a complex evolution of the landslide mass, involving incorporation of underlying seafloor sediment and resulting in discrete morphological facies through the region affected by the mass movement. In order to test the process of landslide deposition and transition, sediment coring sites were selected at several locations across the deposit. The aim of the coring was to collect samples of the sediment stratigraphy directly associated with the landslide (e.g. the distal turbidite deposits) and the stratigraphy that could provide additional context to understanding landslide behaviour (e.g. stratigraphy E of Ritter Island, providing a background record of volcanic activity at Ritter prior to the landslide; and samples of seafloor sediment outside the margins of the landslide deposit, providing information on the nature of the seafloor material incorporated within the landslide).

Previous attempts at sediment coring in the area used both a piston and gravity corer (Day et al., 2015; S. Day, pers. comm.), and failed to retrieve material with either approach. The sites attempted were in the medial part of the landslide deposit (W of the channel between Umboi and Sakar). A gravity corer was again used here, but given the past failure of this approach in sediments dominated by volcaniclastic sands, we selected sites beyond the thickest (and inferred coarsest) parts of the landslide deposit.

The gravity coring system used a 2 tonne weight attached to a 12.5 cm (internal diameter) steel core barrel, 5.75 m in length. This was lined with a PVC liner (5 + 0.75 m pieces) with the core catcher nailed into grooves at the end of the core barrel. The corer was lowered at 1 m/s to a height of 50 m above the seafloor. The winch then paused for 2 minutes at that height, to allow any swinging to dissipate, and then lowered again at 1 m/s to the seafloor. The winch tension was monitored: the first sharp drop was assumed to mark contact with the seafloor; a further 15 m was then paid out. The corer was heaved back at 0.2 m/s until the winch tension increased to downgoing values, and then to deck at 1 m/s.

Sites for coring were selected based on initial interpretations of the Ritter deposit using published maps and newly collected bathymetry and Parasound data. Nine core attempts were completed in total, from seven separate sites. None of these retrieved any material inside the core liner. Six of them recovered material within the core catcher. In every attempt, the winch tension showed a sharp spike after the initial drop, suggesting that the corer failed to penetrate deeply (i.e. beyond a few tens of cm at most) in the seafloor, and fell over. This was evident in several cases by mud and sand adhered to the outside of the core barrel. At each site, we infer that thick volcaniclastic sands or coarser sediment were present and prevented penetration into the seafloor.

Core sites and recovered samples are described below (Tab. 6). The sites were selected from a larger number of initial planned sites, and the site numbers are therefore not sequential. Cores were collected during two overnight shifts (local time) on 18th and 19th November 2016.

Table 6: Core sites and recovered samples.

Date UTC	Launch time UTC	CORE SITE	Core name	Rationale	Latitude	Longitude	Water Depth (m)	Core recovered (cm)	Core catcher sample
18/11/2016	09:30	CORE SITE 1	SO252-1-A	Volcanic stratigraphy E of Ritter	-5.4837	148.2034	1317	0	No
18/11/2016	11:15	CORE SITE 1	SO252-1-B	Volcanic stratigraphy E of Ritter	-5.4879	148.2132	1321	0	No
18/11/2016	13:49	CORE SITE 2	SO252-2-A	Volcanic stratigraphy E of Ritter	-5.5372	148.1534	1077	0	Yes
18/11/2016	16:03	CORE SITE 3	SO252-3-A	Stratigraphy at W foot of post-event cone	-5.5179	148.0908	706	0	Yes
18/11/2016	17:40	CORE SITE 4	SO252-4-A	Flat part of proximal debris avalanche deposit, S of Sakar	-5.4732	148.0643	904	0	Yes
19/11/2016	09:55	CORE SITE 13	SO252-13-A	Farthest mapped part of distal deposit (turbidite)	-4.8954	147.7605	1839	0	Yes
19/11/2016	11:45	CORE SITE 13	SO252-13-B	Farthest mapped part of distal deposit (turbidite)	-4.8954	147.7605	1839	0	Yes
19/11/2016	14:20	CORE SITE 19	SO252-19-A	Beyond lateral margins of debris flow (as visible on parasound)	-4.9519	147.8918	1833	0	No
19/11/2016	16:45	CORE SITE 16	SO252-16-A	At lateral margins of debris flow, where parasound suggests deposit is absent, exposing underlying sediment surface	-5.0821	147.9268	1821	0	Yes

6.9 Heat flow measurements

Experimental setup

To characterize the thermal state of crust surrounding the Ritter Island, we (Wu-Cheng Chi and Kuan-Ting Lin) have conducted heat flow measurements during the nights of 26 and 30 December. The original plan was to sample the background heat flow values from the east of the Ritter Island, then gradually move toward the Ritter Island, and then make two NE-SW transects to the NW of the Ritter Island (Fig. 53, 54; Tab 7, 8).

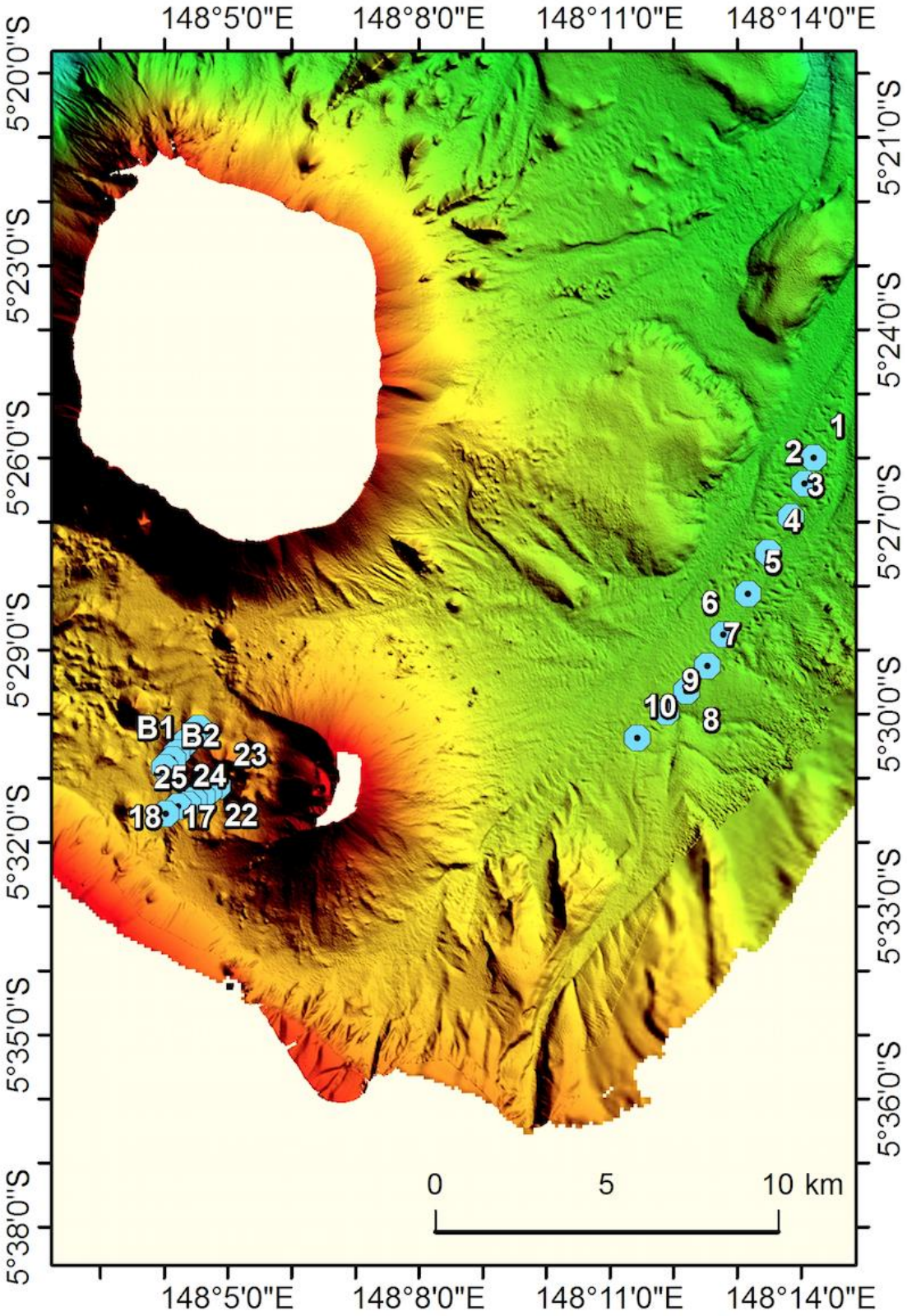

Figure 53: The location map of the heat flow stations
(the blue dots; the bathymetry of figure is based on a geotiff file).

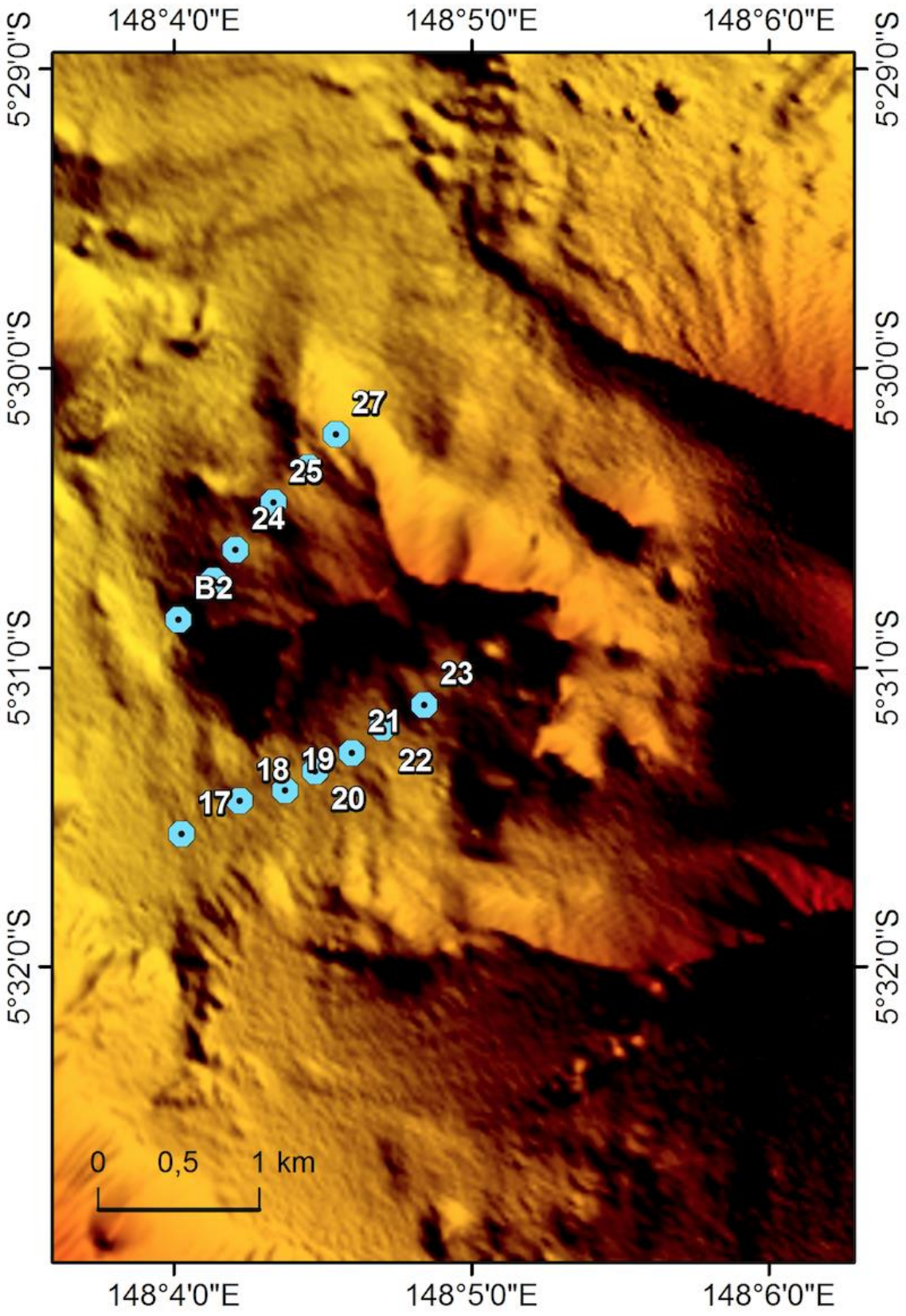

Figure 54: Zoom to the location map of the heat flow stations west of the Ritter Island (the blue dots; the bathymetry of figure is based on a geotiff file).

In situ sediment temperature and thermal conductivity measurements were conducted using a 6 m-long heat flow probe. The probe has a Lister-type violin bow design. The sensor strings contain 22 thermistors spaced at an interval of 26 cm and a heater wire along the entire length of the string. The electronics are integrated into the head of the probe. Four 8-channels 22-bit A/D converters are used to record temperature readings at a sampling interval of 1 s. The probe can be operated in an autonomous mode or with real-time data transmission when using the ship's coax wire. During this cruise, measurements were conducted with real-time data transmission in so called ‘pogo-style’, performing several penetrations in a row at small distances. Each penetration consisted of raising the probe some hundred meters above the sea floor from the previous penetration, slowly moving the ship to the next penetration site and letting the wire angle become nearly vertical before dropping the probe into the sediment for the next penetration. Once the probe had penetrated the seafloor, it was left undisturbed for 7 minutes for the sediment temperature measurement and another 7 minutes, in case a thermal conductivity measurement was conducted. For the spacing of stations used in this survey, the transit between measurements took between 30 and 120 minutes. Transit speed was governed by the trade-off between keeping the wire angle small and minimizing the time between measurements.

Winch speed during payout and retrieval of wire was 1 m/s. Deployment of the instrument was from amid ship on the starboard side, employing a beam crane and assistance crane. This procedure ensured safe operation even during medium sea state and minimum interference due to the ships vertical movement during station work. For precise positioning of the probe at the seafloor, an IXSEA Posidonia transponder was mounted on the wire 100 m above the instrument. The IXSEA Oceanos Abyss positioning system was used to track the probe at depth.

Totally, 11+12=23 measurements have been attempted (Tab. 7, 8). However, due to the hard sea bottom of the survey area, only one successful penetration has been achieved. It has been difficult to conduct heat flow measurements in the survey area. It appears the only possible way to obtain heat flow information in the study area is to conduct sea floor drilling.

Preliminary Results

At station 9 on 26 December (5°29.972S, 148°11.889E) we were able to retreat some heat flow data (Fig. 55). Five thermistors have recorded the frictional heating when the lance entered into the seafloor. Preliminary results give a very high geothermal gradient (0.13 K/1.3 m = 0.1 K/m), and a thermal conductivity of 1.3 W/mK, translating to a heat flow of 0.13 W/m^2.

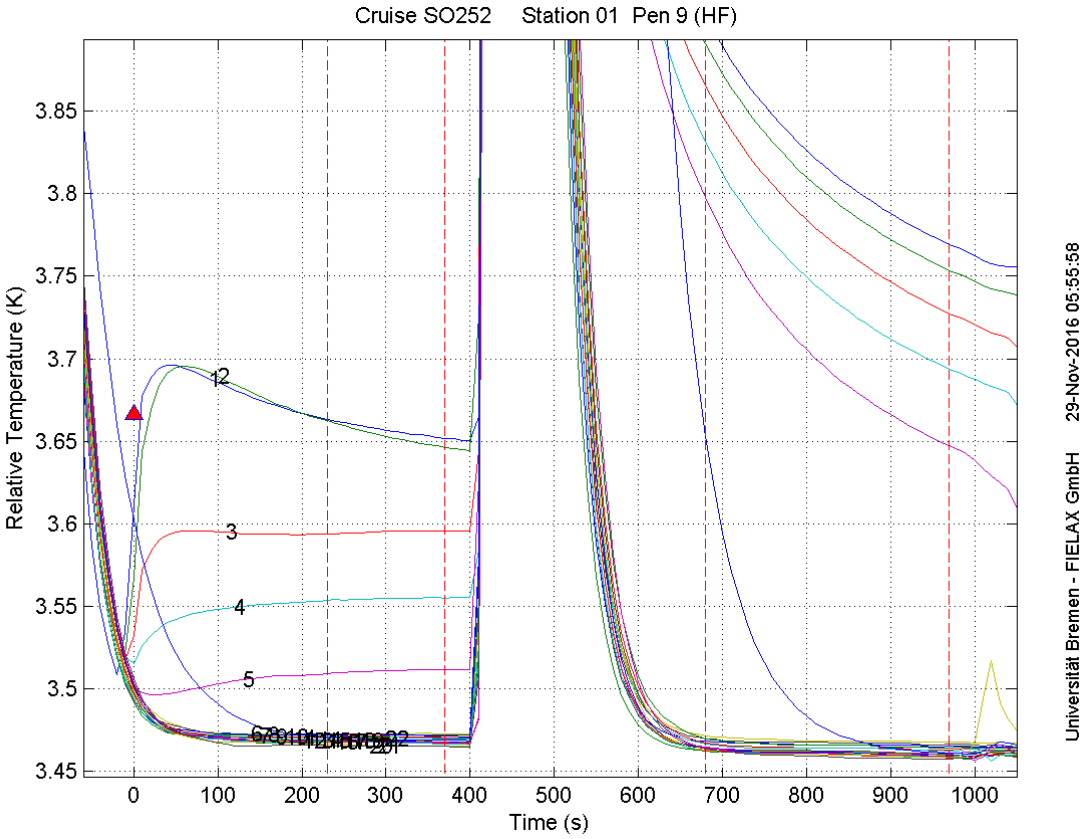

Figure 55: Temperature as a function of time for heat flow measurements at station 9. Temperature data from the first time window (marked by dashed brown lines) are used to derive the ambient temperature at different subbottom depths, and thus the geothermal grad gradient (>0.0223 K/m). A heat pulse was generated at 400 sec to use the temperature decay rate to derive the thermal conductivity. Date from the second time window were fitted to derive a very preliminary thermal conductivity (1.35 W/mK).

Table 7: Heat flow stations, date 26.11.2016

Heat flow – Ritter Island

Station:								Date: 2016/11/26	
Penetration	Latitude	Longitude	Water Depth [m]	HP	Time in [hh:mm:ss]	Time out [hh:mm:ss]	Wire out [m]	Remarks	String #
calibration	5°26.003	148°14.202	1431		10:29	10:34	1300		
01	5°26.003	148°14.202	1432	x	10:42:31	10:59:12	1447	First try failed, this is second try.	
02	5°26.407	148°14.066	1418	x	11:48:40	12:04:20	1436	§	
03	5°26.926	148°13.851	1400	x	13:23:40	13:39:40	1419		
04	5°27.479	148°13.488	1380	x	14:30:55	14:46:40	1397		
05	5°28.127	148°13.175	1377	x	15:43:20	15:59:20	1398	§ *	
06	5°28.757	148°12.785	1347	x	17:45:40	18:01:10	1370	Failed?	
07	5°29.252	148°12.533	1321	x	18:48:00	19:03:20	1344	Failed?	
08	5°29.643	148°12.211	1298	x	19:46:10	20:02:00	1321	Failed?	
09	5°29.972	148°11.889	1286	x	20:44:40	21:01:30	1310	Success!?	
10	5°30.375	148°11.435	1245	x	21:43:30	21:44	1264	Failed?+	
11									
12									
13									
14									
15									
16									

§ Check the heat flow probe on the sea surface after the penetration. Good.
* Heat flow probe fasten next to the deck while moving to the next waypoint.

Table 8: Heat flow stations, date 30.11.2016

Heat flow – Ritter Island

Station: West								Date: 2016/11/30	
Penetration	Latitude	Longitude	Water Depth [m]	HP	Time in [hh:mm:ss]	Time out [hh:mm:ss]	Wire out [m]	Remarks	String #
23	5°31.125	148°4.843	792			12:49:10	810	Failed. (Reverse sites sequence)	
22	5°31.202	148°4.702	822	x	13:16:20	13:32:50	840	Success? Small angle?	
21	5°31.285	148°4.599	834		13:55:30	13:56:40	845	Failed.	
20	5°31.348	148°4.475	848		14:22:50	14:24:20	860	Failed.	
19	5°31.412	148°4.375	855		14:50:00	14:51:20	866	Failed.	
18	5°31.446	148°4.223	870		15:18:00	15:19:10	884	Failed.	
17	5°31.557	148°4.027	883	x	15:47:50	16:04:15	902	Not sure.	
								§*Probe on deck and move.	
27	5°30.221	148°4.546	799		17:48:10	17:49:30	814	Failed.	
26	5°30.332	148°4.452	792		18:16:00	18:32:00	807	Not sure.	
25	5°30.450	148°4.335	803		19:03:00	19:18:40	816	Not good.	
24	5°30.607	148°4.208	833		19:44:20	19:46:00	846	Failed.	
B1	5°30.709	148°4.133	860		20:10:20	20:11:40	869	Failed.	
					20:30:00			USBL stock? ++++++++++++++++	
B2	5°30.840	148°4.015	904		20:47:00	20:48:20	920	Ship location.	
B3									
B4									

§ Check the heat flow probe on the sea surface after the penetration. Good.

6.10 Air-borne drone survey

During SO252 we used a DJI Phantom 4 drone. The drone is equipped with a HD camera and can travel as far as 5 km. The maximum flight altitude was set to 180 m. The video data were recorded as mp4 movie files including subtitles to record the position of the drone at any time.

We operated the drone six times. During the first two flights we surveyed the eastern flank of Ritter Island, but only the first of these recorded data because recording was not switched on during the second flight. The third flight was used to survey the P-Cable system from above to understand better how the system is towing. The fourth and fifth flight were used to survey the western flank of Ritter Island. During the six flight we checked the P-Cable system to check the new rigging of the lead-in cables improved the towing behaviour which was indeed the case. Unfortunately the drone crashed during the attempt to land it on the moving vessel, collided with the A-frame and fell into the water which led to a loss of the drone.

The video images are now being evaluated for constructing a 3D model of Ritter Island by extracting still images and using a 3D reconstruction software (Fig. 56).

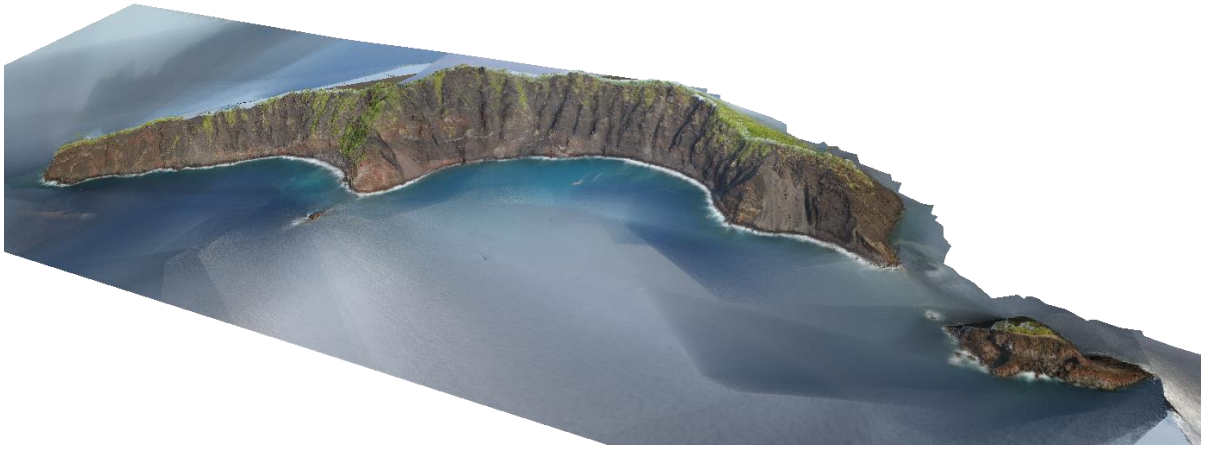

Figure 56: 3D-model of the western side of Ritter Island constructed from drone images.

6.11 CTD Mariana Trench

Time span: Thursday 10 November 10 UTC – Friday 11 November 10 UTC.
Location: around 11°20´N, 142°11´E.
Aim: to collect shipborne CTD data to great depths of about 10,850 m and to deploy a 7 km long mooring with current meters and two sets of high-resolution temperature sensors near the deepest point on Earth.
Purpose: to study internal wave turbulence processes in deep trenches to understand the existence of life near their bottom.

On Thursday 10 November, early night local time, the R/V Sonne arrived above the Challenger Deep, the southern extension of the Mariana Trench arc. Steaming with its advanced EM122 Multibeam echosounder system, a sweep was made over the Challenger Deep to establish its deepest point for activities (Fig. 24). The days before, the overboard instrumentation had been prepared by the crew. This involved the lay-out of mooring winch, cable drums, buoys and instruments on the aft-deck. The ship's Conductivity-Temperature-Depth CTD is unsuitable for the activities as it is rated to 6,000 m. It was thus completely stripped and replaced by a 10,500 m rated CTD on loan from Detlev Quadfasel/University of Hamburg and connected to the ship's 12 km-long 18 mm-diameter steel cable with optic fiber. The CTD was placed in horizontal position on the bottom of Rosette frame, as is common on R/V Sonne.

At 11:50 UTC (21:50 LT) the CTD was lowered into the water at 11°19.75´N, 142°11.26´E to 8,000 m, the greatest depth possible without damaging the pressure sensor. After being brought back to deck, the pressure sensor was blocked by replacing its oil-filled entrance to the capillary by a custom-made dummy plug. At 18:05 UTC the CTD was lowered again into the water, this time for its journey to the bottom of the Challenger Deep. It was the second CTD-cast to great depths of the Challenger Deep, after the one described by Taira et al. (2005). The length of cable out, checked against CTD-depth during the first cast, was used for depth determination. As the exact water depth was not known at the time, because the Multibeam data were only later corrected with the local sound velocity profile from the same CTD data, it was decided to stop the CTD at 10,850 m. This is 56±12 m from the bottom. Except for two single spikes, the CTD-data are flawless.

Figure 57: Deployment of the top-buoy of the 7 km long mooring. In the center, the spooling winch with the first 2,000 m of Dyneema rope. To the right, the first drum with 200 m cable holding 100 temperature sensors.

On Friday 11 November around 02 UTC, R/V Sonne was 15 km south-southwest from the CTD-site, steaming at about 1 knot in NNE direction for the mooring deployment. The top-buoy went first into the water (Fig. 57), followed by 2,000 m of Dyneema rope. No steel cable was used for this length, because of the heavy weight. After spooling the rope, drums were exchanged in the spooling winch and the first section of high-resolution temperature sensors were spooled into the water. This was repeated for the other mooring parts (Fig. 58), until the acoustic releases and the bottom weight were reached. These occured just after 06:30 UTC, when R/V Sonne was at 2.5 km from the CTD-site towing a nearly 7 km-long cable behind it. A further one hour of steaming later and some 600 m beyond the target point, the weight was dropped in free fall: at 09:39 UTC, 11°20.09´N, 142°11.33´E. It was estimated to fall 600 m into the direction of the top-buoys, landing some two hours later near the target spot to establish the longest ocean mooring ever deployed. The near-bottom instrumentation, consisting of two acoustic releases and a 600 m-long cable holding 300 temperature sensors have to withstand an ambient static pressure of some 1,100 bars. Triangulation for precise position establishment was not possible considering the great depth and the 12 km maximum range of the acoustic releases. Instead, the shut-down of satellite transmission from the top-buoy is considered sufficient knowledge that the mooring is indeed under water. It will stay there for a period of 1-2 years before recovery. The entire operation went very smoothly, with an experienced crew.

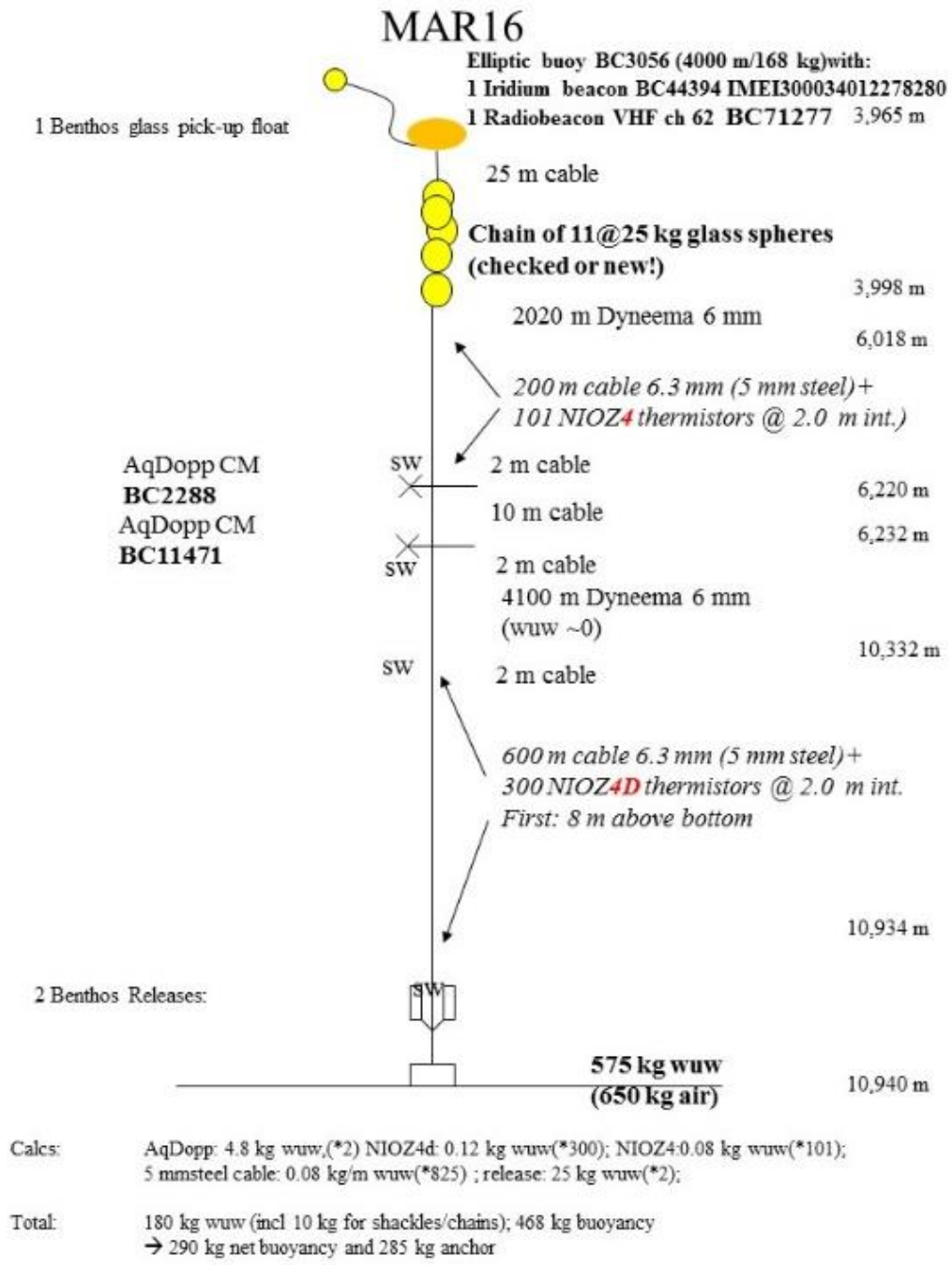

Figure 58: Sketch of the 7 km long mooring with current meters and high-resolution temperature sensors.

Preliminary results

The bottom topography is re-analyzed after inserting the sound velocity profile from the local CTD-data. It results in a new position and new depth for the deepest point, with respect to the most recent estimate by Gardner et al. 2014 of the University of New Hampshire (NH in Figure 59). The new point (Fig. 59) is 400 m northeast from and 60 m less deep than NH. The newly established deepest point is at 10,925±12 m, 11° 19.945'N, 142° 12.123'E.

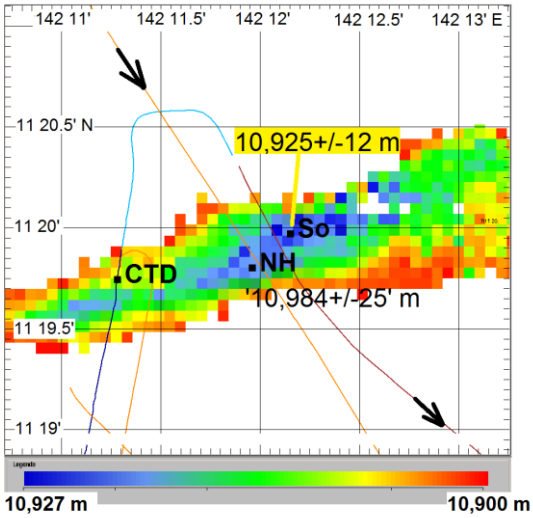

Figure 59: Detail of R/V Sonne's Multibeam map of the deepest area in the Challenger Deep, with depths only coloured when greater than 10,900 m. CTD indicates the site of our operations. NH indicates the deepest point established by Gardner et al. (2014). So indicates the deepest point in this map.

The CTD-data result in an improvement over the data obtained by Taira et al. (2005), who showed profiles of density and salinity that are unrealistically unstable over 2,000 m below 6,000 m. Like the Taira et al. (2005) profiles, the present temperature profile decreases with depth, which, given the salinity increase with depth, provides a stable weak stratification towards the bottom (Fig. 60). This is very useful information for establishing the temperature-density relationship for the moored temperature sensors. In this case, temperature can be used as a tracer for density to estimate turbulence parameters using the method of reordering density profiles into statically stable ones.

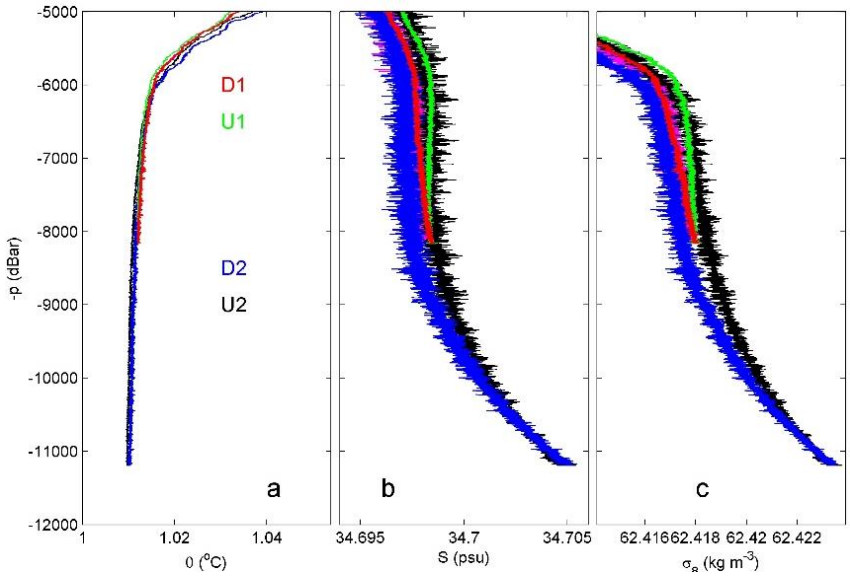

Figure 60: Lower 6,000 dbar detail of the 2016 CTD-profiles from the Challenger Deep for comparison with Figs 5 and 6 in Taira et al. (2005). In red and green, the down- and up-profiles of cast 1, respectively. In blue and black, down- and upcasts for cast 2, respectively. In blue and black, down- and upcasts for cast 2, res respectively. Cast 2-data are noisier than cast 1, because of the coupling with winch-cable data in which no correction is made for ship's motions. (a) Potential temperature. (b) Practical salinity, with the horizontal axis range matching that of (a) in terms of contributions to density variations. (c) Potential density anomaly, referenced to the 8000 dbar.

Turbulence parameters are also estimated using the CTD-data, after considerable filtering of the ship's motions (Fig. 61). Near the bottom, the relatively strong stratification allows little vertical exchange with turbulence values comparable with those from the open ocean. Between 6,000 and 8,000 m stratification is weakest, although still not homogeneously mixed. There, turbulence values are an order of magnitude larger than near the bottom, allowing for considerable vertical exchange generated by vertical overturns larger than 100 m. The future mooring data details are needed to establish the dominant processes generating this turbulence. From previous similar mooring deployment in the Puerto Rico Trench it is expected to be a combination of tidal and inertial internal wave motions coming from above and interacting with larger scale flows through the trench (van Haren and Gostiaux, 2016). Such analysis for the Challenger Deep has to await at least one year.

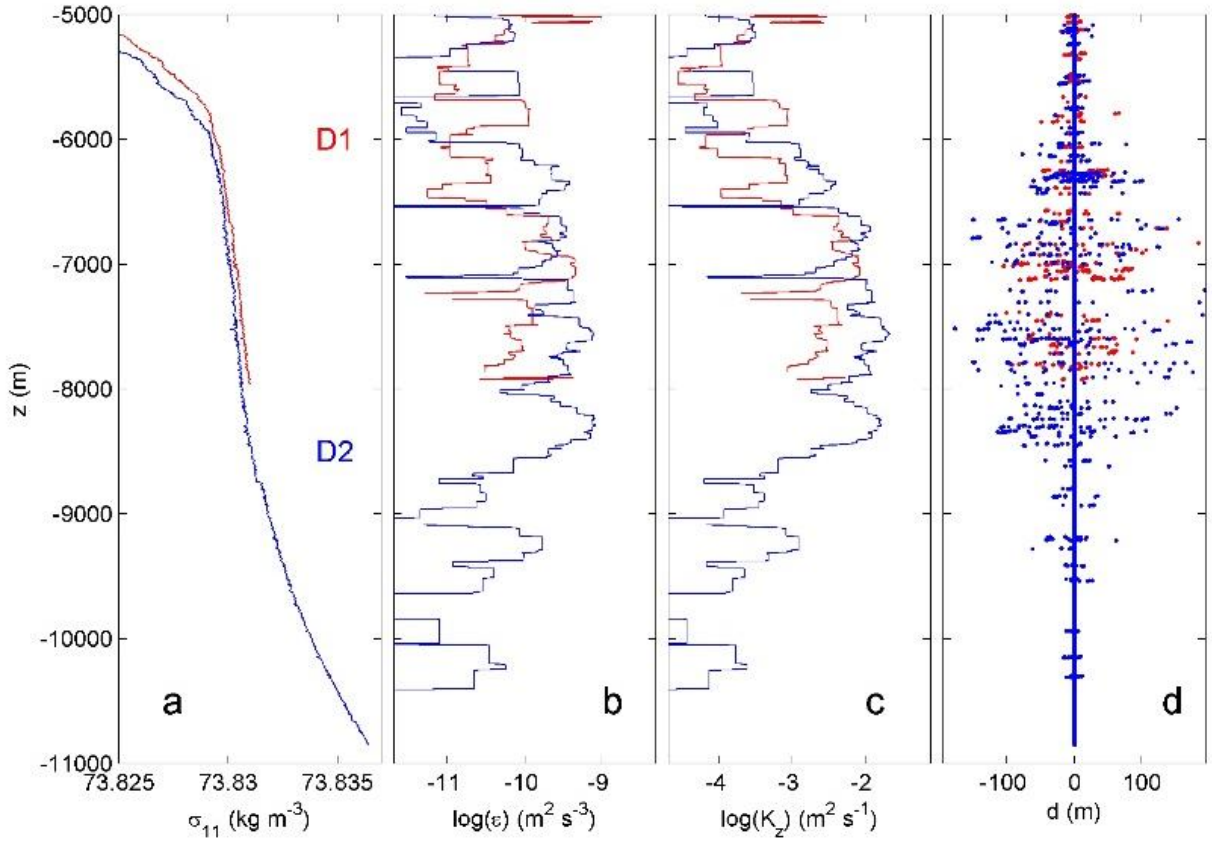

Figure 61: Lower 6,000 m of turbulence characteristics computed from <0.05 cps low-pass filtered downcast data applying a threshold of 7x10-5 kg m-3. In red CTD-cast 1, in blue cast 2. (a) Unordered, 'raw' profile of density anomaly referenced to 11,000 dbar. (b) Logarithm of dissipation rate computed from the profiles in (a), averaged over 200 m intervals. (c) As (b), but for eddy diffusivity. (d) Overturn displacements following reordering of the profiles in (a).

7. Acknowledgements / Danksagung

We thank the Federal Ministry of Education and Science (BMBF)'s SONNE program for funding the expedition. We would also like to thank the master and the ship's crew of R/V Sonne for their relentless support and making our research possible. We would also like to thank Prof. Russel Perembo of the University of Papua New Guinea, Prof. Eli Silver of University of California Santa Cruz, and Dr. Simon Day of University College London for their help during cruise planning, as well as Dr. Morelia Urlaub (GEOMAR) and Dr. Sascha Bruhne (GFZ-Potsdam) during preparation of the cruise.

Figure 62: Science crew of SO252. Photographer: Lars Hoffsommer.

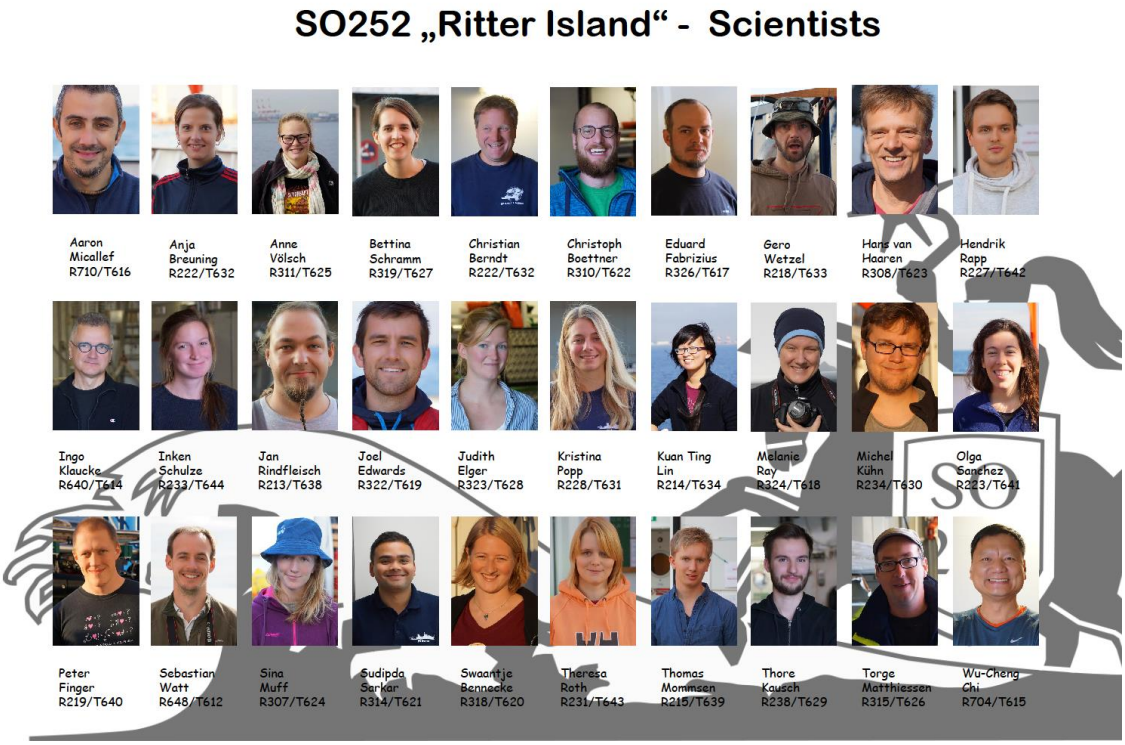

Figure 63: Cruise poster SO252. Created by Theresa Roth, Michel Kühn, Thomas Mommsen.

8. References / Literaturverzeichnis

Baldwin SL, Fitzgerald PG and Webb LE 2012. Tectonics of the New Guinea region. Annual Review of Earth and Planetary Sciences 40: 495-520.

Berndt C et al 2009. Tsunami modeling of a submarine landslide in the Fram Strait. Geochemistry Geophysics Geosystems, 10, 4.

Brune S et al 2009. Submarine landslides at the eastern Sunda margin: observations and tsunami impact assessment. Natural Hazards, 54, 2, 547-562.

Brune S et al 2010. Hazard assessment of underwater landslide-generated tsunamis: a case study in the Padang region, Indonesia. Natural Hazards, 53, 2, 205-218.

Cooke RJS 1981. Eruptive history of the volcano at Ritter Island. Geol Surv Papua New Guinea Mem, 10:115-124.

Day, S., Llanes, P., Silver, E., Hoffmann, G., Ward, S., & Driscoll, N. (2015). Submarine landslide deposits of the historical lateral collapse of Ritter Island, Papua New Guinea. Marine and Petroleum Geology, 67, 419-438.

Dugan B 2012. Petrophysical and consolidation behavior of mass transport deposits from the northern Gulf of Mexico, IODP Expedition 308. Marine Geology, 315, 98-107.

Gardner et al. 2014. So, How Deep Is the Mariana Trench? Marine Geodesy, 37:1-13.

Gardner et al. 2014. So, How Deep Is the Mariana Trench? Marine Geodesy, 37:1-13.

Harbitz CB, Løvholt F and Bungum H 2013. Submarine landslide tsunamis: how extreme and how likely? Natural Hazards: 1-34.

Hunt JE et al 2011. Sedimentological and geochemical evidence for multistage failure of volcanic island landslides: A case study from Icod landslide on north Tenerife, Canary Islands. Geochem.Geophys. Geosyst., 12:Q12007.

Imamura F 1997. Long waves in two layer, governing equations and numerical model. Sci Tsunami Hazards 13:3–24.

Johnson RW 1987. Large-scale volcanic cone collapse: the 1888 slope failure of Ritter volcano, and other examples from Papua New Guinea. Bull Volc, 49: 669-679.

Leroueil S 2001. Natural slopes and cuts: movement and failure mechanisms. Geotechnique, 51(3), 197-243.

Løvholt F, Pedersen G and Gisler G 2008. Oceanic propagation of a potential tsunami from the La Palma Island. Journal of Geophysical Research: Oceans (1978–2012) 113.C9.

Nakanishi, M., & Hashimoto, J. (2011). A precise bathymetric map of the world's deepest seafloor, Challenger Deep in the Mariana Trench. Marine Geophysical Research, 32(4), 455-463.

Silver E et al. 2005. Island arc debris avalanches and tsunami generation. Eos, Transactions American Geophysical Union, 86(47), 485-489.

Silver E et al. 2009. Volcano collapse and tsunami generation in the Bismarck Volcanic Arc, Papua New Guinea. J Volc Geotherm Res, 186: 210-222. Taira et al. 2005. J. Oceanogr., 60: 919-926.

Taira et al. 2005. Super-deep CTD Measurements in the Izu-Ogasawara Trench and a Comparison of Geostrophic Shears with Direct Measurements. J. Oceanogr., 60: 919-926

van Haren and Gostiaux, Convective mixing by internal waves in the Puerto Rico Trench. J. 2016. Mar. Res., 74: 161-173.

Voight B et al 1981. Catastrophic rockslide avalanche of May 18. US Geol. Surv. Prof. Pap, 1250, 347-378.

Ward SN and Day S 2003. Ritter Island Volcano— lateral collapse and the tsunami of 1888. Geophysical Journal International, 154(3), 891-902.

Watt SFL et al 2012. Relationships between volcanic failure, sediment accumulation and landslide generation offshore Montserrat, Lesser Antilles. Marine Geology, 323–325, 69–94.

Waythomas, CF et al 2009. Pacific Basin tsunami hazards associated with mass flows in the Aleutian arc of Alaska. Quaternary Science Reviews 28.11: 1006-1019.

Yamazaki Y et al 2012. Surges along the Honolulu coast from the 2011 Tohoku tsunami. Geophysical Research Letters 39.

9. Abbreviations / Abkürzungen

AD	analog-to-digital	**HyFOS**	HyBis with the OFOS video sledge
AUV	Autonomous Underwater Vehicle	**NH**	New Hampshire
AVG	angle varying gain	**NMO**	normal moveout
CSIRO	Commonwealth Scientific and Industrial Research Organisation	**OBS**	Ocean Bottom Seismometer
CTD	Conductivity, Temperature, Depth	**OFOS**	Ocean Floor Observation System
CW	Continuous Wave	**RU**	Remote Units
DGPS	Differential Global Positioning System	**SIS**	Seafloor Information System
FM	Frequency Modulated	**SLF**	secondary low frequency
GEBCO	General Bathymetric Chart of the Oceans	**TCP/IP**	Transmission Control Protocol/Internet Protocol
GI-Gun	Generator Injector Gun	**TVG**	time varying gain
GMT	Generic Mapping Tools	**USBL**	Ultra Short Baseline
GPS	Global Positioning System		

10. Appendices / Anhänge

Appendix A: Participating Institutions / Liste der teilnehmenden Institutionen

GEOMAR Helmholtz-Zentrum für Ozeanforschung Kiel
Kiel
Germany

University of Birmingham (**UBirmingham**)
Birmingham
U.K.

NIOZ - Royal Netherlandic Institute for Sea Research
Texel
The Netherlands

UCL - University College London
London
U.K.

University of Malta
La Valleta
Malta

Academia Sinica (**SINICA**)
Taipei
Taiwan

IEO - Spanish Institute of Oceanography
Malaga
Spain

UC Santa Cruz – University California Santa Cruz
Santa Cruz
U.S.A.

Geoforschungszentrum Potsdam (**GFZ**)
Potsdam
Germany

Appendix B: OBS Protocols / OBS Protokolle

Station	Latitude	Longitude	Depth *[m]*	Deployment	Recovery	Skew *[ms]*	Recorder
OBS1	5°29,365'S	148°03,365'E	1148	16.11.2016	26.11.2016	-255	MBS
OBS2	5°31,044'S	148°09,342'E	1129	16.11.2016	27.11.2016	-251	MBS
OBS3	5°33,074'S	148°08,561'E	968	16.11.2016	26.11.2016	32	MBS
OBS4	5°33,916'S	148°07,838'E	902	16.11.2016	26.11.2016	-	MBS
OBS5	5°31,583'S	148°04,438'E	844	16.11.2016	26.11.2016	8	MBS
OBS6	5°31,166'S	148°04,053'E	853	16.11.2016	26.11.2016	38	MBS
OBS7	5°30,699'S	148°03,720'E	913	16.11.2016	26.11.2016	86	MBS
OBS8	5°30,340'S	148°03,691'E	926	16.11.2016	26.11.2016	17	MBS
OBS9	5°29,898'S	148°03,207'E	957	16.11.2016	26.11.2016	49	MBS
OBS10	5°29,448'S	148°02,899'E	952	16.11.2016	26.11.2016	19	MBS
OBS11	5°28,992'S	148°02,408'E	960	16.11.2016	26.11.2016	-	MBS
Trigger	-	-	-	16.11.2016	28.11.2016	-18	MBS

Appendix C: Biological sampling summary

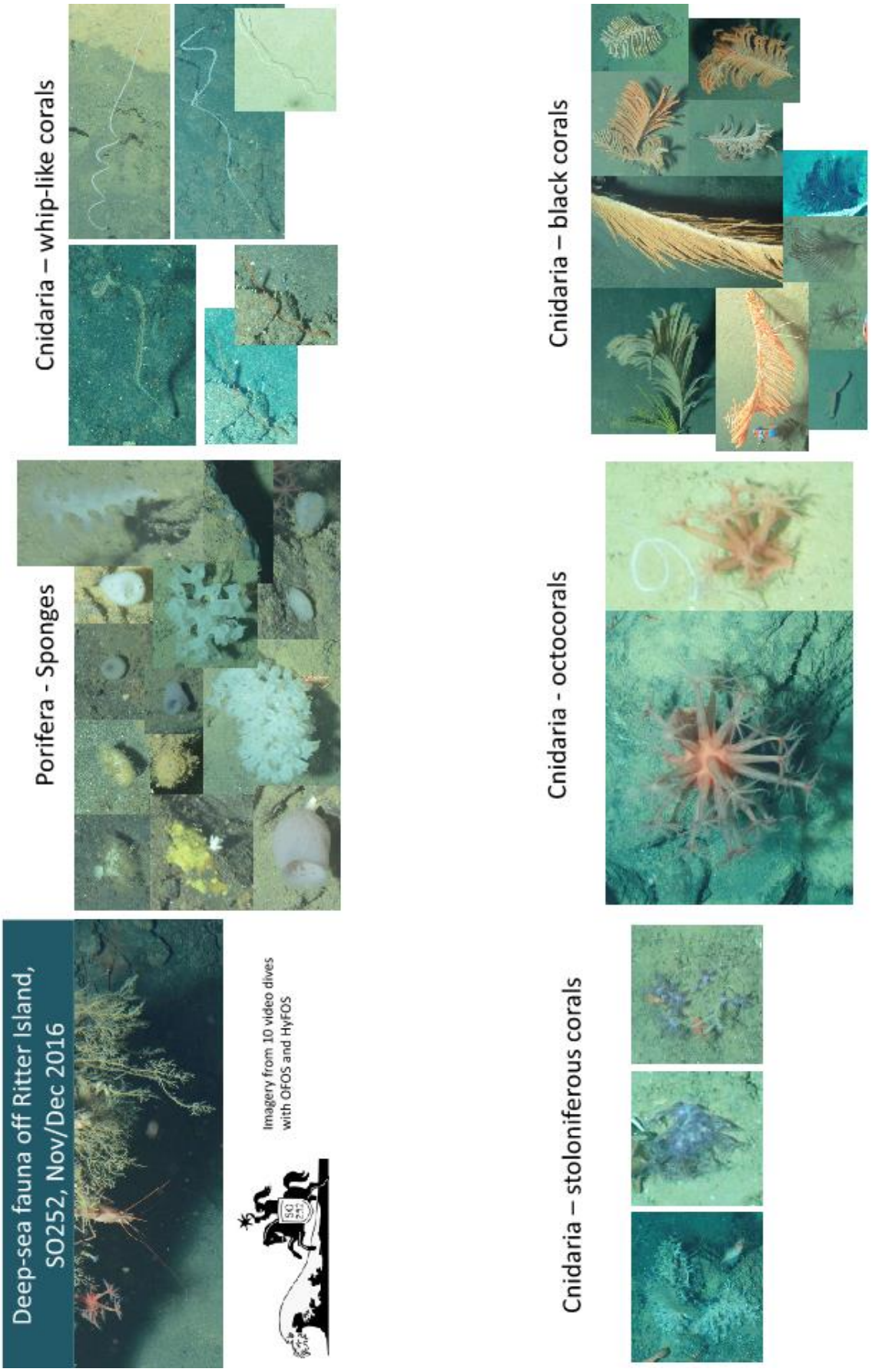

Cnidaria – bamboo corals

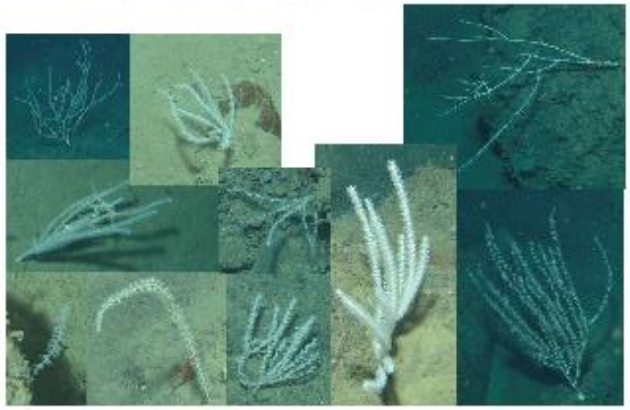

Cnidaria – bamboo corals

Cnidaria – stony corals

Cnidaria - octocorals

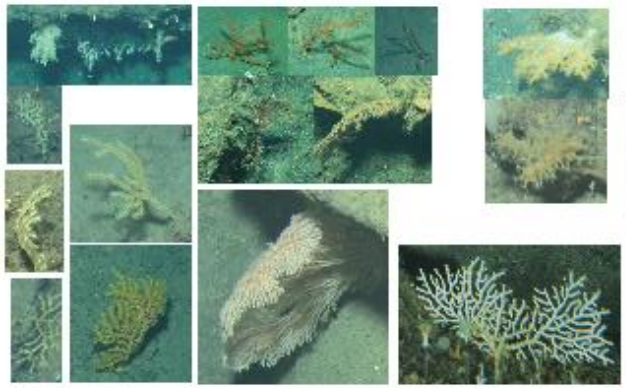

Cnidaria - corals

Cnidaria - corals

Cnidaria - corals

Cnidaria - corals

Cnidaria - corals

Cnidaria - corals

Cnidaria - corals

Cnidaria - corals
Cnidaria - corals
Cnidaria - corals
Cnidaria – anemones
Cnidaria - corals
Cnidaria - corals

Cnidaria
Cnidaria – colonial anemones
Cnidaria – anemones
Cnidaria - Siphonophores
Cnidaria
Cnidaria – jelly fish

Molluscs

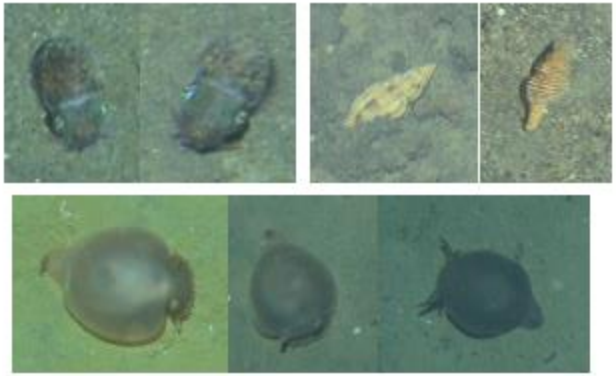

Annelida

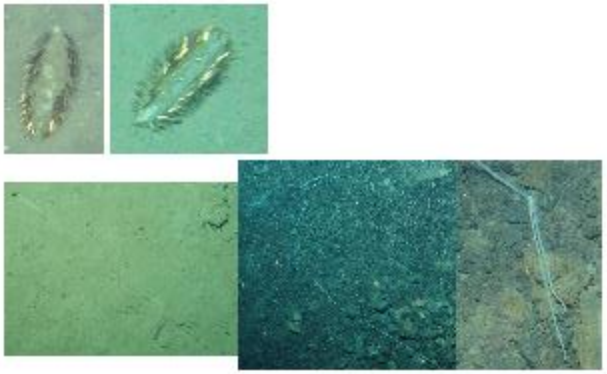

Arthropoda - Crustacea

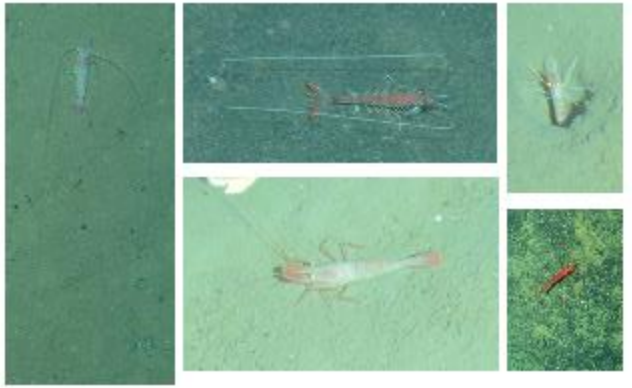

Arthropoda - Crustacea

Arthropoda - Crustacea

Arthropoda - Crustacea

Arthropoda - Crustacea

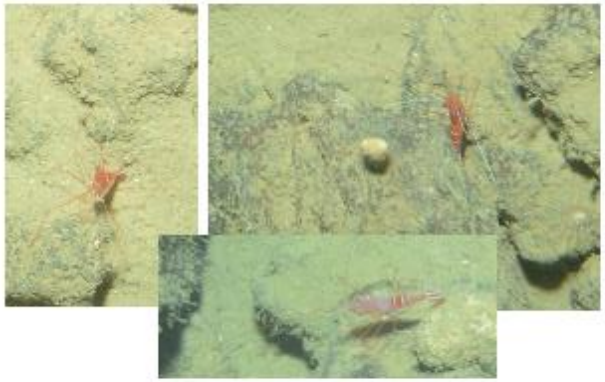

Arthropoda - Crustacea

Arthropoda - Crustacea

Arthropoda - Crustacea

Arthropoda - Crustacea

Arthropoda - Crustacea

Arthropoda - Crustacea
Arthropoda
Arthropoda - Crustacea
Arthropoda – hermit crabs
Echinoderms - starfish
Arthropoda - Crustacea

Echinoderms – sea lilies

Echinoderms – sea urchins

Echinoderms – sea lilies

Echinoderms – sea urchins

Echinoderms - crinoids

Echinoderms – brittle stars

Echinoderms – sea cucumbers
Echinoderms – sea cucumbers
Echinoderms – sea urchins
Chordata - fish
Chordata - fish
Chordata - fish

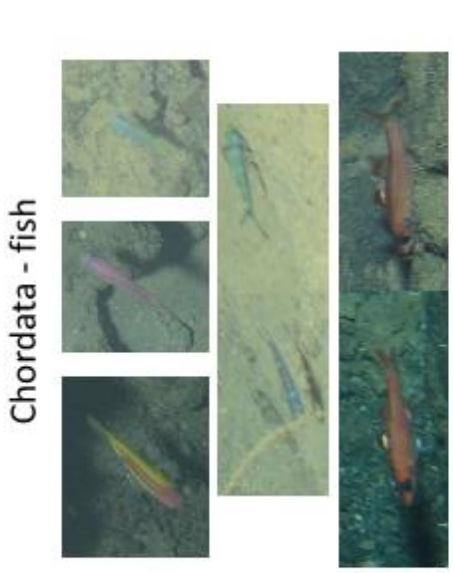
Chordata - fish

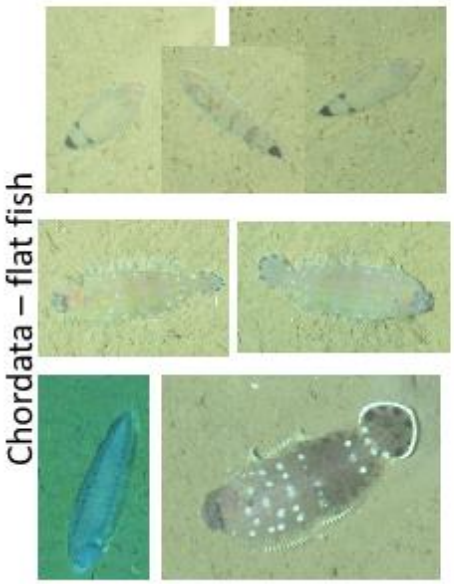
Chordata – flat fish

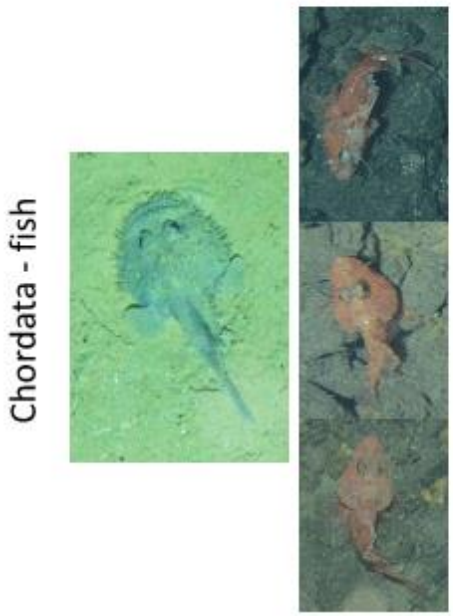
Chordata - fish

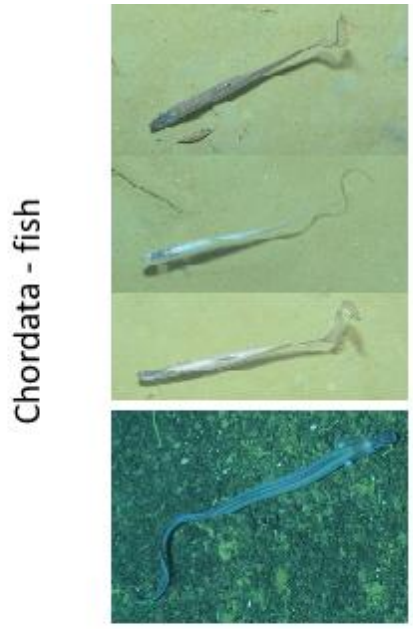
Chordata - fish

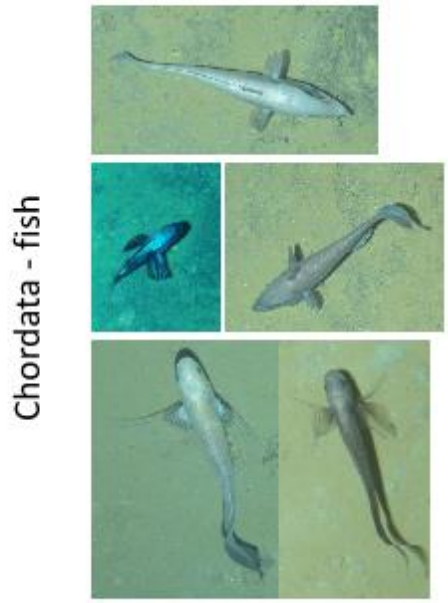
Chordata - fish

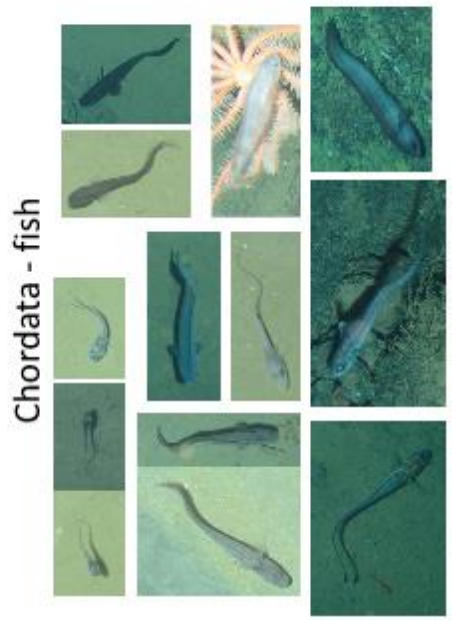
Chordata - fish

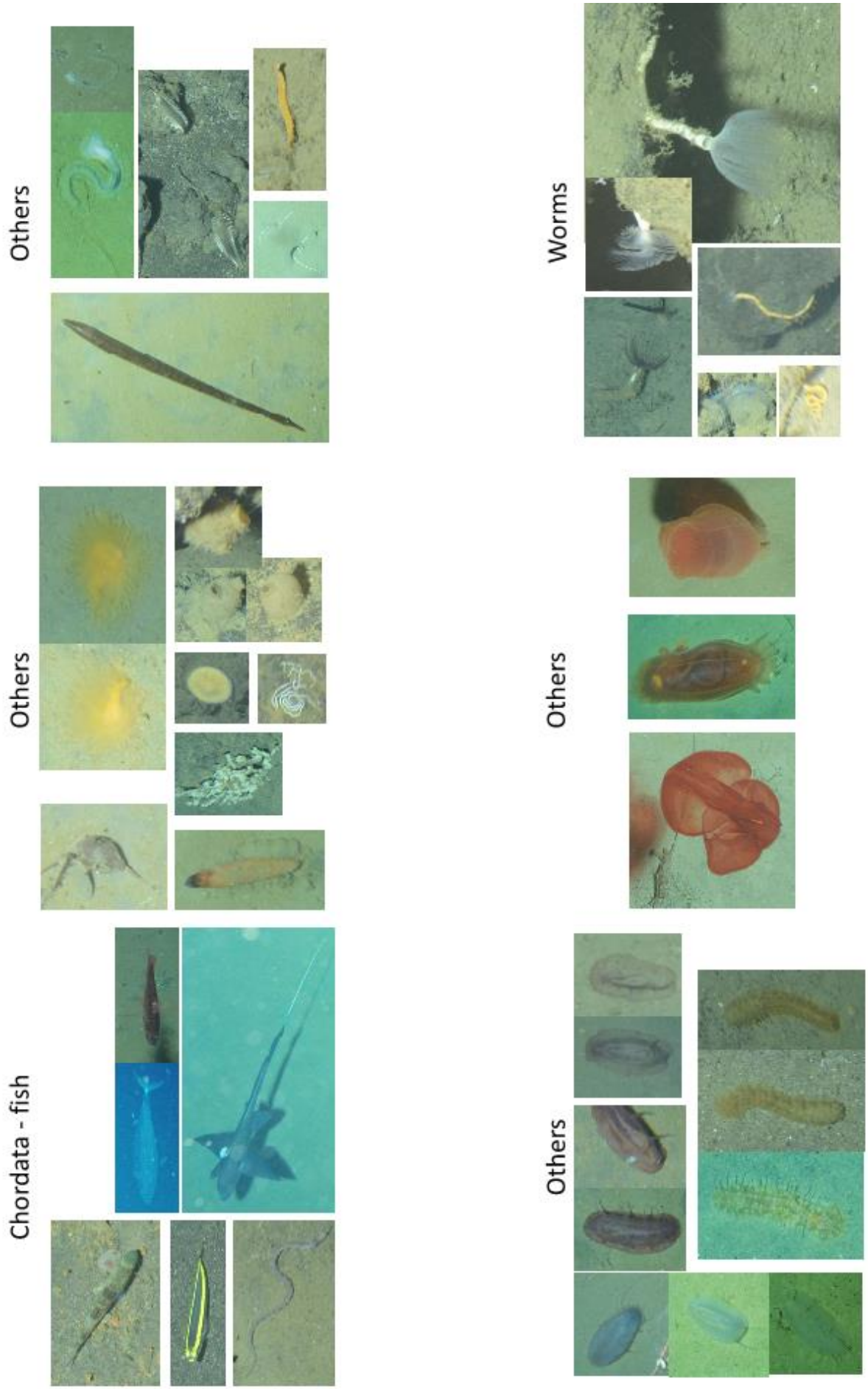
Others
Others
Chordata - fish
Worms
Others
Others

Wood with legs

Appendix D: Station List / Stationsliste

Abkürzungen / Abbreviation		**Eingesetzte Geräte / Equiopment used**	**Einsätze / tasks**	
z.W	zu Wasser / into water			
a.D.	an Deck / on deck	CTD	3	
Slmax	(maximale) Seillänge / max. rope-length	Verankerung	1	
LT	Lottiefe nach EM 122 / Depth of EM 122	Drohne	4	
W ...	eingesetzte Winde / Winch used	2D-Seismik	3	
nm	Seemeilen / nautical miles	3D-Seismik	3	
EM/PS	SIMRAD Multibeam / Parasound	Heat Flow	23	
rwk / COG:	Rechtweisender Kurs / true course	Schwerelot	10	
d:	Distanz / distance	Hybis	17	
v:	Geschwindigkeit in Knoten / SOG in knots	OBS auslegen	1	11 Stück
SL:	Seillänge / rope-length	OBS einholen	1	11 Stück
SZ:	Seilzug / rope tension	Parasound-Profil	1	
		OFOS	7	
		EM 122-Profil	10	
		TV-Greifer	1	
		Σ	85	
		Geräteverluste / lost Equipment:	1 Drohne	

Station	Date / Time UTC	Device	Device Abbreviation	Action	Latitude	Longitude	Depth (m)
SO252_2-1	10/11/2016 22:00:00	Autonomous Underwater Vehicle	AUV	station start	11° 19,751' N	142° 11,278' E	10885
SO252_2-1	10/11/2016 22:01:12	Autonomous Underwater Vehicle	AUV	profile start	11° 19,750' N	142° 11,278' E	10884.1
SO252_2-1	10/11/2016 22:11:31	Autonomous Underwater Vehicle	AUV	on deck	11° 19,754' N	142° 11,276' E	10882.1
SO252_2-1	10/11/2016 22:12:47	Autonomous Underwater Vehicle	AUV	station end	11° 19,754' N	142° 11,275' E	10882.7
SO252_1-1	10/11/2016 11:46:12	CTD	CTD	station start	11° 19,738' N	142° 11,244' E	10884.9
SO252_1-1	10/11/2016 11:48:48	CTD	CTD	in the water	11° 19,744' N	142° 11,257' E	10880.8
SO252_1-1	10/11/2016 15:12:19	CTD	CTD	max depth/on ground	11° 19,755' N	142° 11,278' E	10884.5
SO252_1-1	10/11/2016 15:18:59	CTD	CTD	hoisting	11° 19,756' N	142° 11,278' E	10891.7
SO252_1-1	10/11/2016 17:42:52	CTD	CTD	on deck	11° 19,755' N	142° 11,279' E	10885.8
SO252_1-1	10/11/2016 17:44:00	CTD	CTD	station end	11° 19,753' N	142° 11,278' E	10884.3
SO252_1-2	10/11/2016 18:02:35	CTD	CTD	station start	11° 19,757' N	142° 11,278' E	10884.9
SO252_1-2	10/11/2016 18:04:21	CTD	CTD	in the water	11° 19,757' N	142° 11,279' E	10887.6
SO252_1-2	10/11/2016 22:45:34	CTD	CTD	max depth/on ground	11° 19,754' N	142° 11,276' E	10885
SO252_1-2	10/11/2016 22:46:56	CTD	CTD	hoisting	11° 19,756' N	142° 11,276' E	10887.3
SO252_1-2	11/11/2016 02:13:22	CTD	CTD	on deck	11° 19,754' N	142° 11,274' E	10902.7
SO252_1-2	11/11/2016 02:14:40	CTD	CTD	station end	11° 19,753' N	142° 11,274' E	10907.3
SO252_3-1	11/11/2016 03:23:03	Mooring	MOOR	station start	11° 11,842' N	142° 9,829' E	9509.6
SO252_3-1	11/11/2016 03:24:47	Mooring	MOOR	in the water	11° 11,867' N	142° 9,845' E	9512.2
SO252_3-1	11/11/2016 03:29:11	Mooring	MOOR	information	11° 11,941' N	142° 9,867' E	9540.9
SO252_3-1	11/11/2016 05:03:12	Mooring	MOOR	information	11° 13,583' N	142° 10,163' E	9914.6
SO252_3-1	11/11/2016 05:17:36	Mooring	MOOR	information	11° 13,821' N	142° 10,205' E	9882

Station	Date / Time UTC	Device	Device Abbreviation	Action	Latitude	Longitude	Depth (m)
SO252_3-1	11/11/2016 05:28:37	Mooring	MOOR	information	11° 14,001' N	142° 10,238' E	9937.3
SO252_3-1	11/11/2016 05:39:13	Mooring	MOOR	information	11° 14,176' N	142° 10,269' E	10004.2
SO252_3-1	11/11/2016 05:39:56	Mooring	MOOR	information	11° 14,187' N	142° 10,270' E	10004.1
SO252_3-1	11/11/2016 07:23:25	Mooring	MOOR	information	11° 16,713' N	142° 10,728' E	10061.8
SO252_3-1	11/11/2016 07:41:36	Mooring	MOOR	information	11° 17,073' N	142° 10,792' E	10142.4
SO252_3-1	11/11/2016 08:39:18	Mooring	MOOR	information	11° 18,509' N	142° 11,052' E	10335.2
SO252_3-1	11/11/2016 09:39:00	Mooring	MOOR	in the water	11° 20,093' N	142° 11,335' E	10861
SO252_3-1	11/11/2016 09:41:27	Mooring	MOOR	station end	11° 20,213' N	142° 11,354' E	10851.7
SO252_4-1	14/11/2016 21:25:01	CTD	CTD	station start	5° 15,271' S	148° 13,821' E	1651.7
SO252_4-1	14/11/2016 21:26:29	CTD	CTD	in the water	5° 15,274' S	148° 13,823' E	1652.3
SO252_4-1	14/11/2016 22:15:05	CTD	CTD	max depth/on ground	5° 15,275' S	148° 13,819' E	1652.5
SO252_4-1	14/11/2016 22:16:19	CTD	CTD	hoisting	5° 15,277' S	148° 13,820' E	1654.4
SO252_4-1	14/11/2016 22:50:04	CTD	CTD	on deck	5° 15,269' S	148° 13,819' E	1653.4
SO252_4-1	14/11/2016 23:00:25	CTD	CTD	station end	5° 15,269' S	148° 13,823' E	1652.8
SO252_5-1	15/11/2016 02:00:00	Seismic Source	SEISSRC	station start	5° 15,277' S	148° 13,824' E	0
SO252_5-1	15/11/2016 02:03:07	Seismic Source	SEISSRC	information	5° 15,317' S	148° 13,796' E	0
SO252_5-1	15/11/2016 02:16:36	Seismic Source	SEISSRC	information	5° 15,643' S	148° 13,644' E	0
SO252_5-1	15/11/2016 02:24:57	Seismic Source	SEISSRC	information	5° 15,896' S	148° 13,533' E	0
SO252_5-1	15/11/2016 02:28:21	Seismic Source	SEISSRC	information	5° 16,000' S	148° 13,485' E	1652.2
SO252_5-1	15/11/2016 02:47:45	Seismic Source	SEISSRC	information	5° 16,592' S	148° 13,220' E	1651.3
SO252_5-1	15/11/2016 02:54:33	Seismic Source	SEISSRC	Airgun in water	5° 16,802' S	148° 13,126' E	1649.4
SO252_5-1	15/11/2016 02:59:07	Seismic Source	SEISSRC	profile start	5° 16,959' S	148° 13,064' E	1647.7
SO252_5-1	15/11/2016 03:07:18	Seismic Source	SEISSRC	information	5° 17,366' S	148° 12,936' E	1652.6

Station	Date / Time UTC	Device	Device Abbreviation	Action	Latitude	Longitude	Depth (m)
SO252_5-1	15/11/2016 03:07:38	Seismic Source	SEISSRC	information	5° 17,380' S	148° 12,931' E	1652.6
SO252_5-1	15/11/2016 03:13:48	Seismic Source	SEISSRC	information	5° 17,635' S	148° 12,837' E	1585.3
SO252_5-1	15/11/2016 03:30:02	Seismic Source	SEISSRC	information	5° 18,178' S	148° 12,522' E	1454.4
SO252_5-1	15/11/2016 03:34:34	Seismic Source	SEISSRC	information	5° 18,292' S	148° 12,462' E	1453.5
SO252_5-1	15/11/2016 03:37:03	Seismic Source	SEISSRC	information	5° 18,381' S	148° 12,423' E	1449.5
SO252_5-1	15/11/2016 03:42:30	Seismic Source	SEISSRC	information	5° 18,640' S	148° 12,305' E	1437
SO252_5-1	15/11/2016 03:45:30	Seismic Source	SEISSRC	information	5° 18,809' S	148° 12,220' E	1433.3
SO252_5-1	15/11/2016 03:53:57	Seismic Source	SEISSRC	profile start	5° 19,403' S	148° 11,966' E	1409.7
SO252_5-1	15/11/2016 06:07:12	Seismic Source	SEISSRC	alter course	5° 28,555' S	148° 7,879' E	1074.5
SO252_5-1	15/11/2016 07:20:06	Seismic Source	SEISSRC	alter course	5° 33,049' S	148° 4,847' E	768.2
SO252_5-1	15/11/2016 07:35:03	Seismic Source	SEISSRC	alter course	5° 32,784' S	148° 3,856' E	668.5
SO252_5-1	15/11/2016 08:41:39	Seismic Source	SEISSRC	alter course	5° 28,772' S	148° 6,718' E	947.5
SO252_5-1	15/11/2016 08:52:19	Seismic Source	SEISSRC	alter course	5° 28,289' S	148° 6,375' E	904.2
SO252_5-1	15/11/2016 10:00:02	Seismic Source	SEISSRC	alter course	5° 32,054' S	148° 2,974' E	684.6
SO252_5-1	15/11/2016 10:11:34	Seismic Source	SEISSRC	alter course	5° 31,894' S	148° 2,250' E	506.6
SO252_5-1	15/11/2016 11:09:52	Seismic Source	SEISSRC	alter course	5° 28,637' S	148° 5,026' E	849
SO252_5-1	15/11/2016 11:22:45	Seismic Source	SEISSRC	alter course	5° 27,987' S	148° 4,484' E	764.3
SO252_5-1	15/11/2016 12:27:21	Seismic Source	SEISSRC	alter course	5° 31,404' S	148° 1,192' E	410.9
SO252_5-1	15/11/2016 12:39:11	Seismic Source	SEISSRC	alter course	5° 31,057' S	148° 0,457' E	308.7
SO252_5-1	15/11/2016 13:12:38	Seismic Source	SEISSRC	information	5° 29,140' S	148° 1,857' E	1026.5
SO252_5-1	15/11/2016 13:34:20	Seismic Source	SEISSRC	information	5° 27,912' S	148° 2,936' E	954.7
SO252_5-1	15/11/2016 13:41:38	Seismic Source	SEISSRC	alter course	5° 27,504' S	148° 3,293' E	896.1
SO252_5-1	15/11/2016 13:51:50	Seismic Source	SEISSRC	alter course	5° 26,917' S	148° 2,976' E	738.3

Station	Date / Time UTC	Device	Device Abbreviation	Action	Latitude	Longitude	Depth (m)
SO252_5-1	15/11/2016 14:55:01	Seismic Source	SEISSRC	alter course	5° 30,402' S	147° 59,878' E	370.3
SO252_5-1	15/11/2016 15:09:43	Seismic Source	SEISSRC	alter course	5° 29,905' S	147° 58,997' E	439.9
SO252_5-1	15/11/2016 16:16:06	Seismic Source	SEISSRC	alter course	5° 26,171' S	148° 2,128' E	797.5
SO252_5-1	15/11/2016 17:06:59	Seismic Source	SEISSRC	information	5° 22,655' S	148° 0,651' E	1442.9
SO252_5-1	15/11/2016 17:27:01	Seismic Source	SEISSRC	information	5° 21,285' S	148° 0,039' E	1580.2
SO252_5-1	15/11/2016 17:31:00	Seismic Source	SEISSRC	information	5° 21,010' S	147° 59,917' E	1605.3
SO252_5-1	16/11/2016 00:17:03	Seismic Source	SEISSRC	alter course	4° 53,117' S	147° 47,449' E	1661.1
SO252_5-1	16/11/2016 00:45:01	Seismic Source	SEISSRC	alter course	4° 53,788' S	147° 45,492' E	1839.2
SO252_5-1	16/11/2016 08:44:31	Seismic Source	SEISSRC	alter course	5° 26,523' S	148° 0,050' E	1346
SO252_5-1	16/11/2016 10:20:47	Seismic Source	SEISSRC	alter course	5° 31,065' S	148° 5,764' E	656.2
SO252_5-1	16/11/2016 10:36:02	Seismic Source	SEISSRC	alter course	5° 31,983' S	148° 5,272' E	643.6
SO252_5-1	16/11/2016 12:21:53	Seismic Source	SEISSRC	alter course	5° 27,135' S	147° 59,082' E	1252.6
SO252_5-1	16/11/2016 19:36:49	Seismic Source	SEISSRC	alter course	4° 57,886' S	147° 44,552' E	1840.3
SO252_5-1	16/11/2016 21:00:27	Seismic Source	SEISSRC	alter course	5° 2,591' S	147° 41,115' E	1783.2
SO252_5-1	17/11/2016 00:11:10	Seismic Source	SEISSRC	alter course	4° 56,924' S	147° 53,902' E	1833.7
SO252_5-1	17/11/2016 01:57:07	Seismic Source	SEISSRC	alter course	5° 3,444' S	147° 58,194' E	1807.5
SO252_5-1	17/11/2016 05:29:00	Seismic Source	SEISSRC	alter course	5° 10,261' S	147° 44,012' E	1778
SO252_5-1	17/11/2016 06:54:09	Seismic Source	SEISSRC	alter course	5° 16,434' S	147° 45,265' E	1600.4
SO252_5-1	17/11/2016 10:45:49	Seismic Source	SEISSRC	alter course	5° 8,920' S	148° 0,716' E	1791.5
SO252_5-1	17/11/2016 12:02:52	Seismic Source	SEISSRC	alter course	5° 13,916' S	148° 3,496' E	1771.1
SO252_5-1	17/11/2016 15:36:50	Seismic Source	SEISSRC	alter course	5° 22,626' S	147° 50,072' E	1367.7
SO252_5-1	17/11/2016 15:55:04	Seismic Source	SEISSRC	alter course	5° 23,544' S	147° 50,865' E	1212.5
SO252_5-1	17/11/2016 18:28:36	Seismic Source	SEISSRC	alter course	5° 17,383' S	148° 0,578' E	1759.4

Station	Date / Time UTC	Device	Device Abbreviation	Action	Latitude	Longitude	Depth (m)
SO252_5-1	17/11/2016 18:46:11	Seismic Source	SEISSRC	alter course	5° 18,320' S	148° 1,522' E	1734
SO252_5-1	17/11/2016 21:14:16	Seismic Source	SEISSRC	alter course	5° 24,559' S	147° 52,594' E	1185.7
SO252_5-1	17/11/2016 21:40:12	Seismic Source	SEISSRC	alter course	5° 25,911' S	147° 53,776' E	942.4
SO252_5-1	18/11/2016 00:12:40	Seismic Source	SEISSRC	alter course	5° 19,343' S	148° 3,120' E	1641.2
SO252_5-1	18/11/2016 03:20:09	Seismic Source	SEISSRC	alter course	5° 15,684' S	147° 49,749' E	1791
SO252_5-1	18/11/2016 06:00:00	Seismic Source	SEISSRC	alter course	5° 24,305' S	147° 57,362' E	1551.5
SO252_5-1	18/11/2016 07:56:48	Seismic Source	SEISSRC	profile end	5° 29,515' S	148° 4,379' E	896.1
SO252_5-1	18/11/2016 08:04:44	Seismic Source	SEISSRC	on deck	5° 29,911' S	148° 4,591' E	871.5
SO252_5-1	18/11/2016 08:09:35	Seismic Source	SEISSRC	on deck	5° 30,087' S	148° 4,682' E	847.6
SO252_5-1	18/11/2016 08:14:55	Seismic Source	SEISSRC	on deck	5° 30,281' S	148° 4,791' E	813
SO252_5-1	18/11/2016 08:17:11	Seismic Source	SEISSRC	on deck	5° 30,363' S	148° 4,839' E	784.9
SO252_5-1	18/11/2016 08:23:07	Seismic Source	SEISSRC	on deck	5° 30,577' S	148° 4,961' E	672.9
SO252_5-1	18/11/2016 08:24:03	Seismic Source	SEISSRC	station end	5° 30,611' S	148° 4,981' E	632.7
SO252_6-1	18/11/2016 09:23:23	Gravity Corer	GC	station start	5° 29,027' S	148° 12,204' E	1316.9
SO252_6-1	18/11/2016 09:28:56	Gravity Corer	GC	in the water	5° 29,019' S	148° 12,204' E	1317
SO252_6-1	18/11/2016 09:56:13	Gravity Corer	GC	max depth/on ground	5° 29,026' S	148° 12,209' E	1316.5
SO252_6-1	18/11/2016 09:57:05	Gravity Corer	GC	hoisting	5° 29,027' S	148° 12,209' E	1316.8
SO252_6-1	18/11/2016 10:32:29	Gravity Corer	GC	on deck	5° 29,025' S	148° 12,209' E	1318.4
SO252_6-1	18/11/2016 10:46:30	Gravity Corer	GC	station end	5° 29,023' S	148° 12,210' E	1318.4
SO252_6-2	18/11/2016 11:08:31	Gravity Corer	GC	station start	5° 29,264' S	148° 12,796' E	1315.8
SO252_6-2	18/11/2016 11:17:37	Gravity Corer	GC	in the water	5° 29,276' S	148° 12,796' E	1314.9
SO252_6-2	18/11/2016 11:44:44	Gravity Corer	GC	max depth/on ground	5° 29,278' S	148° 12,792' E	1322.8
SO252_6-2	18/11/2016 11:45:20	Gravity Corer	GC	hoisting	5° 29,278' S	148° 12,792' E	1322.2

Station	Date / Time UTC	Device	Device Abbreviation	Action	Latitude	Longitude	Depth (m)
SO252_6-2	18/11/2016 12:23:37	Gravity Corer	GC	on deck	5° 29,273' S	148° 12,788' E	1323.1
SO252_6-2	18/11/2016 12:28:22	Gravity Corer	GC	station end	5° 29,277' S	148° 12,790' E	1320.5
SO252_7-1	18/11/2016 13:45:28	Gravity Corer	GC	station start	5° 32,227' S	148° 9,164' E	1084.4
SO252_7-1	18/11/2016 13:50:15	Gravity Corer	GC	in the water	5° 32,227' S	148° 9,202' E	1077.3
SO252_7-1	18/11/2016 14:13:55	Gravity Corer	GC	max depth/on ground	5° 32,230' S	148° 9,206' E	1075.1
SO252_7-1	18/11/2016 14:14:21	Gravity Corer	GC	hoisting	5° 32,230' S	148° 9,206' E	1074.2
SO252_7-1	18/11/2016 14:44:26	Gravity Corer	GC	on deck	5° 32,231' S	148° 9,204' E	1075.3
SO252_7-1	18/11/2016 14:51:50	Gravity Corer	GC	station end	5° 32,229' S	148° 9,205' E	1077.5
SO252_8-1	18/11/2016 16:00:10	Gravity Corer	GC	station start	5° 31,031' S	148° 5,457' E	706.4
SO252_8-1	18/11/2016 16:04:49	Gravity Corer	GC	in the water	5° 31,068' S	148° 5,445' E	706
SO252_8-1	18/11/2016 16:24:21	Gravity Corer	GC	max depth/on ground	5° 31,074' S	148° 5,446' E	706.3
SO252_8-1	18/11/2016 16:24:27	Gravity Corer	GC	hoisting	5° 31,074' S	148° 5,446' E	706.2
SO252_8-1	18/11/2016 16:45:46	Gravity Corer	GC	on deck	5° 31,071' S	148° 5,449' E	706.2
SO252_8-1	18/11/2016 16:51:15	Gravity Corer	GC	station end	5° 31,074' S	148° 5,447' E	705.8
SO252_9-1	18/11/2016 17:34:52	Gravity Corer	GC	station start	5° 28,407' S	148° 3,872' E	903.6
SO252_9-1	18/11/2016 17:38:52	Gravity Corer	GC	in the water	5° 28,393' S	148° 3,858' E	903.1
SO252_9-1	18/11/2016 17:59:57	Gravity Corer	GC	max depth/on ground	5° 28,394' S	148° 3,858' E	904
SO252_9-1	18/11/2016 18:00:12	Gravity Corer	GC	hoisting	5° 28,394' S	148° 3,858' E	904.4
SO252_9-1	18/11/2016 18:26:37	Gravity Corer	GC	on deck	5° 28,396' S	148° 3,860' E	903.7
SO252_9-1	18/11/2016 18:32:49	Gravity Corer	GC	station end	5° 28,397' S	148° 3,859' E	903.5
SO252_10-1	18/11/2016 19:40:22	Gravity Corer	GC	station start	5° 20,908' S	147° 57,467' E	1686
SO252_10-1	18/11/2016 19:43:38	Gravity Corer	GC	in the water	5° 20,911' S	147° 57,465' E	1688.3
SO252_10-1	18/11/2016 20:55:06	Gravity Corer	GC	on deck	5° 20,907' S	147° 57,470' E	1686.9

Station	Date / Time UTC	Device	Device Abbreviation	Action	Latitude	Longitude	Depth (m)
SO252_10-1	18/11/2016 21:08:03	Gravity Corer	GC	station end	5° 20,905' S	147° 57,468' E	1686.3
SO252_11-1	18/11/2016 23:07:43	Autonomous Underwater Vehicle	AUV	station start	5° 31,463' S	148° 7,208' E	290
SO252_11-1	18/11/2016 23:15:51	Autonomous Underwater Vehicle	AUV	in the water	5° 31,465' S	148° 7,218' E	298.2
SO252_11-1	18/11/2016 23:30:26	Autonomous Underwater Vehicle	AUV	on deck	5° 31,467' S	148° 7,215' E	296.4
SO252_11-1	18/11/2016 23:33:41	Autonomous Underwater Vehicle	AUV	in the water	5° 31,468' S	148° 7,215' E	295.1
SO252_11-1	18/11/2016 23:44:23	Autonomous Underwater Vehicle	AUV	on deck	5° 31,466' S	148° 7,218' E	300.8
SO252_11-1	18/11/2016 23:45:50	Autonomous Underwater Vehicle	AUV	station end	5° 31,465' S	148° 7,219' E	300.4
SO252_12-1	19/11/2016 00:00:47	Seismic Ocean Bottom Receiver	SEISOBR	station start	5° 30,921' S	148° 7,670' E	645
SO252_12-1	19/11/2016 00:25:03	Seismic Ocean Bottom Receiver	SEISOBR	station start	5° 29,294' S	148° 9,000' E	1142.2
SO252_12-1	19/11/2016 00:34:34	Seismic Ocean Bottom Receiver	SEISOBR	OBS deployed	5° 29,364' S	148° 9,026' E	1147.3
SO252_12-2	19/11/2016 00:58:44	Seismic Ocean Bottom Receiver	SEISOBR	OBS deployed	5° 31,045' S	148° 9,342' E	1127.6
SO252_12-3	19/11/2016 01:22:30	Seismic Ocean Bottom Receiver	SEISOBR	OBS deployed	5° 33,073' S	148° 8,567' E	969
SO252_12-4	19/11/2016 01:41:08	Seismic Ocean Bottom Receiver	SEISOBR	OBS deployed	5° 33,916' S	148° 7,408' E	903.3
SO252_12-5	19/11/2016 02:15:55	Seismic Ocean Bottom Receiver	SEISOBR	OBS deployed	5° 31,591' S	148° 4,403' E	850.5
SO252_12-6	19/11/2016 02:31:42	Seismic Ocean Bottom Receiver	SEISOBR	OBS deployed	5° 31,166' S	148° 4,054' E	892.6
SO252_12-7	19/11/2016 02:48:47	Seismic Ocean Bottom Receiver	SEISOBR	OBS deployed	5° 30,698' S	148° 3,721' E	919.8
SO252_12-8	19/11/2016 03:00:07	Seismic Ocean Bottom Receiver	SEISOBR	OBS deployed	5° 30,355' S	148° 3,433' E	923.6
SO252_12-9	19/11/2016 03:16:34	Seismic Ocean Bottom Receiver	SEISOBR	OBS deployed	5° 29,899' S	148° 3,098' E	969.1
SO252_12-10	19/11/2016 03:32:40	Seismic Ocean Bottom Receiver	SEISOBR	OBS deployed	5° 29,447' S	148° 2,724' E	980.7
SO252_12-11	19/11/2016 03:48:11	Seismic Ocean Bottom Receiver	SEISOBR	OBS deployed	5° 28,992' S	148° 2,329' E	965.5
SO252_13-1	19/11/2016 04:35:39	KONGSBERG EM122	EM122	station start	5° 28,924' S	147° 59,017' E	824.1
SO252_13-1	19/11/2016 04:35:50	KONGSBERG EM122	EM122	profile start	5° 28,909' S	147° 58,998' E	825.8
SO252_13-1	19/11/2016 06:35:09	KONGSBERG EM122	EM122	alter course	5° 18,069' S	147° 47,259' E	1486.4

Station	Date / Time UTC	Device	Device Abbreviation	Action	Latitude	Longitude	Depth (m)
SO252_13-1	19/11/2016 07:15:51	KONGSBERG EM122	EM122	alter course	5° 13,207' S	147° 49,579' E	1790.7
SO252_13-1	19/11/2016 08:41:14	KONGSBERG EM122	EM122	profile end	5° 3,245' S	147° 43,915' E	1820.7
SO252_13-1	19/11/2016 08:41:22	KONGSBERG EM122	EM122	station end	5° 3,229' S	147° 43,906' E	1818.8
SO252_14-1	19/11/2016 09:46:00	Gravity Corer	GC	station start	4° 53,770' S	147° 45,654' E	1838.9
SO252_14-1	19/11/2016 09:54:25	Gravity Corer	GC	in the water	4° 53,751' S	147° 45,642' E	1839
SO252_14-1	19/11/2016 10:32:50	Gravity Corer	GC	max depth/on ground	4° 53,725' S	147° 45,631' E	1838.8
SO252_14-1	19/11/2016 10:34:07	Gravity Corer	GC	hoisting	4° 53,727' S	147° 45,631' E	1839.2
SO252_14-1	19/11/2016 11:22:42	Gravity Corer	GC	on deck	4° 53,726' S	147° 45,632' E	1839.2
SO252_14-1	19/11/2016 11:38:15	Gravity Corer	GC	station end	4° 53,725' S	147° 45,630' E	1839.5
SO252_14-2	19/11/2016 11:40:08	Gravity Corer	GC	station start	4° 53,725' S	147° 45,631' E	1839
SO252_14-2	19/11/2016 11:46:57	Gravity Corer	GC	in the water	4° 53,724' S	147° 45,634' E	1838.1
SO252_14-2	19/11/2016 12:26:50	Gravity Corer	GC	max depth/on ground	4° 53,721' S	147° 45,631' E	1839.2
SO252_14-2	19/11/2016 12:27:01	Gravity Corer	GC	hoisting	4° 53,721' S	147° 45,631' E	1839
SO252_14-2	19/11/2016 13:14:01	Gravity Corer	GC	on deck	4° 53,728' S	147° 45,630' E	1838.6
SO252_14-2	19/11/2016 13:15:25	Gravity Corer	GC	station end	4° 53,728' S	147° 45,630' E	1838.6
SO252_15-1	19/11/2016 14:18:26	Gravity Corer	GC	station start	4° 57,095' S	147° 53,483' E	1835.6
SO252_15-1	19/11/2016 14:21:39	Gravity Corer	GC	in the water	4° 57,095' S	147° 53,488' E	1833.8
SO252_15-1	19/11/2016 14:57:29	Gravity Corer	GC	max depth/on ground	4° 57,112' S	147° 53,507' E	1833.1
SO252_15-1	19/11/2016 14:58:15	Gravity Corer	GC	hoisting	4° 57,112' S	147° 53,507' E	1832.8
SO252_15-1	19/11/2016 15:40:24	Gravity Corer	GC	on deck	4° 57,107' S	147° 53,511' E	1833
SO252_15-1	19/11/2016 15:42:45	Gravity Corer	GC	station end	4° 57,107' S	147° 53,510' E	1833.1
SO252_16-1	19/11/2016 16:41:30	Gravity Corer	GC	station start	5° 4,869' S	147° 55,580' E	1822.1
SO252_16-1	19/11/2016 16:45:24	Gravity Corer	GC	in the water	5° 4,936' S	147° 55,608' E	1821.4

Station	Date / Time UTC	Device	Device Abbreviation	Action	Latitude	Longitude	Depth (m)
SO252_16-1	19/11/2016 17:19:56	Gravity Corer	GC	max depth/on ground	5° 4,924' S	147° 55,610' E	1821.4
SO252_16-1	19/11/2016 17:20:17	Gravity Corer	GC	hoisting	5° 4,924' S	147° 55,610' E	1821.2
SO252_16-1	19/11/2016 18:02:17	Gravity Corer	GC	on deck	5° 4,930' S	147° 55,610' E	1821
SO252_16-1	19/11/2016 18:27:12	Gravity Corer	GC	station end	5° 4,920' S	147° 55,616' E	1820.7
SO252_17-1	19/11/2016 22:24:56	Seismic Towed Receiver	SEISTR	station start	5° 29,912' S	148° 7,905' E	917.2
SO252_17-1	19/11/2016 22:26:25	Seismic Towed Receiver	SEISTR	in the water	5° 29,941' S	148° 7,910' E	915
SO252_17-1	19/11/2016 23:45:09	Seismic Towed Receiver	SEISTR	in the water	5° 31,371' S	148° 8,186' E	871.4
SO252_17-1	19/11/2016 23:53:07	Seismic Towed Receiver	SEISTR	in the water	5° 31,503' S	148° 8,190' E	879.9
SO252_17-1	20/11/2016 00:07:30	Seismic Towed Receiver	SEISTR	information	5° 31,750' S	148° 8,223' E	894.4
SO252_17-1	20/11/2016 00:19:02	Seismic Towed Receiver	SEISTR	in the water	5° 32,164' S	148° 8,186' E	898.4
SO252_17-1	20/11/2016 00:23:36	Seismic Towed Receiver	SEISTR	on deck	5° 32,342' S	148° 8,163' E	925.6
SO252_17-1	20/11/2016 00:25:06	Seismic Towed Receiver	SEISTR	in the water	5° 32,405' S	148° 8,155' E	936.4
SO252_17-1	20/11/2016 00:30:39	Seismic Towed Receiver	SEISTR	information	5° 32,636' S	148° 8,122' E	957.2
SO252_17-1	20/11/2016 00:31:37	Seismic Towed Receiver	SEISTR	alter course	5° 32,677' S	148° 8,117' E	960.3
SO252_17-1	20/11/2016 01:03:24	Seismic Towed Receiver	SEISTR	alter course	5° 33,035' S	148° 6,720' E	716.7
SO252_17-1	20/11/2016 01:10:08	Seismic Towed Receiver	SEISTR	profile start	5° 32,895' S	148° 6,369' E	654.7
SO252_17-1	20/11/2016 01:30:25	Seismic Towed Receiver	SEISTR	information	5° 32,203' S	148° 5,277' E	669.6
SO252_17-1	20/11/2016 03:25:00	Seismic Towed Receiver	SEISTR	alter course	5° 28,435' S	147° 59,232' E	987.9
SO252_17-1	20/11/2016 03:47:00	Seismic Towed Receiver	SEISTR	alter course	5° 27,494' S	147° 59,743' E	1216.2
SO252_17-1	20/11/2016 06:25:19	Seismic Towed Receiver	SEISTR	alter course	5° 31,262' S	148° 5,873' E	590.6
SO252_17-1	20/11/2016 06:44:38	Seismic Towed Receiver	SEISTR	alter course	5° 32,082' S	148° 5,448' E	606.4
SO252_17-1	20/11/2016 08:52:52	Seismic Towed Receiver	SEISTR	alter course	5° 28,487' S	147° 59,364' E	935.6
SO252_17-1	20/11/2016 09:14:31	Seismic Towed Receiver	SEISTR	alter course	5° 27,503' S	147° 59,704' E	1210.3

Station	Date / Time UTC	Device	Device Abbreviation	Action	Latitude	Longitude	Depth (m)
SO252_17-1	20/11/2016 12:00:18	Seismic Towed Receiver	SEISTR	alter course	5° 31,128' S	148° 5,831' E	615.2
SO252_17-1	20/11/2016 12:20:34	Seismic Towed Receiver	SEISTR	alter course	5° 32,101' S	148° 5,429' E	615.5
SO252_17-1	20/11/2016 14:20:06	Seismic Towed Receiver	SEISTR	alter course	5° 28,415' S	147° 59,314' E	986.6
SO252_17-1	20/11/2016 14:50:23	Seismic Towed Receiver	SEISTR	alter course	5° 27,389' S	147° 59,682' E	1221.4
SO252_17-1	20/11/2016 17:41:55	Seismic Towed Receiver	SEISTR	alter course	5° 31,136' S	148° 5,895' E	576.4
SO252_17-1	20/11/2016 18:00:00	Seismic Towed Receiver	SEISTR	alter course	5° 31,978' S	148° 5,540' E	570.3
SO252_17-1	20/11/2016 20:05:57	Seismic Towed Receiver	SEISTR	alter course	5° 28,384' S	147° 59,347' E	1003.8
SO252_17-1	20/11/2016 20:26:50	Seismic Towed Receiver	SEISTR	alter course	5° 27,430' S	147° 59,745' E	1224.2
SO252_17-1	20/11/2016 22:56:22	Seismic Towed Receiver	SEISTR	profile end	5° 31,139' S	148° 5,952' E	495
SO252_17-1	20/11/2016 23:10:00	Seismic Towed Receiver	SEISTR	on deck	5° 31,615' S	148° 6,073' E	404
SO252_17-1	20/11/2016 23:40:44	Seismic Towed Receiver	SEISTR	on deck	5° 32,315' S	148° 6,364' E	457.6
SO252_17-1	21/11/2016 00:11:00	Seismic Towed Receiver	SEISTR	on deck	5° 32,855' S	148° 6,808' E	666
SO252_17-1	21/11/2016 00:21:18	Seismic Towed Receiver	SEISTR	on deck	5° 33,050' S	148° 6,966' E	778.5
SO252_17-1	21/11/2016 00:22:43	Seismic Towed Receiver	SEISTR	station end	5° 33,078' S	148° 6,991' E	792.7
SO252_18-1	21/11/2016 00:30:03	Seismic Source	SEISSRC	station start	5° 33,231' S	148° 7,113' E	832.7
SO252_18-1	21/11/2016 00:32:16	Seismic Source	SEISSRC	Airgun in water	5° 33,276' S	148° 7,144' E	844
SO252_18-1	21/11/2016 00:38:13	Seismic Source	SEISSRC	information	5° 33,394' S	148° 7,228' E	877.3
SO252_18-1	21/11/2016 01:08:20	Seismic Source	SEISSRC	alter course	5° 35,220' S	148° 7,179' E	733.2
SO252_18-1	21/11/2016 01:18:21	Seismic Source	SEISSRC	alter course	5° 35,027' S	148° 6,209' E	742.1
SO252_18-1	21/11/2016 01:24:52	Seismic Source	SEISSRC	profile start	5° 34,675' S	148° 6,300' E	676.9
SO252_18-1	21/11/2016 02:55:01	Seismic Source	SEISSRC	alter course	5° 31,043' S	148° 11,472' E	1205.5
SO252_18-1	21/11/2016 03:54:20	Seismic Source	SEISSRC	alter course	5° 34,704' S	148° 10,425' E	877.9
SO252_18-1	21/11/2016 05:47:13	Seismic Source	SEISSRC	alter course	5° 26,914' S	148° 8,496' E	1078

Station	Date / Time UTC	Device	Device Abbreviation	Action	Latitude	Longitude	Depth (m)
SO252_18-1	21/11/2016 06:28:52	Seismic Source	SEISSRC	alter course	5° 28,476' S	148° 10,332' E	1258.7
SO252_18-1	21/11/2016 08:24:45	Seismic Source	SEISSRC	alter course	5° 32,386' S	148° 2,687' E	401.7
SO252_18-1	21/11/2016 09:51:43	Seismic Source	SEISSRC	alter course	5° 26,210' S	147° 59,700' E	1388.7
SO252_18-1	21/11/2016 12:53:35	Seismic Source	SEISSRC	profile end	5° 34,800' S	148° 7,071' E	788
SO252_18-1	21/11/2016 12:59:45	Seismic Source	SEISSRC	on deck	5° 34,915' S	148° 7,229' E	791.5
SO252_18-1	21/11/2016 13:00:50	Seismic Source	SEISSRC	station end	5° 34,918' S	148° 7,251' E	793.4
SO252_19-1	21/11/2016 14:49:12	OFOS	OFOS	station start	5° 28,646' S	148° 3,643' E	890
SO252_19-1	21/11/2016 14:50:33	OFOS	OFOS	in the water	5° 28,646' S	148° 3,638' E	890
SO252_19-1	21/11/2016 14:52:40	OFOS	OFOS	max depth/on ground	5° 28,647' S	148° 3,639' E	890
SO252_19-1	21/11/2016 14:57:56	OFOS	OFOS	on deck	5° 28,648' S	148° 3,643' E	890
SO252_19-1	21/11/2016 14:59:04	OFOS	OFOS	station end	5° 28,648' S	148° 3,644' E	890
SO252_19-2	21/11/2016 15:10:23	OFOS	OFOS	station start	5° 28,643' S	148° 3,644' E	891
SO252_19-2	21/11/2016 15:12:29	OFOS	OFOS	in the water	5° 28,645' S	148° 3,643' E	890
SO252_19-2	21/11/2016 15:46:21	OFOS	OFOS	max depth/on ground	5° 28,643' S	148° 3,644' E	892
SO252_19-2	21/11/2016 17:24:06	OFOS	OFOS	hoisting	5° 29,397' S	148° 2,987' E	0
SO252_19-2	21/11/2016 17:30:47	OFOS	OFOS	information	5° 29,390' S	148° 2,989' E	0
SO252_19-2	21/11/2016 17:57:27	OFOS	OFOS	max depth/on ground	5° 29,393' S	148° 2,993' E	963
SO252_19-2	21/11/2016 18:04:25	OFOS	OFOS	hoisting	5° 29,414' S	148° 2,976' E	0
SO252_19-2	21/11/2016 18:37:26	OFOS	OFOS	on deck	5° 29,413' S	148° 2,974' E	919
SO252_19-2	21/11/2016 18:39:43	OFOS	OFOS	station end	5° 29,413' S	148° 2,973' E	917
SO252_20-1	21/11/2016 19:05:23	OFOS	OFOS	station start	5° 29,950' S	148° 3,532' E	732
SO252_20-1	21/11/2016 19:07:38	OFOS	OFOS	in the water	5° 29,950' S	148° 3,526' E	0
SO252_20-1	21/11/2016 19:34:00	OFOS	OFOS	max depth/on ground	5° 29,979' S	148° 3,542' E	0

Station	Date / Time UTC	Device	Device Abbreviation	Action	Latitude	Longitude	Depth (m)
SO252_20-1	21/11/2016 20:48:57	OFOS	OFOS	hoisting	5° 29,886' S	148° 3,384' E	0
SO252_20-1	21/11/2016 21:07:16	OFOS	OFOS	on deck	5° 29,889' S	148° 3,391' E	0
SO252_20-1	21/11/2016 21:07:41	OFOS	OFOS	station end	5° 29,889' S	148° 3,391' E	815
SO252_21-1	21/11/2016 22:00:04	Seismic Towed Receiver	SEISTR	station start	5° 29,940' S	148° 3,409' E	0
SO252_21-1	21/11/2016 22:18:03	Seismic Towed Receiver	SEISTR	in the water	5° 30,269' S	148° 3,654' E	926
SO252_21-1	21/11/2016 23:11:27	Seismic Towed Receiver	SEISTR	in the water	5° 30,947' S	148° 4,489' E	724
SO252_21-1	21/11/2016 23:13:37	Seismic Towed Receiver	SEISTR	in the water	5° 30,962' S	148° 4,523' E	717
SO252_21-1	21/11/2016 23:33:01	Seismic Towed Receiver	SEISTR	in the water	5° 31,334' S	148° 4,999' E	728
SO252_21-1	21/11/2016 23:35:44	Seismic Towed Receiver	SEISTR	information	5° 31,356' S	148° 5,067' E	725.6
SO252_21-1	21/11/2016 23:36:28	Seismic Towed Receiver	SEISTR	information	5° 31,362' S	148° 5,089' E	713.4
SO252_21-1	22/11/2016 00:00:02	Seismic Towed Receiver	SEISTR	alter course	5° 31,825' S	148° 6,011' E	339.7
SO252_21-1	22/11/2016 00:07:46	Seismic Towed Receiver	SEISTR	alter course	5° 32,184' S	148° 5,936' E	486.7
SO252_21-1	22/11/2016 00:16:35	Seismic Towed Receiver	SEISTR	profile start	5° 32,177' S	148° 5,490' E	601
SO252_21-1	22/11/2016 00:51:30	Seismic Towed Receiver	SEISTR	alter course	5° 31,059' S	148° 3,677' E	904.5
SO252_21-1	22/11/2016 02:12:54	Seismic Towed Receiver	SEISTR	alter course	5° 28,363' S	147° 59,404' E	1005.9
SO252_21-1	22/11/2016 02:33:15	Seismic Towed Receiver	SEISTR	alter course	5° 27,356' S	147° 59,768' E	1227.5
SO252_21-1	22/11/2016 05:00:28	Seismic Towed Receiver	SEISTR	alter course	5° 31,021' S	148° 5,862' E	607.5
SO252_21-1	22/11/2016 05:17:08	Seismic Towed Receiver	SEISTR	alter course	5° 31,897' S	148° 5,576' E	599.1
SO252_21-1	22/11/2016 06:57:02	Seismic Towed Receiver	SEISTR	alter course	5° 28,359' S	147° 59,450' E	1025.1
SO252_21-1	22/11/2016 07:16:34	Seismic Towed Receiver	SEISTR	alter course	5° 27,407' S	147° 59,757' E	1223.2
SO252_21-1	22/11/2016 10:00:00	Seismic Towed Receiver	SEISTR	alter course	5° 30,957' S	148° 5,832' E	650
SO252_21-1	22/11/2016 10:22:26	Seismic Towed Receiver	SEISTR	alter course	5° 31,917' S	148° 5,566' E	591.7
SO252_21-1	22/11/2016 12:16:17	Seismic Towed Receiver	SEISTR	alter course	5° 28,343' S	147° 59,497' E	1056.4

Station	Date / Time UTC	Device	Device Abbreviation	Action	Latitude	Longitude	Depth (m)
SO252_21-1	22/11/2016 12:37:57	Seismic Towed Receiver	SEISTR	alter course	5° 27,374' S	147° 59,768' E	1226.2
SO252_21-1	22/11/2016 15:09:11	Seismic Towed Receiver	SEISTR	alter course	5° 31,019' S	148° 5,983' E	508.7
SO252_21-1	22/11/2016 15:27:00	Seismic Towed Receiver	SEISTR	alter course	5° 31,886' S	148° 5,597' E	599.4
SO252_21-1	22/11/2016 17:27:00	Seismic Towed Receiver	SEISTR	alter course	5° 28,189' S	147° 59,372' E	1080.2
SO252_21-1	22/11/2016 17:45:52	Seismic Towed Receiver	SEISTR	alter course	5° 27,356' S	147° 59,799' E	1233
SO252_21-1	22/11/2016 20:16:26	Seismic Towed Receiver	SEISTR	alter course	5° 30,961' S	148° 5,971' E	547.9
SO252_21-1	22/11/2016 20:33:58	Seismic Towed Receiver	SEISTR	alter course	5° 31,873' S	148° 5,604' E	604.9
SO252_21-1	22/11/2016 22:33:51	Seismic Towed Receiver	SEISTR	alter course	5° 28,244' S	147° 59,500' E	1084.9
SO252_21-1	22/11/2016 22:52:57	Seismic Towed Receiver	SEISTR	alter course	5° 27,350' S	147° 59,806' E	1236.7
SO252_21-1	23/11/2016 01:20:23	Seismic Towed Receiver	SEISTR	alter course	5° 30,925' S	148° 5,993' E	546.4
SO252_21-1	23/11/2016 01:25:14	Seismic Towed Receiver	SEISTR	information	5° 31,175' S	148° 6,018' E	493.3
SO252_21-1	23/11/2016 01:33:02	Seismic Towed Receiver	SEISTR	on deck	5° 31,546' S	148° 5,816' E	615.8
SO252_21-1	23/11/2016 01:40:51	Seismic Towed Receiver	SEISTR	in the water	5° 31,789' S	148° 5,751' E	567.4
SO252_21-1	23/11/2016 01:45:32	Seismic Towed Receiver	SEISTR	alter course	5° 31,985' S	148° 5,751' E	471.3
SO252_21-1	23/11/2016 02:00:46	Seismic Towed Receiver	SEISTR	information	5° 31,757' S	148° 5,121' E	739.6
SO252_21-1	23/11/2016 03:49:08	Seismic Towed Receiver	SEISTR	alter course	5° 28,148' S	147° 59,426' E	1103.6
SO252_21-1	23/11/2016 04:08:09	Seismic Towed Receiver	SEISTR	alter course	5° 27,245' S	147° 59,877' E	1257.9
SO252_21-1	23/11/2016 06:44:09	Seismic Towed Receiver	SEISTR	information	5° 30,877' S	148° 6,012' E	549
SO252_21-1	23/11/2016 06:50:20	Seismic Towed Receiver	SEISTR	information	5° 30,968' S	148° 6,105' E	455.3
SO252_21-1	23/11/2016 07:37:33	Seismic Towed Receiver	SEISTR	information	5° 32,415' S	148° 6,272' E	491.4
SO252_21-1	23/11/2016 07:39:40	Seismic Towed Receiver	SEISTR	information	5° 32,348' S	148° 6,178' E	476.4
SO252_21-1	23/11/2016 09:47:58	Seismic Towed Receiver	SEISTR	alter course	5° 28,177' S	147° 59,518' E	1107.4
SO252_21-1	23/11/2016 10:05:28	Seismic Towed Receiver	SEISTR	alter course	5° 27,286' S	147° 59,842' E	1247.8

Station	Date / Time UTC	Device	Device Abbreviation	Action	Latitude	Longitude	Depth (m)
SO252_21-1	23/11/2016 12:37:41	Seismic Towed Receiver	SEISTR	alter course	5° 30,840' S	148° 6,006' E	558.8
SO252_21-1	23/11/2016 13:00:07	Seismic Towed Receiver	SEISTR	alter course	5° 31,827' S	148° 5,568' E	641.5
SO252_21-1	23/11/2016 15:00:00	Seismic Towed Receiver	SEISTR	alter course	5° 28,148' S	147° 59,544' E	1122.4
SO252_21-1	23/11/2016 15:18:00	Seismic Towed Receiver	SEISTR	information	5° 27,135' S	147° 59,985' E	1242.8
SO252_21-1	23/11/2016 16:35:35	Seismic Towed Receiver	SEISTR	information	5° 28,807' S	148° 2,819' E	945
SO252_21-1	23/11/2016 16:46:55	Seismic Towed Receiver	SEISTR	information	5° 29,061' S	148° 3,235' E	928.7
SO252_21-1	23/11/2016 16:50:42	Seismic Towed Receiver	SEISTR	information	5° 29,099' S	148° 3,319' E	928.9
SO252_21-1	23/11/2016 17:08:32	Seismic Towed Receiver	SEISTR	information	5° 29,361' S	148° 3,714' E	900.6
SO252_21-1	23/11/2016 17:12:51	Seismic Towed Receiver	SEISTR	information	5° 29,422' S	148° 3,818' E	910.2
SO252_21-1	23/11/2016 18:11:27	Seismic Towed Receiver	SEISTR	alter course	5° 30,835' S	148° 6,048' E	534.2
SO252_21-1	23/11/2016 18:27:22	Seismic Towed Receiver	SEISTR	alter course	5° 31,713' S	148° 5,684' E	631.9
SO252_21-1	23/11/2016 20:30:09	Seismic Towed Receiver	SEISTR	alter course	5° 28,129' S	147° 59,581' E	1132.5
SO252_21-1	23/11/2016 20:51:40	Seismic Towed Receiver	SEISTR	alter course	5° 27,184' S	147° 59,913' E	1261.8
SO252_21-1	23/11/2016 23:15:12	Seismic Towed Receiver	SEISTR	alter course	5° 30,755' S	148° 6,011' E	585.2
SO252_21-1	23/11/2016 23:18:45	Seismic Towed Receiver	SEISTR	information	5° 30,876' S	148° 6,132' E	472.2
SO252_21-1	23/11/2016 23:24:56	Seismic Towed Receiver	SEISTR	on deck	5° 31,144' S	148° 6,056' E	468.4
SO252_21-1	23/11/2016 23:30:01	Seismic Towed Receiver	SEISTR	in the water	5° 31,377' S	148° 5,906' E	573.3
SO252_21-1	23/11/2016 23:32:58	Seismic Towed Receiver	SEISTR	information	5° 31,501' S	148° 5,828' E	610.4
SO252_21-1	23/11/2016 23:37:51	Seismic Towed Receiver	SEISTR	alter course	5° 31,724' S	148° 5,687' E	633.1
SO252_21-1	24/11/2016 01:52:40	Seismic Towed Receiver	SEISTR	alter course	5° 28,112' S	147° 59,611' E	1139.4
SO252_21-1	24/11/2016 02:15:06	Seismic Towed Receiver	SEISTR	alter course	5° 27,167' S	147° 59,931' E	1261.5
SO252_21-1	24/11/2016 02:15:21	Seismic Towed Receiver	SEISTR	information	5° 27,160' S	147° 59,936' E	1261
SO252_21-1	24/11/2016 02:21:31	Seismic Towed Receiver	SEISTR	information	5° 27,077' S	148° 0,110' E	1230.3

Station	Date / Time UTC	Device	Device Abbreviation	Action	Latitude	Longitude	Depth (m)
SO252_21-1	24/11/2016 02:26:37	Seismic Towed Receiver	SEISTR	information	5° 27,176' S	148° 0,323' E	1272.8
SO252_21-1	24/11/2016 02:45:52	Seismic Towed Receiver	SEISTR	information	5° 27,612' S	147° 59,920' E	1211.2
SO252_21-1	24/11/2016 02:49:43	Seismic Towed Receiver	SEISTR	information	5° 27,547' S	147° 59,809' E	1218.3
SO252_21-1	24/11/2016 03:09:15	Seismic Towed Receiver	SEISTR	information	5° 27,148' S	148° 0,274' E	1279.4
SO252_21-1	24/11/2016 05:25:04	Seismic Towed Receiver	SEISTR	alter course	5° 30,807' S	148° 6,122' E	502.1
SO252_21-1	24/11/2016 05:44:00	Seismic Towed Receiver	SEISTR	alter course	5° 31,735' S	148° 5,684' E	632.7
SO252_21-1	24/11/2016 08:14:16	Seismic Towed Receiver	SEISTR	alter course	5° 28,050' S	147° 59,594' E	1154.5
SO252_21-1	24/11/2016 08:35:22	Seismic Towed Receiver	SEISTR	alter course	5° 27,127' S	147° 59,957' E	1257.1
SO252_21-1	24/11/2016 10:37:57	Seismic Towed Receiver	SEISTR	alter course	5° 30,738' S	148° 6,119' E	535.6
SO252_21-1	24/11/2016 10:54:01	Seismic Towed Receiver	SEISTR	alter course	5° 31,631' S	148° 5,766' E	625.9
SO252_21-1	24/11/2016 13:29:07	Seismic Towed Receiver	SEISTR	alter course	5° 28,040' S	147° 59,644' E	1150.8
SO252_21-1	24/11/2016 13:51:10	Seismic Towed Receiver	SEISTR	alter course	5° 27,131' S	147° 59,955' E	1260.4
SO252_21-1	24/11/2016 16:00:00	Seismic Towed Receiver	SEISTR	alter course	5° 30,843' S	148° 6,203' E	450
SO252_21-1	24/11/2016 16:16:04	Seismic Towed Receiver	SEISTR	alter course	5° 31,586' S	148° 5,797' E	625.7
SO252_21-1	24/11/2016 17:57:51	Seismic Towed Receiver	SEISTR	information	5° 29,465' S	148° 1,996' E	1023.5
SO252_21-1	24/11/2016 18:06:30	Seismic Towed Receiver	SEISTR	information	5° 29,302' S	148° 1,730' E	1035.9
SO252_21-1	24/11/2016 18:49:16	Seismic Towed Receiver	SEISTR	information	5° 28,450' S	148° 0,369' E	989.9
SO252_21-1	24/11/2016 18:56:07	Seismic Towed Receiver	SEISTR	information	5° 28,304' S	148° 0,132' E	814.6
SO252_21-1	24/11/2016 19:07:30	Seismic Towed Receiver	SEISTR	alter course	5° 27,998' S	147° 59,653' E	1167.2
SO252_21-1	24/11/2016 19:29:27	Seismic Towed Receiver	SEISTR	alter course	5° 27,069' S	147° 59,986' E	1250.5
SO252_21-1	24/11/2016 21:32:02	Seismic Towed Receiver	SEISTR	alter course	5° 30,657' S	148° 6,136' E	555.7
SO252_21-1	24/11/2016 21:50:27	Seismic Towed Receiver	SEISTR	alter course	5° 31,494' S	148° 5,858' E	598.6
SO252_21-1	25/11/2016 00:18:14	Seismic Towed Receiver	SEISTR	information	5° 29,766' S	148° 2,550' E	983.1

Station	Date / Time UTC	Device	Device Abbreviation	Action	Latitude	Longitude	Depth (m)
SO252_21-1	25/11/2016 00:23:45	Seismic Towed Receiver	SEISTR	on deck	5° 29,649' S	148° 2,360' E	1011.3
SO252_21-1	25/11/2016 01:19:42	Seismic Towed Receiver	SEISTR	in the water	5° 28,615' S	148° 0,721' E	1124.7
SO252_21-1	25/11/2016 01:21:34	Seismic Towed Receiver	SEISTR	information	5° 28,571' S	148° 0,660' E	1159.2
SO252_21-1	25/11/2016 01:43:51	Seismic Towed Receiver	SEISTR	alter course	5° 27,970' S	147° 59,674' E	1163.4
SO252_21-1	25/11/2016 02:05:36	Seismic Towed Receiver	SEISTR	alter course	5° 26,991' S	148° 0,056' E	1250.5
SO252_21-1	25/11/2016 03:00:00	Seismic Towed Receiver	SEISTR	alter course	5° 28,568' S	148° 2,860' E	910.3
SO252_21-1	25/11/2016 03:57:37	Seismic Towed Receiver	SEISTR	information	5° 30,503' S	148° 5,439' E	681.2
SO252_21-1	25/11/2016 03:58:16	Seismic Towed Receiver	SEISTR	information	5° 30,538' S	148° 5,437' E	693.4
SO252_21-1	25/11/2016 04:00:00	Seismic Towed Receiver	SEISTR	information	5° 30,632' S	148° 5,433' E	705.8
SO252_21-1	25/11/2016 04:40:11	Seismic Towed Receiver	SEISTR	information	5° 32,134' S	148° 6,492' E	379.8
SO252_21-1	25/11/2016 05:34:13	Seismic Towed Receiver	SEISTR	information	5° 31,699' S	148° 5,754' E	610.9
SO252_21-1	25/11/2016 08:03:30	Seismic Towed Receiver	SEISTR	alter course	5° 27,941' S	147° 59,706' E	1171.9
SO252_21-1	25/11/2016 08:24:51	Seismic Towed Receiver	SEISTR	alter course	5° 26,979' S	148° 0,055' E	1254.2
SO252_21-1	25/11/2016 10:22:42	Seismic Towed Receiver	SEISTR	alter course	5° 30,623' S	148° 6,204' E	531.7
SO252_21-1	25/11/2016 10:40:18	Seismic Towed Receiver	SEISTR	alter course	5° 31,531' S	148° 5,828' E	615
SO252_21-1	25/11/2016 13:03:22	Seismic Towed Receiver	SEISTR	alter course	5° 27,898' S	147° 59,711' E	1180.8
SO252_21-1	25/11/2016 13:21:29	Seismic Towed Receiver	SEISTR	alter course	5° 27,014' S	148° 0,027' E	1244.8
SO252_21-1	25/11/2016 15:13:51	Seismic Towed Receiver	SEISTR	alter course	5° 30,588' S	148° 6,238' E	509
SO252_21-1	25/11/2016 15:35:02	Seismic Towed Receiver	SEISTR	alter course	5° 31,528' S	148° 5,794' E	629.6
SO252_21-1	25/11/2016 18:14:02	Seismic Towed Receiver	SEISTR	alter course	5° 27,854' S	147° 59,711' E	1186
SO252_21-1	25/11/2016 18:33:53	Seismic Towed Receiver	SEISTR	alter course	5° 26,889' S	148° 0,113' E	1322.9
SO252_21-1	25/11/2016 20:41:24	Seismic Towed Receiver	SEISTR	alter course	5° 30,495' S	148° 6,178' E	529.7
SO252_21-1	25/11/2016 21:00:04	Seismic Towed Receiver	SEISTR	alter course	5° 31,424' S	148° 5,894' E	582.2

Station	Date / Time UTC	Device	Device Abbreviation	Action	Latitude	Longitude	Depth (m)
SO252_21-1	25/11/2016 23:13:49	Seismic Towed Receiver	SEISTR	profile end	5° 27,833' S	147° 59,746' E	1192.2
SO252_21-1	25/11/2016 23:14:15	Seismic Towed Receiver	SEISTR	information	5° 27,822' S	147° 59,728' E	1195.9
SO252_21-1	25/11/2016 23:20:03	Seismic Towed Receiver	SEISTR	on deck	5° 27,706' S	147° 59,521' E	1185.8
SO252_21-1	25/11/2016 23:45:57	Seismic Towed Receiver	SEISTR	on deck	5° 27,175' S	147° 58,718' E	1230.3
SO252_21-1	26/11/2016 00:15:45	Seismic Towed Receiver	SEISTR	on deck	5° 26,603' S	147° 57,927' E	1315.1
SO252_21-1	26/11/2016 00:20:24	Seismic Towed Receiver	SEISTR	on deck	5° 26,520' S	147° 57,808' E	1319.7
SO252_21-1	26/11/2016 00:21:06	Seismic Towed Receiver	SEISTR	station end	5° 26,508' S	147° 57,791' E	1318
SO252_22-1	26/11/2016 01:12:38	Seismic Ocean Bottom Receiver	SEISOBR	station start	5° 29,379' S	148° 2,214' E	975.5
SO252_22-1	26/11/2016 01:15:52	Seismic Ocean Bottom Receiver	SEISOBR	information	5° 29,356' S	148° 2,221' E	980.7
SO252_22-1	26/11/2016 01:20:02	Seismic Ocean Bottom Receiver	SEISOBR	information	5° 29,324' S	148° 2,217' E	994.6
SO252_22-1	26/11/2016 01:36:01	Seismic Ocean Bottom Receiver	SEISOBR	information	5° 29,250' S	148° 2,252' E	993.9
SO252_22-1	26/11/2016 01:39:09	Seismic Ocean Bottom Receiver	SEISOBR	information	5° 29,147' S	148° 2,293' E	945
SO252_22-1	26/11/2016 01:47:23	Seismic Ocean Bottom Receiver	SEISOBR	information	5° 29,057' S	148° 2,418' E	960.5
SO252_22-1	26/11/2016 01:58:54	Seismic Ocean Bottom Receiver	SEISOBR	information	5° 29,488' S	148° 2,514' E	992.4
SO252_22-1	26/11/2016 02:05:38	Seismic Ocean Bottom Receiver	SEISOBR	information	5° 29,562' S	148° 2,857' E	938.2
SO252_22-1	26/11/2016 02:10:03	Seismic Ocean Bottom Receiver	SEISOBR	information	5° 29,597' S	148° 2,953' E	946.8
SO252_22-1	26/11/2016 02:19:33	Seismic Ocean Bottom Receiver	SEISOBR	information	5° 29,763' S	148° 3,202' E	941.1
SO252_22-1	26/11/2016 02:32:48	Seismic Ocean Bottom Receiver	SEISOBR	information	5° 30,030' S	148° 3,223' E	955.7
SO252_22-1	26/11/2016 02:34:54	Seismic Ocean Bottom Receiver	SEISOBR	information	5° 30,074' S	148° 3,250' E	956.6
SO252_22-1	26/11/2016 03:00:07	Seismic Ocean Bottom Receiver	SEISOBR	information	5° 30,410' S	148° 3,573' E	915.2
SO252_22-1	26/11/2016 03:15:16	Seismic Ocean Bottom Receiver	SEISOBR	information	5° 30,501' S	148° 3,707' E	923.5
SO252_22-1	26/11/2016 03:17:15	Seismic Ocean Bottom Receiver	SEISOBR	information	5° 30,510' S	148° 3,723' E	923.4
SO252_22-1	26/11/2016 03:34:14	Seismic Ocean Bottom Receiver	SEISOBR	information	5° 30,552' S	148° 3,720' E	920.9

Station	Date / Time UTC	Device	Device Abbreviation	Action	Latitude	Longitude	Depth (m)
SO252_22-1	26/11/2016 03:48:24	Seismic Ocean Bottom Receiver	SEISOBR	information	5° 30,842' S	148° 3,914' E	912.7
SO252_22-1	26/11/2016 03:50:03	Seismic Ocean Bottom Receiver	SEISOBR	information	5° 30,857' S	148° 3,915' E	912.6
SO252_22-1	26/11/2016 04:05:05	Seismic Ocean Bottom Receiver	SEISOBR	information	5° 31,159' S	148° 4,079' E	890.3
SO252_22-1	26/11/2016 04:23:17	Seismic Ocean Bottom Receiver	SEISOBR	information	5° 31,383' S	148° 4,356' E	853.4
SO252_22-1	26/11/2016 04:27:25	Seismic Ocean Bottom Receiver	SEISOBR	information	5° 31,381' S	148° 4,513' E	843.8
SO252_22-1	26/11/2016 04:38:32	Seismic Ocean Bottom Receiver	SEISOBR	information	5° 31,586' S	148° 4,405' E	849.3
SO252_22-1	26/11/2016 04:42:16	Seismic Ocean Bottom Receiver	SEISOBR	information	5° 31,642' S	148° 4,461' E	837.4
SO252_22-1	26/11/2016 05:05:52	Seismic Ocean Bottom Receiver	SEISOBR	information	5° 33,330' S	148° 6,282' E	769.6
SO252_22-1	26/11/2016 05:17:55	Seismic Ocean Bottom Receiver	SEISOBR	information	5° 34,101' S	148° 7,089' E	873.1
SO252_22-1	26/11/2016 06:01:29	Seismic Ocean Bottom Receiver	SEISOBR	information	5° 34,154' S	148° 7,875' E	903.4
SO252_22-1	26/11/2016 06:05:05	Seismic Ocean Bottom Receiver	SEISOBR	information	5° 34,160' S	148° 7,989' E	900.2
SO252_22-1	26/11/2016 06:20:10	Seismic Ocean Bottom Receiver	SEISOBR	information	5° 33,411' S	148° 8,926' E	929.1
SO252_22-1	26/11/2016 06:40:40	Seismic Ocean Bottom Receiver	SEISOBR	information	5° 33,282' S	148° 8,682' E	948.7
SO252_22-1	26/11/2016 06:41:45	Seismic Ocean Bottom Receiver	SEISOBR	information	5° 33,311' S	148° 8,671' E	940.6
SO252_22-1	26/11/2016 07:47:00	Seismic Ocean Bottom Receiver	SEISOBR	information	5° 31,203' S	148° 9,552' E	1143.8
SO252_22-1	26/11/2016 08:07:04	Seismic Ocean Bottom Receiver	SEISOBR	information	5° 29,995' S	148° 9,484' E	1174.8
SO252_22-1	26/11/2016 08:28:12	Seismic Ocean Bottom Receiver	SEISOBR	information	5° 29,410' S	148° 9,156' E	1160.7
SO252_22-1	26/11/2016 08:42:16	Seismic Ocean Bottom Receiver	SEISOBR	information	5° 29,379' S	148° 9,272' E	1166.1
SO252_22-1	26/11/2016 09:00:07	Seismic Ocean Bottom Receiver	SEISOBR	station end	5° 29,675' S	148° 9,815' E	1207.9
SO252_23-1	26/11/2016 09:52:27	Heat-Flow probe	HF	station start	5° 26,025' S	148° 14,217' E	1432
SO252_23-1	26/11/2016 10:00:00	Heat-Flow probe	HF	in the water	5° 26,031' S	148° 14,215' E	1433.9
SO252_23-1	26/11/2016 10:05:12	Heat-Flow probe	HF	in the water	5° 26,028' S	148° 14,215' E	1432.3
SO252_23-1	26/11/2016 10:36:52	Heat-Flow probe	HF	max depth/on ground	5° 26,014' S	148° 14,197' E	1430.3

Station	Date / Time UTC	Device	Device Abbreviation	Action	Latitude	Longitude	Depth (m)
SO252_23-1	26/11/2016 10:38:44	Heat-Flow probe	HF	hoisting	5° 26,017' S	148° 14,198' E	1433.2
SO252_23-1	26/11/2016 10:41:54	Heat-Flow probe	HF	lowering	5° 26,015' S	148° 14,199' E	1431.4
SO252_23-1	26/11/2016 10:43:17	Heat-Flow probe	HF	max depth/on ground	5° 26,012' S	148° 14,197' E	1431.2
SO252_23-1	26/11/2016 11:00:03	Heat-Flow probe	HF	hoisting	5° 26,011' S	148° 14,201' E	1431.8
SO252_23-1	26/11/2016 11:02:33	Heat-Flow probe	HF	information	5° 26,009' S	148° 14,200' E	1436.3
SO252_23-1	26/11/2016 11:03:52	Heat-Flow probe	HF	station end	5° 26,009' S	148° 14,201' E	1435.2
SO252_23-2	26/11/2016 11:34:49	Heat-Flow probe	HF	station start	5° 26,418' S	148° 14,064' E	1417
SO252_23-2	26/11/2016 11:45:47	Heat-Flow probe	HF	lowering	5° 26,416' S	148° 14,060' E	1418.6
SO252_23-2	26/11/2016 11:49:17	Heat-Flow probe	HF	max depth/on ground	5° 26,416' S	148° 14,060' E	1420
SO252_23-2	26/11/2016 12:04:54	Heat-Flow probe	HF	hoisting	5° 26,438' S	148° 14,057' E	1418.2
SO252_23-2	26/11/2016 12:05:54	Heat-Flow probe	HF	information	5° 26,417' S	148° 14,065' E	1419.3
SO252_23-2	26/11/2016 12:33:24	Heat-Flow probe	HF	information	5° 26,565' S	148° 14,005' E	1411.8
SO252_23-2	26/11/2016 12:35:45	Heat-Flow probe	HF	information	5° 26,564' S	148° 14,002' E	1413.8
SO252_23-2	26/11/2016 12:39:45	Heat-Flow probe	HF	in the water	5° 26,565' S	148° 14,001' E	1411.7
SO252_23-2	26/11/2016 12:42:35	Heat-Flow probe	HF	information	5° 26,567' S	148° 14,004' E	1411.2
SO252_23-2	26/11/2016 12:50:11	Heat-Flow probe	HF	station end	5° 26,578' S	148° 13,995' E	1409.8
SO252_23-3	26/11/2016 13:13:56	Heat-Flow probe	HF	station start	5° 26,937' S	148° 13,848' E	1399.1
SO252_23-3	26/11/2016 13:19:22	Heat-Flow probe	HF	lowering	5° 26,932' S	148° 13,847' E	1399.4
SO252_23-3	26/11/2016 13:24:21	Heat-Flow probe	HF	max depth/on ground	5° 26,933' S	148° 13,849' E	1400
SO252_23-3	26/11/2016 13:39:15	Heat-Flow probe	HF	hoisting	5° 26,938' S	148° 13,847' E	1399.3
SO252_23-3	26/11/2016 13:45:46	Heat-Flow probe	HF	information	5° 26,938' S	148° 13,850' E	1402.1
SO252_23-3	26/11/2016 13:46:28	Heat-Flow probe	HF	station end	5° 26,939' S	148° 13,849' E	1399.9
SO252_23-4	26/11/2016 14:24:25	Heat-Flow probe	HF	station start	5° 27,499' S	148° 13,490' E	1381

Station	Date / Time UTC	Device	Device Abbreviation	Action	Latitude	Longitude	Depth (m)
SO252_23-4	26/11/2016 14:28:30	Heat-Flow probe	HF	lowering	5° 27,501' S	148° 13,486' E	1381.3
SO252_23-4	26/11/2016 14:31:06	Heat-Flow probe	HF	max depth/on ground	5° 27,500' S	148° 13,485' E	1380.4
SO252_23-4	26/11/2016 14:46:12	Heat-Flow probe	HF	hoisting	5° 27,498' S	148° 13,489' E	1382.5
SO252_23-4	26/11/2016 14:54:00	Heat-Flow probe	HF	information	5° 27,498' S	148° 13,487' E	1380.5
SO252_23-4	26/11/2016 14:54:21	Heat-Flow probe	HF	station end	5° 27,498' S	148° 13,487' E	1379.6
SO252_23-5	26/11/2016 15:38:18	Heat-Flow probe	HF	station start	5° 28,139' S	148° 13,173' E	1376.5
SO252_23-5	26/11/2016 15:38:37	Heat-Flow probe	HF	lowering	5° 28,139' S	148° 13,174' E	1376.9
SO252_23-5	26/11/2016 15:43:39	Heat-Flow probe	HF	max depth/on ground	5° 28,142' S	148° 13,173' E	1376.6
SO252_23-5	26/11/2016 15:58:41	Heat-Flow probe	HF	hoisting	5° 28,137' S	148° 13,177' E	1377.5
SO252_23-5	26/11/2016 16:28:02	Heat-Flow probe	HF	information	5° 28,138' S	148° 13,175' E	1378
SO252_23-5	26/11/2016 16:31:27	Heat-Flow probe	HF	information	5° 28,136' S	148° 13,175' E	1376.5
SO252_23-5	26/11/2016 16:37:26	Heat-Flow probe	HF	station end	5° 28,139' S	148° 13,175' E	1378
SO252_23-6	26/11/2016 17:15:29	Heat-Flow probe	HF	station start	5° 28,746' S	148° 12,806' E	1347.5
SO252_23-6	26/11/2016 17:19:15	Heat-Flow probe	HF	lowering	5° 28,751' S	148° 12,804' E	1339.9
SO252_23-6	26/11/2016 17:22:38	Heat-Flow probe	HF	information	5° 28,753' S	148° 12,800' E	1345.3
SO252_23-6	26/11/2016 17:23:13	Heat-Flow probe	HF	lowering	5° 28,752' S	148° 12,800' E	1347.4
SO252_23-6	26/11/2016 17:46:06	Heat-Flow probe	HF	max depth/on ground	5° 28,750' S	148° 12,803' E	1346.8
SO252_23-6	26/11/2016 18:00:18	Heat-Flow probe	HF	hoisting	5° 28,750' S	148° 12,799' E	1345.8
SO252_23-6	26/11/2016 18:03:51	Heat-Flow probe	HF	information	5° 28,749' S	148° 12,801' E	1346.2
SO252_23-6	26/11/2016 18:04:22	Heat-Flow probe	HF	station end	5° 28,748' S	148° 12,801' E	1346.2
SO252_23-7	26/11/2016 18:40:18	Heat-Flow probe	HF	station start	5° 29,242' S	148° 12,555' E	1320.5
SO252_23-7	26/11/2016 18:44:26	Heat-Flow probe	HF	lowering	5° 29,245' S	148° 12,550' E	1320
SO252_23-7	26/11/2016 18:48:28	Heat-Flow probe	HF	max depth/on ground	5° 29,248' S	148° 12,552' E	1323.3

Station	Date / Time UTC	Device	Device Abbreviation	Action	Latitude	Longitude	Depth (m)
SO252_23-7	26/11/2016 19:02:24	Heat-Flow probe	HF	hoisting	5° 29,241' S	148° 12,555' E	1321.5
SO252_23-7	26/11/2016 19:11:49	Heat-Flow probe	HF	station end	5° 29,244' S	148° 12,554' E	1320.9
SO252_23-8	26/11/2016 19:40:57	Heat-Flow probe	HF	station start	5° 29,633' S	148° 12,233' E	1299.3
SO252_23-8	26/11/2016 19:41:36	Heat-Flow probe	HF	lowering	5° 29,635' S	148° 12,231' E	1306.2
SO252_23-8	26/11/2016 19:47:12	Heat-Flow probe	HF	max depth/on ground	5° 29,634' S	148° 12,228' E	1301.2
SO252_23-8	26/11/2016 20:01:30	Heat-Flow probe	HF	hoisting	5° 29,635' S	148° 12,228' E	1299.1
SO252_23-8	26/11/2016 20:08:21	Heat-Flow probe	HF	station end	5° 29,634' S	148° 12,232' E	1300.4
SO252_23-9	26/11/2016 20:39:55	Heat-Flow probe	HF	station start	5° 29,968' S	148° 11,908' E	1285
SO252_23-9	26/11/2016 20:41:17	Heat-Flow probe	HF	lowering	5° 29,967' S	148° 11,908' E	1283.5
SO252_23-9	26/11/2016 20:45:07	Heat-Flow probe	HF	max depth/on ground	5° 29,965' S	148° 11,907' E	1284.3
SO252_23-9	26/11/2016 21:00:19	Heat-Flow probe	HF	hoisting	5° 29,967' S	148° 11,905' E	1284.6
SO252_23-9	26/11/2016 21:07:27	Heat-Flow probe	HF	station end	5° 29,969' S	148° 11,904' E	1283
SO252_23-10	26/11/2016 21:41:23	Heat-Flow probe	HF	station start	5° 30,368' S	148° 11,454' E	1245
SO252_23-10	26/11/2016 21:41:43	Heat-Flow probe	HF	lowering	5° 30,368' S	148° 11,454' E	1243.8
SO252_23-10	26/11/2016 21:44:09	Heat-Flow probe	HF	max depth/on ground	5° 30,369' S	148° 11,454' E	1244.3
SO252_23-10	26/11/2016 21:45:01	Heat-Flow probe	HF	hoisting	5° 30,370' S	148° 11,454' E	1245.2
SO252_23-10	26/11/2016 22:18:09	Heat-Flow probe	HF	on deck	5° 30,370' S	148° 11,457' E	1245.1
SO252_23-10	26/11/2016 22:20:56	Heat-Flow probe	HF	station end	5° 30,368' S	148° 11,459' E	1250.5
SO252_24-1	26/11/2016 22:30:22	Seismic Ocean Bottom Receiver	SEISOBR	station start	5° 30,496' S	148° 11,149' E	1234.2
SO252_24-1	26/11/2016 22:31:24	Seismic Ocean Bottom Receiver	SEISOBR	released	5° 30,536' S	148° 11,034' E	1233.7
SO252_24-1	26/11/2016 23:53:00	Seismic Ocean Bottom Receiver	SEISOBR	information	5° 31,073' S	148° 9,340' E	1122.8
SO252_24-1	27/11/2016 00:27:42	Seismic Ocean Bottom Receiver	SEISOBR	station end	5° 31,071' S	148° 9,339' E	1122
SO252_25-1	27/11/2016 00:54:56	HyBIS	HyBIS	station start	5° 31,073' S	148° 9,338' E	1122.1

Station	Date / Time UTC	Device	Device Abbreviation	Action	Latitude	Longitude	Depth (m)
SO252_25-1	27/11/2016 01:14:30	HyBIS	HyBIS	in the water	5° 31,070' S	148° 9,342' E	1122
SO252_25-1	27/11/2016 01:19:07	HyBIS	HyBIS	in the water	5° 31,072' S	148° 9,342' E	1121
SO252_25-1	27/11/2016 01:50:55	HyBIS	HyBIS	information	5° 31,071' S	148° 9,341' E	1123.5
SO252_25-1	27/11/2016 04:05:19	HyBIS	HyBIS	information	5° 31,064' S	148° 9,313' E	1119.1
SO252_25-1	27/11/2016 04:13:57	HyBIS	HyBIS	on deck	5° 31,060' S	148° 9,316' E	1119.3
SO252_25-1	27/11/2016 04:18:52	HyBIS	HyBIS	on deck	5° 31,060' S	148° 9,315' E	1118.5
SO252_25-1	27/11/2016 04:20:22	HyBIS	HyBIS	information	5° 31,060' S	148° 9,315' E	1119.9
SO252_25-1	27/11/2016 04:22:01	HyBIS	HyBIS	station end	5° 31,060' S	148° 9,316' E	1118
SO252_26-1	27/11/2016 04:29:45	KONGSBERG EM122	EM122	station start	5° 31,060' S	148° 9,072' E	1085.6
SO252_26-1	27/11/2016 05:02:27	KONGSBERG EM122	EM122	alter course	5° 32,236' S	148° 6,245' E	420.6
SO252_26-1	27/11/2016 05:11:33	KONGSBERG EM122	EM122	alter course	5° 31,611' S	148° 6,026' E	482.4
SO252_26-1	27/11/2016 05:22:13	KONGSBERG EM122	EM122	alter course	5° 30,644' S	148° 6,348' E	438.9
SO252_26-1	27/11/2016 05:40:40	KONGSBERG EM122	EM122	station end	5° 30,984' S	148° 6,506' E	260.3
SO252_27-1	27/11/2016 05:42:29	Drone	DRONE	station start	5° 30,981' S	148° 6,514' E	261.4
SO252_27-1	27/11/2016 05:45:00	Drone	DRONE	information	5° 30,995' S	148° 6,509' E	253.2
SO252_27-1	27/11/2016 06:00:13	Drone	DRONE	information	5° 30,997' S	148° 6,512' E	254.5
SO252_27-1	27/11/2016 06:02:31	Drone	DRONE	information	5° 30,996' S	148° 6,512' E	254.3
SO252_27-1	27/11/2016 06:18:02	Drone	DRONE	information	5° 30,997' S	148° 6,510' E	252.2
SO252_27-1	27/11/2016 06:19:47	Drone	DRONE	station end	5° 30,998' S	148° 6,510' E	252.9
SO252_28-1	27/11/2016 08:50:00	Seismic Towed Receiver	SEISTR	station start	5° 35,255' S	148° 9,178' E	767.2
SO252_28-1	27/11/2016 08:55:11	Seismic Towed Receiver	SEISTR	information	5° 35,120' S	148° 9,029' E	793.7
SO252_28-1	27/11/2016 08:57:24	Seismic Towed Receiver	SEISTR	information	5° 35,067' S	148° 8,973' E	787.3
SO252_28-1	27/11/2016 09:46:25	Seismic Towed Receiver	SEISTR	information	5° 34,165' S	148° 8,206' E	904.1

Station	Date / Time UTC	Device	Device Abbreviation	Action	Latitude	Longitude	Depth (m)
SO252_28-1	27/11/2016 09:51:30	Seismic Towed Receiver	SEISTR	information	5° 34,090' S	148° 8,131' E	908
SO252_28-1	27/11/2016 10:07:28	Seismic Towed Receiver	SEISTR	in the water	5° 33,808' S	148° 7,822' E	925.6
SO252_28-1	27/11/2016 10:18:53	Seismic Towed Receiver	SEISTR	information	5° 33,525' S	148° 7,562' E	923.3
SO252_28-1	27/11/2016 11:17:07	Seismic Towed Receiver	SEISTR	profile start	5° 31,561' S	148° 5,801' E	628.2
SO252_28-1	27/11/2016 13:33:42	Seismic Towed Receiver	SEISTR	alter course	5° 27,824' S	147° 59,800' E	1206.9
SO252_28-1	27/11/2016 13:52:55	Seismic Towed Receiver	SEISTR	alter course	5° 26,894' S	148° 0,103' E	1326.8
SO252_28-1	27/11/2016 15:57:51	Seismic Towed Receiver	SEISTR	alter course	5° 30,447' S	148° 6,235' E	489.1
SO252_28-1	27/11/2016 16:21:30	Seismic Towed Receiver	SEISTR	alter course	5° 31,339' S	148° 5,952' E	546.7
SO252_28-1	27/11/2016 19:02:04	Seismic Towed Receiver	SEISTR	alter course	5° 27,773' S	147° 59,789' E	1203.9
SO252_28-1	27/11/2016 19:21:21	Seismic Towed Receiver	SEISTR	alter course	5° 26,851' S	148° 0,132' E	1324.1
SO252_28-1	27/11/2016 21:24:10	Seismic Towed Receiver	SEISTR	alter course	5° 30,414' S	148° 6,256' E	469.4
SO252_28-1	27/11/2016 21:42:18	Seismic Towed Receiver	SEISTR	alter course	5° 31,416' S	148° 5,848' E	606.2
SO252_28-1	27/11/2016 23:43:11	Seismic Towed Receiver	SEISTR	alter course	5° 27,613' S	147° 59,739' E	1206.4
SO252_28-1	28/11/2016 00:00:40	Seismic Towed Receiver	SEISTR	alter course	5° 26,711' S	148° 0,266' E	1307
SO252_28-1	28/11/2016 00:34:45	Seismic Towed Receiver	SEISTR	information	5° 27,613' S	148° 1,838' E	961.4
SO252_28-1	28/11/2016 00:45:31	Seismic Towed Receiver	SEISTR	information	5° 27,892' S	148° 2,286' E	914.1
SO252_28-1	28/11/2016 00:50:29	Seismic Towed Receiver	SEISTR	on deck	5° 28,001' S	148° 2,463' E	982
SO252_28-1	28/11/2016 01:10:16	Seismic Towed Receiver	SEISTR	information	5° 28,403' S	148° 3,111' E	892.3
SO252_28-1	28/11/2016 01:12:05	Seismic Towed Receiver	SEISTR	on deck	5° 28,436' S	148° 3,165' E	900.9
SO252_28-1	28/11/2016 01:31:21	Seismic Towed Receiver	SEISTR	on deck	5° 28,860' S	148° 3,836' E	891.4
SO252_28-1	28/11/2016 01:39:26	Seismic Towed Receiver	SEISTR	alter course	5° 29,041' S	148° 4,137' E	888.1
SO252_28-1	28/11/2016 02:02:45	Seismic Towed Receiver	SEISTR	information	5° 29,450' S	148° 5,025' E	841.8
SO252_28-1	28/11/2016 02:15:45	Seismic Towed Receiver	SEISTR	information	5° 29,645' S	148° 5,468' E	780.9

Station	Date / Time UTC	Device	Device Abbreviation	Action	Latitude	Longitude	Depth (m)
SO252_28-1	28/11/2016 02:21:22	Seismic Towed Receiver	SEISTR	information	5° 29,716' S	148° 5,653' E	751.9
SO252_28-1	28/11/2016 02:29:33	Seismic Towed Receiver	SEISTR	information	5° 29,839' S	148° 5,932' E	682.6
SO252_28-1	28/11/2016 02:47:11	Seismic Towed Receiver	SEISTR	information	5° 30,072' S	148° 6,509' E	523.5
SO252_28-1	28/11/2016 03:03:13	Seismic Towed Receiver	SEISTR	PCable in water	5° 30,290' S	148° 7,179' E	557.7
SO252_28-1	28/11/2016 03:03:35	Seismic Towed Receiver	SEISTR	information	5° 30,296' S	148° 7,194' E	565.5
SO252_28-1	28/11/2016 03:05:12	Seismic Towed Receiver	SEISTR	information	5° 30,321' S	148° 7,263' E	586.2
SO252_28-1	28/11/2016 03:21:38	Seismic Towed Receiver	SEISTR	information	5° 30,614' S	148° 7,897' E	806.1
SO252_28-1	28/11/2016 03:25:41	Seismic Towed Receiver	SEISTR	information	5° 32,305' S	148° 6,467' E	448.4
SO252_28-1	28/11/2016 04:42:14	Seismic Towed Receiver	SEISTR	information	5° 31,491' S	148° 5,881' E	586.7
SO252_28-1	28/11/2016 07:03:27	Seismic Towed Receiver	SEISTR	alter course	5° 27,715' S	147° 59,842' E	1208.3
SO252_28-1	28/11/2016 07:22:29	Seismic Towed Receiver	SEISTR	alter course	5° 26,769' S	148° 0,175' E	1319
SO252_28-1	28/11/2016 09:27:25	Seismic Towed Receiver	SEISTR	alter course	5° 30,371' S	148° 6,325' E	422
SO252_28-1	28/11/2016 09:45:28	Seismic Towed Receiver	SEISTR	alter course	5° 31,258' S	148° 5,997' E	513.3
SO252_28-1	28/11/2016 11:57:48	Seismic Towed Receiver	SEISTR	alter course	5° 27,664' S	147° 59,836' E	1205.6
SO252_28-1	28/11/2016 12:15:17	Seismic Towed Receiver	SEISTR	alter course	5° 26,788' S	148° 0,168' E	1321
SO252_28-1	28/11/2016 14:19:12	Seismic Towed Receiver	SEISTR	alter course	5° 30,392' S	148° 6,401' E	365.5
SO252_28-1	28/11/2016 14:37:02	Seismic Towed Receiver	SEISTR	alter course	5° 31,256' S	148° 6,002' E	512.4
SO252_28-1	28/11/2016 17:11:02	Seismic Towed Receiver	SEISTR	alter course	5° 27,525' S	147° 59,795' E	1217.3
SO252_28-1	28/11/2016 17:27:42	Seismic Towed Receiver	SEISTR	alter course	5° 26,677' S	148° 0,246' E	1312.7
SO252_28-1	28/11/2016 19:28:02	Seismic Towed Receiver	SEISTR	alter course	5° 30,296' S	148° 6,355' E	391.1
SO252_28-1	28/11/2016 19:46:06	Seismic Towed Receiver	SEISTR	alter course	5° 31,215' S	148° 6,011' E	499.7
SO252_28-1	28/11/2016 21:51:09	Seismic Towed Receiver	SEISTR	alter course	5° 27,602' S	147° 59,879' E	1215
SO252_28-1	28/11/2016 22:09:04	Seismic Towed Receiver	SEISTR	alter course	5° 26,701' S	148° 0,210' E	1314.6

Station	Date / Time UTC	Device	Device Abbreviation	Action	Latitude	Longitude	Depth (m)
SO252_28-1	29/11/2016 00:26:51	Seismic Towed Receiver	SEISTR	alter course	5° 30,241' S	148° 6,327' E	388.9
SO252_28-1	29/11/2016 00:44:17	Seismic Towed Receiver	SEISTR	alter course	5° 31,125' S	148° 6,089' E	440.5
SO252_28-1	29/11/2016 02:55:00	Seismic Towed Receiver	SEISTR	alter course	5° 27,559' S	147° 59,883' E	1217.2
SO252_28-1	29/11/2016 03:17:36	Seismic Towed Receiver	SEISTR	alter course	5° 26,585' S	148° 0,317' E	1325.9
SO252_28-1	29/11/2016 05:28:12	Seismic Towed Receiver	SEISTR	alter course	5° 30,274' S	148° 6,438' E	357
SO252_28-1	29/11/2016 05:44:43	Seismic Towed Receiver	SEISTR	alter course	5° 31,128' S	148° 6,083' E	447.7
SO252_28-1	29/11/2016 08:00:00	Seismic Towed Receiver	SEISTR	alter course	5° 27,441' S	147° 59,741' E	1218
SO252_28-1	29/11/2016 10:52:01	Seismic Towed Receiver	SEISTR	alter course	5° 31,109' S	148° 5,794' E	633.7
SO252_28-1	29/11/2016 11:09:09	Seismic Towed Receiver	SEISTR	alter course	5° 31,955' S	148° 5,529' E	593
SO252_28-1	29/11/2016 13:13:18	Seismic Towed Receiver	SEISTR	alter course	5° 28,392' S	147° 59,355' E	996.8
SO252_28-1	29/11/2016 13:33:26	Seismic Towed Receiver	SEISTR	alter course	5° 27,425' S	147° 59,789' E	1223.6
SO252_28-1	29/11/2016 15:20:52	Seismic Towed Receiver	SEISTR	alter course	5° 31,152' S	148° 5,970' E	523.9
SO252_28-1	29/11/2016 15:32:49	Seismic Towed Receiver	SEISTR	alter course	5° 31,945' S	148° 5,499' E	615.5
SO252_28-1	29/11/2016 16:18:08	Seismic Towed Receiver	SEISTR	information	5° 30,508' S	148° 2,921' E	925.7
SO252_28-1	29/11/2016 17:39:02	Seismic Towed Receiver	SEISTR	information	5° 27,977' S	147° 59,051' E	1062.4
SO252_28-1	29/11/2016 17:42:43	Seismic Towed Receiver	SEISTR	information	5° 27,919' S	147° 58,978' E	1070.3
SO252_28-1	29/11/2016 17:43:21	Seismic Towed Receiver	SEISTR	information	5° 27,908' S	147° 58,965' E	1072.8
SO252_28-1	29/11/2016 18:04:22	Seismic Towed Receiver	SEISTR	information	5° 27,563' S	147° 58,593' E	1125.7
SO252_28-1	29/11/2016 18:05:17	Seismic Towed Receiver	SEISTR	information	5° 27,547' S	147° 58,574' E	1133.8
SO252_28-1	29/11/2016 18:51:53	Seismic Towed Receiver	SEISTR	information	5° 26,955' S	147° 57,460' E	1187.2
SO252_28-1	29/11/2016 19:15:36	Seismic Towed Receiver	SEISTR	information	5° 26,686' S	147° 56,951' E	1253.5
SO252_28-1	29/11/2016 19:23:28	Seismic Towed Receiver	SEISTR	information	5° 26,634' S	147° 56,819' E	1263.6
SO252_28-1	30/11/2016 22:00:23	Seismic Towed Receiver	SEISTR	information	5° 30,842' S	148° 4,013' E	904.2

Station	Date / Time UTC	Device	Device Abbreviation	Action	Latitude	Longitude	Depth (m)
SO252_28-1	30/11/2016 22:20:00	Seismic Towed Receiver	SEISTR	in the water	5° 30,480' S	148° 3,501' E	913.2
SO252_28-1	01/12/2016 00:04:12	Seismic Towed Receiver	SEISTR	in the water	5° 28,310' S	148° 0,248' E	838.6
SO252_28-1	01/12/2016 00:05:01	Seismic Towed Receiver	SEISTR	in the water	5° 28,299' S	148° 0,220' E	830.3
SO252_28-1	01/12/2016 00:23:41	Seismic Towed Receiver	SEISTR	in the water	5° 28,009' S	147° 59,471' E	1140.2
SO252_28-1	01/12/2016 00:28:07	Seismic Towed Receiver	SEISTR	information	5° 27,940' S	147° 59,283' E	1123
SO252_28-1	01/12/2016 00:34:22	Seismic Towed Receiver	SEISTR	alter course	5° 27,819' S	147° 58,938' E	1091
SO252_28-1	01/12/2016 00:44:03	Seismic Towed Receiver	SEISTR	information	5° 27,405' S	147° 58,846' E	1158.5
SO252_28-1	01/12/2016 00:53:54	Seismic Towed Receiver	SEISTR	alter course	5° 26,922' S	147° 59,167' E	1296.5
SO252_28-1	01/12/2016 00:57:23	Seismic Towed Receiver	SEISTR	in the water	5° 26,845' S	147° 59,312' E	1305
SO252_28-1	01/12/2016 01:11:08	Seismic Towed Receiver	SEISTR	profile start	5° 27,195' S	147° 59,958' E	1253.2
SO252_28-1	01/12/2016 03:15:18	Seismic Towed Receiver	SEISTR	alter course	5° 30,973' S	148° 5,904' E	598.7
SO252_28-1	01/12/2016 03:27:45	Seismic Towed Receiver	SEISTR	alter course	5° 31,514' S	148° 5,818' E	617.3
SO252_28-1	01/12/2016 05:42:35	Seismic Towed Receiver	SEISTR	alter course	5° 28,070' S	147° 59,464' E	1126.4
SO252_28-1	01/12/2016 06:01:12	Seismic Towed Receiver	SEISTR	alter course	5° 27,260' S	147° 59,872' E	1254.7
SO252_28-1	01/12/2016 08:09:46	Seismic Towed Receiver	SEISTR	alter course	5° 30,844' S	148° 5,957' E	591.9
SO252_28-1	01/12/2016 08:26:05	Seismic Towed Receiver	SEISTR	alter course	5° 31,577' S	148° 5,750' E	646.6
SO252_28-1	01/12/2016 10:31:55	Seismic Towed Receiver	SEISTR	alter course	5° 27,906' S	147° 59,586' E	1175.4
SO252_28-1	01/12/2016 10:46:48	Seismic Towed Receiver	SEISTR	alter course	5° 27,195' S	147° 59,915' E	1261.3
SO252_28-1	01/12/2016 13:01:17	Seismic Towed Receiver	SEISTR	alter course	5° 30,719' S	148° 6,025' E	587.2
SO252_28-1	01/12/2016 13:16:01	Seismic Towed Receiver	SEISTR	alter course	5° 31,427' S	148° 5,861' E	597.1
SO252_28-1	01/12/2016 15:22:36	Seismic Towed Receiver	SEISTR	alter course	5° 27,816' S	147° 59,722' E	1193.3
SO252_28-1	01/12/2016 15:41:06	Seismic Towed Receiver	SEISTR	alter course	5° 27,004' S	148° 0,050' E	1247.6
SO252_28-1	01/12/2016 17:55:01	Seismic Towed Receiver	SEISTR	alter course	5° 30,641' S	148° 6,181' E	538.7

Station	Date / Time UTC	Device	Device Abbreviation	Action	Latitude	Longitude	Depth (m)
SO252_28-1	01/12/2016 18:08:48	Seismic Towed Receiver	SEISTR	alter course	5° 31,268' S	148° 5,948' E	548.8
SO252_28-1	01/12/2016 20:14:44	Seismic Towed Receiver	SEISTR	alter course	5° 27,732' S	147° 59,731' E	1194.4
SO252_28-1	01/12/2016 20:31:21	Seismic Towed Receiver	SEISTR	alter course	5° 26,917' S	148° 0,101' E	1322.6
SO252_28-1	01/12/2016 22:51:16	Seismic Towed Receiver	SEISTR	alter course	5° 30,530' S	148° 6,301' E	460.3
SO252_28-1	01/12/2016 23:05:14	Seismic Towed Receiver	SEISTR	alter course	5° 31,107' S	148° 6,062' E	464.4
SO252_28-1	02/12/2016 01:05:57	Seismic Towed Receiver	SEISTR	alter course	5° 27,598' S	147° 59,958' E	1213.7
SO252_28-1	02/12/2016 01:21:49	Seismic Towed Receiver	SEISTR	alter course	5° 26,805' S	148° 0,152' E	1322.4
SO252_28-1	02/12/2016 03:47:02	Seismic Towed Receiver	SEISTR	alter course	5° 30,391' S	148° 6,282' E	450.9
SO252_28-1	02/12/2016 04:04:01	Seismic Towed Receiver	SEISTR	alter course	5° 31,187' S	148° 6,031' E	491.1
SO252_28-1	02/12/2016 04:15:04	Seismic Towed Receiver	SEISTR	information	5° 31,001' S	148° 5,559' E	705.4
SO252_28-1	02/12/2016 04:19:13	Seismic Towed Receiver	SEISTR	information	5° 30,933' S	148° 5,437' E	687.6
SO252_28-1	02/12/2016 04:23:21	Seismic Towed Receiver	SEISTR	information	5° 30,886' S	148° 5,355' E	612.6
SO252_28-1	02/12/2016 04:42:00	Seismic Towed Receiver	SEISTR	information	5° 30,618' S	148° 4,941' E	670.2
SO252_28-1	02/12/2016 04:48:56	Seismic Towed Receiver	SEISTR	information	5° 30,514' S	148° 4,797' E	712.7
SO252_28-1	02/12/2016 05:14:33	Seismic Towed Receiver	SEISTR	information	5° 30,142' S	148° 4,181' E	894.6
SO252_28-1	02/12/2016 05:56:51	Seismic Towed Receiver	SEISTR	information	5° 29,504' S	148° 3,105' E	957.9
SO252_28-1	02/12/2016 05:59:15	Seismic Towed Receiver	SEISTR	information	5° 29,465' S	148° 3,032' E	937.9
SO252_28-1	02/12/2016 06:16:29	Seismic Towed Receiver	SEISTR	information	5° 29,043' S	148° 2,344' E	962.9
SO252_28-1	02/12/2016 06:20:51	Seismic Towed Receiver	SEISTR	information	5° 28,935' S	148° 2,175' E	968.8
SO252_28-1	02/12/2016 07:04:39	Seismic Towed Receiver	SEISTR	alter course	5° 27,558' S	147° 59,943' E	1223.2
SO252_28-1	02/12/2016 07:22:51	Seismic Towed Receiver	SEISTR	alter course	5° 26,683' S	148° 0,227' E	1316.5
SO252_28-1	02/12/2016 09:44:19	Seismic Towed Receiver	SEISTR	alter course	5° 30,216' S	148° 6,396' E	403.9
SO252_28-1	02/12/2016 10:00:27	Seismic Towed Receiver	SEISTR	alter course	5° 31,015' S	148° 6,151' E	399.4

Station	Date / Time UTC	Device	Device Abbreviation	Action	Latitude	Longitude	Depth (m)
SO252_28-1	02/12/2016 12:03:19	Seismic Towed Receiver	SEISTR	alter course	5° 27,501' S	147° 59,936' E	1219.7
SO252_28-1	02/12/2016 12:18:30	Seismic Towed Receiver	SEISTR	alter course	5° 26,800' S	148° 0,146' E	1323.9
SO252_28-1	02/12/2016 14:36:37	Seismic Towed Receiver	SEISTR	alter course	5° 30,454' S	148° 6,404' E	372.2
SO252_28-1	02/12/2016 14:50:50	Seismic Towed Receiver	SEISTR	alter course	5° 31,245' S	148° 5,960' E	539.1
SO252_28-1	02/12/2016 17:00:00	Seismic Towed Receiver	SEISTR	alter course	5° 27,583' S	147° 59,772' E	1213.5
SO252_28-1	02/12/2016 17:15:14	Seismic Towed Receiver	SEISTR	alter course	5° 26,853' S	148° 0,119' E	1328
SO252_28-1	02/12/2016 19:35:28	Seismic Towed Receiver	SEISTR	alter course	5° 30,477' S	148° 6,237' E	493.4
SO252_28-1	02/12/2016 19:54:31	Seismic Towed Receiver	SEISTR	alter course	5° 31,428' S	148° 5,854' E	597.2
SO252_28-1	02/12/2016 21:52:20	Seismic Towed Receiver	SEISTR	alter course	5° 27,927' S	147° 59,586' E	1174
SO252_28-1	02/12/2016 22:12:10	Seismic Towed Receiver	SEISTR	alter course	5° 26,955' S	148° 0,039' E	1267.7
SO252_28-1	03/12/2016 00:34:13	Seismic Towed Receiver	SEISTR	alter course	5° 30,547' S	148° 6,137' E	557.1
SO252_28-1	03/12/2016 00:55:17	Seismic Towed Receiver	SEISTR	alter course	5° 31,572' S	148° 5,764' E	638.2
SO252_28-1	03/12/2016 02:42:21	Seismic Towed Receiver	SEISTR	alter course	5° 27,953' S	147° 59,487' E	1158
SO252_28-1	03/12/2016 03:02:07	Seismic Towed Receiver	SEISTR	alter course	5° 26,973' S	148° 0,038' E	1252.6
SO252_28-1	03/12/2016 05:30:00	Seismic Towed Receiver	SEISTR	alter course	5° 30,627' S	148° 6,156' E	552.9
SO252_28-1	03/12/2016 05:55:40	Seismic Towed Receiver	SEISTR	alter course	5° 31,858' S	148° 5,543' E	640.6
SO252_28-1	03/12/2016 07:42:29	Seismic Towed Receiver	SEISTR	alter course	5° 28,223' S	147° 59,428' E	1084.8
SO252_28-1	03/12/2016 08:04:22	Seismic Towed Receiver	SEISTR	alter course	5° 27,176' S	147° 59,906' E	1262.4
SO252_28-1	03/12/2016 10:34:30	Seismic Towed Receiver	SEISTR	alter course	5° 30,726' S	148° 6,052' E	571.5
SO252_28-1	03/12/2016 11:00:31	Seismic Towed Receiver	SEISTR	alter course	5° 31,817' S	148° 5,588' E	632.9
SO252_28-1	03/12/2016 12:46:54	Seismic Towed Receiver	SEISTR	alter course	5° 28,233' S	147° 59,303' E	1046.3
SO252_28-1	03/12/2016 13:06:17	Seismic Towed Receiver	SEISTR	alter course	5° 27,316' S	147° 59,799' E	1237.5
SO252_28-1	03/12/2016 15:40:28	Seismic Towed Receiver	SEISTR	alter course	5° 30,927' S	148° 6,024' E	522.3

Station	Date / Time UTC	Device	Device Abbreviation	Action	Latitude	Longitude	Depth (m)
SO252_28-1	03/12/2016 16:00:49	Seismic Towed Receiver	SEISTR	alter course	5° 32,011' S	148° 5,449' E	593.3
SO252_28-1	03/12/2016 17:51:14	Seismic Towed Receiver	SEISTR	alter course	5° 28,295' S	147° 59,259' E	1028.8
SO252_28-1	03/12/2016 18:09:49	Seismic Towed Receiver	SEISTR	alter course	5° 27,455' S	147° 59,699' E	1216.2
SO252_28-1	03/12/2016 20:33:00	Seismic Towed Receiver	SEISTR	alter course	5° 31,068' S	148° 5,849' E	608.7
SO252_28-1	03/12/2016 20:54:02	Seismic Towed Receiver	SEISTR	alter course	5° 27,675' S	147° 59,697' E	1077.2
SO252_28-1	03/12/2016 22:20:16	Seismic Towed Receiver	SEISTR	information	5° 29,074' S	148° 0,438' E	1052.6
SO252_28-1	03/12/2016 22:29:01	Seismic Towed Receiver	SEISTR	on deck	5° 28,809' S	148° 0,009' E	880.4
SO252_28-1	03/12/2016 22:43:22	Seismic Towed Receiver	SEISTR	in the water	5° 28,406' S	147° 59,361' E	991.9
SO252_28-1	03/12/2016 22:46:03	Seismic Towed Receiver	SEISTR	information	5° 28,328' S	147° 59,243' E	1016.6
SO252_28-1	03/12/2016 22:49:20	Seismic Towed Receiver	SEISTR	alter course	5° 28,209' S	147° 59,066' E	1028.8
SO252_28-1	03/12/2016 23:19:48	Seismic Towed Receiver	SEISTR	alter course	5° 26,836' S	147° 59,512' E	1290
SO252_28-1	04/12/2016 02:09:25	Seismic Towed Receiver	SEISTR	alter course	5° 30,650' S	148° 6,147' E	552.4
SO252_28-1	04/12/2016 02:40:48	Seismic Towed Receiver	SEISTR	alter course	5° 32,060' S	148° 5,492' E	587.3
SO252_28-1	04/12/2016 04:22:17	Seismic Towed Receiver	SEISTR	alter course	5° 28,356' S	147° 59,269' E	1012.3
SO252_28-1	04/12/2016 04:42:00	Seismic Towed Receiver	SEISTR	alter course	5° 27,438' S	147° 59,712' E	1218.9
SO252_28-1	04/12/2016 07:21:03	Seismic Towed Receiver	SEISTR	alter course	5° 31,023' S	148° 5,881' E	592.9
SO252_28-1	04/12/2016 07:44:40	Seismic Towed Receiver	SEISTR	alter course	5° 32,071' S	148° 5,473' E	597.1
SO252_28-1	04/12/2016 09:27:25	Seismic Towed Receiver	SEISTR	alter course	5° 28,421' S	147° 59,277' E	994
SO252_28-1	04/12/2016 09:44:48	Seismic Towed Receiver	SEISTR	alter course	5° 27,546' S	147° 59,646' E	1208.6
SO252_28-1	04/12/2016 12:45:37	Seismic Towed Receiver	SEISTR	alter course	5° 31,066' S	148° 5,812' E	629.6
SO252_28-1	04/12/2016 13:08:11	Seismic Towed Receiver	SEISTR	alter course	5° 32,013' S	148° 5,506' E	567.6
SO252_28-1	04/12/2016 14:50:20	Seismic Towed Receiver	SEISTR	alter course	5° 28,417' S	147° 59,302' E	990.5
SO252_28-1	04/12/2016 15:32:11	Seismic Towed Receiver	SEISTR	alter course	5° 26,538' S	148° 0,312' E	1324

Station	Date / Time UTC	Device	Device Abbreviation	Action	Latitude	Longitude	Depth (m)
SO252_28-1	04/12/2016 18:15:39	Seismic Towed Receiver	SEISTR	alter course	5° 30,187' S	148° 6,391' E	431
SO252_28-1	04/12/2016 18:55:02	Seismic Towed Receiver	SEISTR	alter course	5° 32,075' S	148° 5,485' E	592
SO252_28-1	04/12/2016 20:39:01	Seismic Towed Receiver	SEISTR	alter course	5° 28,482' S	147° 59,325' E	963.4
SO252_28-1	04/12/2016 21:17:39	Seismic Towed Receiver	SEISTR	alter course	5° 26,585' S	148° 0,268' E	1333
SO252_28-1	05/12/2016 00:00:02	Seismic Towed Receiver	SEISTR	alter course	5° 30,131' S	148° 6,372' E	472.1
SO252_28-1	05/12/2016 00:22:34	Seismic Towed Receiver	SEISTR	alter course	5° 31,076' S	148° 6,087' E	439
SO252_28-1	05/12/2016 02:08:41	Seismic Towed Receiver	SEISTR	alter course	5° 27,277' S	147° 59,687' E	1252.6
SO252_28-1	05/12/2016 02:37:07	Seismic Towed Receiver	SEISTR	alter course	5° 26,801' S	148° 0,080' E	1334.7
SO252_28-1	05/12/2016 05:21:30	Seismic Towed Receiver	SEISTR	information	5° 30,352' S	148° 5,884' E	660.9
SO252_28-1	05/12/2016 05:23:12	Seismic Towed Receiver	SEISTR	information	5° 30,381' S	148° 5,941' E	644.1
SO252_28-1	05/12/2016 05:27:58	Seismic Towed Receiver	SEISTR	information	5° 30,437' S	148° 6,035' E	606.5
SO252_28-1	05/12/2016 05:28:51	Seismic Towed Receiver	SEISTR	information	5° 30,465' S	148° 6,051' E	602.7
SO252_28-1	05/12/2016 05:45:33	Seismic Towed Receiver	SEISTR	information	5° 31,059' S	148° 5,972' E	530.8
SO252_28-1	05/12/2016 05:47:01	Seismic Towed Receiver	SEISTR	information	5° 31,107' S	148° 5,958' E	538.3
SO252_28-1	05/12/2016 05:51:46	Seismic Towed Receiver	SEISTR	information	5° 31,241' S	148° 5,892' E	579.5
SO252_28-1	05/12/2016 06:17:29	Seismic Towed Receiver	SEISTR	on deck	5° 31,925' S	148° 5,664' E	533.4
SO252_28-1	05/12/2016 06:21:55	Seismic Towed Receiver	SEISTR	on deck	5° 32,040' S	148° 5,626' E	492.2
SO252_28-1	05/12/2016 06:23:19	Seismic Towed Receiver	SEISTR	station end	5° 32,077' S	148° 5,617' E	488.7
SO252_29-1	29/11/2016 20:55:00	KONGSBERG EM122	EM122	station start	5° 28,543' S	148° 9,657' E	1216.6
SO252_29-1	29/11/2016 20:55:04	KONGSBERG EM122	EM122	profile start	5° 28,535' S	148° 9,663' E	1216.6
SO252_29-1	29/11/2016 21:31:38	KONGSBERG EM122	EM122	alter course	5° 24,168' S	148° 12,022' E	1381.8
SO252_29-1	29/11/2016 21:42:45	KONGSBERG EM122	EM122	alter course	5° 24,864' S	148° 13,124' E	1395
SO252_29-1	29/11/2016 22:20:35	KONGSBERG EM122	EM122	profile end	5° 29,049' S	148° 10,577' E	1262.1

Station	Date / Time UTC	Device	Device Abbreviation	Action	Latitude	Longitude	Depth (m)
SO252_29-1	29/11/2016 22:21:08	KONGSBERG EM122	EM122	station end	5° 29,102' S	148° 10,538' E	1257.4
SO252_30-1	29/11/2016 23:20:15	OFOS	OFOS	station start	5° 29,926' S	148° 3,543' E	734.4
SO252_30-1	29/11/2016 23:23:23	OFOS	OFOS	in the water	5° 29,915' S	148° 3,544' E	730.7
SO252_30-1	29/11/2016 23:54:11	OFOS	OFOS	information	5° 29,917' S	148° 3,541' E	736.5
SO252_30-1	30/11/2016 00:28:19	OFOS	OFOS	alter course	5° 29,901' S	148° 3,492' E	758.2
SO252_30-1	30/11/2016 01:16:15	OFOS	OFOS	hoisting	5° 29,957' S	148° 3,523' E	757.5
SO252_30-1	30/11/2016 01:39:33	OFOS	OFOS	on deck	5° 29,959' S	148° 3,525' E	758.2
SO252_30-1	30/11/2016 01:44:23	OFOS	OFOS	station end	5° 29,954' S	148° 3,527' E	758.2
SO252_30-1	30/11/2016 01:44:56	OFOS	OFOS	station end	5° 29,954' S	148° 3,527' E	755.4
SO252_30-1	30/11/2016 01:44:59	OFOS	OFOS	station end	5° 29,954' S	148° 3,526' E	754.6
SO252_31-1	30/11/2016 02:47:09	OFOS	OFOS	station start	5° 30,473' S	148° 6,583' E	215.2
SO252_31-1	30/11/2016 02:48:40	OFOS	OFOS	in the water	5° 30,481' S	148° 6,578' E	213.4
SO252_31-1	30/11/2016 03:00:00	OFOS	OFOS	max depth/on ground	5° 30,480' S	148° 6,580' E	214.8
SO252_31-1	30/11/2016 06:23:07	OFOS	OFOS	information	5° 31,099' S	148° 6,155' E	393.5
SO252_31-1	30/11/2016 06:44:19	OFOS	OFOS	hoisting	5° 31,178' S	148° 6,216' E	340.9
SO252_31-1	30/11/2016 06:56:39	OFOS	OFOS	on deck	5° 31,177' S	148° 6,210' E	343.8
SO252_31-1	30/11/2016 07:00:03	OFOS	OFOS	station end	5° 31,180' S	148° 6,210' E	345.8
SO252_32-1	30/11/2016 08:00:00	OFOS	OFOS	station start	5° 30,943' S	148° 2,431' E	926.6
SO252_32-1	30/11/2016 08:07:15	OFOS	OFOS	in the water	5° 30,926' S	148° 2,403' E	937.4
SO252_32-1	30/11/2016 08:33:44	OFOS	OFOS	information	5° 30,924' S	148° 2,401' E	936.8
SO252_32-1	30/11/2016 10:30:46	OFOS	OFOS	profile end	5° 31,176' S	148° 2,001' E	820.5
SO252_32-1	30/11/2016 10:31:13	OFOS	OFOS	hoisting	5° 31,175' S	148° 2,002' E	820.1
SO252_32-1	30/11/2016 10:55:50	OFOS	OFOS	on deck	5° 31,173' S	148° 2,003' E	822.8

Station	Date / Time UTC	Device	Device Abbreviation	Action	Latitude	Longitude	Depth (m)
SO252_32-1	30/11/2016 11:00:10	OFOS	OFOS	station end	5° 31,175' S	148° 2,000' E	820.8
SO252_33-1	30/11/2016 11:45:15	Heat-Flow probe	HF	station start	5° 31,131' S	148° 4,856' E	791.6
SO252_33-1	30/11/2016 12:18:18	Heat-Flow probe	HF	in the water	5° 31,123' S	148° 4,837' E	791.2
SO252_33-1	30/11/2016 12:28:03	Heat-Flow probe	HF	in the water	5° 31,126' S	148° 4,835' E	792.2
SO252_33-1	30/11/2016 12:50:08	Heat-Flow probe	HF	max depth/on ground	5° 31,128' S	148° 4,835' E	793.1
SO252_33-1	30/11/2016 12:52:38	Heat-Flow probe	HF	hoisting	5° 31,129' S	148° 4,834' E	792.2
SO252_33-1	30/11/2016 12:54:09	Heat-Flow probe	HF	information	5° 31,129' S	148° 4,834' E	794.2
SO252_33-2	30/11/2016 13:12:57	Heat-Flow probe	HF	lowering	5° 31,209' S	148° 4,691' E	822.8
SO252_33-2	30/11/2016 13:16:31	Heat-Flow probe	HF	max depth/on ground	5° 31,208' S	148° 4,691' E	825.2
SO252_33-2	30/11/2016 13:32:17	Heat-Flow probe	HF	hoisting	5° 31,205' S	148° 4,692' E	823.1
SO252_33-2	30/11/2016 13:38:55	Heat-Flow probe	HF	information	5° 31,209' S	148° 4,685' E	822.3
SO252_33-3	30/11/2016 13:52:58	Heat-Flow probe	HF	lowering	5° 31,288' S	148° 4,590' E	833.7
SO252_33-3	30/11/2016 13:55:50	Heat-Flow probe	HF	max depth/on ground	5° 31,289' S	148° 4,590' E	835.2
SO252_33-3	30/11/2016 13:56:23	Heat-Flow probe	HF	hoisting	5° 31,289' S	148° 4,590' E	833.3
SO252_33-3	30/11/2016 13:58:10	Heat-Flow probe	HF	information	5° 31,289' S	148° 4,590' E	833.5
SO252_33-4	30/11/2016 14:20:04	Heat-Flow probe	HF	lowering	5° 31,352' S	148° 4,465' E	849
SO252_33-4	30/11/2016 14:23:32	Heat-Flow probe	HF	max depth/on ground	5° 31,352' S	148° 4,465' E	847.7
SO252_33-4	30/11/2016 14:24:05	Heat-Flow probe	HF	hoisting	5° 31,352' S	148° 4,465' E	848.2
SO252_33-4	30/11/2016 14:28:35	Heat-Flow probe	HF	information	5° 31,352' S	148° 4,465' E	847.1
SO252_33-5	30/11/2016 14:47:15	Heat-Flow probe	HF	lowering	5° 31,414' S	148° 4,364' E	854.9
SO252_33-5	30/11/2016 14:50:15	Heat-Flow probe	HF	max depth/on ground	5° 31,415' S	148° 4,364' E	855.6
SO252_33-5	30/11/2016 14:50:54	Heat-Flow probe	HF	hoisting	5° 31,416' S	148° 4,364' E	855
SO252_33-5	30/11/2016 14:55:33	Heat-Flow probe	HF	information	5° 31,415' S	148° 4,364' E	855.2

Station	Date / Time UTC	Device	Device Abbreviation	Action	Latitude	Longitude	Depth (m)
SO252_33-6	30/11/2016 15:15:09	Heat-Flow probe	HF	lowering	5° 31,494' S	148° 4,214' E	869.5
SO252_33-6	30/11/2016 15:18:33	Heat-Flow probe	HF	max depth/on ground	5° 31,497' S	148° 4,214' E	869.6
SO252_33-6	30/11/2016 15:18:41	Heat-Flow probe	HF	hoisting	5° 31,497' S	148° 4,214' E	869.4
SO252_33-6	30/11/2016 15:24:25	Heat-Flow probe	HF	information	5° 31,496' S	148° 4,214' E	869.5
SO252_33-7	30/11/2016 15:44:33	Heat-Flow probe	HF	lowering	5° 31,562' S	148° 4,019' E	883
SO252_33-7	30/11/2016 15:48:20	Heat-Flow probe	HF	max depth/on ground	5° 31,565' S	148° 4,017' E	884
SO252_33-7	30/11/2016 16:03:08	Heat-Flow probe	HF	hoisting	5° 31,564' S	148° 4,017' E	884.4
SO252_33-7	30/11/2016 16:24:03	Heat-Flow probe	HF	information	5° 31,562' S	148° 4,019' E	883.1
SO252_33-7	30/11/2016 16:29:44	Heat-Flow probe	HF	information	5° 31,562' S	148° 4,019' E	883
SO252_33-7	30/11/2016 16:30:03	Heat-Flow probe	HF	information	5° 31,562' S	148° 4,019' E	882.7
SO252_33-8	30/11/2016 17:30:36	Heat-Flow probe	HF	in the water	5° 30,223' S	148° 4,543' E	800.2
SO252_33-8	30/11/2016 17:34:44	Heat-Flow probe	HF	information	5° 30,220' S	148° 4,539' E	800.9
SO252_33-8	30/11/2016 17:35:10	Heat-Flow probe	HF	lowering	5° 30,220' S	148° 4,539' E	800.3
SO252_33-8	30/11/2016 17:48:35	Heat-Flow probe	HF	max depth/on ground	5° 30,224' S	148° 4,539' E	799.8
SO252_33-8	30/11/2016 17:49:02	Heat-Flow probe	HF	hoisting	5° 30,224' S	148° 4,539' E	798.8
SO252_33-8	30/11/2016 17:54:16	Heat-Flow probe	HF	information	5° 30,224' S	148° 4,539' E	799.4
SO252_33-9	30/11/2016 18:12:12	Heat-Flow probe	HF	lowering	5° 30,340' S	148° 4,443' E	792.4
SO252_33-9	30/11/2016 18:16:33	Heat-Flow probe	HF	max depth/on ground	5° 30,340' S	148° 4,443' E	791.7
SO252_33-9	30/11/2016 18:32:03	Heat-Flow probe	HF	hoisting	5° 30,339' S	148° 4,446' E	790.7
SO252_33-9	30/11/2016 18:37:02	Heat-Flow probe	HF	information	5° 30,339' S	148° 4,446' E	791.1
SO252_33-10	30/11/2016 18:59:20	Heat-Flow probe	HF	lowering	5° 30,454' S	148° 4,321' E	797.3
SO252_33-10	30/11/2016 19:01:47	Heat-Flow probe	HF	max depth/on ground	5° 30,456' S	148° 4,322' E	802.1
SO252_33-10	30/11/2016 19:18:16	Heat-Flow probe	HF	hoisting	5° 30,453' S	148° 4,329' E	801

Station	Date / Time UTC	Device	Device Abbreviation	Action	Latitude	Longitude	Depth (m)
SO252_33-10	30/11/2016 19:22:18	Heat-Flow probe	HF	information	5° 30,453' S	148° 4,328' E	804.6
SO252_33-11	30/11/2016 19:42:16	Heat-Flow probe	HF	lowering	5° 30,607' S	148° 4,210' E	833.1
SO252_33-11	30/11/2016 19:45:12	Heat-Flow probe	HF	max depth/on ground	5° 30,607' S	148° 4,208' E	834.3
SO252_33-11	30/11/2016 19:45:24	Heat-Flow probe	HF	hoisting	5° 30,607' S	148° 4,208' E	834.6
SO252_33-11	30/11/2016 19:50:55	Heat-Flow probe	HF	information	5° 30,611' S	148° 4,209' E	834.5
SO252_33-12	30/11/2016 20:07:31	Heat-Flow probe	HF	lowering	5° 30,711' S	148° 4,122' E	862.2
SO252_33-12	30/11/2016 20:10:37	Heat-Flow probe	HF	max depth/on ground	5° 30,710' S	148° 4,122' E	861.7
SO252_33-12	30/11/2016 20:11:21	Heat-Flow probe	HF	hoisting	5° 30,710' S	148° 4,122' E	862.1
SO252_33-12	30/11/2016 20:17:43	Heat-Flow probe	HF	information	5° 30,711' S	148° 4,126' E	857.2
SO252_33-13	30/11/2016 20:43:41	Heat-Flow probe	HF	lowering	5° 30,839' S	148° 4,012' E	903.8
SO252_33-13	30/11/2016 20:47:23	Heat-Flow probe	HF	max depth/on ground	5° 30,839' S	148° 4,014' E	903.6
SO252_33-13	30/11/2016 20:48:15	Heat-Flow probe	HF	hoisting	5° 30,840' S	148° 4,014' E	903.9
SO252_33-13	30/11/2016 21:08:52	Heat-Flow probe	HF	information	5° 30,836' S	148° 4,018' E	903.8
SO252_33-13	30/11/2016 21:18:38	Heat-Flow probe	HF	on deck	5° 30,836' S	148° 4,017' E	904
SO252_33-13	30/11/2016 21:24:12	Heat-Flow probe	HF	station end	5° 30,837' S	148° 4,013' E	904
SO252_34-1	05/12/2016 06:23:29	Seismic Towed Receiver	SEISTR	station start	5° 32,082' S	148° 5,616' E	489.9
SO252_34-1	05/12/2016 07:09:08	Seismic Towed Receiver	SEISTR	PCable in water	5° 33,315' S	148° 5,693' E	796.3
SO252_34-1	05/12/2016 07:15:02	Seismic Towed Receiver	SEISTR	in the water	5° 33,471' S	148° 5,733' E	804
SO252_34-1	05/12/2016 07:25:58	Seismic Towed Receiver	SEISTR	profile start	5° 33,773' S	148° 5,834' E	825
SO252_34-1	05/12/2016 08:01:33	Seismic Towed Receiver	SEISTR	profile end	5° 35,227' S	148° 6,569' E	433.6
SO252_34-1	05/12/2016 08:08:53	Seismic Towed Receiver	SEISTR	on deck	5° 35,480' S	148° 6,697' E	406.5
SO252_34-1	05/12/2016 08:16:10	Seismic Towed Receiver	SEISTR	on deck	5° 35,634' S	148° 6,779' E	433.4
SO252_34-1	05/12/2016 08:18:05	Seismic Towed Receiver	SEISTR	station end	5° 35,672' S	148° 6,799' E	431.5

Station	Date / Time UTC	Device	Device Abbreviation	Action	Latitude	Longitude	Depth (m)
SO252_35-1	05/12/2016 10:36:26	KONGSBERG EM122	EM122	station start	5° 18,981' S	147° 48,622' E	1594.6
SO252_35-1	05/12/2016 10:49:04	KONGSBERG EM122	EM122	profile start	5° 18,225' S	147° 49,452' E	1772.1
SO252_35-1	05/12/2016 12:40:05	KONGSBERG EM122	EM122	alter course	5° 13,951' S	148° 1,731' E	1781
SO252_35-1	05/12/2016 13:00:01	KONGSBERG EM122	EM122	alter course	5° 11,755' S	148° 1,253' E	1786.2
SO252_35-1	05/12/2016 14:57:00	KONGSBERG EM122	EM122	alter course	5° 16,151' S	147° 48,523' E	1691.9
SO252_35-1	05/12/2016 15:35:00	KONGSBERG EM122	EM122	alter course	5° 12,110' S	147° 46,955' E	1782.7
SO252_35-1	05/12/2016 17:29:00	KONGSBERG EM122	EM122	alter course	5° 7,807' S	147° 59,490' E	1799.2
SO252_35-1	05/12/2016 17:43:06	KONGSBERG EM122	EM122	alter course	5° 9,687' S	147° 45,927' E	1790.7
SO252_35-1	05/12/2016 17:43:06	KONGSBERG EM122	EM122	alter course	5° 6,224' S	147° 59,130' E	1801.3
SO252_35-1	05/12/2016 19:39:57	KONGSBERG EM122	EM122	profile end	5° 9,691' S	147° 45,914' E	1789.8
SO252_35-1	05/12/2016 19:40:03	KONGSBERG EM122	EM122	station end	5° 9,694' S	147° 45,902' E	1792.7
SO252_36-1	05/12/2016 22:50:52	HyBIS	HyBIS	station start	5° 30,969' S	148° 6,379' E	287.6
SO252_36-1	05/12/2016 23:18:59	HyBIS	HyBIS	in the water	5° 30,986' S	148° 6,389' E	277.4
SO252_36-1	05/12/2016 23:37:48	HyBIS	HyBIS	max depth/on ground	5° 30,988' S	148° 6,388' E	278.7
SO252_36-1	05/12/2016 23:39:40	HyBIS	HyBIS	profile start	5° 30,988' S	148° 6,387' E	279.7
SO252_36-1	06/12/2016 00:17:33	HyBIS	HyBIS	profile end	5° 31,040' S	148° 6,398' E	245
SO252_36-1	06/12/2016 00:18:42	HyBIS	HyBIS	hoisting	5° 31,040' S	148° 6,398' E	245
SO252_36-1	06/12/2016 00:26:52	HyBIS	HyBIS	on deck	5° 31,040' S	148° 6,396' E	246.6
SO252_36-1	06/12/2016 00:31:17	HyBIS	HyBIS	on deck	5° 31,040' S	148° 6,395' E	247.4
SO252_36-2	06/12/2016 00:56:46	HyBIS	HyBIS	in the water	5° 31,036' S	148° 6,398' E	246.9
SO252_36-2	06/12/2016 01:00:38	HyBIS	HyBIS	in the water	5° 31,036' S	148° 6,399' E	246.1
SO252_36-2	06/12/2016 01:12:39	HyBIS	HyBIS	max depth/on ground	5° 31,037' S	148° 6,393' E	250.5
SO252_36-2	06/12/2016 01:17:19	HyBIS	HyBIS	profile start	5° 31,040' S	148° 6,391' E	247.9

Station	Date / Time UTC	Device	Device Abbreviation	Action	Latitude	Longitude	Depth (m)
SO252_36-2	06/12/2016 01:25:36	HyBIS	HyBIS	information	5° 31,050' S	148° 6,391' E	243.7
SO252_36-2	06/12/2016 01:26:45	HyBIS	HyBIS	hoisting	5° 31,051' S	148° 6,392' E	242.1
SO252_36-2	06/12/2016 01:36:00	HyBIS	HyBIS	on deck	5° 31,053' S	148° 6,391' E	236
SO252_36-2	06/12/2016 01:39:28	HyBIS	HyBIS	on deck	5° 31,052' S	148° 6,390' E	241.2
SO252_36-2	06/12/2016 01:44:00	HyBIS	HyBIS	station end	5° 31,050' S	148° 6,392' E	239.2
SO252_37-1	06/12/2016 02:07:04	HyBIS	HyBIS	station start	5° 30,701' S	148° 6,446' E	345.4
SO252_37-1	06/12/2016 02:16:32	HyBIS	HyBIS	in the water	5° 30,702' S	148° 6,443' E	364.2
SO252_37-1	06/12/2016 02:19:33	HyBIS	HyBIS	information	5° 30,702' S	148° 6,447' E	358.2
SO252_37-1	06/12/2016 02:31:33	HyBIS	HyBIS	max depth/on ground	5° 30,705' S	148° 6,449' E	355.9
SO252_37-1	06/12/2016 02:44:54	HyBIS	HyBIS	information	5° 30,706' S	148° 6,446' E	362.2
SO252_37-1	06/12/2016 02:55:39	HyBIS	HyBIS	information	5° 30,708' S	148° 6,441' E	365.9
SO252_37-1	06/12/2016 02:58:37	HyBIS	HyBIS	on deck	5° 30,706' S	148° 6,438' E	367.2
SO252_37-1	06/12/2016 03:00:05	HyBIS	HyBIS	station end	5° 30,705' S	148° 6,438' E	368.3
SO252_38-1	06/12/2016 03:54:54	HyBIS	HyBIS	station start	5° 28,979' S	148° 3,379' E	926.4
SO252_38-1	06/12/2016 03:56:14	HyBIS	HyBIS	in the water	5° 28,981' S	148° 3,382' E	926.2
SO252_38-1	06/12/2016 03:58:54	HyBIS	HyBIS	information	5° 28,983' S	148° 3,384' E	927.5
SO252_38-1	06/12/2016 04:20:14	HyBIS	HyBIS	max depth/on ground	5° 28,983' S	148° 3,386' E	928.8
SO252_38-1	06/12/2016 04:47:11	HyBIS	HyBIS	hoisting	5° 28,995' S	148° 3,379' E	928
SO252_38-1	06/12/2016 05:46:00	HyBIS	HyBIS	information	5° 28,990' S	148° 3,386' E	926.9
SO252_38-1	06/12/2016 05:48:19	HyBIS	HyBIS	on deck	5° 28,991' S	148° 3,386' E	927
SO252_38-1	06/12/2016 05:49:11	HyBIS	HyBIS	station end	5° 28,991' S	148° 3,386' E	928.4
SO252_39-1	06/12/2016 07:07:00	KONGSBERG EM122	EM122	station start	5° 29,882' S	148° 5,226' E	817.4
SO252_39-1	06/12/2016 07:07:06	KONGSBERG EM122	EM122	profile start	5° 29,879' S	148° 5,237' E	816.2

Station	Date / Time UTC	Device	Device Abbreviation	Action	Latitude	Longitude	Depth (m)
SO252_39-1	06/12/2016 08:23:31	KONGSBERG EM122	EM122	alter course	5° 28,653' S	148° 14,063' E	1340.9
SO252_39-1	06/12/2016 08:58:21	KONGSBERG EM122	EM122	alter course	5° 24,727' S	148° 14,650' E	1478.2
SO252_39-1	06/12/2016 10:00:03	KONGSBERG EM122	EM122	alter course	5° 19,018' S	148° 10,245' E	1422.3
SO252_39-1	06/12/2016 10:27:20	KONGSBERG EM122	EM122	alter course	5° 16,472' S	148° 8,315' E	1676.1
SO252_39-1	06/12/2016 11:57:21	KONGSBERG EM122	EM122	alter course	5° 10,883' S	147° 59,411' E	1794.2
SO252_39-1	06/12/2016 13:53:52	KONGSBERG EM122	EM122	alter course	4° 59,377' S	147° 52,138' E	1836.4
SO252_39-1	06/12/2016 14:39:06	KONGSBERG EM122	EM122	alter course	4° 55,543' S	147° 55,600' E	1825.2
SO252_39-1	06/12/2016 16:00:00	KONGSBERG EM122	EM122	alter course	4° 51,329' S	147° 47,940' E	939.9
SO252_39-1	06/12/2016 16:36:15	KONGSBERG EM122	EM122	alter course	4° 51,975' S	147° 43,733' E	1566.1
SO252_39-1	06/12/2016 17:49:42	KONGSBERG EM122	EM122	alter course	4° 59,531' S	147° 39,712' E	1832.9
SO252_39-1	06/12/2016 18:25:01	KONGSBERG EM122	EM122	alter course	5° 3,538' S	147° 40,717' E	1765.8
SO252_39-1	06/12/2016 20:09:24	KONGSBERG EM122	EM122	alter course	5° 13,827' S	147° 47,243' E	1776.9
SO252_39-1	06/12/2016 23:47:04	KONGSBERG EM122	EM122	profile end	5° 30,787' S	148° 4,864' E	656.5
SO252_39-1	06/12/2016 23:48:01	KONGSBERG EM122	EM122	station end	5° 30,788' S	148° 4,863' E	661
SO252_40-1	07/12/2016 03:56:36	OFOS	OFOS	station start	5° 30,866' S	148° 5,403' E	675.6
SO252_40-1	07/12/2016 03:58:48	OFOS	OFOS	in the water	5° 30,866' S	148° 5,404' E	675
SO252_40-1	07/12/2016 04:21:43	OFOS	OFOS	max depth/on ground	5° 30,863' S	148° 5,399' E	667.7
SO252_40-1	07/12/2016 08:08:29	OFOS	OFOS	hoisting	5° 31,186' S	148° 4,292' E	827.9
SO252_40-1	07/12/2016 08:30:02	OFOS	OFOS	on deck	5° 31,184' S	148° 4,293' E	829.8
SO252_40-1	07/12/2016 08:36:24	OFOS	OFOS	station end	5° 31,179' S	148° 4,289' E	837.1
SO252_41-1	07/12/2016 09:45:04	KONGSBERG EM122	EM122	station start	5° 28,421' S	148° 13,205' E	1367.2
SO252_41-1	07/12/2016 09:45:12	KONGSBERG EM122	EM122	profile start	5° 28,405' S	148° 13,211' E	1367.5
SO252_41-1	07/12/2016 11:20:07	KONGSBERG EM122	EM122	alter course	5° 19,608' S	148° 9,221' E	1505.2

Station	Date / Time UTC	Device	Device Abbreviation	Action	Latitude	Longitude	Depth (m)
SO252_41-1	07/12/2016 12:06:07	KONGSBERG EM122	EM122	alter course	5° 16,651' S	148° 5,691' E	1702.9
SO252_41-1	07/12/2016 14:54:43	KONGSBERG EM122	EM122	alter course	5° 1,178' S	147° 58,928' E	1804.5
SO252_41-1	07/12/2016 17:55:12	KONGSBERG EM122	EM122	profile end	5° 8,413' S	147° 42,510' E	1777.4
SO252_41-1	07/12/2016 17:55:20	KONGSBERG EM122	EM122	station end	5° 8,420' S	147° 42,499' E	1779.2
SO252_42-1	07/12/2016 22:00:40	HyBIS	HyBIS	station start	5° 29,371' S	148° 2,323' E	954.6
SO252_42-1	07/12/2016 23:49:15	HyBIS	HyBIS	in the water	5° 29,368' S	148° 2,322' E	954.8
SO252_42-1	07/12/2016 23:52:28	HyBIS	HyBIS	in the water	5° 29,367' S	148° 2,322' E	954.9
SO252_42-1	08/12/2016 00:07:25	HyBIS	HyBIS	information	5° 29,368' S	148° 2,326' E	955.7
SO252_42-1	08/12/2016 00:24:37	HyBIS	HyBIS	on deck	5° 29,368' S	148° 2,322' E	954.5
SO252_42-1	08/12/2016 00:26:04	HyBIS	HyBIS	on deck	5° 29,368' S	148° 2,321' E	954.3
SO252_42-1	08/12/2016 00:30:23	HyBIS	HyBIS	in the water	5° 29,367' S	148° 2,325' E	954.6
SO252_42-1	08/12/2016 00:33:12	HyBIS	HyBIS	in the water	5° 29,370' S	148° 2,323' E	956
SO252_42-1	08/12/2016 00:55:39	HyBIS	HyBIS	max depth/on ground	5° 29,364' S	148° 2,330' E	964.5
SO252_42-1	08/12/2016 00:57:51	HyBIS	HyBIS	profile start	5° 29,365' S	148° 2,329' E	965.1
SO252_42-1	08/12/2016 02:14:40	HyBIS	HyBIS	hoisting	5° 29,713' S	148° 2,185' E	976.4
SO252_42-1	08/12/2016 02:34:38	HyBIS	HyBIS	information	5° 29,713' S	148° 2,180' E	978.5
SO252_42-1	08/12/2016 02:37:14	HyBIS	HyBIS	on deck	5° 29,714' S	148° 2,181' E	976.8
SO252_42-1	08/12/2016 02:39:18	HyBIS	HyBIS	station end	5° 29,714' S	148° 2,182' E	976.9
SO252_43-1	08/12/2016 03:46:55	HyBIS	HyBIS	station start	5° 28,753' S	148° 1,289' E	835.3
SO252_43-1	08/12/2016 03:48:43	HyBIS	HyBIS	in the water	5° 28,768' S	148° 1,296' E	800.7
SO252_43-1	08/12/2016 03:51:31	HyBIS	HyBIS	information	5° 28,777' S	148° 1,309' E	807.9
SO252_43-1	08/12/2016 04:12:51	HyBIS	HyBIS	max depth/on ground	5° 28,811' S	148° 1,354' E	848.9
SO252_43-1	08/12/2016 05:18:52	HyBIS	HyBIS	hoisting	5° 29,062' S	148° 1,011' E	1072

Station	Date / Time UTC	Device	Device Abbreviation	Action	Latitude	Longitude	Depth (m)
SO252_43-1	08/12/2016 06:54:31	HyBIS	HyBIS	on deck	5° 29,137' S	148° 0,942' E	1111.3
SO252_43-1	08/12/2016 06:56:54	HyBIS	HyBIS	station end	5° 29,138' S	148° 0,944' E	1109.3
SO252_44-1	08/12/2016 07:40:36	KONGSBERG EM122	EM122	station start	5° 31,528' S	148° 2,761' E	877.9
SO252_44-1	08/12/2016 07:40:42	KONGSBERG EM122	EM122	profile start	5° 31,531' S	148° 2,748' E	852.3
SO252_44-1	08/12/2016 07:52:44	KONGSBERG EM122	EM122	alter course	5° 31,817' S	148° 1,436' E	259.7
SO252_44-1	08/12/2016 09:22:37	KONGSBERG EM122	EM122	alter course	5° 26,304' S	147° 54,312' E	978.3
SO252_44-1	08/12/2016 11:46:18	KONGSBERG EM122	EM122	alter course	5° 17,220' S	147° 43,155' E	1317
SO252_44-1	08/12/2016 13:40:15	KONGSBERG EM122	EM122	alter course	5° 6,094' S	147° 40,561' E	1753.9
SO252_44-1	08/12/2016 16:36:20	KONGSBERG EM122	EM122	alter course	4° 58,792' S	147° 56,516' E	1825.7
SO252_44-1	08/12/2016 19:42:35	KONGSBERG EM122	EM122	alter course	4° 55,015' S	147° 38,742' E	1838.7
SO252_44-1	08/12/2016 20:36:07	KONGSBERG EM122	EM122	alter course	4° 50,161' S	147° 40,463' E	1844.3
SO252_44-1	08/12/2016 22:06:39	KONGSBERG EM122	EM122	profile end	4° 55,714' S	147° 47,407' E	1839.8
SO252_44-1	08/12/2016 22:07:32	KONGSBERG EM122	EM122	station end	4° 55,773' S	147° 47,470' E	1838.8
SO252_45-1	08/12/2016 23:41:47	HyBIS	HyBIS	station start	4° 56,505' S	147° 46,495' E	1839.9
SO252_45-1	08/12/2016 23:48:12	HyBIS	HyBIS	in the water	4° 56,503' S	147° 46,495' E	1839.9
SO252_45-1	08/12/2016 23:51:24	HyBIS	HyBIS	in the water	4° 56,503' S	147° 46,494' E	1839.5
SO252_45-1	09/12/2016 00:36:02	HyBIS	HyBIS	max depth/on ground	4° 56,511' S	147° 46,495' E	1840
SO252_45-1	09/12/2016 00:38:57	HyBIS	HyBIS	profile start	4° 56,511' S	147° 46,495' E	1839.9
SO252_45-1	09/12/2016 00:42:48	HyBIS	HyBIS	information	4° 56,503' S	147° 46,494' E	1839.8
SO252_45-1	09/12/2016 00:45:08	HyBIS	HyBIS	alter course	4° 56,501' S	147° 46,495' E	1840.5
SO252_45-1	09/12/2016 00:51:11	HyBIS	HyBIS	information	4° 56,502' S	147° 46,488' E	1840.2
SO252_45-1	09/12/2016 00:52:56	HyBIS	HyBIS	hoisting	4° 56,501' S	147° 46,489' E	1840.5
SO252_45-1	09/12/2016 01:40:57	HyBIS	HyBIS	on deck	4° 56,507' S	147° 46,492' E	1843.6

Station	Date / Time UTC	Device	Device Abbreviation	Action	Latitude	Longitude	Depth (m)
SO252_45-1	09/12/2016 01:43:46	HyBIS	HyBIS	on deck	4° 56,507' S	147° 46,491' E	1840.4
SO252_45-1	09/12/2016 01:44:02	HyBIS	HyBIS	station end	4° 56,507' S	147° 46,491' E	1840.5
SO252_46-1	09/12/2016 02:58:16	HyBIS	HyBIS	station start	5° 4,784' S	147° 50,220' E	1829.5
SO252_46-1	09/12/2016 03:04:09	HyBIS	HyBIS	in the water	5° 4,720' S	147° 50,190' E	1830.3
SO252_46-1	09/12/2016 03:07:01	HyBIS	HyBIS	information	5° 4,724' S	147° 50,192' E	1829.4
SO252_46-1	09/12/2016 03:53:33	HyBIS	HyBIS	max depth/on ground	5° 4,721' S	147° 50,191' E	1830.3
SO252_46-1	09/12/2016 03:55:51	HyBIS	HyBIS	hoisting	5° 4,720' S	147° 50,192' E	1829.6
SO252_46-1	09/12/2016 04:55:56	HyBIS	HyBIS	information	5° 4,720' S	147° 50,193' E	1829.5
SO252_46-1	09/12/2016 05:00:00	HyBIS	HyBIS	on deck	5° 4,717' S	147° 50,192' E	1829.7
SO252_46-1	09/12/2016 05:01:07	HyBIS	HyBIS	station end	5° 4,717' S	147° 50,192' E	1829.3
SO252_47-1	09/12/2016 06:12:15	HyBIS	HyBIS	station start	5° 13,110' S	147° 52,406' E	1790.2
SO252_47-1	09/12/2016 06:18:57	HyBIS	HyBIS	in the water	5° 13,103' S	147° 52,416' E	1790.6
SO252_47-1	09/12/2016 07:10:23	HyBIS	HyBIS	max depth/on ground	5° 13,105' S	147° 52,418' E	67
SO252_47-1	09/12/2016 07:14:44	HyBIS	HyBIS	information	5° 13,105' S	147° 52,416' E	73
SO252_47-1	09/12/2016 07:15:16	HyBIS	HyBIS	hoisting	5° 13,106' S	147° 52,416' E	61
SO252_47-1	09/12/2016 08:01:12	HyBIS	HyBIS	on deck	5° 13,104' S	147° 52,414' E	57
SO252_47-1	09/12/2016 08:02:41	HyBIS	HyBIS	station end	5° 13,105' S	147° 52,414' E	63
SO252_48-1	09/12/2016 09:03:09	HyBIS	HyBIS	station start	5° 21,635' S	147° 54,074' E	1718.4
SO252_48-1	09/12/2016 09:07:57	HyBIS	HyBIS	in the water	5° 21,626' S	147° 54,071' E	1719
SO252_48-1	09/12/2016 09:10:04	HyBIS	HyBIS	information	5° 21,615' S	147° 54,070' E	1718.2
SO252_48-1	09/12/2016 09:54:48	HyBIS	HyBIS	information	5° 21,604' S	147° 54,067' E	1718.3
SO252_48-1	09/12/2016 09:58:35	HyBIS	HyBIS	information	5° 21,605' S	147° 54,065' E	1719.2
SO252_48-1	09/12/2016 09:58:50	HyBIS	HyBIS	hoisting	5° 21,605' S	147° 54,065' E	1718.8

Station	Date / Time UTC	Device	Device Abbreviation	Action	Latitude	Longitude	Depth (m)
SO252_48-1	09/12/2016 10:38:36	HyBIS	HyBIS	on deck	5° 21,607' S	147° 54,071' E	1718.4
SO252_48-1	09/12/2016 10:42:32	HyBIS	HyBIS	on deck	5° 21,607' S	147° 54,071' E	1719.1
SO252_48-1	09/12/2016 10:43:18	HyBIS	HyBIS	station end	5° 21,607' S	147° 54,071' E	1717.9
SO252_49-1	09/12/2016 11:39:24	KONGSBERG EM122	EM122	station start	5° 21,482' S	148° 1,707' E	1485.7
SO252_49-1	09/12/2016 11:47:33	KONGSBERG EM122	EM122	profile start	5° 22,154' S	148° 2,022' E	1208.9
SO252_49-1	09/12/2016 12:25:19	KONGSBERG EM122	EM122	alter course	5° 25,948' S	148° 2,272' E	620.8
SO252_49-1	09/12/2016 13:00:03	KONGSBERG EM122	EM122	alter course	5° 27,885' S	148° 5,098' E	652.3
SO252_49-1	09/12/2016 13:19:40	KONGSBERG EM122	EM122	alter course	5° 27,904' S	148° 7,064' E	947.8
SO252_49-1	09/12/2016 13:35:10	KONGSBERG EM122	EM122	alter course	5° 26,703' S	148° 8,007' E	977.1
SO252_49-1	09/12/2016 14:22:24	KONGSBERG EM122	EM122	alter course	5° 21,961' S	148° 8,044' E	1159.7
SO252_49-1	09/12/2016 15:06:23	KONGSBERG EM122	EM122	alter course	5° 20,632' S	148° 3,909' E	959.3
SO252_49-1	09/12/2016 15:28:44	KONGSBERG EM122	EM122	alter course	5° 21,968' S	148° 2,155' E	1222.6
SO252_49-1	09/12/2016 15:34:17	KONGSBERG EM122	EM122	alter course	5° 21,853' S	148° 1,802' E	1394.1
SO252_49-1	09/12/2016 16:00:05	KONGSBERG EM122	EM122	station end	5° 20,160' S	148° 3,730' E	1260.1
SO252_50-1	09/12/2016 17:27:00	Parasound P70	PS	station start	5° 15,006' S	148° 10,379' E	1691.1
SO252_50-1	09/12/2016 19:12:27	Parasound P70	PS	alter course	5° 23,571' S	148° 16,619' E	1471.3
SO252_50-1	09/12/2016 20:28:11	Parasound P70	PS	profile end	5° 25,688' S	148° 9,567' E	1089.7
SO252_50-1	09/12/2016 20:28:15	Parasound P70	PS	station end	5° 25,690' S	148° 9,560' E	1086.1
SO252_51-1	09/12/2016 21:56:46	HyBIS	HyBIS	station start	5° 30,951' S	148° 2,379' E	930.5
SO252_51-1	09/12/2016 21:58:38	HyBIS	HyBIS	in the water	5° 30,950' S	148° 2,379' E	930.3
SO252_51-1	09/12/2016 21:59:03	HyBIS	HyBIS	in the water	5° 30,950' S	148° 2,380' E	930.2
SO252_51-1	09/12/2016 22:33:09	HyBIS	HyBIS	profile start	5° 30,946' S	148° 2,385' E	929.7
SO252_51-1	09/12/2016 22:41:09	HyBIS	HyBIS	alter course	5° 30,951' S	148° 2,367' E	931.1

Station	Date / Time UTC	Device	Device Abbreviation	Action	Latitude	Longitude	Depth (m)
SO252_51-1	09/12/2016 22:53:25	HyBIS	HyBIS	alter course	5° 30,992' S	148° 2,324' E	929.1
SO252_51-1	09/12/2016 23:03:02	HyBIS	HyBIS	alter course	5° 30,942' S	148° 2,321' E	936
SO252_51-1	09/12/2016 23:08:51	HyBIS	HyBIS	alter course	5° 30,939' S	148° 2,328' E	937.1
SO252_51-1	09/12/2016 23:22:26	HyBIS	HyBIS	alter course	5° 30,939' S	148° 2,387' E	930.3
SO252_51-1	09/12/2016 23:27:29	HyBIS	HyBIS	alter course	5° 30,948' S	148° 2,398' E	929.9
SO252_51-1	09/12/2016 23:36:38	HyBIS	HyBIS	information	5° 30,948' S	148° 2,386' E	929.8
SO252_51-1	09/12/2016 23:37:24	HyBIS	HyBIS	hoisting	5° 30,948' S	148° 2,386' E	929.5
SO252_51-1	10/12/2016 00:00:52	HyBIS	HyBIS	on deck	5° 30,948' S	148° 2,382' E	930.3
SO252_51-1	10/12/2016 00:05:09	HyBIS	HyBIS	on deck	5° 30,945' S	148° 2,383' E	930
SO252_51-1	10/12/2016 00:06:39	HyBIS	HyBIS	station end	5° 30,945' S	148° 2,383' E	929.9
SO252_52-1	10/12/2016 00:40:36	HyBIS	HyBIS	station start	5° 29,559' S	148° 2,237' E	970.6
SO252_52-1	10/12/2016 00:45:58	HyBIS	HyBIS	in the water	5° 29,568' S	148° 2,232' E	992.5
SO252_52-1	10/12/2016 00:49:29	HyBIS	HyBIS	in the water	5° 29,572' S	148° 2,233' E	1057.7
SO252_52-1	10/12/2016 01:13:28	HyBIS	HyBIS	max depth/on ground	5° 29,567' S	148° 2,239' E	989
SO252_52-1	10/12/2016 01:14:23	HyBIS	HyBIS	profile start	5° 29,568' S	148° 2,237' E	993.4
SO252_52-1	10/12/2016 01:15:20	HyBIS	HyBIS	alter course	5° 29,568' S	148° 2,236' E	1061.8
SO252_52-1	10/12/2016 01:25:17	HyBIS	HyBIS	alter course	5° 29,567' S	148° 2,225' E	996.6
SO252_52-1	10/12/2016 01:36:41	HyBIS	HyBIS	max depth/on ground	5° 29,561' S	148° 2,222' E	990.6
SO252_52-1	10/12/2016 01:37:13	HyBIS	HyBIS	hoisting	5° 29,560' S	148° 2,222' E	998.1
SO252_52-1	10/12/2016 02:03:42	HyBIS	HyBIS	information	5° 29,561' S	148° 2,224' E	989.8
SO252_52-1	10/12/2016 02:06:36	HyBIS	HyBIS	on deck	5° 29,560' S	148° 2,221' E	992.8
SO252_52-1	10/12/2016 02:07:38	HyBIS	HyBIS	station end	5° 29,560' S	148° 2,221' E	980.2
SO252_53-1	10/12/2016 02:43:59	HyBIS	HyBIS	station start	5° 29,902' S	148° 3,490' E	760

Station	Date / Time UTC	Device	Device Abbreviation	Action	Latitude	Longitude	Depth (m)
SO252_53-1	10/12/2016 02:46:02	HyBIS	HyBIS	in the water	5° 29,904' S	148° 3,492' E	750
SO252_53-1	10/12/2016 02:48:56	HyBIS	HyBIS	information	5° 29,906' S	148° 3,493' E	748.1
SO252_53-1	10/12/2016 03:10:03	HyBIS	HyBIS	max depth/on ground	5° 29,901' S	148° 3,487' E	759.1
SO252_53-1	10/12/2016 03:26:02	HyBIS	HyBIS	hoisting	5° 29,901' S	148° 3,494' E	747.6
SO252_53-1	10/12/2016 03:44:30	HyBIS	HyBIS	information	5° 29,902' S	148° 3,493' E	746.2
SO252_53-1	10/12/2016 03:46:40	HyBIS	HyBIS	on deck	5° 29,902' S	148° 3,493' E	951.6
SO252_53-1	10/12/2016 03:47:19	HyBIS	HyBIS	station end	5° 29,902' S	148° 3,493' E	747
SO252_54-1	10/12/2016 04:24:36	HyBIS	HyBIS	station start	5° 29,066' S	148° 3,299' E	930
SO252_54-1	10/12/2016 04:25:40	HyBIS	HyBIS	in the water	5° 29,075' S	148° 3,303' E	931.2
SO252_54-1	10/12/2016 04:29:11	HyBIS	HyBIS	information	5° 29,068' S	148° 3,304' E	930.2
SO252_54-1	10/12/2016 04:55:31	HyBIS	HyBIS	max depth/on ground	5° 29,071' S	148° 3,303' E	930.5
SO252_54-1	10/12/2016 05:19:58	HyBIS	HyBIS	hoisting	5° 29,141' S	148° 3,333' E	931.7
SO252_54-1	10/12/2016 05:42:48	HyBIS	HyBIS	information	5° 29,135' S	148° 3,330' E	927.4
SO252_54-1	10/12/2016 05:46:18	HyBIS	HyBIS	on deck	5° 29,135' S	148° 3,331' E	931.3
SO252_54-1	10/12/2016 05:47:17	HyBIS	HyBIS	station end	5° 29,135' S	148° 3,332' E	928.3
SO252_55-1	10/12/2016 07:52:05	KONGSBERG EM710	EM710	station start	5° 30,443' S	148° 0,498' E	655.2
SO252_55-1	10/12/2016 07:52:11	KONGSBERG EM710	EM710	profile start	5° 30,446' S	148° 0,503' E	652.7
SO252_55-1	10/12/2016 09:10:48	KONGSBERG EM710	EM710	alter course	5° 33,164' S	148° 5,016' E	781.9
SO252_55-1	10/12/2016 10:34:33	KONGSBERG EM710	EM710	alter course	5° 30,286' S	148° 0,629' E	720.5
SO252_55-1	10/12/2016 12:06:16	KONGSBERG EM710	EM710	alter course	5° 32,919' S	148° 5,223' E	736.1
SO252_55-1	10/12/2016 13:34:39	KONGSBERG EM710	EM710	alter course	5° 29,939' S	148° 0,714' E	827
SO252_55-1	10/12/2016 15:04:36	KONGSBERG EM710	EM710	alter course	5° 32,625' S	148° 5,385' E	696.8
SO252_55-1	10/12/2016 16:27:47	KONGSBERG EM710	EM710	alter course	5° 29,762' S	148° 1,032' E	1005

Station	Date / Time UTC	Device	Device Abbreviation	Action	Latitude	Longitude	Depth (m)
SO252_55-1	10/12/2016 17:13:39	KONGSBERG EM710	EM710	alter course	5° 27,100' S	148° 2,233' E	984.1
SO252_55-1	10/12/2016 18:31:21	KONGSBERG EM710	EM710	alter course	5° 29,782' S	148° 6,573' E	684.2
SO252_55-1	10/12/2016 19:56:01	KONGSBERG EM710	EM710	alter course	5° 26,741' S	148° 2,109' E	971
SO252_55-1	10/12/2016 21:21:39	KONGSBERG EM710	EM710	alter course	5° 29,533' S	148° 6,755' E	786.3
SO252_55-1	10/12/2016 22:20:06	KONGSBERG EM710	EM710	profile end	5° 27,403' S	148° 3,659' E	767.8
SO252_55-1	10/12/2016 22:21:45	KONGSBERG EM710	EM710	station end	5° 27,322' S	148° 3,546' E	687.1
SO252_56-1	10/12/2016 23:10:08	HyBIS	HyBIS	station start	5° 31,367' S	148° 6,326' E	288.3
SO252_56-1	10/12/2016 23:14:41	HyBIS	HyBIS	in the water	5° 31,359' S	148° 6,323' E	286.6
SO252_56-1	10/12/2016 23:17:18	HyBIS	HyBIS	in the water	5° 31,364' S	148° 6,324' E	287.1
SO252_56-1	10/12/2016 23:29:17	HyBIS	HyBIS	max depth/on ground	5° 31,364' S	148° 6,319' E	290
SO252_56-1	10/12/2016 23:33:53	HyBIS	HyBIS	alter course	5° 31,363' S	148° 6,321' E	292.3
SO252_56-1	11/12/2016 00:06:51	HyBIS	HyBIS	information	5° 31,285' S	148° 6,405' E	200.5
SO252_56-1	11/12/2016 00:18:35	HyBIS	HyBIS	alter course	5° 31,268' S	148° 6,415' E	196.3
SO252_56-1	11/12/2016 01:00:07	HyBIS	HyBIS	information	5° 31,472' S	148° 6,410' E	189.4
SO252_56-1	11/12/2016 01:02:40	HyBIS	HyBIS	information	5° 31,475' S	148° 6,409' E	179
SO252_56-1	11/12/2016 01:05:16	HyBIS	HyBIS	information	5° 31,489' S	148° 6,409' E	159.7
SO252_56-1	11/12/2016 01:06:06	HyBIS	HyBIS	hoisting	5° 31,493' S	148° 6,409' E	155.4
SO252_56-1	11/12/2016 01:16:51	HyBIS	HyBIS	on deck	5° 31,507' S	148° 6,394' E	126.8
SO252_56-1	11/12/2016 01:20:21	HyBIS	HyBIS	on deck	5° 31,507' S	148° 6,394' E	128.1
SO252_56-1	11/12/2016 01:24:51	HyBIS	HyBIS	station end	5° 31,504' S	148° 6,398' E	141
SO252_57-1	11/12/2016 02:28:57	HyBIS	HyBIS	station start	5° 31,481' S	148° 7,334' E	393.3
SO252_57-1	11/12/2016 02:30:00	HyBIS	HyBIS	in the water	5° 31,479' S	148° 7,336' E	392.6
SO252_57-1	11/12/2016 02:31:46	HyBIS	HyBIS	information	5° 31,478' S	148° 7,337' E	394

Station	Date / Time UTC	Device	Device Abbreviation	Action	Latitude	Longitude	Depth (m)
SO252_57-1	11/12/2016 02:44:24	HyBIS	HyBIS	max depth/on ground	5° 31,474' S	148° 7,334' E	390.7
SO252_57-1	11/12/2016 06:24:53	HyBIS	HyBIS	hoisting	5° 32,188' S	148° 6,144' E	419.1
SO252_57-1	11/12/2016 06:39:10	HyBIS	HyBIS	on deck	5° 32,185' S	148° 6,140' E	424.2
SO252_57-1	11/12/2016 06:44:00	HyBIS	HyBIS	station end	5° 32,202' S	148° 6,130' E	432.4
SO252_58-1	11/12/2016 08:39:52	KONGSBERG EM122	EM122	station start	5° 14,820' S	148° 12,052' E	1681.3
SO252_58-1	11/12/2016 08:40:00	KONGSBERG EM122	EM122	profile start	5° 14,814' S	148° 12,037' E	1681.3
SO252_58-1	11/12/2016 09:31:12	KONGSBERG EM122	EM122	alter course	5° 12,656' S	148° 6,842' E	1740
SO252_58-1	11/12/2016 11:34:51	KONGSBERG EM122	EM122	alter course	5° 0,443' S	148° 1,278' E	1631.3
SO252_58-1	11/12/2016 13:49:02	KONGSBERG EM122	EM122	alter course	4° 52,838' S	147° 48,882' E	1422.2
SO252_58-1	11/12/2016 14:17:07	KONGSBERG EM122	EM122	alter course	4° 50,001' S	147° 49,742' E	1713
SO252_58-1	11/12/2016 15:39:13	KONGSBERG EM122	EM122	alter course	4° 53,258' S	147° 57,807' E	1654
SO252_58-1	11/12/2016 16:11:16	KONGSBERG EM122	EM122	alter course	4° 56,646' S	147° 58,581' E	1735.1
SO252_58-1	11/12/2016 17:00:00	KONGSBERG EM122	EM122	alter course	4° 59,421' S	148° 3,041' E	1536.9
SO252_58-1	11/12/2016 18:58:34	KONGSBERG EM122	EM122	alter course	5° 11,167' S	148° 8,249' E	1734.4
SO252_58-1	11/12/2016 19:59:57	KONGSBERG EM122	EM122	alter course	5° 13,079' S	148° 14,584' E	1623.8
SO252_58-1	11/12/2016 21:00:27	KONGSBERG EM122	EM122	profile end	5° 19,096' S	148° 12,030' E	1412.4
SO252_58-1	11/12/2016 21:00:28	KONGSBERG EM122	EM122	station end	5° 19,097' S	148° 12,029' E	1412.4
SO252_59-1	11/12/2016 22:44:25	GRAB	GRAB	station start	5° 29,072' S	148° 3,303' E	930.5
SO252_59-1	11/12/2016 23:01:06	GRAB	GRAB	in the water	5° 29,074' S	148° 3,306' E	930.9
SO252_59-1	11/12/2016 23:05:42	GRAB	GRAB	in the water	5° 29,072' S	148° 3,304' E	931
SO252_59-1	11/12/2016 23:25:14	GRAB	GRAB	information	5° 29,072' S	148° 3,305' E	929.5
SO252_59-1	11/12/2016 23:26:03	GRAB	GRAB	max depth/on ground	5° 29,072' S	148° 3,305' E	930
SO252_59-1	11/12/2016 23:28:27	GRAB	GRAB	hoisting	5° 29,073' S	148° 3,304' E	930.2

Station	Date / Time UTC	Device	Device Abbreviation	Action	Latitude	Longitude	Depth (m)
SO252_59-1	11/12/2016 23:49:53	GRAB	GRAB	on deck	5° 29,075' S	148° 3,303' E	930.6
SO252_59-1	11/12/2016 23:53:35	GRAB	GRAB	on deck	5° 29,074' S	148° 3,301' E	931.2
SO252_59-1	12/12/2016 00:34:03	GRAB	GRAB	station end	5° 29,071' S	148° 3,303' E	930.8